MONASH University

Characterization of the mechanism of z-FA-FMK anti-proliferative effects and cyst induction in *Toxoplasma gondii*

YEO ENG HWA

A thesis submitted for the degree of Doctor of Philosophy at
Monash University in 2020
SCHOOL OF SCIENCE

Contents

ABSTRACT

Toxoplasma gondii is an obligate intracellular parasitic protozoan of the phylum apicomplexa which causes zoonotic infection across wide range of homeothermic animals worldwide. The parasite possesses three distinctive proliferative stages: rapidly multiplying tachyzoites, slowly replicating bradyzoites in tissue cysts and sporozoites in oocysts. The dynamic life cycle of *T. gondii* facilitates its transmission and persistence across a wide range of hosts. During an acute infection, the immune system drives *T. gondii* tachyzoites into bradyzoites (cyst form) which leads to chronic infection. The mechanisms of *T. gondii* differentiation remains elusive and elucidating the factors that drive stage conversion may shed light to the development of novel anti-toxoplasma drug targets and therapeutics against toxoplasmosis.

The cathepsin B inhibitor and potential pro-oxidant, Benzyloxycarbonyl-phenylalanine-alanine-fluoromethylketone (z-FA-FMK) was shown to inhibit *T. gondii* (RH strain and ME49 strain) infectivity and proliferation in Hs68 cells which subsequently led to cyst formation. The intracellular cysts were shown to reactivate and regain proliferation upon z-FA-FMK withdrawal. Using this *in vitro* model which facilitates interconversion between tachyzoites and bradyzoites in Hs68 cells, the anti-proliferative effects of z-FA-FMK and mechanism of *T. gondii* differentiation were further studied.

The z-FA-FMK analogue, Benzyloxycarbonyl-phenylalanine-alanine-diazomethylketone (z-FA-DMK) which is more specific in cathepsin B inhibition blocked *T. gondii* parasite proliferation in Hs68 cells and induced cyst formation in a similar manner to z-FA-FMK. Results further showed that both z-FA-FMK and z-FA-DMK readily inhibited cathepsin B activity in host cells and *T. gondii* parasites. These results strongly suggest that the anti-proliferative effects of z-FA-FMK are mediated through cathepsin B inhibition, which is associated with the proteolytic activity of the parasite vacuolar compartment (VAC). z-FA-FMK treated parasites were also shown to depend on autophagy to regain proliferation. The results collectively indicate that the disruption of VAC causes starvation in parasites which could drive cyst formation and induce autophagy as a stress response to preserve intracellular parasite survival.

The results further demonstrated that z-FA-FMK did not increase ROS levels in both Hs68 cells and *T. gondii* parasites. However, the co-treatment of z-FA-FMK with BSO which blocks GSH synthesis exhibited synergistic effect in inhibiting *T. gondii* RH strain proliferation. The results collectively imply that z-FA-FMK and BSO appears to exert different form of stress to *T. gondii*, where the effect of z-FA-FMK is not attributed to oxidative stress but could be potentially enhanced in combination with redox stress inducers.

DECLARATION

This thesis is an original work of my research and contains no material which has been accepted for the award of any other degree or diploma at any university or equivalent institution and that, to the best of my knowledge and belief, this thesis contains no material previously published or written by another person, except where due reference is made in the text of the thesis.

Signature:

Print Name: YEO ENG HWA

Date: 5th January 2020

ACKNOWLEDGEMENT

Firstly, I would like to express my deepest appreciation and gratitude to my supervisor, Professor Chow Sek Chuen for his dedicated commitment, encouragement, invaluable guidance and opportunities given throughout my honours research year and the entire journey of my postgraduate research. To me, you have been a great mentor and teacher in which your guidance has deeply inspired and motivated me in pursuing research.

I would like to express my sincere appreciation to my senior Wai Leong, whom I often seek for regarding scientific discussions even after his completion of his postgraduate studies. The same goes for my other seniors Kiat Yee, Eveline and Tanuja for guiding me in my early phase of my research experience during the honours research year. A special appreciation also goes to my lab mates: Athena, Timothy, Karl Vern, Moinul and Tammy. Thank you all for all the moments, laughter and smiles we shared. I truly enjoyed the process of learning from each other and appreciate you all being part of this journey.

The same acknowledgement and gratitude goes to many other supportive peers and the staffs of Monash School of Science who have given me support and a helping hand. Next, I would like to express my gratitude to my parents Yeo Chin Tat and Chan Swee Fun as well as my siblings. They are my source of motivation, perseverance and strength to keep moving forward. Finally, I would like to once again thank and acknowledge everyone that I have mentioned to have given me support and assistance to pursue and achieve excellence.

LIST OF TABLES

LIST OF FIGURES

LIST OF ABBREVIATION OF TERMS

%	Percentage
:	Ratio
°C	Degree Celsius
µg	Microgram
µm	Micron
µM	Micromolar
AIDS	Acquired immunodeficiency syndrome
AMA1	Apical membrane antigen 1
ANOVA	Analysis of variance
AP	Alkaline phosphatase
ATG	Autophagy-related genes
ATP	Adenosine triphosphate
BSA	Bovine serum albumin
BSO	Buthionine sulfoximine
CAT	Catalase
CMK	Chloromethylketone
CNS	Central nervous system
CO_2	Carbon dioxide
CQ	Chloroquine
CSF	Cerebrospinal fluid
DBA	*Dolichos biflorus* agglutinin
DCF	2,7-dichlorofluorescein
DCFH-DA	Dichloro-dihydro-fluorescein diacetate
DF	Dilution factor
DFHR	Dihydrofolate reductase
dH_2O	Deionized water
DHE	Dihydroethidium
DHPS	Dihydropteroate synthetase
DMEM	Dulbecco's modified eagle's medium
DMSO	Dimethyl sulfoxide
DNA	Deoxyribonucleotide
DTT	Dithiothreitol
EDTA	Ethylenediaminetetraacetic acid
EE	Early endosome
ELISA	Enzyme linked immunosorbent assay

FBS	Fetal bovine serum
FMK	Fluoromethylketone
GPx	Glutathione peroxidase
GR	Glutathione reductase
GSH	Glutathione
GSSH	Glutathione disulfide
GST	Glutathione-s-transferase
h	Hour
H_2O_2	Hydrogen peroxide
HIV	Human immunodeficiency virus
HRP	Horseradish peroxidase
IFN-γ	Interferon gamma
IMC	Inner membrane complex
LD_{100}	Absolute lethal dose
LE	Late endosome
LHVS	Morpholinurea-leucyl-homophenyl-vinyl sulfonephenyl
MBD	Methylene blue dye
MCB	Monoclorobimane
MJ	Moving junction
ml	Milliliters
mM	Millimolar
MP	Micropore
MTS	3-(4,5-dimethylthiazol-2-yl)-5-(3-carboxymethoxyphenyl)-2-(4-sulfophenyl)-2H-tetrazolium
NAC	N-acetylcysteine
nm	Nanometer
PABA	p-aminobenzoic acid
PBS	Phosphate buffer saline
PCR	Polymerase chain reaction
PI-3K	Phosphatidylinositol 3-kinases
PMS	Phenazine methosulphate
PV	Parasitophorous vacuole
PVM	Parasitophorous vacuole membrane
R	Arginine
RFLP	Restriction length polymorphism
RIPA	Radio-immunoprecipitation assay

RNA	Ribonucleic acid
RON	Rhoptry neck
ROS	Reactive oxygen species
rpm	Revolutions per minute
SEM	Standard error of the mean
SFDT	Sabin-Feldman dye test
SOD	Superoxide dismutase
*Tg*CPB	*Toxoplasma gondii* cathepsin B-like protease
*Tg*CPL	*Toxoplasma gondii* cathepsin L-like protease
*Tg*CRT	*Toxoplasma gondii* chloroquine transporter protein
*Tg*IF2α	Toxoplasma eukaryotic initiation factor-2α
TNFα	Tumor necrosis factor α
v/v	Volume / volume
VAC	Vacuolar compartment
z-FA-DMK	Benzyloxycarbonyl-phenylalanine-alanine-diazomethylketone
z-FA-FMK	Benzyloxycarbonyl-phenylalanine-alanine-fluoromethylketone
z-RR-AMC	Benzyloxycarbonyl-arginine-arginine-7-amido-4-methylcoumarin hydrochloride
γ-GCS	γ-glutamylcysteine synthetase

CHAPTER ONE

INTRODUCTION

1.1 *Toxoplasma gondii* and toxoplasmosis

Toxoplasmosis is one of the most prevalent and widespread parasitic infections in the world, yet one of the most overlooked disease. The causative agent of toxoplasmosis is *Toxoplasma gondii* (*T. gondii*), an obligate intracellular parasitic protozoan belonging to the apicomplexan phylum (Hill and Dubey, 2002, Hill and Dubey, 2018, Kim and Weiss, 2004). Other members of parasites from the phylum apicomplexan are responsible for several major human and animal diseases. This includes *Plasmodium* which infects human and replicate within erythrocytes causing malaria. *Eimeria* and *Neospora* are of veterinary importance as they inflict diseases among livestock animals including cattle and sheep. Lastly, *Cryptosporidium* is a well-established opportunistic human pathogen which causes gastrointestinal and respiratory illness (Hu *et al*., 2004, Saeij *et al*., 2005).

T. gondii can infect any nucleated cells of homeothermic animals including humans and marine mammals, rendering them one of the most successful parasites on earth (Hill and Dubey, 2002, Tu *et al*., 2018). Although *T. gondii* infection is widespread throughout the world, its prevalence varies and depends on the geographical location, cultural habits and hygiene standards (Hill *et al*., 2005, Robert-Gangneux and Dardé, 2012). Toxoplasmosis prevalence in the United Kingdom and the United States is estimated to be around 16 - 40% of the population, whereas it can increase up to 50 - 80% in Central and South America as well as some parts of Europe (Hill *et al*., 2005). Generally, cold-temperate or arid regions have lower prevalence compared to warm and humid regions (Kasper, 2001). Apart from climate influences, socio-economic background is also a major determinant as toxoplasmosis are often reported in communities with poor hygiene and sanitation (Flegr *et al*., 2014). Serological studies estimate that about 30% of the global human population have been infected with *T. gondii*, thus making toxoplasmosis one of the most prevalent chronic infections that is faced by humans (Hill and Dubey, 2018, Nath and Sinai, 2003, Tenter *et al*., 2000).

Morphologically, *T. gondii* is crescent shaped and is approximately 5µm long and 2µm wide as depicted in Figure 1.1. It has a pointed anterior and a rounded posterior end that contains a complex cytoskeletal and organellar arrangement (Black and Boothroyd, 2000, Tu *et al*., 2018). *T. gondii* possess several basic organelles including a nucleus, a single elongated tubular mitochondrion, ribosomes, Golgi apparatus, smooth and rough endoplasmic reticulum (Hill and Dubey, 2018, Khan and Grigg, 2017, Clough and Frickel, 2017). The parasite also possesses specialized secretory organelles such as micronemes, rhoptries and dense granules which carry out specialized functions during parasite infection and proliferation (Harker *et al*., 2015, Hill and Dubey, 2002, Hu *et al*., 2006). *T. gondii* parasites are motile and they move by gliding, flexing, undulating, and rotating despite the lack of locomotion structures such as cilia, flagella, or pseudopodia (Besteiro *et al*., 2011b, Blader *et al*., 2015, Dubey *et al*., 1998).

To date, *T. gondii* can be classified into 3 major clonal lineages, namely type-1, 2 and 3 based on restriction fragment length polymorphism (RFLP) analysis and their virulence in laboratory mice (Niehus *et al*., 2014, Saeij *et al*., 2005, Simon *et al*., 2019). Type-1 strain is the most virulent, with LD_{100} of less than 10 parasites in mice (Simon *et al*., 2019). On the other hand, both type-2 and type-3 strains are less virulent, with LD_{50} of 100 and 10^5 respectively (Kim and Weiss, 2004). The three *T. gondii* strains only have a genetic difference of 1 - 2% despite their marked differences in virulence (Saeij *et al*., 2005, Su *et al*., 2003). In general, type-1 (RH) strain is the most virulent and is associated with high replication rate within any kind of host cells (Saeij *et al*., 2005, Sullivan *et al*., 2009). Although type-2 (ME49) and type-3 (VEG) strains have lower virulence and replication at a slower rate, they have the ability to differentiate into tissue cysts easily (Niehus *et al*., 2014, Skariah *et al*., 2010). According to epidemiological survey, the type-2 (ME49) strain has the highest prevalence cause of human toxoplasmosis especially in immunosuppressed patients (Araujo and Slifer, 2003, Tu *et al*., 2018).

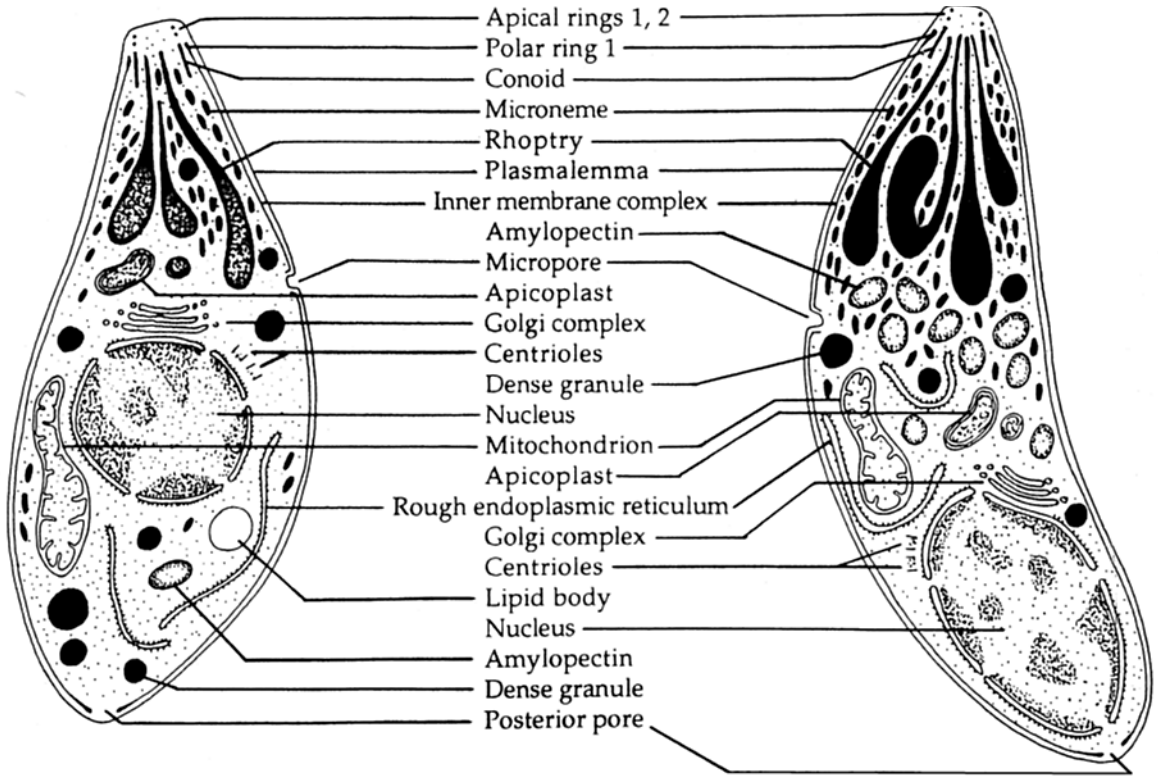

Figure 1.1. Schematic structure illustration of a tachyzoite (left) and a bradyzoite (right) of *T. gondii* parasite

Tachyzoites and bradyzoites share high structural similarities with slight variations in organelles and their positioning within the parasite. For instance, the nucleus of bradyzoites is located towards the posterior end as compared to tachyzoites while the nucleus of the tachyzoites is located centrally. Additionally, bradyzoites also contains amylopectin granules which serve as energy storage while these granules are usually absent in tachyzoites (Adapted from Dubey *et al*., 1998).

Toxoplasmosis is characterized by cellular and tissue destruction, presenting as necrotic lesions in the body due to actively multiplying parasites (Elsheikha and Khan, 2010). The parts of our body most commonly invaded and infected by *Toxoplasma* parasites are the brain, eyes, liver, lungs and skeletal muscles (Tenter *et al*., 2000, Uttah *et al*., 2013). Depending on the type of tissues or organs that are infected, toxoplasmosis can lead to diverse range of clinical complications (Tenter *et al*., 2000). Individuals having toxoplasmosis typically display mild flu-like symptoms, such as mild fever, malaise, myalgia and headache or can be asymptomatic in healthy individuals having a functional immune system (Dubey and Jones, 2008, Dunay *et al*., 2018, Foulon *et al*., 1988). The primary infection is usually acute and self-limiting where the parasites are subjugated by the immune system. However, the parasite may escape immunological clearance and differentiate into bradyzoite cysts leading to chronic infection (Bharti *et al*., 2016, Jeffers *et al*., 2018, Sutterland *et al*., 2015). The infected individual will acquire a lifelong immunity against *T. gondii* parasites following the primary infection as long as the host retains a competent immune system (Bharti *et al*., 2016, Sutterland *et al*., 2015). Nevertheless, individuals that have a weakened or suppressed immune system, such as having acquired immunodeficiency syndrome (AIDS) due to infection of human immunodeficiency virus (HIV) or under immunosuppressive therapy may suffer from toxoplasmosis as the bradyzoite tissue cysts will reactivate into highly infectious tachyzoites (Bharti *et al*., 2016, Ozgonul and Besirli, 2017, Sutterland *et al*., 2015).

On the other hand, vertical transmission or known as congenital transmission of *Toxoplasma* occurs when the expecting mother acquires primary infection or the chronically infected mother become immunocompromised during gestation (Jones *et al*., 2003, Many and Koren, 2006, McAuley, 2014, Montoya and Remington, 2008). The acute primary infection can lead to parasitemia where the parasites can cross the placenta and infect the developing fetus (McAuley, 2014, Uttah *et al*., 2013). The risk of transplacental transmission and the severity of the resulting fetal infection depend on the time of maternal infection (Hill *et al*., 2005, Tenter *et al*., 2000). The severity of the disease is inversely related to the transmission risk. The risk of transmission is the lower (~25%) when the maternal infection is acquired during

the first trimester and higher risk (~70%) during third trimester (Capobiango *et al*., 2016, Capobiango *et al*., 2014, Many and Koren, 2006). Fetal infection acquired during the first trimester often have a higher risk of miscarriage or neonatal death, which occurs in approximately 10% of all congenital toxoplasmosis cases (Montoya and Liesenfeld, 2004, Montoya and Remington, 2008, Remington *et al*., 1985). The fetus who are infected later during gestation may develop other clinical complications such as microcephaly, hydrocephalus, chorioretinitis, seizures and deafness (Jones *et al*., 2003, McAuley, 2014). Although newborn that survives congenital infection may appear asymptomatic at birth, they may subsequently develop visual impairment, learning disabilities, or mental retardation later in life (Capobiango *et al*., 2016, Jones *et al*., 2003, Uttah *et al*., 2013). The incidence of congenital toxoplasmosis is affected by the immunity of women entering pregnancy and risk of exposure to *T. gondii* during pregnancy, with an everage infection between 1 in 3000 to 1 in 10 000 live births in the United States (McAuley, 2014).

1.2 Life cycle and transmission of *T. gondii*

The life cycle of *T. gondii* parasites can be classified into two distinct phases, namely the sexual and asexual cycle that is associated to specific differentiation stages of the parasite (Blader *et al*., 2015, Dzierszinski *et al*., 2004, Ferguson, 2004). The *T. gondii* life cycle is highly adaptive in order to ensure successful transmission, pathogenesis and persistence in the infected host (Dzierszinski *et al*., 2004, Ferguson, 2004, Nath and Sinai, 2003). *T. gondii* is usually transmissible via ingestion of either: (i) oocysts (sporozoites) which are shed into the environment from the feline host, (ii) viable tissue cysts (bradyzoites) in infected meat of intermediate hosts or (iii) vertical transmission (tachyzoites) from infected mother to developing fetus (Figure 1.2) (Dubey, 1998, Hill and Dubey, 2018, Jeffers *et al*., 2018).

1.2.1 Sexual cycle

As depicted in Figure 1.2, the sexual phase of the *T. gondii* life cycle occurs exclusively in the Felidae family, which makes feline hosts the primary host (Blader *et al*., 2015, Dubey,

1998, Hill and Dubey, 2018). The sexual cycle occurs solely within the intestines of the definitive host, generating and expelling oocysts which sporulates and become infectious (Skariah *et al*., 2010). The sexual cycle begins upon ingestion of tissue cysts by a feline, the gastric enzymes destroys the cyst wall and release with bradyzoites (Robert-Gangneux and Dardé, 2012). The bradyzoites then proceed to invade the intestinal enterocytes of the feline host and undergo the sexual reproduction cycle (entero-epithelial cycle) (Robert-Gangneux and Dardé, 2012). Alternatively, the parasite may differentiate into tachyzoites and actively disseminate throughout the body known as the extra-intestinal cycle (Blader *et al*., 2015, Dubey, 1995, Hill and Dubey, 2018). The sexual cycle begins with the bradyzoites undergoing asexual multiplication to form schizonts, which further develop into merozoites via schizogony in the feline intestinal epithelial cells (Dubey, 1995, Ferguson, 2004, Hussain *et al*., 2017). The resulting merozoites undergo sexual differentiation to form microgametocytes (male) and macrogametocytes (female), which further forms haploid flagellated microgamete and macrogamete respectively to allow fertilization (Dumetre and Darde, 2003, Ferguson, 2004, Harker *et al*., 2015). A diploid zygote is formed following gamete fertilization, in which the zygote then develops into an unsporulated oocyst which is eventually passed out into the environment via the intestinal lumen (McAuley, 2014).

The duration between initial infection and the shedding of unsporulated oocysts into the environment by the feline host is known as the prepatent period, which goes on for 3-10 days (Dubey, 1988, Dubey, 1995, Hill and Dubey, 2002). Following the prepatent period, the infected feline host expels millions of highly resilient unsporulated oocysts in the feces for about 2 weeks (Blader *et al*., 2015, Dubey, 1995). Although the parasite's definitive hosts include various felids such as ocelots, bobcats, tigers and domestic cats, oocyst excretion was found to be the greatest in domestic cats (Dubey, 1995). The shedding of oocysts halts once the infected feline develops immunity towards *T. gondii* parasites and re-shedding of oocysts is extremely uncommon (Dubey, 1995, Dubey and Jones, 2008). The expelled oocysts are highly resilient towards adverse environmental conditions while remaining infectious in the environment for up to a year (Dzierszinski *et al*., 2004, Ferguson, 2004). The expelled oocyst

undergoes sporulation over time and is disseminated further across the environment via insects and rodents, contaminating soil, food and water in the process (Cook *et al*., 2000, Tenter *et al*., 2000). As shown in Figure 1.2, infection in all mammals including humans is normally acquired by ingestion of oocysts, followed by differentiation into the tachyzoite form which replicates and disseminates rapidly, causing an acute infection driven by the asexual cycle (Dubey, 1998, Hill and Dubey, 2018, Tu *et al*., 2018). Upon infection, the proliferative form of the parasite (tachyzoite) may differentiate into a tissue cyst (bradyzoite) that can be transmitted to new hosts when consumed, particularly in raw or uncooked meat of previously infected intermediate hosts (Dzierszinski *et al*., 2004, Ferguson, 2004).

1.2.2 Asexual cycle (Acute phase)

As shown in Figure 1.2, the asexual phase of the *T. gondii* life cycle occurs in the intermediate host and can be classified into two distinct stages of infection, known as the acute and chronic phase (Black and Boothroyd, 2000). The acute phase of toxoplasmosis is characterized by active dissemination of tachyzoites within the infected host (Blader *et al*., 2015, Joyce *et al*., 2011). The acute phase of the asexual cycle of *T. gondii* begins when an intermediate host ingests sporulated oocyst (sporozoites) or viable tissue cyst (bradyzoites). The sporozoites or bradyzoites are released from oocyst and cyst, respectively by proteolytic enzymes in the gut (Yan *et al*., 2016) before invading the intestinal epithelial cells and differentiate into tachyzoites (Robert-Gangneux and Dardé, 2012, Yan *et al*., 2016). Tachyzoites are defined as the infectious and rapidly multiplying form of the parasite during acute toxoplasmosis, which can be easily subjugated by a functional immune system (Black and Boothroyd, 2000, Hill and Dubey, 2018, Jeffers *et al*., 2018, Tu *et al*., 2018).

1.2.3 Asexual cycle (Chronic phase)

In contrast, the chronic infection stage of toxoplasmosis is defined by the development of tissue cysts, through the differentiation from tachyzoites to bradyzoites (Black and Boothroyd, 2000, Joyce *et al*., 2011). Tachyzoites could avoid immunological clearance by

differentiating into the slow replicating bradyzoite encapsulated in a resilient cyst wall, which resides primarily in the muscle tissues, central nervous system (CNS) and retina (Blader *et al*., 2015, Dubey, 1988, Dubey and Jones, 2008). Bradyzoites appears morphologically identical to tachyzoites but grows much slower and more resistant to proteolytic degradation than tachyzoites (Dzierszinski *et al*., 2004, Hill and Dubey, 2018, Jacobs *et al*., 1960). Tissue cysts containing bradyzoites are metabolically quiescent and replicates very slowly, evading immune detection and does not invoke any immune response (Harker *et al*., 2015, Nath and Sinai, 2003, Tomita *et al*., 2013). However, *T. gondii* cysts sporadically reactivate, thus sustaining chronic infection over the lifetime of the host (Dzierszinski *et al*., 2004, Guimaraes *et al*., 2009, Jeffers *et al*., 2018). Studies have shown that *T. gondii* cysts undergoes episodic cycles of differentiation between tachyzoites and bradyzoites even while under control by the immune system (Watts *et al*., 2015). During the formation of cysts, the parasitophorous vacuole membrane (PVM) undergoes modification through addition of chitin, glycoproteins, and glycolipids to form the cyst wall. Additionally, the differentiating parasite shows increase in amylopectin granules presumably to increase glucose storage (Sugi *et al*., 2017). The bradyzoites is generally characterized by subcellular reorganization such as relocation of the nucleus to the posterior end and redistribution of the secretory organelles (Dzierszinski *et al*., 2004).

T. gondii is a highly virulent parasite that also affects domesticated animals. Infected livestock presents a major source of transmission, contributing to the high prevalence of toxoplasmosis in humans through the consumption of meat harboring viable tissue cysts (Hussain *et al*., 2017, Wilking *et al*., 2016). *T. gondii* cysts ingested through raw or undercooked infected meat rupture along the digestive tract, releasing bradyzoites which proceeds to infect the epithelium of the intestinal lumen (Black and Boothroyd, 2000). This is followed by differentiation of the bradyzoites back to the highly virulent tachyzoite, thereby initiating the acute phase of the asexual cycle (Black and Boothroyd, 2000, Blader *et al*., 2015).

Chronic toxoplasmosis and its complications are due to the ability of *T. gondii* parasites to respond to the host's immune system and form resilient tissue cysts (Jeffers *et al*., 2018, Nath and Sinai, 2003, Tenter *et al*., 2000). In healthy individuals, *Toxoplasma* cyst is constantly suppressed by the immune system and may undergo cycles of differentiation between active tachyzoites and dormant bradyzoite without clinical complications (Chew *et al*., 2012, Takashima *et al*., 2008). However, the infection in immune-privileged organs such as the eyes (ocular toxoplasmosis) even in healthy individuals leads to progressive degeneration of vision and may result in permanent blindness (Bosch-Driessen *et al*., 2002a). Clinical manifestation of chronic toxoplasmosis occurs in the absence of immune surveillance, particularly the loss of T-cell immunity which facilitates the reactivation of tissue cysts and leads to the uncontrolled tachyzoite replication (Israelski *et al*., 1993, Khan *et al*., 2019, Watts *et al*., 2015).

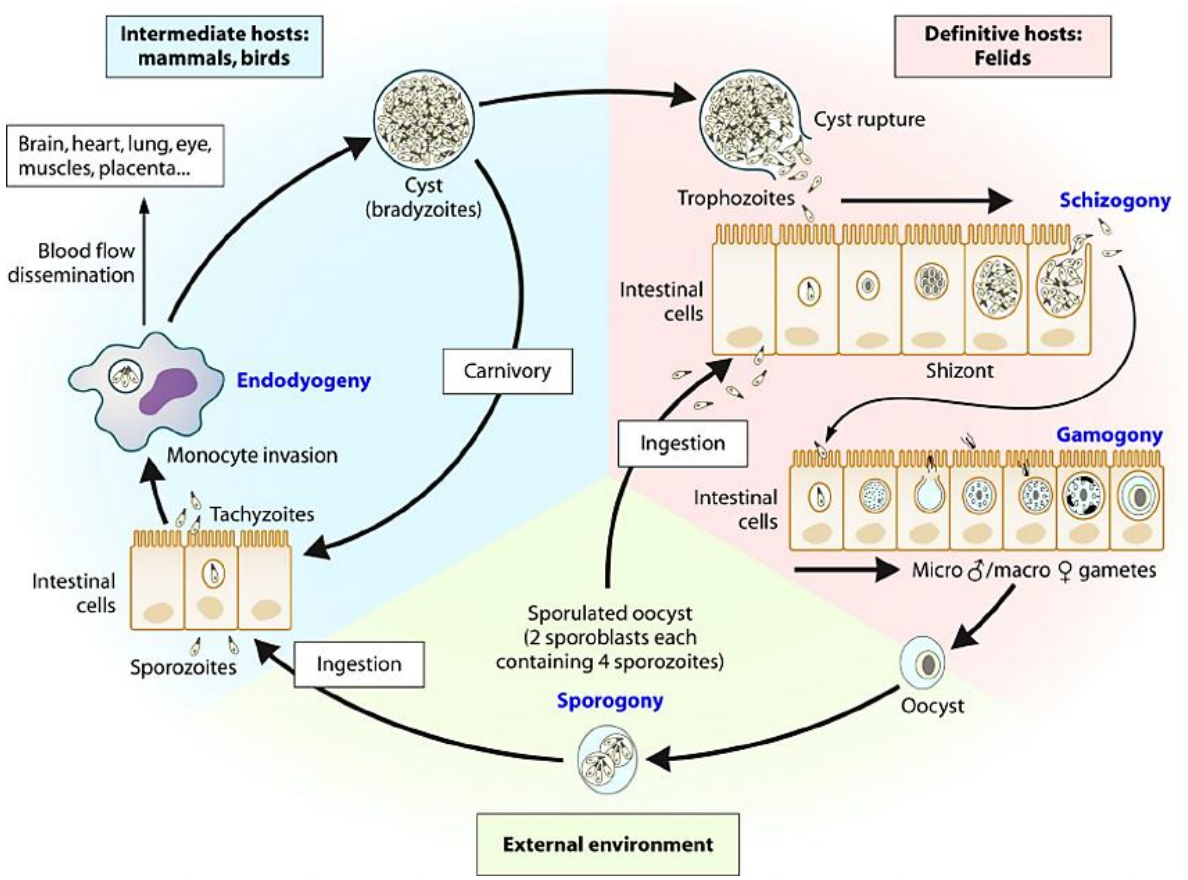

Figure 1.2. Life cycle of *Toxoplasma gondii*

T. gondii parasites undergo sexual replication exclusively in felines (definitive host). The sexual cycle occurs in the gut of the feline host where parasites transform into schizonts in the intestinal epithelial cells. The schizonts undergo schizogony to form merozoites, which further differentiates into microgametocytes (male) and macrogametocytes (female) via gamogony. The fusion of the resulting gametes completes the fertilization process which produces oocyst which is excreted into the environment via the feline's feces. On the other hand, the *T. gondii* asexual cycle occurs in the intermediate host via ingestion of oocysts or tissue cysts. Excysted sporozoites and bradyzoites infects the intestinal cells and differentiates into tachyzoites which further disseminate across the infected host body. Under the pressure of the immune system, invaded tachyzoites can convert into latent bradyzoites residing in tissue cysts (Adapted from Robert-Gangenux and Dardé, 2012).

1.3 *T. gondii* proliferation and lytic cycle

1.3.1 Host cell invasion

In both primary and secondary hosts, the *T. gondii* infection process is often described as the lytic cycle, which consist of parasite invasion, replication and egress (Uttah *et al*., 2013). Apicomplexans such as *T. gondii* possess specialized secretory organelles such as micronemes, rhoptries and dense granules, which deploy proteins in a regulated manner during the parasite invasion process (Carruthers, 1999, Hill and Dubey, 2018). As shown in Figure 1.3, the parasite invasion begins by active adhesion of the posterior end via calcium dependent micronemal secretion of adhesins, which facilitates the initial attachment and penetration into the host cell (Carruthers, 2002, Drewry and Sibley, 2015). One of the adhesin known as apical membrane antigen 1 (AMA1) interacts with rhoptry neck (RON) proteins secreted by the rhoptries to form the moving junction (MJ) (Blader *et al*., 2015, Gilson and Crabb, 2009). This provides a strong anchorage on to the host cytoskeleton to facilitate penetration into the host cell (Alexander *et al*., 2005, Besteiro *et al*., 2011b, Drewry and Sibley, 2015).

During active penetration of the host cell, the parasite moves across the MJ from the apical end to the posterior end. Throughout this process, the MJ also serves to prevent association of host membrane integral proteins to the forming PVM (Blader *et al*., 2015, Laliberte and Carruthers, 2008). Rhoptry protein secretions is also associated with the establishment of the PVM that envelops and delimits the PVM from the host cell cytoplasm (Guimaraes *et al*., 2009, Hoppe *et al*., 2000, Uttah *et al*., 2013). The composition of the PVM consist of parasite rhoptry secretions (20%), while the majority of the PVM are derived from the infected host cell (Clough and Frickel, 2017, Harker *et al*., 2015, Suss-Toby *et al*., 1996). The PVM is a subcellular compartment that serves as a selective barrier between the parasite and the host cell and protects the parasite against free radicals, pH, osmolarity stress and immunological detection (Guimaraes *et al*., 2009). Most importantly, the parasitophorous vacuole (PV) resist

fusion with the host endocytic lysosomal compartments and allow parasite persistence within the host cell (Guimaraes *et al*., 2009, Harker *et al*., 2015).

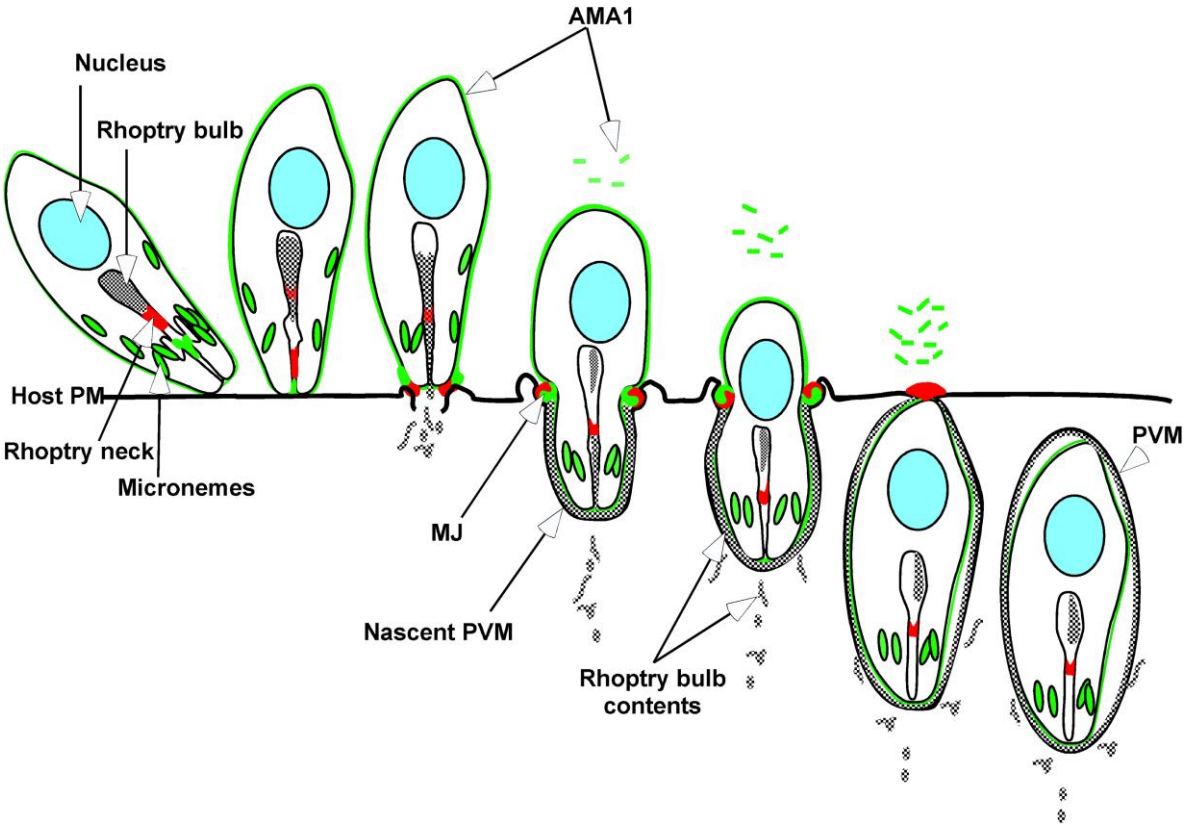

Figure 1.3. Host cell invasion process by *T. gondii* tachyzoites

The *T. gondii* invasion process begins with attachment of the parasite to the host cell membrane mediated via secretion of adhesin. Subsequently, the parasite apically attaches to the host cell membrane surface and secretes AMA1 and RON proteins. This results in the formation of the MJ, which allows the parasite to actively penetrate the cell membrane. The parasite moves across the MJ as the PVM is formed. The invasion process is completed when the parasite is fully internalized and enclosed within a PVM (Adapted from Alexander *et al*., 2005).

1.3.2 Replication via endodyogeny and egress

T. gondii parasites replicate asexually within the host cell by repeated endodyogeny, a specialized form of reproduction in which two clonal progenies form within the cytoplasm of a single mother parasite (Hill *et al*., 2005, Nishi *et al*., 2008, Sheffield and Melton, 1968). As shown in Figure 1.4, endodyogeny begins with the division of the Golgi apparatus and the formation of nascent conoid at the apical end. This is followed by the formation of the inner membrane complex (IMC) and the subpellicular microtubules, which elongates from the apical nascent conoid towards the posterior end (Jacot *et al*., 2013, Nishi *et al*., 2008). Subsequently, the apicoplast, nucleus and all the other cytoplasm contents is divided across each forming daughter cell (Carruthers, 2002, van Dooren *et al*., 2009). As the development progresses, the IMC of the two daughter parasites will enclose the divided cellular contents and replace the mother cell's IMC (Carruthers, 2002, Jacot *et al*., 2013). Towards the end of endodyogeny, the specialized organelles such as the rhoptries and micronemes are regenerated *de novo* from the Golgi apparatus (Jacot *et al*., 2013, Morlon-Guyot *et al*., 2014). The newly formed tachyzoites maintains a residual linkage at the posterior end which results in the "rosette" arrangement as the parasite continues to further replicate within the PVM (Carruthers, 2002, Bisio *et al*., 2019).

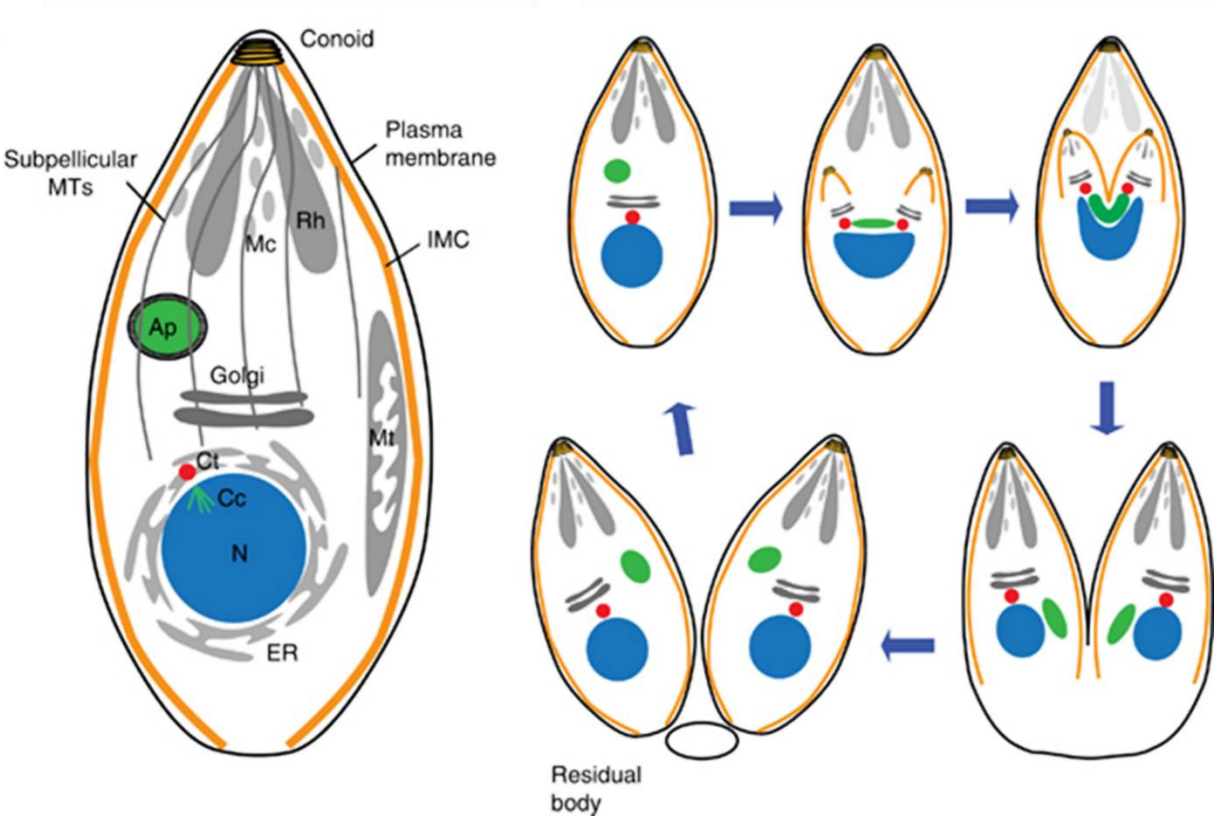

Figure 1.4. Endodyogeny of *T. gondii* tachyzoites

Endodyogeny begins with the formation of two nascent conoid at the apical end of the parent parasite. Subsequently, the subpellicular microtubules and IMC forms and extends from the conoid to the posterior end. The organelles divide and segregate into each daughter cell before being fully enveloped by the extending IMC. The daughter parasite's IMC replaces the parent IMC while the parent plasmalemma is retained to envelope the newly formed daughter parasites. The daughter parasite then separates to form independent bodies while leaving behind a residual body of the parent parasite (Adapted from Jacot *et al*., 2013).

T. gondii are parasitic auxotrophs which needs to obtain nutrients such as phospholipids, cholesterol, arginine, polyamines, tryptophan and purine nucleosides across the PVM for sustenance to drive proliferation (Charron and Sibley, 2002, Clough and Frickel, 2017, de Melo and de Souza, 1996, Sehgal *et al*., 2005). *T. gondii* parasites acquire these nutrients from the host cell cytoplasm through diffusion and active transport across the PVM (Coppens *et al*., 2000). The PVM is formed by structural modification from the *T. gondii* dense granule secretory proteins to confer protection to the parasites and facilitate nutrient transfer from the host cytoplasm (Carruthers, 1999, Cesbron-Delauw, 1994, Zhou *et al*., 2005).

As *T. gondii* parasites undergo synchronous replication via endodyogeny, the PV swells in volume and eventually rupture the infected host cell, thus completing the lytic cycle with the egress of parasites to continue infecting adjacent cells (Figure 1.5) (Black and Boothroyd, 2000, Hortua Triana *et al*., 2018, Watts *et al*., 2015). Intracellular *T. gondii* parasites replicate with a doubling time of 6 - 8h *in vitro* and yields approximately 64 - 128 parasites after a single complete lytic cycle (Black and Boothroyd, 2000, Khan and Grigg, 2017).

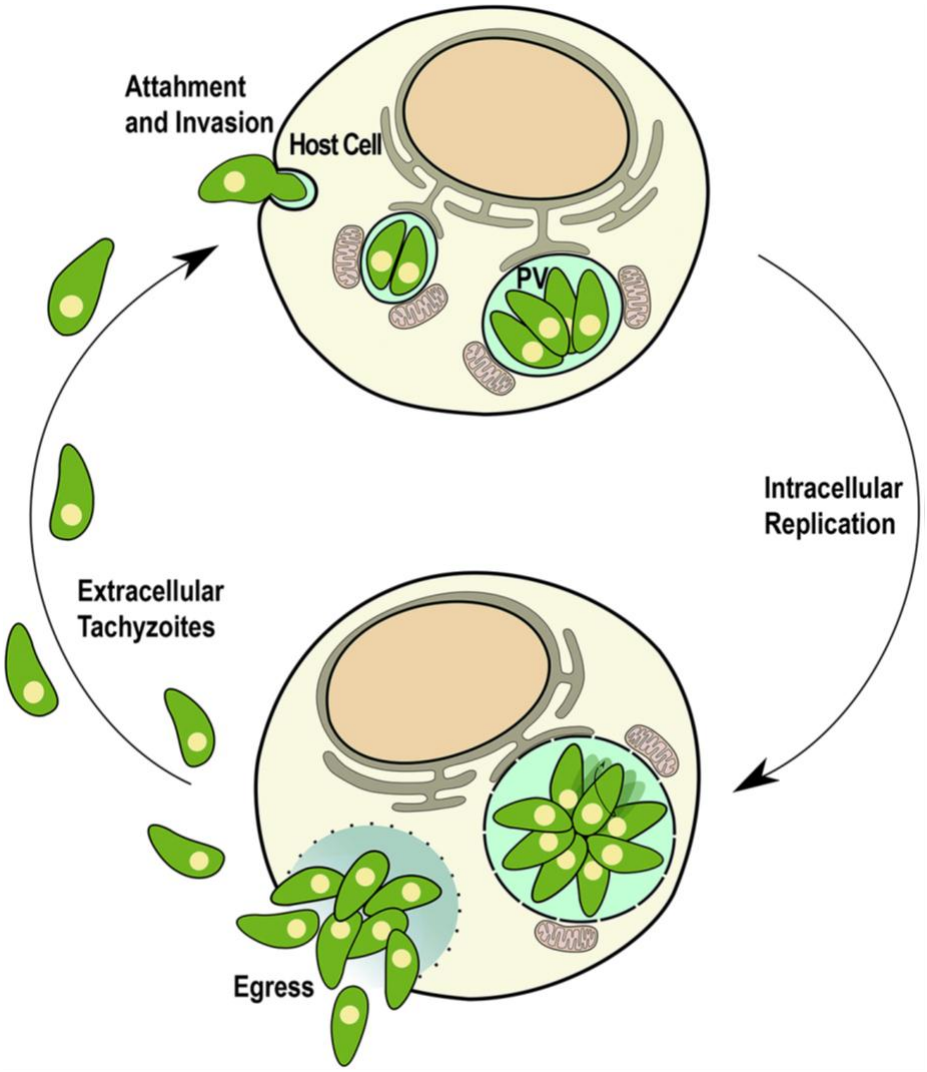

Figure 1.5. Lytic cycle of *T. gondii* tachyzoites

The lytic cycle of *T. gondii* tachyzoite proliferation begins with the attachment and invasion of a target host cell. The intracellular *T. gondii* parasites undergoes synchronous replication via endodyogeny and doubles in number exponentially until the infected host cell ruptures. The tachyzoites then egress from the PV as the host cell ruptures and completes the lytic cycle. The egressed parasites actively seek out and invades adjacent cells, repeating the lytic cycle (Adapted from Hortua Triana *et al*., 2018).

1.4 Diagnosis of toxoplasmosis

1.4.1 Serological tests

The gold standard for *Toxoplasma* diagnosis is the Sabin-Feldman dye test (SFDT) or also known as the methylene blue dye (MBD) test (Sabin and Feldman, 1948, Uttah *et al*., 2013). It is a serological test and involves methylene blue staining of live *T. gondii* parasites to determine the presence of anti-*Toxoplasma* antibodies in a patient's serum. A positive anti-*Toxoplasma* antibody test serum saturates the parasite surface antigen, which prevents methylene blue dye uptake (Ozgonul and Besirli, 2017, Udonsom *et al*., 2010, Villard *et al*., 2016) . MBD test is highly reliable and accurate, however it requires availability and routine maintenance of viable *T. gondii* parasites in a diagnostic facility (Ozgonul and Besirli, 2017).

1.4.2 Enzyme-linked immunosorbent assay (ELISA)

Another highly utilized diagnosis for toxoplasmosis is ELISA, widely utilized to diagnose *Toxoplasma* infection in both humans and livestock. The ELISA detects the presence of specific IgG, IgM or IgA antibodies against *T. gondii* in test serums (Ozgonul and Besirli, 2017, Villard *et al*., 2016). In this technique, *T. gondii* antigens are immobilized on the surface of microwells, which binds antibodies present in the test serum samples. A positive anti-*Toxoplasma* antibody test serum allows binding of a horseradish peroxidase (HRP) or alkaline phosphatase (AP) conjugated secondary antibody, which catalyzes chromogenic enzyme reaction detectable using a spectrophotometer (Hammouda *et al*., 2006, Liu *et al*., 2015). ELISA is the preferred diagnostic approach used in epidemiological studies as it is rapid and the test kits are highly reliable and commercially available (Glor *et al*., 2013, Liu *et al*., 2015).

1.4.3 Biological tests

Another approach to the diagnosis for toxoplasmosis involves the use of immunohistological staining of biopsy samples or examining the presence of *T. gondii* in isolated tissue samples and bodily fluids (Hill *et al*., 2005, Montoya and Remington, 2008). Extracellular *T. gondii* parasites are usually scarce in bodily fluids and tissues due to immunological suppression which renders isolation for histological examination challenging (Uttah *et al*., 2013). However, this approach is predominantly suitable for diagnosing toxoplasmosis in immunocompromised individuals, which lacks production of antibodies used for conventional serological diagnosis (Villard *et al*., 2016).

1.4.4 Molecular diagnosis (polymerase chain reaction)

Polymerase chain reaction (PCR) diagnosis of toxoplasmosis utilizes a set of *T. gondii* specific primers to selectively amplify parasite genetic sequences. PCR based *Toxoplasma* diagnosis and detection was first developed in 1984, and the *Toxoplasma* B1 gene was targeted for amplification as this gene was found to be conserved specifically in all strains of *Toxoplasma* parasite (Remington *et al*., 2004). Diagnosis of toxoplasmosis using PCR has been extensively applied in prenatal screening using amniotic fluid, as well as in suspected patients using bodily fluids such as blood, urine, cerebrospinal fluid (CSF) and ocular samples (Basavaraju, 2016, Remington *et al*., 2004).

1.5 Treatment of toxoplasmosis

Several chemotherapeutic drugs are used to treat symptomatic toxoplasmosis or to prevent clinical manifestation. The most effective and established therapy for the treatment of toxoplasmosis is the synergistic combination of pyrimethamine and sulfadiazine, which impairs folic acid biosynthesis and metabolism in the parasites (Dunay *et al*., 2018, Montoya and Remington, 2008). Pyrimethamine works by inhibiting the enzymes dihydrofolate reductase (DFHR) in the folic-folinic acid cycle while sulfonamides inhibit dihydropteroate synthetase (DHPS) of the p-aminobenzoic acid (PABA) pathway (Alday and Doggett, 2017). Symptomatic toxoplasmosis may require combination therapy of pyrimethamine, sulfadiazine and folinic acid with minimum of two to a maximum of six weeks (Ben-Harari *et al*., 2017).

Although this treatment is effective towards the tachyzoites (acute phase), it is accompanied by many adverse effects and is not effective towards encysted bradyzoites (chronic phase), allowing possibility of recurrence after treatment (Dunay *et al*., 2018, Montazeri *et al*., 2017, Montoya and Liesenfeld, 2004). This treatment regimen is usually supplemented with folinic acid to reduce the risk of bone marrow suppression (Remington *et al*., 2004). Unfortunately, these drugs have other potential side effects such as thrombocytopenia, neutropenia, leucopenia and hypersensitivity reactions (Dunay *et al*., 2018, Montazeri *et al*., 2017).

Other alternative anti-*Toxoplasma* drugs that are commonly used include atovaquone, spiramycin, clindamycin, or diaminodiphenylsulphone (Hill and Dubey, 2002). Side effects of these drugs have been reported, particularly spiramycin which is a teratogen and cannot be used to circumvent prenatal toxoplasmosis (Montoya and Remington, 2008). Since these drugs possess side effects and are ineffective against tissue cysts, there has been a continuous need to develop new anti-*Toxoplasma* drugs (Alday and Doggett, 2017, Montazeri *et al*., 2018).

1.6 Peptidyl methyl ketones

Peptidyl halomethyl ketones are synthetic protease inhibitors specifically designed to elucidate enzyme function and reaction mechanisms of serine and cysteine proteases (Liow and Chow, 2013, Rajah and Chow, 2015). Both peptidyl chloromethylketone (CMK) and peptidyl fluoromethylketone (FMK) are widely used as pharmacological and biochemical tools, where the peptidyl moiety serves as the affinity group complementary to the S1 and S2 sites of the enzyme. The halomethyl ketone moiety functions as the reactive entity and forms irreversible thiomethyl ketone with the cysteine or serine residue at the active site and subsequently inactivates the enzyme (Lawrence *et al*., 2006, Powers *et al*., 2002). Peptidyl CMKs are strong alkylating agents and possess numerous side effects besides blocking serine or cysteine proteases. Peptidyl FMKs on the other hand are poorer alkylating agents and therefore reduce significantly the non-specific alkylating effects. One of the first peptidyl FMK synthesized was z-FA-FMK, which was designed to irreversibly block human cathepsin B (Rasnick, 1985). However, it possesses immunosuppressive effects and blocks T-cell proliferation (Lawrence *et al*., 2006) through oxidative stress (Rajah and Chow, 2015).

Proteases or proteolytic enzymes can be generally classified into 7 major groups based on their catalytic residue: Aspartic, Cysteine, Glutamic, Serine, Threonine, Metallo and Asparagine (Dou and Carruthers, 2011, Powers *et al*., 2002, Grzonka *et al*., 2001). The peptidyl fluoromethylketone z-FA-FMK inhibits cathepsin B, a lysosomal cysteine protease of the papain family involved in protein catabolism hydrolyzing peptide bonds in polypeptides (Dou and Carruthers, 2011, Rasnick, 1985). Cysteine peptidases also called thiol peptidases, are proteases that use a catalytic mechanism involving the nucleophilic thiol group of cysteine for hydrolysis (Dou and Carruthers, 2011, Turk *et al*., 2012). Cathepsin proteases are widely distributed in eukaryotic organisms which act classically as lysosomal hydrolases that digest endogenous and exogenous endocytosed polypeptides (Barrett and Kirschke, 1981). However, it is increasingly appreciated that cathepsins can also play more specialized roles in higher eukaryotic organisms including spermatogenesis, antigen

presentation, tumor invasion, degradation of matrix proteins and TNF-induced apoptosis (Dou and Carruthers, 2011).

Interestingly, similar to higher eukaryotes, protozoan parasites appear to use cathepsin endopeptidases for protein degradation and other specialized functions (Dou and Carruthers, 2011). Cysteine proteases are important for the growth, survival and pathogenesis of apicomplexan parasites that infect humans (Siqueira-Neto *et al*., 2018, Turk *et al*., 2012, Zhao *et al*., 2013). The apicomplexan *T. gondii* expresses five members of the papain-like cysteine proteases, including one cathepsin L-like (*Tg*CPL), one cathepsin B-like (*Tg*CPB) and three cathepsin C-like (*Tg*CPC1, 2 and 3) proteases (Siqueira-Neto *et al*., 2018). Recent genetic, biochemical and structural studies revealed that these cathepsin-like proteases play an important function in microneme and rhoptry protein maturation, host cell invasion, replication and nutrient acquisition (Dou and Carruthers, 2011). Inhibition of *Tg*CPB with antisense RNA was reported to reduce infection in a chick embryo model of toxoplasmosis (Que *et al*., 2004). *Tg*CPL knockout strains and cathepsin L inhibitor treatment blocked autophagy in cysts and reduce their survival (Di Cristina *et al*., 2017). The inhibition of *Tg*CPC1 and *Tg*CPC2 by peptidyl inhibitor, Gly-Phe-dimethylketone reduced intracellular parasite growth and proliferation (Que *et al*., 2007). Since these cathepsin-like cysteine proteases appears to play important roles in *T. gondii* proliferation and infection processes, this makes them potential anti-*Toxoplasma* drug targets.

1.7 Stress response in *T. gondii* parasites

The *T. gondii* parasite possessing high virulence and a broad range of compatible host, reflects the plasticity of the parasite to infect and converting the host nutrients and resources to support its intracellular growth (Tymoshenko *et al*., 2015). As an obligate intracellular parasite, *T. gondii* needs an intracellular environment rich with nutrients and shielded from the host immune response to survive and multiply (Blader and Saeij, 2009, Blume and Seeber, 2018, Clough and Frickel, 2017, Jeffers *et al*., 2018). However, extracellular *T. gondii* parasites are exposed to various forms of stress during acute infection, such as heat shock (fever), oxidative stress and inflammatory cytokines (immune response) (Lyons *et al*., 2002). In addition, host deprived extracellular tachyzoites are deprived of the protection and nutrient provided by the host cell and may only remain viable for a limited duration (Vonlaufen *et al*., 2008, Weiss and Kim, 2000). Hence, the parasites must adapt and cope with these stresses to ensure successful infection and persistence within the host. The differentiation of *T. gondii* between distinct stages, i.e. sporozoites, tachyzoites and bradyzoites is essential for the parasite's survival and transmission between hosts (Ferreira da Silva Mda *et al*., 2008, Hill and Dubey, 2018). Studies over the years have documented that exogenous stress factors, such as alkaline pH, IFN-γ, drugs, heat shock, and nutrient deprivation increases bradyzoite development *in vitro* (Gross *et al*., 1996, Soete *et al*., 1994, Tomavo and Boothroyd, 1995, Weiss *et al*., 1995, Yahiaoui *et al*., 1999). Hence, *T. gondii* differentiation is widely recognized as a stress-related response towards hostile environmental conditions (Vonlaufen *et al*., 2008, Weiss and Kim, 2000).

Translational repression in *T. gondii* parasites towards stress has been reported and it is associated with the elevation of phosphorylated *Toxoplasma* eukaryotic initiation factor-2 (*Tg*IF2α) (Ghosh *et al*., 2012). This stress response pathway involves the phosphorylation of the alpha subunit of the *Tg*IF2α by stress-activated *Tg*IF2α kinases (*Tg*IF2Ks). Phosphorylated *Tg*IF2α represses protein translation, but only allowing translation of a subset of mRNAs associated with stress responsive factors (Narasimhan *et al*., 2008, Sullivan and Jeffers, 2012). Interestingly, elevated *Tg*IF2α phosphorylation was reported during *T. gondii*

differentiation into bradyzoites. This suggests that the translation control is involved in the modulation of gene expression to facilitate *T. gondii* stage conversion (Narasimhan *et al*., 2008, Sullivan and Jeffers, 2012). Furthermore, bradyzoites in the quiescent state were found to have higher levels of phosphorylated *Tg*IF2α compared to actively proliferating tachyzoites (Narasimhan *et al*., 2008). The translational repression mediated via *Tg*IF2α decreases protein synthesis in the parasite while promoting translation of a subset of mRNAs for the expression of genes associated with stress coping mechanisms and stage of differentiation (Gebauer and Hentze, 2004, Jeffers *et al*., 2018, Nguyen *et al*., 2017b). Further understanding on the mechanism of stress mediated response in driving *T. gondii* stage conversion may reveal new approaches to tackle chronic toxoplasmosis (Bohne *et al*., 1999).

1.7.1 Oxidative stress in *T. gondii* parasites

Oxygen plays a critical role in all major metabolic processes in aerobic organisms where it serves as the terminal electron acceptor in the oxidative phosphorylation pathway to drive adenosine triphosphate (ATP) production (Gorlach *et al*., 2015). The incomplete or partial reduction of oxygen leads to generation of Reactive Oxygen Species (ROS) intracellularly as by product of normal cellular aerobic metabolism (Birben *et al*., 2012, Gorlach *et al*., 2015, Rahal *et al*., 2014, Turrens, 2004). Exogenous derived ROS on the other hand are exposed to cells directly possibly originating from environmental insults (Martindale and Holbrook, 2002). To protect against ROS-mediated damages, aerobic organisms are capable of producing enzymes such as catalase, glutathione peroxidase, and superoxide dismutase, which scavenges ROS (Liguori *et al*., 2018, Ozougwu, 2016, Rahal *et al*., 2014, Simon *et al*., 2000). Oxidative stress occurs when there is an imbalance between pro-oxidant and antioxidants which results in excessive levels of ROS (Poljsak *et al*., 2013, Rahal *et al*., 2014). Excessive ROS levels directly causes oxidative damage to vital cellular macromolecules such as DNA, membrane proteins and lipids which could lead to cellular dysfunction (Andreyev *et al*., 2005, Martindale and Holbrook, 2002, Slesak *et al*., 2016, Trachootham *et al*., 2008).

Being an aerobic protozoan parasite, *T. gondii* derives its energy mainly from a single tubular mitochondrion, the main site of cellular respiration and oxidative phosphorylation which drives cellular function (Turrens, 2004). Despite *T. gondii* being adapted to living within the host cell, they are sensitive and continuously challenged by the redox balance within the parasite (Liguori *et al*., 2018, Peng *et al*., 2003, Xue *et al*., 2017). Additionally, the host cell also exerts oxidative stress towards the intracellular parasites due to the cell's higher metabolism and substrate turnover in the cytosol and the mitochondria (Andreyev *et al*., 2005, Bosch *et al*., 2015, Gorlach *et al*., 2015). Therefore, ROS could directly cause harm to the parasite or indirectly via disruption of the redox balance of the infected host cell (Bosch *et al*., 2015, Jones and Go, 2010, Pino *et al*., 2007). Therefore, antioxidants are crucial in providing protection against cellular damage caused by ROS in both *T. gondii* and its host cell.

T. gondii have been shown to have an extensive network of antioxidants which includes glutathione/glutathione disulphide, peroxiredoxins, superoxide dismutase and thioredoxins which play a critical role in regulating the redox levels and to counter ROS mediated damages (Bosch *et al*., 2015, Jones and Go, 2010, Odberg-Ferragut *et al*., 2000, Xue *et al*., 2017). In the early phases of parasitic infection, host macrophages and natural killer cells which serves as the first line of immunological defense, utilize oxidative stress to counter infections (Cabral and DaMatta, 2017, Denkers *et al*., 2003, Mammari *et al*., 2019). Interestingly, *T. gondii* has been shown to differentiate from tachyzoite to bradyzoite form in response to the oxidative stress induced by the immune system (Bohne *et al*., 1999, Bosch *et al*., 2015). Remarkably, many of the current anti-parasitic drugs, such as anti-malarials (chloroquine) and anti-trypanosomal agents (nifurimox and beta-lapachone) are pro-oxidants which induces oxidative stress to counteract parasitic protozoan infections (Alday and Doggett, 2017, Montazeri *et al*., 2018, Pal and Bandyopadhyay, 2012). These accumulating evidences show that parasitic protozoans in general are sensitive and vulnerable to oxidative stress. Hence, investigation of the susceptibility and stress response mechanism of parasitic protozoans toward oxidative stress can certainly provide new insights for novel anti-parasitic

drug targets and formulation of therapeutic strategies by disrupting vital redox reactions and to induce oxidative stress.

1.7.2 Nutrient requirements and starvation in *T. gondii*

T. gondii is an auxotroph which is not capable of synthesizing specific type of nutrients *de novo* and thus must rely on scavenging them from the host cell. These essential nutrients include small molecules such as glucose, arginine, iron, tryptophan, and purine nucleosides (Zhu *et al*., 2019, McGovern *et al*., 2018, Tymoshenko *et al*., 2015). The parasite may acquire these nutrients via diffusion across the PVM and transportation into the parasite via carrier proteins or active membrane transport (Blader and Saeij, 2009, Fox *et al*., 2004). Intracellular *T. gondii* parasites redirects host derived cholesterol into the PV by manipulating and redirecting the host's endosomal transport system (Charron and Sibley, 2002, Coppens *et al*., 2013, Laliberte and Carruthers, 2008). The parasite primarily utilizes glucose for glycolysis or mitochondrial oxidative phosphorylation as energy sources. However, bradyzoites have amylopectin reserves, which is not found in tachyzoites. In this case, amylopectin serves as an energy reserve for encysted bradyzoites during differentiation back into tachyzoite form (Coppens *et al*., 2013). No apicomplexan parasites including *T. gondii* are able to replicate or survive for extended durations in axenic media in the absence of host (Blume and Seeber, 2018, Clough and Frickel, 2017, Hill and Dubey, 2018). This indicates that *T. gondii* parasites are heavily dependent on host to obtain sustenance for survival. The deprivation of the essential amino acid arginine alone was reported to efficiently trigger differentiation of replicative tachyzoites into bradyzoites (Blume and Seeber, 2018, Fox *et al*., 2004). Additionally, nutrient deprivation in *T. gondii* parasites is also reported to lead to *Tg*IF2α phosphorylation, which is stress response mechanism which leads to translational repression (Joyce *et al*., 2011, Narasimhan *et al*., 2008, Nguyen *et al*., 2017b). These findings collectively demonstrate that nutrient starvation is a potent stress factor and inducer of differentiation in *T. gondii* parasites.

T. gondii was reported to possess several cathepsin-like cysteine proteases that are involved in nutrient acquisition and other specialized roles which are important for the growth and survival of apicomplexan parasites (Dou and Carruthers, 2011). The *Toxoplasma* lysosomal vacuolar compartment (VAC) is an acidified organelle that bears resemblance to a plant-like vacuole (Dou and Carruthers, 2011, Miranda *et al*., 2010, Parussini *et al*., 2010). Studies have reported VAC contains two cathepsins, termed *Tg*CPL and *Tg*CPB as mentioned earlier (Dou *et al*., 2013, Miranda *et al*., 2010, Parussini *et al*., 2010) and these proteases are closely associated with lysosomes where protein degradation occurs. This implies that the VAC functions as the terminal compartment of the parasite endolysosomal system (Dou and Carruthers, 2011, Parussini *et al*., 2010). The VAC cathepsins have been reported to possess proteolytic functions which are vital for parasite survival and persistence both *in vitro* and *in vivo*. The disruption of VAC cathepsins has been shown to result in accumulation of parasitic material and organelle remnants which led to the demise of the parasites (Di Cristina *et al*., 2017). The digestion and breakdown of cellular components in the VAC is suggested to be associated with autophagy, which may play an important role in *T. gondii* survival (Di Cristina *et al*., 2017).

1.7.3 Autophagy

The ability to sense nutrient deprivation and respond to starvation is important for cell survival. The most notable features in response to starvation are the induction of both translational repression and autophagy (Ghosh *et al*., 2012). Autophagy is a key catabolic process of targeted degradation of dysfunctional or expendable proteins, cellular organelles and cytoplasm components in eukaryotic cells (Inoue and Klionsky, 2010, Mizushima, 2007, Siqueira-Neto *et al*., 2018). Autophagy is a cytoprotective response towards physiological stresses such as nutrient starvation, oxidative stress, and accumulation of unfolded proteins (Weidberg *et al*., 2011, Yorimitsu and Klionsky, 2005). As depicted in Figure 1.6, the process of autophagy is characterized by the *de novo* formation of the isolation membrane, which comprise of double membranes. The isolation membrane will envelop both cytoplasm and organelle components into an enclosed autophagosome that acts as a containment site for autophagic degradation. The subsequent fusion of the autophagosome with hydrolytic compartments such as lysosomes would lead to specific and contained degradation of the captured cellular components (Ghosh *et al*., 2012, Nguyen *et al*., 2017b, Weidberg *et al*., 2011). The degradation of material within the autophagosome would regenerate building blocks to ensure cellular survival during nutrient limitation (Weidberg *et al*., 2011).

The molecular machinery of autophagy was shown to have a high level of genetic conservation from yeast to higher eukaryotes where 31 of autophagy-related genes (ATG) and their proteins in yeast are largely conserved across mammals (Duszenko *et al*., 2011, Herman *et al*., 2006, Klionsky *et al*., 2011, Yorimitsu and Klionsky, 2005). Although intracellular parasites like *T. gondii* established itself within an intracellular host cell environment which is nutrient rich, they do encode autophagy genes (Ghosh *et al*., 2012). Bioinformatic studies have revealed the presence of homologues of many but not all of the yeast ATG genes across several parasitic protozoa including *T. gondii* (Duszenko *et al*., 2011, Herman *et al*., 2006, Klionsky *et al*., 2011). In line with this, studies have reported presence of autophagosome-like structures in *T. gondii* parasite when subjected to nutrient limiting conditions *in vitro*, but how and when the parasite encounters such conditions *in vivo* remains

unclear (Besteiro *et al*., 2011a, Ghosh *et al*., 2012). Despite the fact that *T. gondii* parasites do not possess lysosomes, autophagosome-like bodies are still formed thus implying that *T. gondii* parasites may not share the exact autophagic pathway as eukaryotes (Duszenko *et al*., 2011, Nguyen *et al*., 2017b, Subauste, 2019). Studies have reported that the knockout or inhibition of the cysteine protease cathepsin L resulted in accumulation of autophagic material in the bradyzoite VAC. This suggest that the VAC functions as part of the parasite endolysosomal system, and associate with autophagosomes in the degradation of autophagic material during chronic infection (Kannan *et al*., 2019, Siqueira-Neto *et al*., 2018). Some studies have also suggested that *T. gondii* could modulate autophagic pathways in the infected host cell and take advantage of the host autophagy to increase nutrient availability to enhance its proliferation (Halonen, 2009, Subauste, 2019, Wang *et al*., 2009). Autophagy in *T. gondii* parasites appears to be activated by stress and may play a critical role in overcoming nutrient limitation via bulk protein turnover to enhance parasite survival during chronic infection (Di Cristina *et al*., 2017, Ghosh *et al*., 2012, Nguyen *et al*., 2017b).

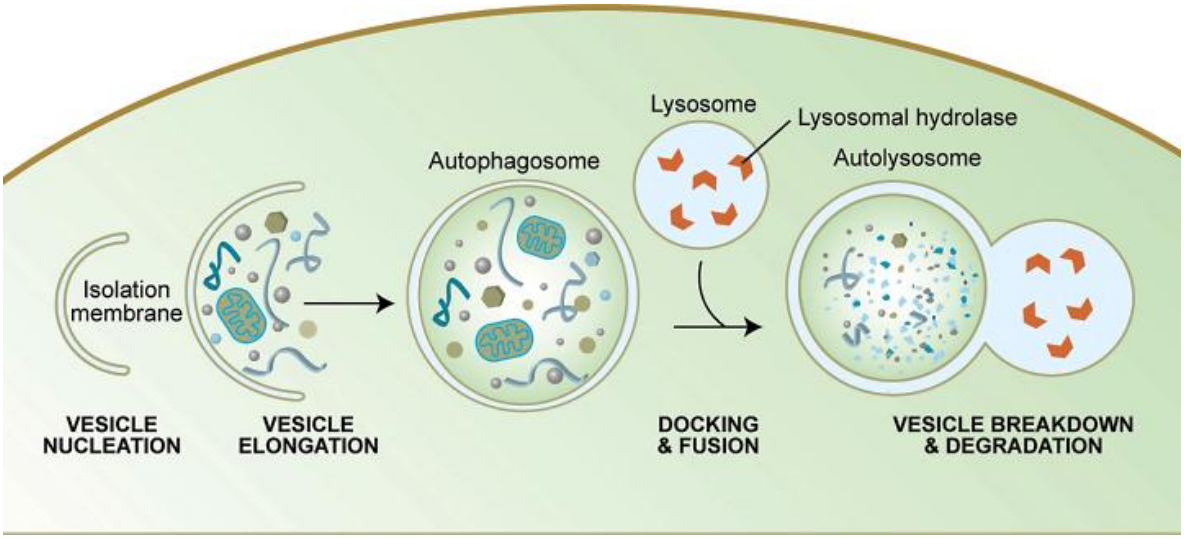

Figure 1.6. Schematic depiction of the mechanism of autophagy

Autophagy begins with the *de novo* formation of the phagophore or isolation membrane. The phagophore vesicle elongates and envelops the targeted cytoplasm and organellar components to form the autophagosome (vesicle elongation). The autophagosome subsequently fuses a lysosome (docking and fusion) to form the autophagolysosome. In the autophagolysosome, the engulfed material is degraded and recycled by the cell (vesicle breakdown and degradation) (Adapted from Meléndez, A. and Levine, B. 2009).

1.8 Aims and objectives

T. gondii is a highly virulent parasite that can infect all nucleated cells of homeothermic animals including humans. *T. gondii* infection is highly prevalent, infecting almost one-third of the global human population (Tu *et al*., 2018). *T. gondii* is the causative agent of toxoplasmosis and it can lead to devastating congenital complications and life-threatening diseases. *T. gondii* is capable of establishing lifelong chronic infection under immunological pressure by differentiating into encysted bradyzoites which remain dormant as tissue cysts. However, tissue cysts are able to reactivate back into a tachyzoite form under favorable conditions, most notably in individuals with a compromised immune system (Bharti *et al*., 2016, Ozgonul and Besirli, 2017, Sutterland *et al*., 2015). The dynamic and adaptive differentiation of *T. gondii* from tachyzoites into bradyzoites in response to various stresses during the chronic phase of toxoplasmosis is unclear. Despite the growing attention in understanding the chronic phase of toxoplasmosis and cysts formation, not much is known about the mechanism of differentiation from tachyzoites into bradyzoites. The interconversion between these two stages of *T. gondii* plays a critical role in establishing chronic infection and disease reactivation. Therefore, understanding the mechanism and triggers of cyst formation is the key to minimizing parasite transmission and managing chronic infection (Sullivan and Jeffers, 2012). The inability of current anti-*Toxoplasma* drugs to eliminate cysts further highlights the importance in elucidating the underlying mechanisms of this parasite differentiation. Understanding the underlying mechanisms of this process could provide valuable insight into bradyzoite biology as well as identifying targets for the treatment of chronic toxoplasmosis and its symptomatic diseases. To this end, our findings indicate that the cathepsin B inhibitor, z-FA-FMK, which induces oxidative stress in T-cells (Rajah and Chow, 2015) is able to inhibit the proliferation of *T. gondii* and induced a cyst-like morphological change in the parasite. Therefore, we sought to characterize the altered morphology of the parasites and to identify the possible mechanisms that underlie the differentiation of *T. gondii*.

CHAPTER TWO

MATERIALS AND METHODS

2.1 MATERIALS

2.1.1 Reagents

Table 1. 1 List of reagents

Reagents	Supplier
3-Methyladenine (3-MA)	Sigma-Aldrich, USA
Ammonium oxalate	Sigma-Aldrich, USA
Bovine serum albumin (BSA)	Merck, Germany
Bradford reagent	Bio-Rad, USA
Buthionine sulfoximine (BSO)	Sigma-Aldrich, USA
CHAPS	Sigma-Aldrich, USA
Chloroquine (CQ)	Sigma-Aldrich, USA
Crystal violet	Sigma-Aldrich, USA
DAPI	Sigma-Aldrich, USA
DBA-FITC	Vector Laboratories, USA
Dichlorofluorescin diacetate (DCFH-DA)	Sigma-Aldrich, USA
Dihydroethidium (DHE)	Molecular Probes, UK
Dimethyl sulfoxide	Sigma-Aldrich, USA
Dithiothreitol	Sigma-Aldrich, USA
Dulbecco's modified eagle's medium (DMEM) high glucose	Gibco, USA
Ethanol	J. Kollin, UK
Fetal bovine serum	Gibco, USA
HEPES	Gibco, USA
L-Glutamine	Sigma-Aldrich, USA
Magic red	ImmunoChemistry Technologies, USA
Monochlorobimane (MCB)	Sigma-Aldrich, USA
MTS	Promega, USA

Paraformaldehyde (PFA)	Sigma-Aldrich, USA
Penicillin/Streptomycin	Gibco, USA
Phosphate buffered saline (PBS)	Calbiochem, USA
Phenazine methosulfate (PMS)	Sigma, Ukraine
ProLong® Gold antifade mountant	Thermo Fisher Scientific, USA
Radio-Immunoprecipitation Assay (RIPA) cell lysis buffer	Thermo Fisher Scientific, USA
Sucrose	Sigma-Aldrich, USA
Trypan blue	Sigma-Aldrich, USA
Trypsin 0.25% in 1mM EDTA	Gibco, USA
z-FA-DMK	Bachem, switzerland
z-FA-FMK	Bachem, switzerland
z-RR-AMC	Bachem, switzerland

2.1.2 Materials

Table 1. 2 List of materials and equipment

Equipment and consumables	Supplier
27-gauge needles	Terumo, Japan
96-well plates	Orange Scientific, Belgium
Automatic pipettor	Finnpipette, Finland
Camera	Nikon Digital Sight (DS-U2), Japan
Cell scraper	SPL life sciences, Korea
Centrifuge	Thermo Fisher Scientific, USA
Centrifuge tubes (15ml)	Orange Scientific, Belgium
Centrifuge tubes (50ml)	Becton Dickinson, USA
Cryovial	Corning, USA
Eppendorf tubes (0.5 and 1.0ml)	Axygen, USA
FACSCalibur flow cytometer	Becton Dickinson, USA
Falcon tube	Becton Dickinson, USA
Fluorescent microscope	Olympus (Model BX51), Japan
Gloves	IRONskin, UK
Hemacytometer and cover slips	Hirschmann Laborgerate, Germany
Humidified cell culture incubator	RS Biotech (Galaxy S), UK
Inverted microscope	Nikon Eclipse TS100, Japan
Lamina flow hood	ESCO Lab Culture Class II Type A2, Singapore
Microtitre plate reader	BIO-TEK M200, USA
Pipette tips	Axygen Scientific, USA
Pipettes (0.5-10µl)	Eppendorf, USA
Pipettes (100-1000µl)	Eppendorf, USA
Pipettes (10-100µl)	Eppendorf, USA
Polycarbonate membrane filter	Whatman, UK
Syringe	Terumo, Japan
Water bath	Stuart, USA

2.2 Cell culture techniques

2.2.1 Culture of human foreskin fibroblast (Hs68) cells

The human neonatal foreskin fibroblast cell line (Hs68) was obtained from ATCC (CRL-1446). Handling of all cell culture procedures were performed in Class II biosafety cabinets. Hs68 cells were maintained in Dulbecco's modified eagle's medium (DMEM) high glucose, supplemented with 10% (v/v) fetal bovine serum (FBS), 2mM L-glutamine and antibiotics (penicillin-100 units/ml and streptomycin-100 μg/ml). The Hs68 cells were cultured in 75cm^2 cell culture flask in a humidified incubator at 37°C with 5% CO_2 in air. The culture medium was replaced every 48h until the Hs68 cells reached confluence. For subculture of Hs68 cells, confluent cells were rinsed with phosphate buffer saline (PBS) before incubating with 0.25% trypsin in 1mM EDTA (2ml) at 37°C for 2min to detach the cells from the culture flask. Once the cells were confirmed detached by observing under the inverted microscope, 10ml of DMEM was added to the cells to inactivate the trypsin. The detached cells in suspension were then subcultured into four 75cm^3 culture flasks.

2.2.2 Cryopreservation and revival of Hs68 cells

Detached Hs68 cells in DMEM were centrifuged at 1200rpm for 10min at 4°C. Following centrifugation, the cell pellet was suspended with 1ml of pre-cooled freezing medium consisting of 95% (v/v) DMEM medium and 5% (v/v) dimethyl sulfoxide (DMSO). The Hs68 cells in freezing medium were transferred to pre-cooled cryovials and stored in a -80°C freezer. After 24h, the frozen vials were transferred and stored in liquid nitrogen for long-term cryopreservation. Revival of cryopreserved Hs68 cells was performed by thawing a frozen vial of cells in 37°C water bath. The thawed cell suspension was transferred to 10ml DMEM media pre-warmed to 37°C and centrifuged at 1200rpm for 10min. The cell pellet was resuspended with 15ml of 37°C pre-warmed DMEM media and transferred into a 75cm^3 tissue culture flasks before incubation in a humidified incubator at 37°C with 5% CO_2 in air.

2.2.3 Continuous *in vitro* culture of *T. gondii* (RH and ME49 strain)

2.2.3.1 Infection of Hs68 cells with *T. gondii* tachyzoites

Hs68 cells were used as host cells for the continuous culture of RH and ME49 strains of *T. gondii*. All the experimental procedures involving *T. gondii* tachyzoites (RH and ME49 strain) were performed in Class II biosafety cabinets. Once the Hs68 cells reach confluence, the media was replaced with infection media (complete DMEM with 1% (v/v) FBS) and simultaneously inoculated with 4×10^6 tachyzoites (RH or ME49 strain). Subsequently, the tachyzoites were allowed to infect the Hs68 cells for 24h and unattached parasites were removed by rinsing the host cells with 10ml pre-warmed infection medium.

2.2.3.2 Harvesting of *T. gondii* from infected Hs68 cells

After 48h post-infection, most of the Hs68 monolayer would lyse, releasing tachyzoites into the culture supernatant. Any intact Hs68 cells harboring tachyzoites were scraped using a cell scraper. Next, both the host cells and tachyzoites in suspension were passed through a 27-gauge needle in order to completely lyse the host cells. This will facilitate the release of every remaining intracellular tachyzoites into the culture medium. The lysed cell suspension containing parasites was centrifuged at 1000g for 15min and the pellet was resuspended in 5ml DMEM media before filtering through a 3μm polycarbonate membrane filter. Cell debris were removed during filtration while the tachyzoites pass through the filter. Finally, the filtered parasite suspension was centrifuged again at 400g for 15min before resuspension in 5ml of infection media. The number of freshly harvested tachyzoites was counted using trypan blue exclusion assay for subsequent experiments, serial passaging or cryopreservation.

2.2.3.3 Cryopreservation of *T. gondii* tachyzoites

Freshly harvested and purified extracellular tachyzoites were centrifuged at 400g for 10min. Following centrifugation, the parasite pellet was resuspended with 1ml of pre-cooled freezing medium consisting of 85% (v/v) FBS and 15% (v/v) DMSO. The tachyzoites in freezing medium were transferred to pre-cooled cryovials and stored in a -80°C freezer for 24h before transferred to liquid nitrogen for long-term cryopreservation.

Revival of cryopreserved tachyzoites was carried out by thawing a frozen vial in a 37°C water bath. The entire thawed parasite suspension was added to confluent Hs68 cells in a culture flask with 10ml of 37°C pre-warmed infection media. The cells inoculated with the parasites were incubated in a humidified incubator at 37°C with 5% CO_2 in air. After 24h post infection, any unattached parasites were removed by rinsing off the Hs68 cells with 10ml of pre-warmed infection medium.

2.2.4 Determination of cell and *T. gondii* density

Trypan blue exclusion assay was used to quantify the density of viable cells present in the cell suspension. Trypan blue is a vital dye that permeates and selectively stains dead cells with compromised membrane integrity (Strober, 2001, Tran *et al*., 2011). Viable cells are able to exclude the entry of trypan blue and thus appear to be translucent and unstained, whereas dead cells will be stained blue. Trypan blue exclusion was therefore used to determine both viability and density of cells and *T. gondii* parasites in suspension.

- For Hs68 cells, 10µl of the Hs68 cell suspension was added with 10µl of 0.4 % (w/v) trypan blue dye (1:2 dilution factor).
- For *T. gondii* parasites, 0.5µl of the parasite suspension was added with 19.5µl of trypan blue dye (1:40 dilution factor).

The cell/parasite suspension with added trypan blue was incubated at room temperature for 1min. Following incubation, 10µl of stained cell/parasite suspension was pipetted onto a haemocytometer and the viability of Hs68 cells and tachyzoites were scored using an inverted microscope at 100× and 200× magnification respectively.

The Hs68 cell and tachyzoite density in number of cells/ml or tachyzoites/ml was calculated using the formula as described below:

$$\textbf{Number of cells / tachyzoites per ml} = N/4 \times DF \times 10^4$$

N = The total number of counted viable cells / parasite across all four quadrants
DF = The dilution factor of cell / parasite suspension added with trypan blue
10^4 = Volume correction factor

2.3 Treatments of tachyzoites

Freshly isolated *T. gondii* tachyzoites from Hs68 cells were treated with various concentrations of benzyloxycarbonyl-phenylalanine-alanine-fluoromethylketone (z-FA-FMK) or benzyloxycarbonyl-phenylalanine-alanine-diazomethylketone (z-FA-DMK) where indicated. z-FA-FMK and z-FA-DMK were dissolved sterile DMSO to obtain stock solution of 50mM. The different concentrations of z-FA-FMK and z-FA-DMK were prepared by diluting the peptidyl FMK with infection media accordingly. To study the role of oxidative stress, tachyzoites were treated with buthionine sulfoximine (BSO) at concentrations where indicated with or without the presence of z-FA-FMK. The final concentration of the carrier solvent (DMSO) in each treatment never exceeded 0.2% (v/v). Chloroquine (CQ), and 3-methyladenine (3-MA) were prepared using sterile deionized water (dH_2O). All tachyzoites were treated at a density of 4×10^6/well in a final volume of 1ml in a humidified incubator at 37°C in 5% atmospheric CO_2. As shown in Figure 2.1., the tachyzoites were allowed to invade the host cells for 24h to establish infection before treatment with various compounds begin where indicated. The treatment duration ranged from 72h or 96h depending on the assay parameters.

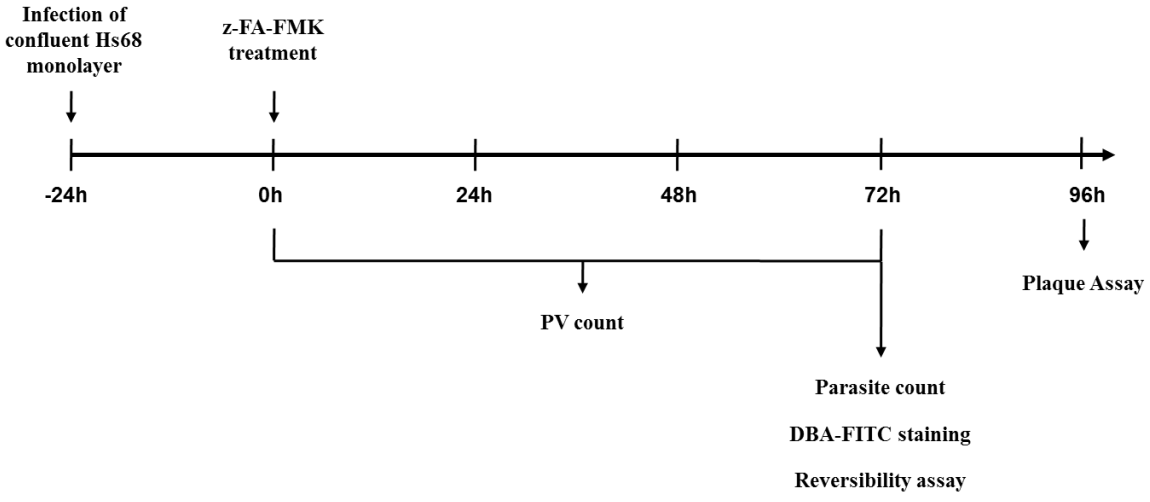

Figure 2.1. *T. gondii* treatment and experimental timeline

2.4 Biochemistry and cell biology assays

2.4.1 MTS cell viability assay

The MTS assay is a colorimetric quantification of cell viability in mammalian cells. It utilizes MTS [3-(4,5-dimethylthiazol-2-yl)-5-(3-carboxymethoxyphenyl)-2-(4-sulfophenyl)-2H-tetrazolium], a tetrazolium salt which is bioreduced into a soluble formazan product by the mitochondrial dehydrogenase enzymes in metabolically active cells (Johnson *et al*., 2000). The bioreduction of MTS requires the presence of PMS (Phenazine methosulphate) as an electron carrier (Hua *et al*., 2019). The absorbance of the formazan formed can be determined at 490nm, and the amount is directly proportional to the number of living cells. After treatments where indicated, 20µl of freshly prepared MTS/PMS solution at (5:1 v/v) were added to the cell culture (100µl media) in the wells of a 96-well plate.

The plate was incubated at 37°C in an incubator with 5% CO_2 in air for 2h before reading the absorbance at 490nm using a Tecan 200 ELISA plate reader. All samples were assayed in triplicate. The absorbance of the supernatant in treated cells was compared to control cells and the percentage of viability was calculated as follows:

$$\text{Percentage of viability } (\%) = \frac{\text{Adjusted absorbance of treated cells}}{\text{Adjusted absorbance of control cells}}\ x\ 100\%$$

(Adjustment of absorbance was done by subtracting the blank absorbance)

2.4.2 Monitoring infectivity of *T. gondii* tachyzoites via parasitophorous vacuole (PV) formation

The lytic proliferation cycle of *T. gondii* tachyzoites involves active invasion and subsequent PV formation in the infected host cell. The number of PVs formed thus correlates directly to the ability of the parasite to infect cells or proliferate and complete the lytic cycle. By monitoring the number of PVs formed, the infectivity and progression of the lytic cycle of the parasites in a monolayer cell can be studied *in vitro*. Hs68 cells were grown to confluence in 24-well plate before inoculated with *T. gondii* tachyzoites for 24h before treatment as described in Section 2.3. Optimized number of tachyzoites were inoculated to the confluent Hs68 cells so that a complete destruction of the monolayer was achieved at the end of the experiment timeline. The infected cultures with treatments were examined every 24h using an inverted microscope with a 40× objective. The number of PV formed directly correlates with the ability of *T. gondii* tachyzoites to infect cells, PVs were scored in 10 randomized microscopic field across the infected Hs68 cells.

2.4.3 Assessment of *T. gondii* tachyzoite proliferation using trypan blue exclusion assay

Trypan blue is a vital dye that selectively stains dead cells with compromised membrane integrity (Strober, 2001, Tran *et al*., 2011). This allows the determination of total viable tachyzoite count following treatment, which correlates to the proliferation of the parasite culture. Confluent Hs68 cells grown in 24-well plate were inoculated with *T. gondii* tachyzoites for 24h before treatment as described in Section 2.3. After 72h treatment, the remaining intact Hs68 cells in the 24-well plate were detached using a cell scraper. The cell and tachyzoite suspension were passed through a 27-gauge needle to release any remaining intracellular tachyzoites into the suspension. The number of viable *T. gondii* parasites in the suspension across all treatment groups was examined using the trypan blue exclusion assay as described in Section 2.2.4. The dilution of the parasite suspension with trypan blue was adjusted accordingly based on the number of tachyzoites present.

2.4.4 Assessment of intracellular *T. gondii* tachyzoites lytic growth using plaque assay

The plaque assay serves as a reliable assessment of *T. gondii* virulence which relies on successful lytic proliferation cycle which requires parasite invasion, replication, egress and subsequent invasion (Ufermann *et al*., 2017, Vinayak *et al*., 2014). Repeated *T. gondii* tachyzoite lytic cycles result in lysis of host cells and leads to formation of visible plaques on monolayer of cells. Confluent Hs68 cells grown in 24-well plates were inoculated with tachyzoites for 24h before treatment as described above (Section 2.3). Following 96h treatment with various compounds where indicated, the monolayer cells were rinsed with PBS twice before fixing using ice-cold absolute ethanol for 5min. The monolayer cells were then stained with crystal violet solution (2.5% crystal violet, 30% ethanol, 1% ammonium oxalate) for 1min. The cells were rinsed with PBS to remove excess crystal violet stain. Intact cells will be stained with crystal violet dye while lysed cells (plaque) appear as empty and unstained regions. The plaques formed were examined and captured across randomized microscopic fields using an inverted microscope under 200× magnification. The measurement of plaque area formed was performed using NIS Elements Basic Research Microscope Imaging Software (Nikon).

2.4.5 Detecting intracellular *T. gondii* cyst using *Dolichos biflorus* agglutinin (DBA) lectin

Confluent Hs68 cells grown in 8-well chamber slides were inoculated with *T. gondii* tachyzoites for 24h prior to treatment where indicated. The formation of cyst wall was determined by detecting a characteristic modification in the cyst membrane component (*N-acetyl*-D-galactosamine) which selectively binds to DBA-lectin (Buchholz *et al*., 2013). Following treatment for 72h, the cells were rinsed with PBS for 10min and subsequently fixed and permeabilised using ice-cold methanol for 5min. The fixed cells were washed with ice-cold PBS for 10min before incubating with DBA-lectin conjugated with fluorescein isothiocyanate (FITC) at the concentration of 20µg/ml in PBS with 3% bovine serum albumin (BSA) for 2h in the dark. Following incubation, the cells were washed with PBS and stained with DAPI before mounted with ProLong® Gold antifade mountant. After mounting with coverslips, the slides were allowed to cure for 24h at 4°C in the dark prior to fluorescence microscopic examination under 60× objectives using Olympus fluorescence microscope (Model BX51).

2.4.6 Assessment of z-FA-FMK withdrawal on *T. gondii* propensity to proliferate in Hs68 cells

As shown in Figure 2.2, confluent Hs68 cells grown in 24-well plate were inoculated with *T. gondii* tachyzoites for 24h before treatment as described earlier (Section 2.3). Following treatments for 72h where indicated, the medium was replaced with 1ml fresh pre-warmed infection medium without z-FA-FMK. Following the withdrawal of z-FA-FMK, the number of PVs were determined across 10 randomized microscopic field in the infected Hs68 cells at the time points where indicated. After 6 days (144h), the monolayer cells were scraped and lysed, and the number of viable tachyzoites determined using trypan blue exclusion assay. At this stage, control treated cultures start to show plaques indicating the destruction of the Hs68 cells.

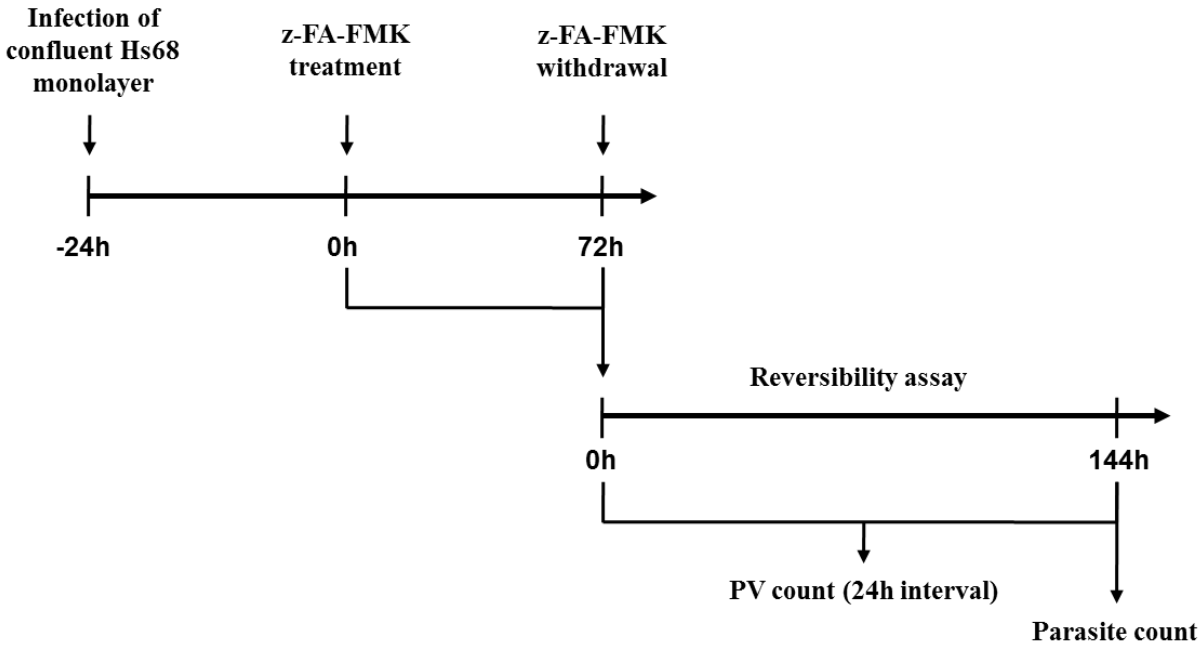

Figure 2.2. Treatment timeline to assess effect of z-FA-FMK withdrawal on the virulence of *T. gondii*

2.4.7 Measurement of intracellular glutathione (GSH) levels using monochlorobimane (MCB)

Monochlorobimane (MCB) is a cell permeable non-fluorescent probe which specifically forms a highly blue fluorogenic adduct when bound to GSH (Kamencic *et al*., 2000). MCB is widely used to measure intracellular GSH levels in both mammalian cells and parasites (Al-Adhami *et al*., 2006, Kathuria *et al*., 2014, Palit *et al*., 2012, Williams *et al*., 2014). Following treatments where indicated, Hs68 cells or *T. gondii* parasites were washed with 100µl of PBS before resuspension in 100µl of MCB (100µM) in PBS. The fluorescence intensity was measured following incubation at 37°C for 30min in the dark, using excitation wavelength of 390nm and emission wavelength of 460nm in a Tecan 200 ELISA plate reader. Complete media with MCB was used as background fluorescence control.

2.4.8 Measurement of intracellular reactive oxygen species (ROS) production in Hs68 cells

2.4.8.1 Intracellular ROS (superoxide) measurement using dihydroethidium (DHE)

The production and intracellular accumulation of superoxide ROS in treated both Hs68 cells and extracellular tachyzoites was detected using DHE probe. DHE is a redox sensitive fluorogenic probe that reacts with superoxides to form 2-hydroxyethidium, which subsequently intercalates with nuclear DNA to emit red fluorescence (Kim *et al*., 2016, Owusu-Ansah *et al*., 2008). Following treatments where indicated, Hs68 cells were trypsinized and transferred to a 5ml tube and centrifuged down at 1000rpm for 10min. The cell pellet was washed with PBS before incubated with 10µM DHE in 500µl serum-free DMEM medium at 37°C in the dark for 30min. For the parasites, treated extracellular tachyzoites were processed the same way as Hs68 cells. Following DHE staining, Hs68 cells or extracellular tachyzoites were washed twice using ice-cold PBS and resuspended in 500µl PBS prior to flow cytometry analysis (FACSCalibur, Becton Dickinson). The fluorescence intensity of DHE was monitored using FL-2 channel (excitation wavelength at 519nm and emission wavelength at 605nm).

2.4.8.2 Intracellular ROS (peroxyl and hydroxyl radicals) measurement using dichloro-fluorescein diacetate (DCFH-DA)

Dichloro-fluorescein diacetate (DCFH-DA) is a cell permeable peroxyl and hydroxyl radical specific probe which is trapped intracellularly following deacetylation by cellular esterases to form DCFH. Intracellular peroxyl and hydroxyl radicals reacts with DCFH to produce the highly fluorescent form 2,7-dichlorofluorescein (DCF) (Aranda *et al*., 2013, Baranwal *et al*., 2014). Accumulation of intracellular peroxyl and hydroxyl radicals in Hs68 cells and extracellular tachyzoites were assessed using flow cytometry analysis. Following treatments where indicated, Hs68 cells were trypsinized and transferred to a 5ml tube and centrifuged down at 1000rpm for 10min. The cell pellet was washed with PBS before incubating with 10µM DCFH-DA in 500µl serum-free DMEM medium at 37°C in the dark for 30min. For parasites, the treated extracellular tachyzoites were transferred to a 5ml tube and centrifuged down at 3000rpm for 10min. The tachyzoite pellet was processed the same procedure as Hs68 cells. Following DCFH-DA staining, Hs68 cells or extracellular tachyzoites were washed twice using ice-cold PBS and resuspended in 500µl PBS prior to flow cytometry analysis (FACSCalibur, Becton Dickinson). The fluorescence intensity of DCFH-DA was monitored using FL-1 channel (excitation wavelength at 488nm and emission wavelength at 525nm).

2.4.9 Preparation of cell lysates and determination of protein concentration

2.4.9.1 Extraction of cell lysates

After treatments where indicated, Hs68 cells were harvested by trypsinization and centrifuged at 1500rpm for 15 min at 4°C. Extracellular tachyzoites were centrifuged at 1000g for 15min at 4°C. The cells or tachyzoites were washed with 1× PBS before resuspended in 25µl Radio-Immunoprecipitation Assay (RIPA) cell lysis buffer and subjected to 3× freeze-thaw cycle using liquid nitrogen to obtain the cell lysates. The cell lysates were stored at -20°C freezer until use. The protein concentrations of the cell lysates were determined using Bradford protein assay and normalized prior to subsequent experiments.

2.4.9.2 Protein quantification using Bradford protein assay

The Bradford protein assay was used to determine the concentration of protein in the cell lysates. The assay utilizes Coomasie Brilliant Blue G-250 dye that converts into a blue unprotonated form in the presence of proteins (Grintzalis *et al*., 2015). The intensity of Coomasie Brilliant Blue which correlates and is proportional to the amount of protein could be quantitatively measured at 595nm. A series of protein standards were prepared using serial dilutions of bovine serum albumin (BSA) (2mg/ml). Cell lysates that were extracted as described earlier (Section 2.4.9.1) were diluted (1:20) with dH_2O prior to Bradford protein assay. Aliquots of 5µl each of protein standards and diluted lysate samples were transferred to a 96-well microtiter plate with 250µl of Bradford reagent. The mixture was incubated at room temperature for 30min in dark, before measuring the absorbance at 595nm using a Tecan 200 ELISA plate reader. A standard curve was constructed from the protein standards and the cell lysate protein concentration was calculated.

2.4.10 Measurement of cathepsin B activity

2.4.10.1 Measurement of cathepsin B activity in lysates using fluorogenic substrate z-RR-AMC

Cathepsin B activity in Hs68 cells or tachyzoite lysates was measured by detecting the cleavage of the fluorogenic substrate z-RR-AMC. The cathepsin B specific substrate contains the fluorescent leaving group, AMC which is released upon cleavage of the P1 and P2 sites (Que *et al*., 2002). The cathepsin B activity in Hs68 cell or tachyzoite lysates was assayed using 30µg protein in a final concentration of 100µM substrate in 1mM HEPES buffer containing 10% sucrose, 0.1% CHAPS, 2% DMSO and 10mM dithiothreitol (DTT) in a final volume of 100µl. The fluorescence signal was measured following incubation at 37°C for 30min using a Tecan 200 ELISA plate reader at excitation and emission wavelength of 370nm and 440nm respectively.

2.4.10.2 Measurement of cathepsin B activity in live cells using Magic Red cathepsin B assay

Magic Red is a cell permeable cathepsin B specific probe that emits red fluorescence upon enzymatic cleavage by cathepsin B at one or both arginine (R) amide linkage sites on the cresyl violet fluorophore conjugated to Magic Red. The Magic Red fluorogenic substrate penetrates across internal cellular organelles such as lysosomes, thus allowing detection of cathepsin B activity in live cells (Kratschmer and Levy, 2018). Magic Red substrate was used to detect cathepsin B activity according to the manufacturer's protocol. Following treatment where indicated, Hs68 cells or extracellular tachyzoites were incubated with Magic Red diluted in 1ml final volume of prewarmed DMEM culture media. The cells or parasites were incubated with the Magic Red staining solution in the dark at 37°C for 60min. Following that, the staining solution was aspirated and the cells or tachyzoites were washed twice with PBS. The fluorescence signal was measured using a Tecan 200 ELISA plate reader at excitation and emission wavelength of 592nm and 628nm respectively. Cathepsin B activity in live cells or tachyzoites was also visualized using a Olympus fluorescence microscope (Model BX51).

2.5 Statistical analysis

The results obtained were analyzed using the GraphPad Prism Software. Results shown were the mean value ± standard error of the mean (SEM) from three independent experiments. Comparisons between two independent groups were analyzed using Student's t-test. Statistical difference between multiple independent groups were analyzed using one-way analysis of variance (ANOVA) followed by *post hoc* comparison using Tukey's test. The statistical *p*-value less than 0.05 were considered as statistically significant.

CHAPTER THREE

The cathepsin B inhibitor, z-FA-FMK inhibits proliferation of *T. gondii* parasites and induces parasite cyst formation

3.1 Introduction

Toxoplasma gondii is a unicellular parasitic protozoan with worldwide distribution and *T. gondii* infection leads to the development of a disease called toxoplasmosis (Hill and Dubey, 2002). Toxoplasmosis can lead to devastating congenital complications, neonatal mortality and various life-threatening diseases in both humans and homeothermic animals alike (Bharti *et al*., 2016, Sutterland *et al*., 2015). Acute toxoplasmosis is usually self-limiting and lack of clinical symptoms as the parasites are usually suppressed by the host immune response (Gross *et al*., 1996, Hill *et al*., 2005, Lyons *et al*., 2002). Toxoplasmosis can progress into chronic stage when tachyzoites differentiates into encysted bradyzoites, which remains dormant and harmless under immunological surveillance (Lyons *et al*., 2002). However, once the individual immune system is weakened due to AIDS, cancer chemotherapy or undergoing immunosuppressive therapy following organ transplant, latent infection reactivates through the differentiation of encysted bradyzoites into tachyzoites which leads to the manifestation of clinical complications (Bharti *et al*., 2016, Sutterland *et al*., 2015).

Pathogen persistence and latency are conserved strategies that are advantageous to various pathogens to increase their chances of successful transmissions. The ability of *Toxoplasma* to form latent cysts is an evolutionary trade-off to enhance parasite persistence and transmission (Sullivan and Jeffers, 2012). The interconversion between tachyzoites and bradyzoites plays a critical role in toxoplasmosis pathogenesis via establishing a chronic infection and enabling disease reactivation (Lyons *et al*., 2002). Additionally, the ability of *T. gondii* to differentiate into encysted bradyzoites prevents their eradication by both immune system and current anti-*Toxoplasma* drugs such as pyrimethamine and sulfadiazine (Montoya and Liesenfeld, 2004, Sullivan and Jeffers, 2012). Despite the growing scientific interest and studies on the chronic toxoplasmosis and cyst biology, not much is known about the mechanism of *T. gondii* differentiation (Watts *et al*., 2015).

In recent years, various stress conditions have been used to trigger tachyzoite differentiation into tissue cysts *in vitro* and this has contributed significantly to the understanding of *T.*

gondii cyst biology (Dzierszinski *et al*., 2004, Singh *et al*., 2002). These approaches to induce *T. gondii* differentiation can be classified into different stress factors such as alkaline medium, interferon gamma (IFN-γ), heat shock, chemicals or drugs and nutrient depletion (Ferreira da Silva Mda *et al*., 2008). One of the simplest and most widely used approaches to induce *T. gondii* cyst formation *in vitro* involves growing the parasites in alkaline medium (Lyons *et al*., 2002, Soete *et al*., 1993). However, alkaline medium stress treatment does not represent a physiological stress condition *in vivo* (Ferreira da Silva Mda *et al*., 2008). On the other hand, formation of bradyzoite cysts via stresses such as heat shock and pro-inflammatory cytokines are more physiological, attributed to fever and various factors in the host immune response respectively *in vivo* (Sullivan *et al*., 2009).

T. gondii are auxotrophic obligatory intracellular parasites, which makes them very sensitive to axenic conditions, deprivation of essential nutrients and growth factors (Black and Boothroyd, 2000, Blader and Koshy, 2014). The highly virulent tachyzoite form has a higher nutritional demand than the slow replicating bradyzoite form. It has also been reported that deprivation of the amino acid arginine inhibits parasite replication and triggers formation of cyst *in vitro* (Fox *et al*., 2004). Other than that, disrupting pyrimidine *de novo* biosynthesis which is essential for producing the building blocks for nucleic acid synthesis appears to induce bradyzoite differentiation in *T. gondii* tachyzoites (Fox and Bzik, 2002). Tachyzoites exposed to axenic conditions briefly have increased tendency to form cyst and exhibit signs of bradyzoite differentiation when they establish infection later on (Yahiaoui *et al*., 1999).

A characteristic hallmark during the differentiation from tachyzoites to bradyzoites is the formation of the cyst wall (Sullivan and Jeffers, 2012). The cyst wall consists of the glycoprotein CST1, which protects the bradyzoites physically and also from the immune system, allowing the bradyzoites to enter a dormant state and establish chronic infection (Tomita *et al*., 2013, Zhang *et al*., 2001). The glycoprotein CST1 consists of N-acetyl-galactosamine and was shown to localize exclusively to cyst wall *in vivo* and *in vitro* (Tomita *et al*., 2013). The highly glycosylated structure of the cyst wall allows it to be readily stained

and identified with *Dolichos biflorus* lectin (DBA) which specifically binds to N-acetyl-galactosamine (Buchholz *et al*., 2013, Tomita *et al*., 2013).

Recent studies have suggested that parasitic cysteine proteases may be potential chemotherapeutic intervention targets across various protozoan pathogens such as *Plasmodium spp.*, *T. brucei*, *T. cruzi* and *T. gondii* (Engel *et al*., 1998, Rosenthal *et al*., 1993, Scory *et al*., 1999, Shaw *et al*., 2002). These pathogens appear to utilize cysteine proteases for similar functions such as establishing infection, virulence and growth (Siqueira-Neto *et al*., 2018). The *T. gondii* cathepsin B cysteine protease has been shown to play a vital role during parasite invasion and proliferation (Chaparro *et al*., 2018, Que *et al*., 2004). One of the earliest cathepsin-B inhibitors synthesized is z-FA-FMK, with amino acids phenylalanine and alanine on the P1 and P2 position respectively (Lawrence *et al*., 2006, Powers *et al*., 2002). This cathepsin B inhibitor is a synthetic peptide inhibitor that irreversibly alkylates the cysteine residue at the cathepsin B active site, thereby irreversibly blocking its proteolytic activity (Ahmed *et al*., 1992, Bang *et al*., 2004, Schotte *et al*., 2001). The main objective in this chapter was to examine the potential anti-proliferative effects of the cathepsin B inhibitor, z-FA-FMK on *T. gondii* tachyzoites (RH and ME49 strains) *in vitro*. Secondly, to examine whether *T. gondii* treated with z-FA-FMK undergoes stage differentiation from tachyzoites into intracellular cysts.

3.2 Results

3.2.1 The cathepsin B inhibitor, z-FA-FMK is non-toxic in Hs68 cells and *T. gondii* tachyzoites

In order to examine the effect of z-FA-FMK on *T. gondii* proliferation, its potential toxic effect on Hs68 host cells and extracellular tachyzoites was first examined. Hs68 cells were treated with various concentrations of z-FA-FMK for different time points and the cell viability was determined using the MTS cell viability assay. As shown in Figure 3.1A, z-FA-FMK did not induce any toxicity in Hs68 cells with increasing concentrations up to 100µM. The viability of z-FA-FMK treated Hs68 cells remained high (>90%) even after 72h treatment. Similarly, z-FA-FMK at concentrations increasing up to 100µM was also non-toxic to extracellular tachyzoites of the RH strain and ME49 strain up to 6h as shown in Figure 3.1B and 3.1C respectively. The results indicate that z-FA-FMK possesses no adverse effects and is non-toxic to Hs68 cells and both RH and ME49 strains of *T. gondii* tachyzoites.

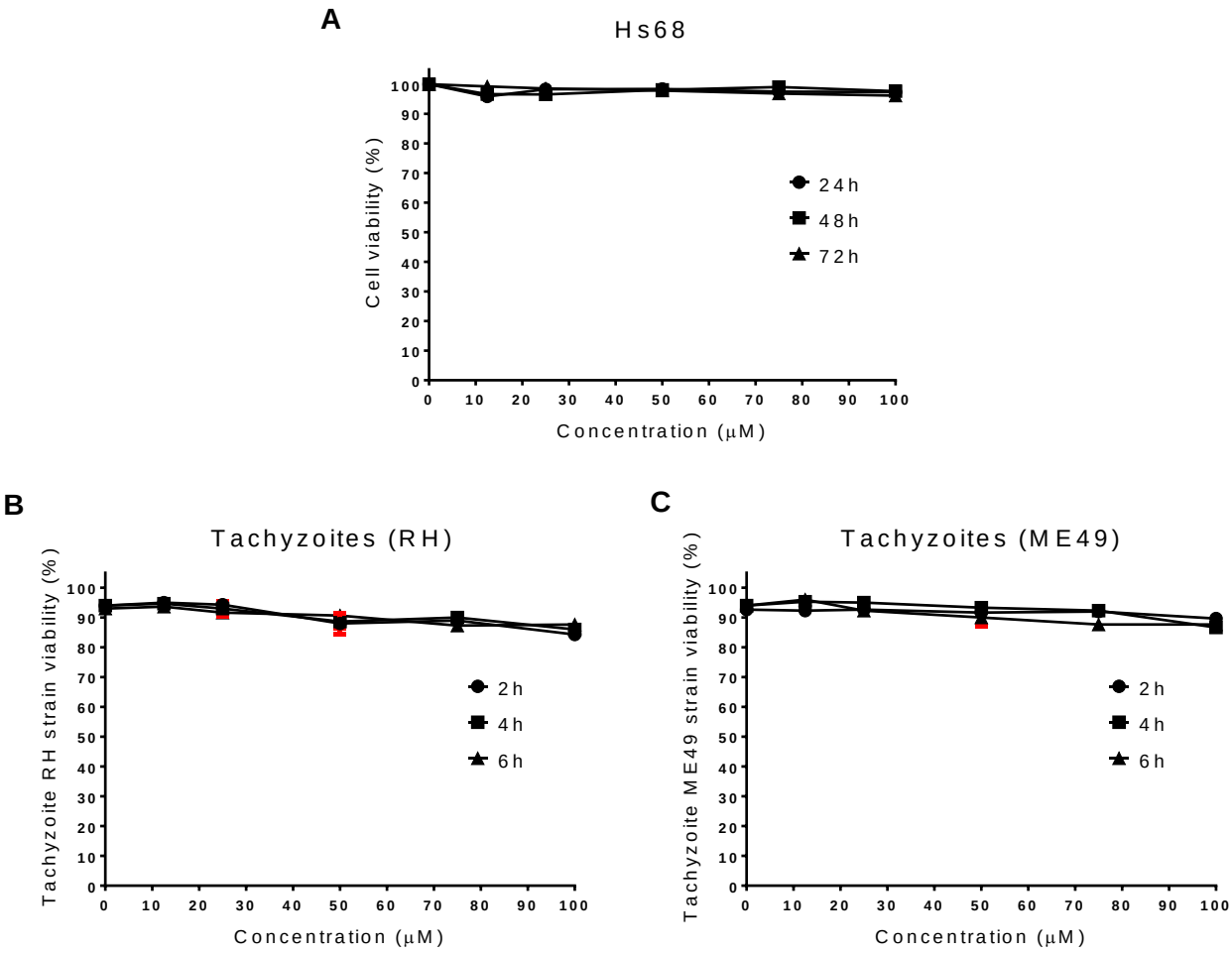

Figure 3.1. Effect of z-FA-FMK on Hs68 cell and tachyzoites (RH and ME49 strain) viability

Hs68 cells were treated with various concentrations of z-FA-FMK and the cell viability (**A**) was determined at different time points where indicated using the MTS assay as described in Materials and Methods. Extracellular *T. gondii* tachyzoites RH strain (**B**) and ME49 strain (**C**) were treated with various concentrations of z-FA-FMK and the number of viable tachyzoites was determined at different time points where indicated using the trypan blue exclusion method as described in Materials and Methods. The results represent the means ± SEM from three independent experiments.

3.2.2 z-FA-FMK reduces the invasion of extracellular *T. gondii* parasites (RH and ME49 strains) into Hs68 cells

Since z-FA-FMK is non-toxic to Hs68 cells and extracellular tachyzoites, the potential anti-proliferative effects of this peptidyl FMK on both Type-1 (RH) and Type-2 (ME49) strains were examined. To this end, confluent Hs68 monolayer cells were inoculated with tachyzoites from RH or ME49 *T. gondii* strains in the presence of z-FA-FMK. The formation of PVs following successful invasion into host cells was assessed after 24h post-infection. As shown in Figure 3.2A, z-FA-FMK significantly reduced the number of PV formed in a dose-dependent manner after 24h in the RH strain, indicating that z-FA-FMK readily blocks the invasion of tachyzoites into Hs68 host cells. On the other hand, z-FA-FMK was less effective with the ME49 strain and much higher concentration (≥75μM) was required to reduce significantly the number of PV formed in the host cells (Figure 3.2B). These results indicate that z-FA-FMK was able to reduce the infectivity of tachyzoites by preventing the invasion of tachyzoites into Hs68 host cells.

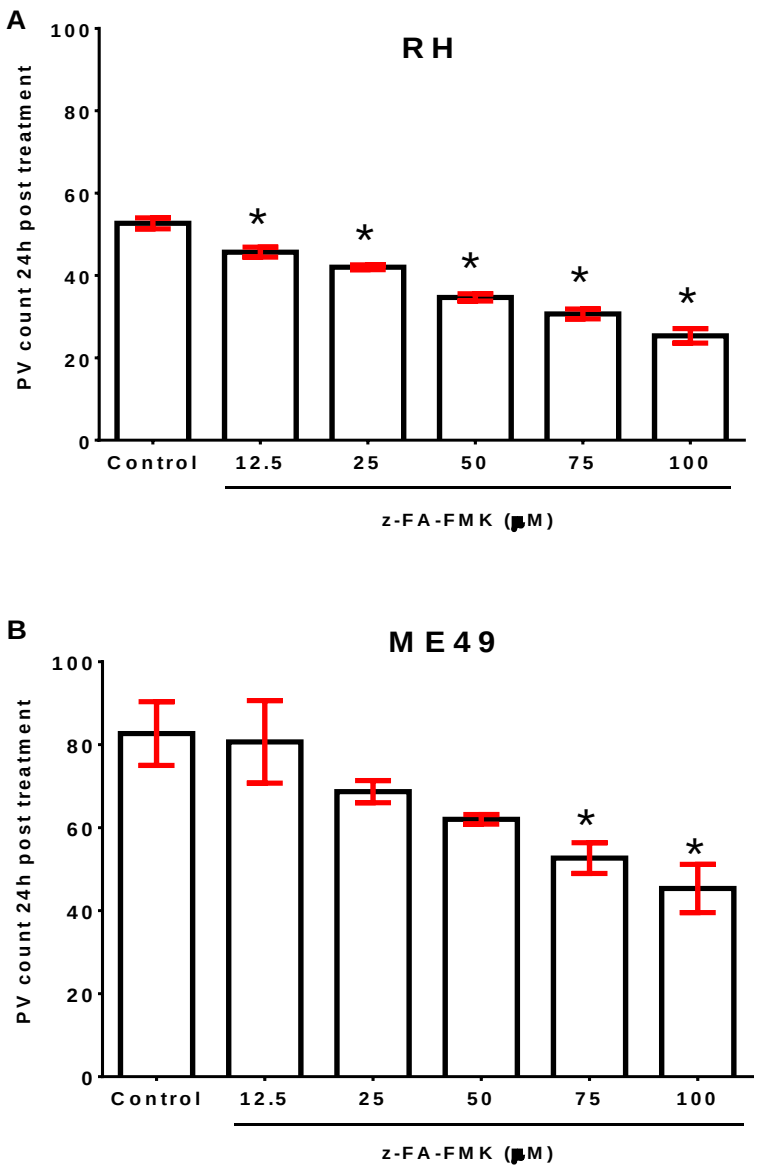

Figure 3.2. Effect of z-FA-FMK on extracellular *T. gondii* (RH and ME49 strain) tachyzoite infectivity

Number of PV formed in Hs68 cells by RH strain (**A**) and ME49 strain (**B**) tachyzoites following parasite inoculation in the presence of z-FA-FMK for 24h. The PVs formed were examined under 40× magnification and the number of PV was scored across 10 randomized microscopic field. The results represent the means ± SEM from three independent experiments, where * indicates $p < 0.05$ versus untreated control.

3.2.3 z-FA-FMK inhibits PV formation and reduces total parasite count in *T. gondii* infected Hs68 cells

The proliferation of *T. gondii* in Hs68 host cells consists of repeated lytic cycle involving host cell invasion, proliferation and rupture. Previous results (Figure 3.2) indicated that host cell invasion or infectivity was blocked by z-FA-FMK. However, it is not clear whether z-FA-FMK could block intracellular tachyzoite proliferation within the PVs. To examine whether z-FA-FMK inhibits intracellular tachyzoite proliferation, the intracellular replication (number of PV and total parasites) was determined. To this end, confluent Hs68 cells were pre-infected with RH or ME49 strain parasites for 24h before exposing the host cell containing with intracellular tachyzoites with various concentrations of z-FA-FMK for another 72h.

As shown in Figure 3.3A and 3.4A, z-FA-FMK effectively reduced the PV formation in Hs68 cells mediated by both strains of *T. gondii* (RH and ME49 strains respectively) in a dose- and time-dependent manner. On the other hand, untreated Hs68 cells infected with tachyzoites showed increase in PV over 72h as a result of normal progression of the parasite proliferation cycle. High concentrations of z-FA-FMK (100µM) almost completely inhibited PV formation mediated by *T. gondii* over 72h. The reduction in tachyzoite proliferation leads to less host cell rupture and subsequently less tachyzoites are available to invade new host cells. This correspond to the decrease in intracellular tachyzoite proliferation and the inability to complete the lytic cycle to establish new infections. Interestingly, z-FA-FMK (100µM) almost completely inhibited PV formation in RH strain while in the ME49 strain, a slight increase in PV was observed (Figure 3.4A). The results suggest that z-FA-FMK at 100µM was more effective in suppressing PV formation in the RH strain than the ME49 strain. In contrast, lower concentrations of z-FA-FMK on the other hand appear to have a greater inhibition of PV formation on the ME49 strain compared to the RH strain.

Since a single PV harbors varying number of tachyzoites, the anti-proliferative effects of z-FA-FMK was further determined by counting the number of viable parasites obtained from the Hs68 cells after 72h culture following treatment with z-FA-FMK. Consistent with the

reduction of PV, the presence of z-FA-FMK induced a dose-dependent decrease in *T. gondii* number compared to control. Our results indicate that all the concentrations of z-FA-FMK used significantly reduced tachyzoite proliferation in both RH strain (Figure 3.3B) and ME49 strain (Figure 3.4B). As observed earlier, the ME49 strain appears to be more susceptible to z-FA-FMK as indicated by a greater reduction in parasite number at lower concentrations of z-FA-FMK (12.5µM and 25µM). Collectively, the results suggest that z-FA-FMK dose-dependently inhibits *T. gondii* replication.

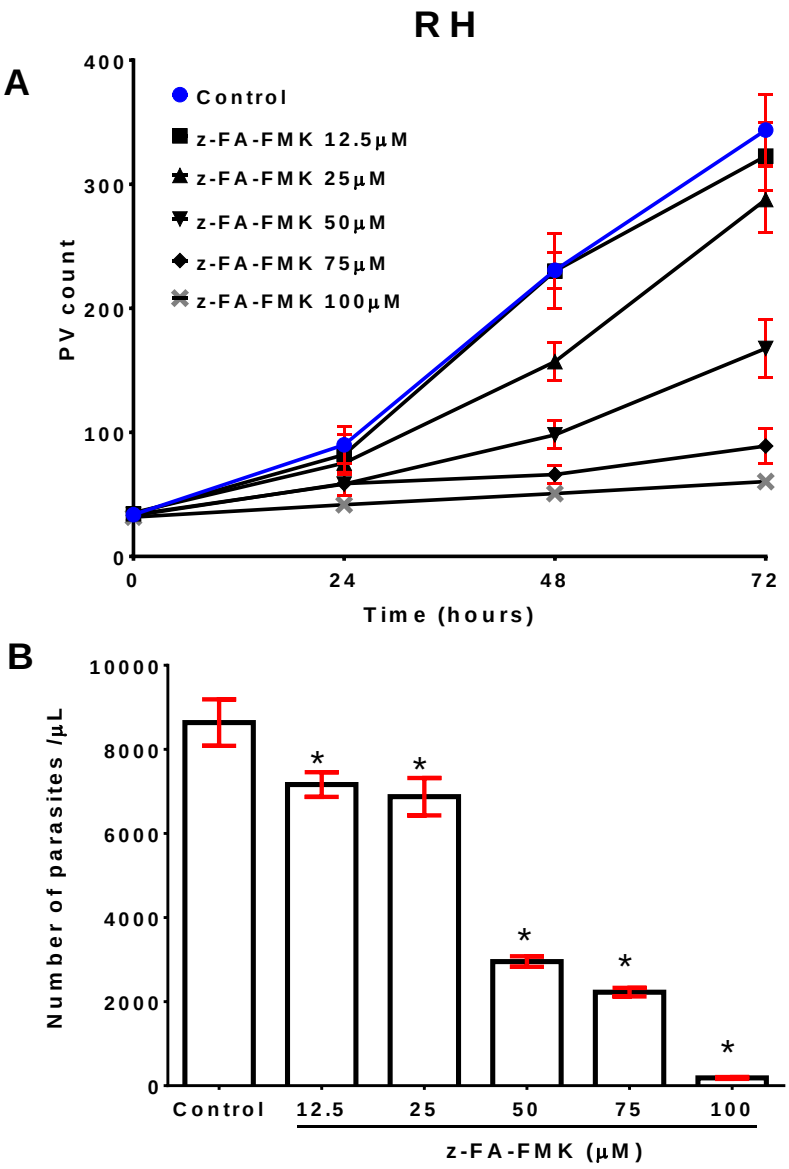

Figure 3.3. Effect of z-FA-FMK on *T. gondii* (RH) tachyzoite proliferation

Time dependent effect of z-FA-FMK on the number of PV (**A**) and total parasite count in Hs68 cells after 72h treatment (**B**). Following treatment, intracellular tachyzoites were examined under 40× magnification and the number of PVs formed were scored across 10 randomized microscopic field. The total number of viable tachyzoites was determined using the trypan blue exclusion method as described in Materials and Methods. The results represent the means ± SEM from three independent experiments, where * indicates $p < 0.05$ versus untreated control.

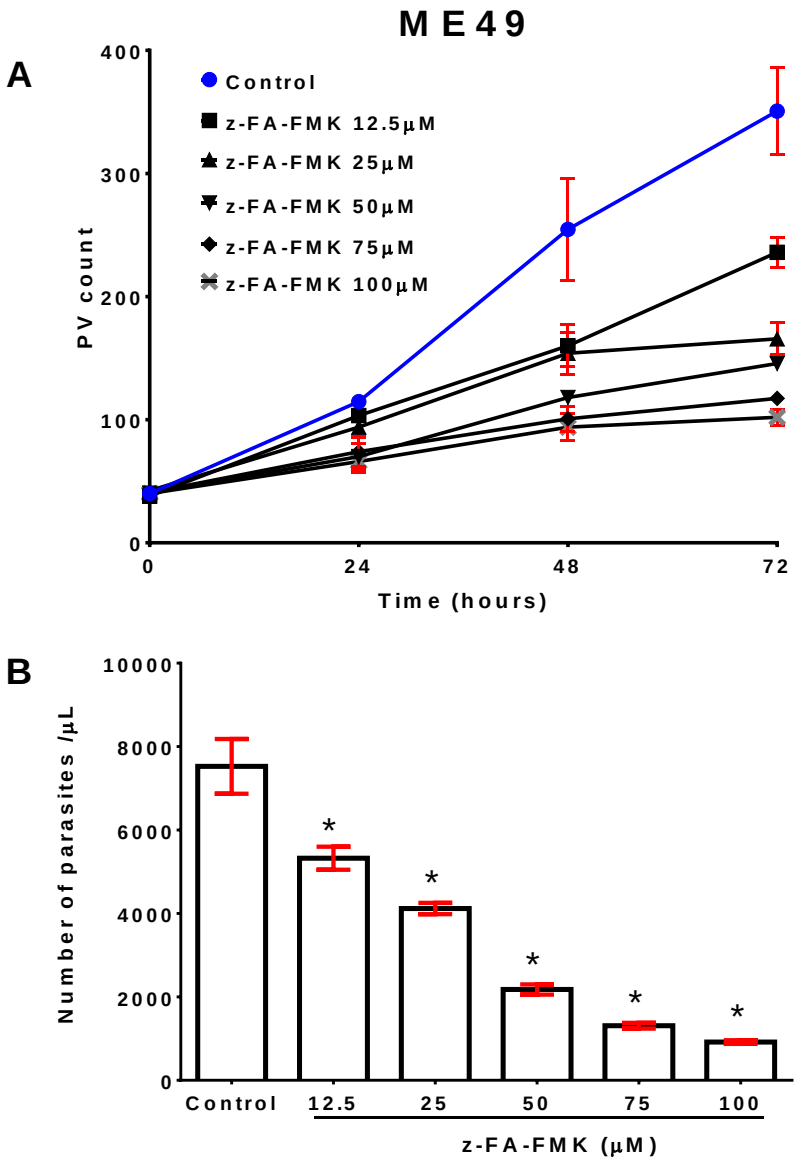

Figure 3.4. Effect of z-FA-FMK on *T. gondii* (ME49) tachyzoite proliferation

Time dependent effect of z-FA-FMK on the number of PV (**A**) and total parasite count in Hs68 cells after 72h treatment (**B**). Following treatment, intracellular tachyzoites were examined under 40× magnification and the number of PVs formed were scored across 10 randomized microscopic field. The total number of viable tachyzoites was determined using the trypan blue exclusion method as described in Materials and Methods. The results represent the means ± SEM from three independent experiments, where * indicates $p < 0.05$ versus untreated control.

3.2.4 z-FA-FMK inhibits plaque formation in Hs68 cells induced by *T. gondii* (RH and ME49 strains)

Our earlier results have shown that z-FA-FMK inhibits *T. gondii* proliferation dose-dependently by blocking PV formation and reducing total parasite number. The lytic cycle of *T. gondii* proliferation ultimately results in rupture of the host cell when the number of parasites overwhelms the physical capacity of the cell. Plaques which reflect the proliferation capability of the parasite and are formed after repeated cycles of host invasion and rupture (Ufermann *et al*., 2017, Vinayak *et al*., 2014). Thus, the visualization and quantification of *T. gondii* plaque area correlates to the tachyzoite replication rate *in vitro*. To further determine if z-FA-FMK has any effects on the *T. gondii* proliferation, confluent Hs68 cells were infected with tachyzoites (RH or ME49 strain) for 24h prior to treatment with z-FA-FMK. The Hs68 cells infected with tachyzoites were incubated for a further 96h in the presence of z-FA-FMK and the plaque area formed was determined.

As shown in Figure 3.5A, Hs68 cells infected with RH strain tachyzoites alone developed ~70% plaques, indicating that a lot of the cells were dying as the parasites proliferate normally. In contrast, uninfected cells have less plaque as the Hs68 cells were not dying. However, the presence of z-FA-FMK was shown to inhibit the formation of plaques in Hs68 cells mediated by the tachyzoites in a dose-dependent manner. At 100µM z-FA-FMK, the amount of plaques induced by the parasite in Hs68 cells was reduced to >30% indicating that less cells were dying compared to the infected Hs68 cells alone.

For the ME49 strain, the same amount of plaques (~70%) were observed in Hs68 cells infected with tachyzoites alone (Figure 3.5B). Similarly, z-FA-FMK also prevented plaque formation induced by the ME49 strain of parasites. At 12.5µM z-FA-FMK there was a marked decrease in plaque area (>40%) and complete inhibition at 50µM. This finding suggests that the ME49 strain may be more sensitive to z-FA-FMK.

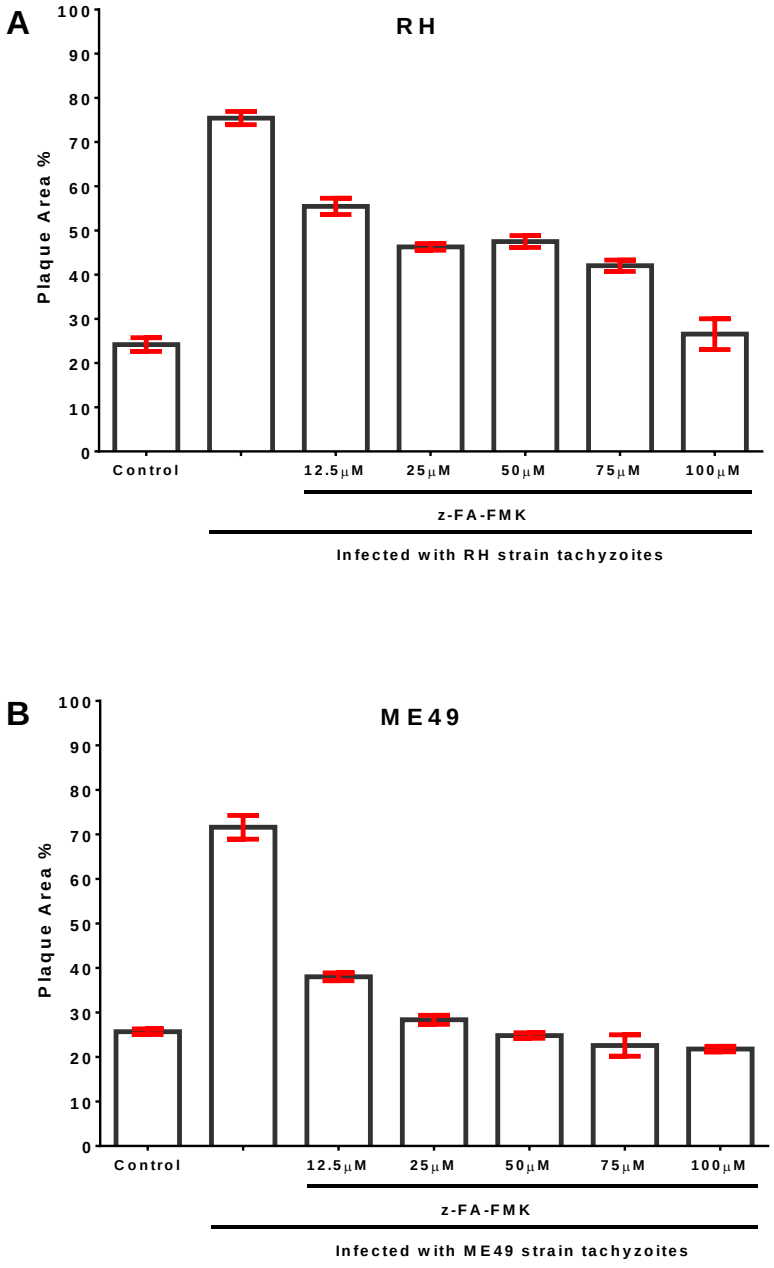

Figure 3.5. Effect of z-FA-FMK on plaque formation in Hs68 cells infected with *T. gondii* (RH and ME49 strain)

Hs68 host cells were infected with RH strain (**A**) and ME49 strain (**B**) *T. gondii* in the absence or presence of various concentrations of z-FA-FMK for 96h. The area of the plaques formed was quantified using the NIS-Elements Microscope Imaging Software. The results represent the means ± SEM from three independent experiments.

3.2.5 z-FA-FMK induces cyst-like organelles in *T. gondii* infected Hs68 cells

Besides blocking PV formation and reduce parasite count in *T. gondii* infected Hs68 cells, z-FA-FMK at high concentrations (≥50μM) was shown to induce morphological changes in the PVs, which resembled intracellular cysts. As depicted in Figure 3.6, the observed cysts-like structures (red arrow) appear as randomly arranged parasites without the classical 'rosette' formation enclosed within an enlarged PV. The results suggest that z-FA-FMK inhibits *T. gondii* proliferation and may have induce cyst formation in Hs68 cells infected with both the RH and ME49 strains. Since z-FA-FMK at 100μM almost completely inhibited parasite proliferation in both strains, this concentration was used in subsequent experiments to determine whether the cyst-like organelles are indeed cysts. To this end, DBA-FITC (a lectin from *Dolichos biflorus*) which specifically binds to N-acetyl-galactosamine on the *T. gondii* cyst wall was used to detect the presence of cyst wall (Buchholz *et al*., 2013). Hs68 cells infected with *T. gondii* parasites (RH or ME49 strains) were treated with 100μM of z-FA-FMK for 72h prior to DBA-FITC staining.

As shown in Figure 3.7A, the untreated *T. gondii* (RH) PVs in Hs68 cells were not stained by DBA-FITC, indicating that the parasites were not developing cyst wall under normal culture conditions. However, spontaneous cyst formation was observed in Hs68 cells infected with the ME49 strain of *T. gondii* as shown by the positive DBA-FITC staining in some of the intracellular organelles (Figure 3.7B). The treatment with z-FA-FMK (100μM) which effectively inhibited proliferation of *T. gondii* in both RH and ME49 strains indicated positive DBA-FITC staining of intracellular organelles (Figure 3.7C and 3.7D respectively). The ME49 strain also exhibited more cysts being formed following z-FA-FMK treatment compared to untreated ME49 parasites. This indicates that treatment with z-FA-FMK (100μM) for 72h leads to the development of cyst wall in both parasite strains (RH and ME49).

The kinetics of cyst wall formation over time for both strains of *T. gondii* following 100μM z-FA-FMK treatment was next examined. As shown in Figure 3.8, cyst wall formation in RH strain intracellular tachyzoites was apparent after 48h which becomes increasingly prominent

after 72h. Since the parasite proliferation was suppressed after 24h following z-FA-FMK treatment, the results showed that the inhibition of parasite proliferation precedes the formation of the cyst wall organelles. For the ME49 strain, the formation of cyst wall organelles was detectable as early as 24h in comparison to RH strain which was only detectable 48h following z-FA-FMK treatment (Figure 3.8 and Figure 3.9). These results suggest that the ME49 strain of *T. gondii* form cyst more readily compared to RH strain after z-FA-FMK treatment.

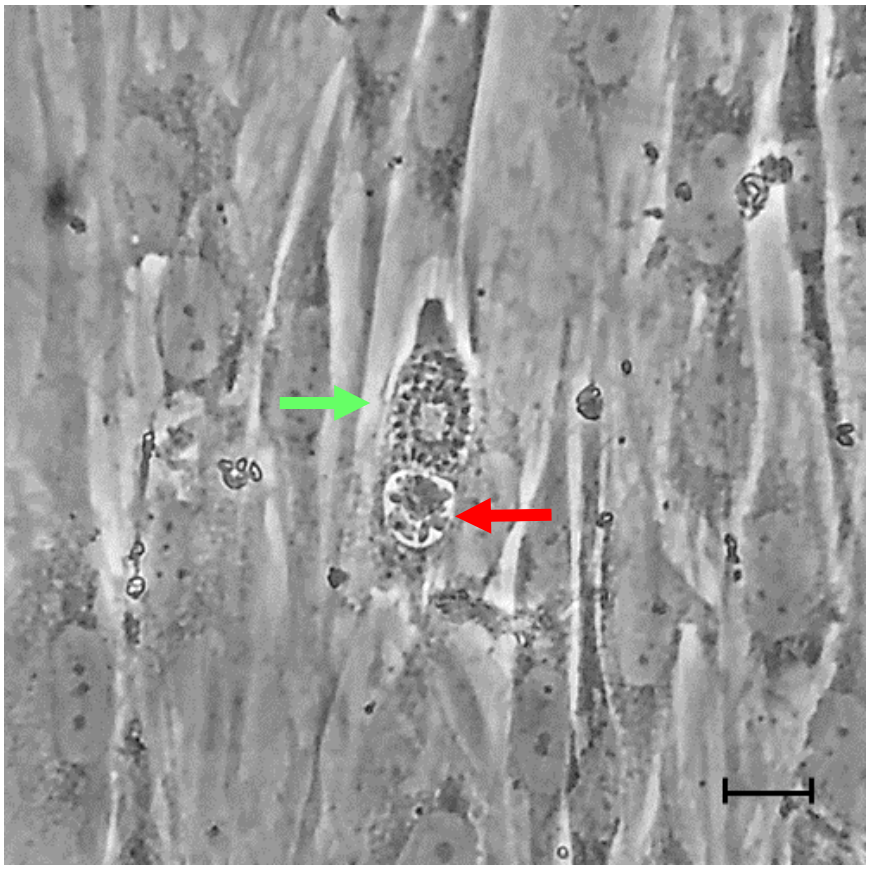

Figure 3.6. Representative image of *T. gondii* cysts-like organelle in Hs68 cells observed following z-FA-FMK treatment

Normal PV with rosette formation (Green arrow). Cysts-like structure having randomly arranged parasites enclosed within an enlarged PV space (Red arrow). Scale bars, 10μm.

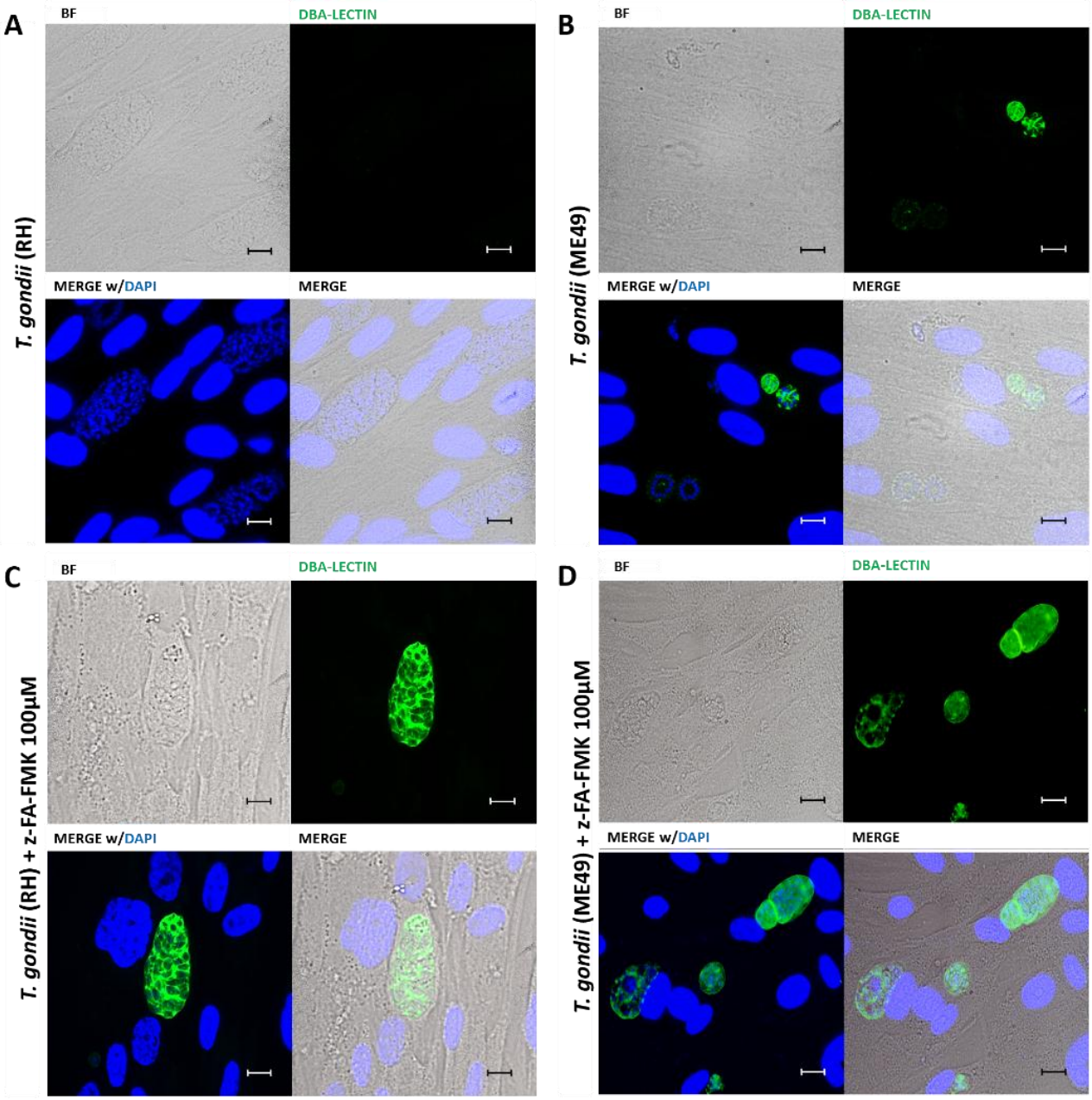

Figure 3.7. Fluorescence microscopy of *T. gondii* stained with DBA-FITC and DAPI

Cells harboring *T. gondii* were fixed and stained with DBA-FITC and DAPI as described in Materials and Methods. Control untreated intracellular *T. gondii*; RH strain (**A**) and ME49 strain (**B**) and after treatment with z-FA-FMK (100µM) for 72h; RH strain (**C**) and ME49 strain (**D**). The parasite morphology and fluorescence staining were examined under 600× magnification using fluorescence microscopy. BF, brightfield. Scale bars, 10µm.

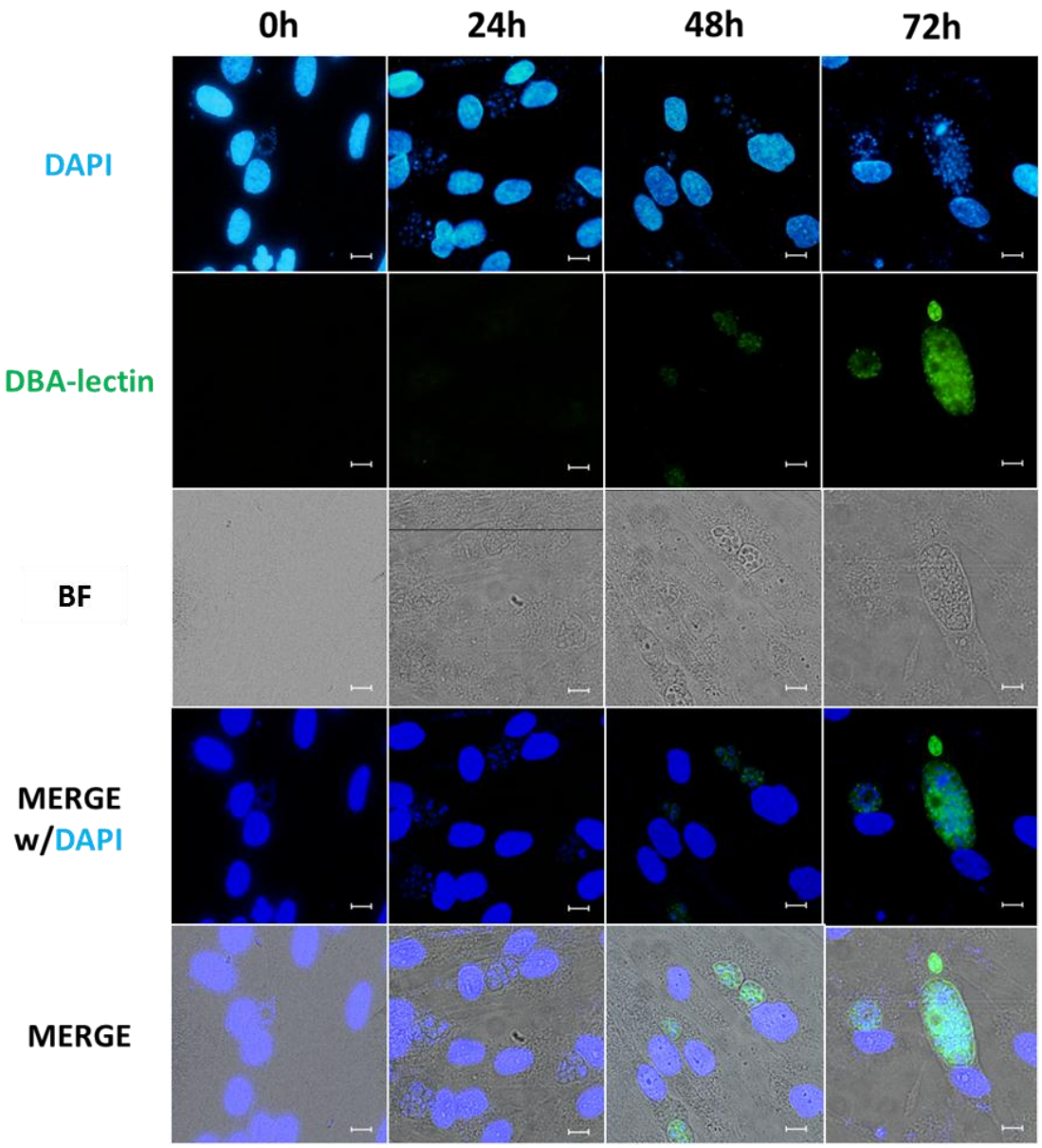

Figure 3.8. Time-dependent development of cyst wall in z-FA-FMK-treated *T. gondii* of RH strain

Following treatment with 100μM z-FA-FMK for various time points where indicated, infected Hs68 cells harboring *T. gondii* (RH strain) were fixed and stained with DBA-FITC and DAPI as described in Materials and Methods. The parasite morphology and fluorescence were examined under 600× magnification using fluorescence microscopy. BF, brightfield. Scale bars, 10μm.

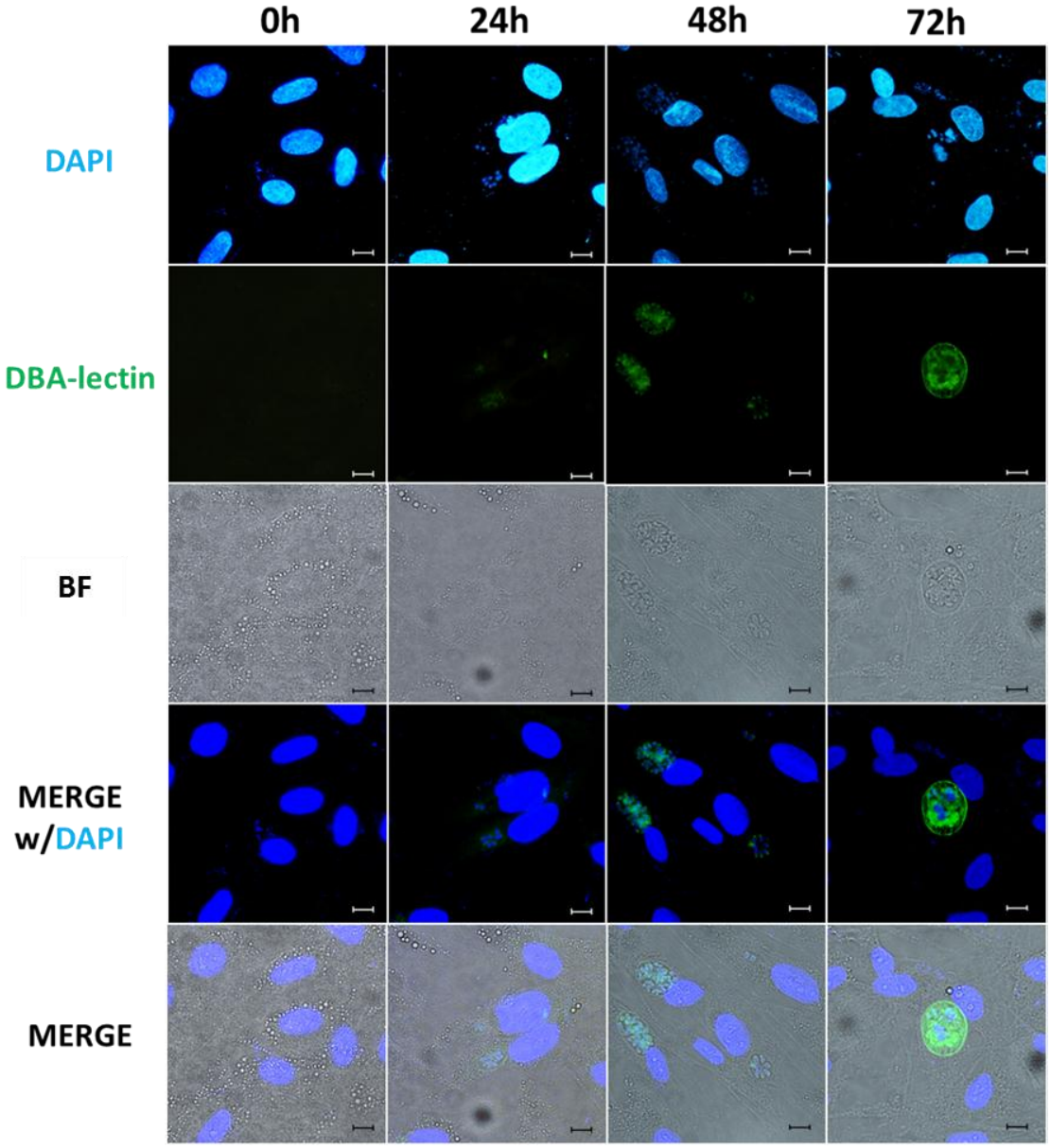

Figure 3.9. Time-dependent development of cyst wall in z-FA-FMK-treated *T. gondii* of ME49 strain

Following treatment with 100μM z-FA-FMK for various time points where indicated, infected Hs68 cells harboring *T. gondii* (ME49 strain) were fixed and stained with DBA-FITC and DAPI as described in Materials and Methods. The parasite morphology and fluorescence were examined under 600× magnification using fluorescence microscopy. BF, brightfield. Scale bars, 10μm.

3.2.6 Anti-proliferative effects of z-FA-FMK on *T. gondii* is reversible

Our collective results have shown that z-FA-FMK at 100µM effectively blocked proliferation of *T. gondii* tachyzoites from both RH and ME49 strains, and induced development of cyst wall. Since the parasites remain viable following z-FA-FMK treatment, their ability to resume proliferation following withdrawal of z-FA-FMK was examined. To this end, Hs68 host cells infected with *T. gondii* (RH or ME49 strains) were treated with z-FA-FMK (100µM) for 72h. The treated infected cells were either continuously exposed to 100µM z-FA-FMK or treated with fresh culture media without z-FA-FMK and cultured for another 144h.

As shown in Figure 3.10A, following withdrawal of z-FA-FMK treatment, RH strain parasites showed a slight increase in PV gradually over 72h followed by a marked recovery up to 144h. Similarly, ME49 strain parasites also indicated a gradual increase in PV number following the removal of z-FA-FMK (Figure 3.10C). These results indicate that after z-FA-FMK withdrawal, the intracellular parasites appear to proliferate within the PVs and resume the lytic cycle. This will release more infectious tachyzoites to invade adjacent cells, leading to an increase in the number of PVs. On the other hand, the presence of z-FA-FMK continued to inhibit the increase in PV formation over 144h.

To further confirm if the parasites resume proliferation after the withdrawal of z-FA-FMK, the total viable parasites were quantified after 144h. Indeed, the number of parasites quantified in both RH and ME49 strains showed a significant increase in parasites (Figure 3.10B and 3.10D, respectively) compared to parasites that were continuously exposed to z-FA-FMK. These findings collectively indicate that the parasites remain viable during z-FA-FMK treatment and the parasites with their proliferation inhibited were able to regain the ability to proliferate upon the withdrawal of z-FA-FMK.

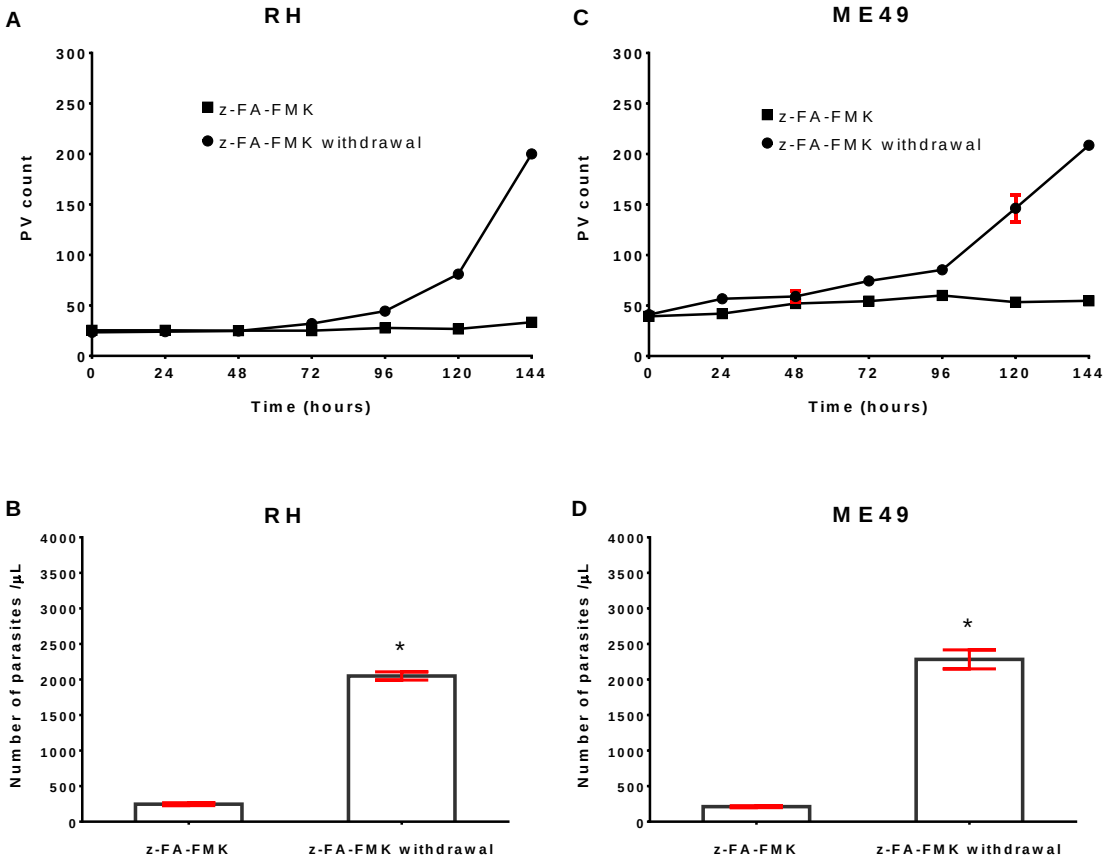

Figure 3.10. Recovery of *T. gondii* proliferation following z-FA-FMK withdrawal

Hs68 cells infected with *T. gondii* (RH and ME49 strains) were treated with 100µM z-FA-FMK. After 72h, the infected Hs68 cells were either continuously exposed to 100µM z-FA-FMK or replaced with normal culture media without z-FA-FMK and maintained in culture for another 144h. The number of PVs (**A, C**) was determined every 24h interval, and the total number of parasite (**B, D**) isolated from Hs68 cells was quantified after 144h. The number of PV was scored across 10 randomized microscopic field under 40× magnification. The number of tachyzoites was determined using the trypan blue exclusion method. The results represent the means ± SEM from three independent experiments, where * indicates $p < 0.05$ versus z-FA-FMK treatment.

3.3 Discussion

T. gondii possess a dynamic and complex life cycle which involves interconversion between proliferative and latent stages (Lyons *et al*., 2002, Sullivan and Jeffers, 2012). The proliferative stage involves the tachyzoite form, which actively replicates intracellularly inside the PVs via endodyogeny. On the other hand, the latent stage is when the tachyzoites differentiate into quiescent bradyzoites within a modified PV known as the cyst wall (Sullivan and Jeffers, 2012). The current anti-*Toxoplasma* drugs are only efficient against the tachyzoites which is responsible for acute infections but remain incapable of eradicating tissue cysts which sustains chronic infection (Lapinskas and Ben-Harari, 2019). At present, there are no effective drugs that prevents cyst formation or eradicate *T. gondii* residing within tissue cysts (Zhu *et al*., 2019). Hence it is important to elucidate the mechanisms of *T. gondii* differentiation to discover new strategies or drug targets to tackle toxoplasmosis at both acute and chronic phase. It is well documented that stress factors that impede the parasite growth plays an important driving force in *T. gondii* stage conversion (Vonlaufen *et al*., 2008). One of the classical *in vitro* approaches is to use alkaline pH treatment, around pH 8.0 - 8.2 (Soete *et al*., 1994). Other stress agents used successfully include heat shock treatment, sodium nitroprusside which causes nitrosative stress and inhibitors of parasite mitochondrial respiratory chain (Bohne *et al*., 1994, Soete *et al*., 1994, Tomavo and Boothroyd, 1995). Nutrient deprivation via axenic culture and arginine starvation were also able to induce tachyzoites differentiation into bradyzoites (Fox *et al*., 2004, Yahiaoui *et al*., 1999). However, it remains unknown whether these stresses directly affect the parasites during extracellular phase of the lytic cycle, and/or indirectly towards intracellular parasites by stressing the host cell altogether (Sullivan and Jeffers, 2012). Hence, it is crucial that novel strategies developed are specifically targeted to suppress or eradicate *T. gondii* in the cyst form while avoiding excessive stress to the host.

In *T. gondii*, cysteine proteases such as cathepsins B are involved in parasite invasion, protein processing and digestion, which are essential processes during parasite invasion and proliferation (Chaparro *et al*., 2018, Dou *et al*., 2014, Que *et al*., 2007, Ramirez-Flores *et al*.,

2019). Studies have shown that the *T. gondii* cysteine protease, cathepsin L (*Tg*CPL) is essential to cyst survival during the chronic phase of infection (Zwicker *et al*., 2018). These studies collectively indicate that cysteine proteases are potential drug targets in *T. gondii* parasites which appears to be effective towards both acute and chronic phase infections.

T. gondii parasites can be classified into different strains according to their genotype and pathogenicity. In this study, we used the RH and ME49 strain to study how these strains with different propensity to differentiate respond to z-FA-FMK treatment. The highly virulent RH strain has been extensively studied in the majority of *T. gondii* studies and associated with acute infections (da Costa-Silva *et al*., 2012). On the other hand, the less virulent ME49 strain accounts for the majority of human toxoplasmosis and also has a higher tendency to form cysts than the RH strain (Araujo and Slifer, 2003, Saeij *et al*., 2005). The Hs68 cells infected with tachyzoites were used as a model to study the effects of the cathepsin B inhibitor, z-FA-FMK on the proliferation of intracellular tachyzoites.

Based on our results, we have shown that the cathepsin B inhibitor, z-FA-FMK is not toxic to Hs68 cells. Our findings are in line with previously reported studies where z-FA-FMK was also shown to be non-toxic towards Jurkat T-cells (Liow and Chow, 2013) and human primary T-cells (Lawrence *et al*., 2006). The average duration required for *T. gondii* tachyzoite to complete the host cell invasion requires only 15 - 30 seconds (Sibley *et al*., 1999), and to this end the results showed that z-FA-FMK is not toxic to both RH and ME49 strain extracellular *T. gondii* tachyzoites up to 6h. This indicates that z-FA-FMK does not cause any toxic effects to the *T. gondii* parasites in a proliferation model using Hs68 cells. Subsequently, it was shown that z-FA-FMK blocks *T. gondii* invasion into Hs68 cells in a dose-dependent manner. *T. gondii* being an obligate intracellular parasite, relies on cell invasion mediated via secretion of microneme and rhoptry neck proteins (RON) to establish entry into host intracellular compartment for its survival (Zhu *et al*., 2019). The micronemes and rhoptries discharge their contents during cell invasion to mediate successful parasite anchorage to host cell membrane followed by entry (Carruthers, 2006). Since cathepsin B has been shown to take part in microneme and rhoptry protein maturation in *T. gondii*

parasites (Di Cristina *et al*., 2017, Dou and Carruthers, 2011, Dou *et al*., 2014, Que *et al*., 2007). Therefore, the cathepsin B inhibitor z-FA-FMK could have interfered with microneme and rhoptry function which prevented *T. gondii* invasion into Hs68 cells.

To further examine if z-FA-FMK continues to affect *T. gondii* after invasion into Hs68 cells, we assessed the ability of intracellular parasites to establish new PVs over time. Our results indicate that z-FA-FMK dose-dependently inhibited the formation of new PVs in the infected Hs68 monolayer. The natural lytic cycle of *T. gondii* begins with invasion into a host cell where the intracellular parasite begins to replicate via endodyogeny within a PV. The parasite continues to proliferate until it ruptures the host cell from within, releases all the tachyzoites to freely invade adjacent cells (Uttah *et al*., 2013). Based on our findings, the intracellular parasites treated with z-FA-FMK were not able to effectively establish new infections as seen from the decreased number of PVs formed. Our earlier results showed that z-FA-FMK could only partially block parasite invasion. However, high concentrations of z-FA-FMK were shown to almost completely block new PV formation. This suggests that z-FA-FMK also blocks replication of intracellular tachyzoites within Hs68 cells. To assess if the *T. gondii* proliferation was indeed blocked by z-FA-FMK, the total number of viable parasites following z-FA-FMK treatment was determined. Our results strongly indicate that the intracellular parasites remain viable and the total parasite number was markedly reduced following z-FA-FMK treatment. Our collective results so far indicate that z-FA-FMK dose-dependently impede *T. gondii* lytic cycle by blocking host cell invasion and intracellular proliferation. In line with this, the plaque assay results demonstrated that z-FA-FMK inhibited plaque formation in Hs68 cells infected with tachyzoites. In summary, z-FA-FMK blocks the lytic cycle of the parasite by blocking both invasion (establishment of PV) and intracellular proliferation (total parasite count), which eventually lead to less parasite egress (plaque formation).

Studies have documented a strong correlation between reduced *T. gondii* tachyzoite growth as a result of stress conditions and propensity to differentiate and form cyst (Bohne *et al*., 1994, Gubbels *et al*., 2008, Radke *et al*., 2003, Sullivan and Jeffers, 2012). Furthermore, *T.*

gondii differentiation/cyst formation is often preceded by a reduction in parasite proliferation. The presence of DBA-lectin positive organelles in Hs68 cells infected with RH and ME49 strains of parasites following z-FA-FMK treatment indicates the development of cyst wall. Time course examination on formation of cysts in response to z-FA-FMK also demonstrated that growth inhibition of the parasites precedes the formation of the cyst wall. The findings from this study that z-FA-FMK inhibits *T. gondii* proliferation prior to cyst wall formation is in line with reported studies, where differentiation into bradyzoites in cysts is often preceded by a decrease in parasite proliferation (Jerome *et al*., 1998, Radke *et al*., 2003). Interestingly, the ME49 strain appears to be more sensitive to the inhibitory effects of z-FA-FMK and formed cysts more readily compared to the RH strain. The difference in propensity to form cysts is in line with previously documented studies where the slower growing type-2 (ME49) and type-3 (VEG) strains have higher cyst forming tendency than the hypervirulent type-1 RH strain (Skariah *et al*., 2010, Soete *et al*., 1994, Sullivan and Jeffers, 2012). Previous study has also suggested that cell cycle arrest does not trigger cyst formation, demonstrating that cell cycle progression is needed for cyst formation (Gubbels *et al*., 2008). Whether the anti-proliferative effects of z-FA-FMK involves cell cycle blockage is unclear and more work is needed to confirm this in the *T. gondii* parasites.

The present results demonstrated that z-FA-FMK inhibits the proliferation of tachyzoites followed by the formation of cysts without killing the parasites. This suggests that the anti-proliferative effects of z-FA-FMK may involve some form of stress induction. However, it is unclear if the effects are dependent on the continuous presence of the z-FA-FMK. Hereafter, we examined the reversibility of z-FA-FMK mediated anti-proliferative effects on *T. gondii* parasites by withdrawing z-FA-FMK after 72h treatment. Interestingly, intracellular *T. gondii* was able to regain proliferation and revert into the fast growing tachyzoites to infect more host cells following the withdrawal of z-FA-FMK, albeit after a latent period. This latent period may be attributed to z-FA-FMK irreversibly alkylating the cysteine residue at the active site and forming a covalent bond (Lawrence *et al*., 2006, Rajah and Chow, 2015). Secondly, a number of studies have indicated a complex and distinct subset of genes being expressed during interconversion between tachyzoite and bradyzoite, e.g. the ribosomal

protein family, dense granule protein family, microneme protein family (MIC proteins) and heat shock protein family (Alonso *et al*., 2019, Chen *et al*., 2018, Pittman *et al*., 2014). Therefore, the latent period following z-FA-FMK withdrawal may involve gene expression during re-differentiation back into tachyzoites to regain virulence and proliferate.

During an acute infection, *T. gondii* parasites are challenged by a variety of cellular stresses from the host immune system and the extracellular environment (Joyce *et al*., 2011, Lyons *et al*., 2002, Weiss and Kim, 2000). Even in between lytic cycles, egressed tachyzoites must cope with the stress of the extracellular environment, which lacks essential nutrients and metabolites necessary for survival. Hence, the only condition where *T. gondii* parasite are able to evade these stresses is within the host cell intracellular environment, where protection and nutrients are available for survival and proliferation (Coppens *et al*., 2000, Zhou *et al*., 2005).

In summary, our results in this chapter showed that the irreversible cathepsin B inhibitor z-FA-FMK blocks *T. gondii* lytic proliferation cycle in both RH and ME49 strains by reducing PV formation and parasite number, leading to decreased plaque formation and cyst formation. Withdrawal of z-FA-FMK treatment resulted in the parasites regaining virulence and proliferation. Collectively, z-FA-FMK treated Hs68 host cells infected with *T. gondii* could be a useful model to study the interconversion between tachyzoites and encysted bradyzoites.

CHAPTER FOUR

T. gondii anti-proliferative effects mediated by z-FA-FMK in Hs68 cells are associated with cathepsin B inhibition, and its recovery involves autophagy

4.1 Introduction

Proteases are enzymes that catalyze the breakdown of proteins into smaller polypeptides or amino acids via hydrolysis of peptide bonds, and are vital to major biological processes, such as protein digestion, enzyme activation and differentiation (Dou and Carruthers, 2011, Siqueira-Neto *et al*., 2018, Zhao *et al*., 2013). There 7 major classes of proteases are classified based on the catalytic residue: Aspartic, Cysteine, Glutamic, Serine, Threonine, Metallo and Asparagine (Dou and Carruthers, 2011, Sajid and McKerrow, 2002). Cathepsins are lysosomal proteases of the cysteine protease family which digests endogenous and exogenous endocytosed polypeptides in eukaryotic cells (Que *et al*., 2007, Que *et al*., 2002, Sajid and McKerrow, 2002, Siqueira-Neto *et al*., 2018). It is now clear that cathepsins are also involved in more specialized cellular functions, including antigen presentation, spermatogenesis, tumor invasion, and TNFα-induced apoptosis (Dou and Carruthers, 2011, Guicciardi *et al*., 2000). Similar to higher eukaryotes, protozoan parasites appear to utilize cathepsin proteases for protein degradation and various specialized functions that are important for survival, making them attractive targets for potential anti-parasitic drug development (Dou and Carruthers, 2011). For example, the cysteine proteinase cathepsin L in *P. falciparum* is vital for the digestion of hemoglobin in the parasite food vacuole during erythrocyte infection (Rosenthal, 2004), while cathepsin B in *T. brucei* is essential for iron acquisition (O'Brien *et al*., 2008).

In *T. gondii*, cysteine proteases have been shown to play a significant role in parasite invasion, processing of functional proteins and digestion of host derived proteins (Dou *et al*., 2014, Que *et al*., 2007, Ramirez-Flores *et al*., 2019). The *Toxoplasma* genome project has indicated a lower redundancy of cathepsin protease genes in *T. gondii* compared to other parasites, further corroborating them as potential anti-*Toxoplasma* drug targets (Siqueira-Neto *et al*., 2018). There are 5 cathepsin-like cysteine proteases (*Tg*CPs) in *T. gondii* which consists of one cathepsin L-like (*Tg*CPL), one cathepsin B-like (*Tg*CPB) and three cathepsin C-like (*Tg*CPC1, 2 and 3) (Dou and Carruthers, 2011). These cathepsins have been shown to play roles in host cell invasion (microneme and rhoptry protein maturation), digestion of host

proteins for nutrition and cyst survival in *T. gondii* parasites (Di Cristina *et al*., 2017, Dou and Carruthers, 2011, Que *et al*., 2007, Que *et al*., 2004).

As shown in Figure 4.1. the *Toxoplasma* lysosomal vacuolar compartment (VAC) is an organelle that contains mainly proteolytic cathepsins and functions as the parasite's endolysosomal system (Dou and Carruthers, 2011, Miranda *et al*., 2010, Parussini *et al*., 2010). The VAC exists in various forms at different stages of the *T. gondii* lytic cycle. It appears as an intact organelle during the initial infection stage but fragments during intracellular replication (Parussini *et al*., 2010). How the parasite regulates the morphological changes that occur to the VAC organelle at different stages of the lytic cycle is still unclear. Nevertheless, VAC dysfunction is known to reduce invasion, replication, and virulence of the *T. gondii* parasite (Parussini *et al*., 2010, Dou *et al*., 2014).

Structurally, the *Toxoplasma* VAC consist of internal membrane tubules and vesicles, resembling multivesicular bodies that are involved in protein degradation and turnover (Dou and Carruthers, 2011). In fact, the VAC may function as the terminal compartment of the parasite endolysosomal system where protein degradation occurs as seen in the lysosomes of metazoans (Dou and Carruthers, 2011, Parussini *et al*., 2010). There are only 4 proteins in the VAC, that is *Tg*CPL, *Tg*CPB (a cathepsin B-like protein), *Tg*CRT (*T. gondii* chloroquine resistance transporter), and *Tg*VP1 (a pyrophosphatase) (Di Cristina *et al*., 2017, Dou and Carruthers, 2011, Warring *et al*., 2014). As depicted in Figure 4.1, both *Tg*CPL and *Tg*CPB serve as the functional component of the VAC, presumably by digesting host-derived proteins to support parasite survival and persistence *in vitro* and *in vivo* (Dou and Carruthers, 2011, Dou *et al*., 2013, Que *et al*., 2002). On the other hand, *Tg*CPC is an exopeptidase that is secreted into the PV digest exogenous proteins (Dou and Carruthers, 2011). Recent studies have reported the critical importance of VAC-localized *Tg*CPL and *Tg*CPB cathepsins in *T. gondii* which plays a role in maturation of invasion effectors, digestion of exogenous proteins and autophagosomes (Dou and Carruthers, 2011, Miranda *et al*., 2010, Parussini *et al*., 2010, Thornton *et al*., 2019).

Interestingly, studies have reported that the knockout of VAC cathepsins resulted in the death of intracellular *T. gondii* which is characterized by excessive accumulation of organellar remnants (Di Cristina *et al*., 2017, Ghosh *et al*., 2012, Nguyen *et al*., 2017c). These findings suggest that the knockout of cathepsins may disrupt autophagy process in the parasites, leading to lack of autophagosome degradation and breakdown of cellular components by VAC (Di Cristina *et al*., 2017). Autophagy is a process of self-engulfment to recycle and remove misfolded proteins and dysfunctional organelles in eukaryotic cells (Di Cristina *et al*., 2017, Inoue and Klionsky, 2010, Mizushima, 2007). The autophagic process serves as a means of cell preservation under nutrient limitation by turnover of excess cellular capacity to sustain cellular function (Di Cristina *et al*., 2017, Kristensen *et al*., 2008, Weidberg *et al*., 2011). To this end, it has been suggested that autophagy may alleviate nutrient limitation experienced by *T. gondii* cysts during chronic infection stage (Di Cristina *et al*., 2017). Accumulating evidence suggests that autophagy plays an important role in facilitating *T. gondii* tachyzoites survival against extracellular stress and persistence in latent infection, despite living in a nutrient rich microenvironment in the host (Di Cristina *et al*., 2017, Ghosh *et al*., 2012). Bioinformatic studies have indicated the presence of autophagy-related genes (ATG) homologues in several parasitic protozoa including *T. gondii* (Duszenko *et al*., 2011, Herman *et al*., 2006, Klionsky *et al*., 2011). Despite the lack of lysosomes and not encoding all the known ATG genes, *T. gondii* was reported to form autophagosomes (Di Cristina *et al*., 2017, Ghosh *et al*., 2012, Nguyen *et al*., 2017c).

Recent studies indicated that the VAC also plays an important role in *T. gondii* autophagy where autophagosomes are degraded to sustain the survival of *T. gondii* during chronic infection (Figure 4.2) (Nguyen *et al*., 2017b, Siqueira-Neto *et al*., 2018, Subauste, 2019). One of the VAC cathepsin, *Tg*CPL have been shown to degrade autophagosomes and blocking this enzyme resulted in accumulation of undigested material in the VAC, and ultimately lead to diminished chronic infection in mice (Di Cristina *et al*., 2017, Parussini *et al*., 2010, Subauste, 2019). This suggest that nutrient limitation within the cyst may be overcome by bulk protein turnover mediated via autophagy to enhance parasite survival during chronic infection (Ghosh *et al*., 2012, Nguyen *et al*., 2017c, Subauste, 2019). The

toxoplasma VAC therefore appears to be involved in protein digestion and degradation of autophagosomes (Figure 4.2). In short, the various cysteine proteases of *T. gondii* play important roles in facilitating *T. gondii* infection and persistence, making them potential therapeutic targets as well as vaccine candidates. Hence, the main objective in this chapter is to characterize the involvement of cathepsin B and autophagy in the anti-proliferative activity mediated by z-FA-FMK in *T. gondii* parasites.

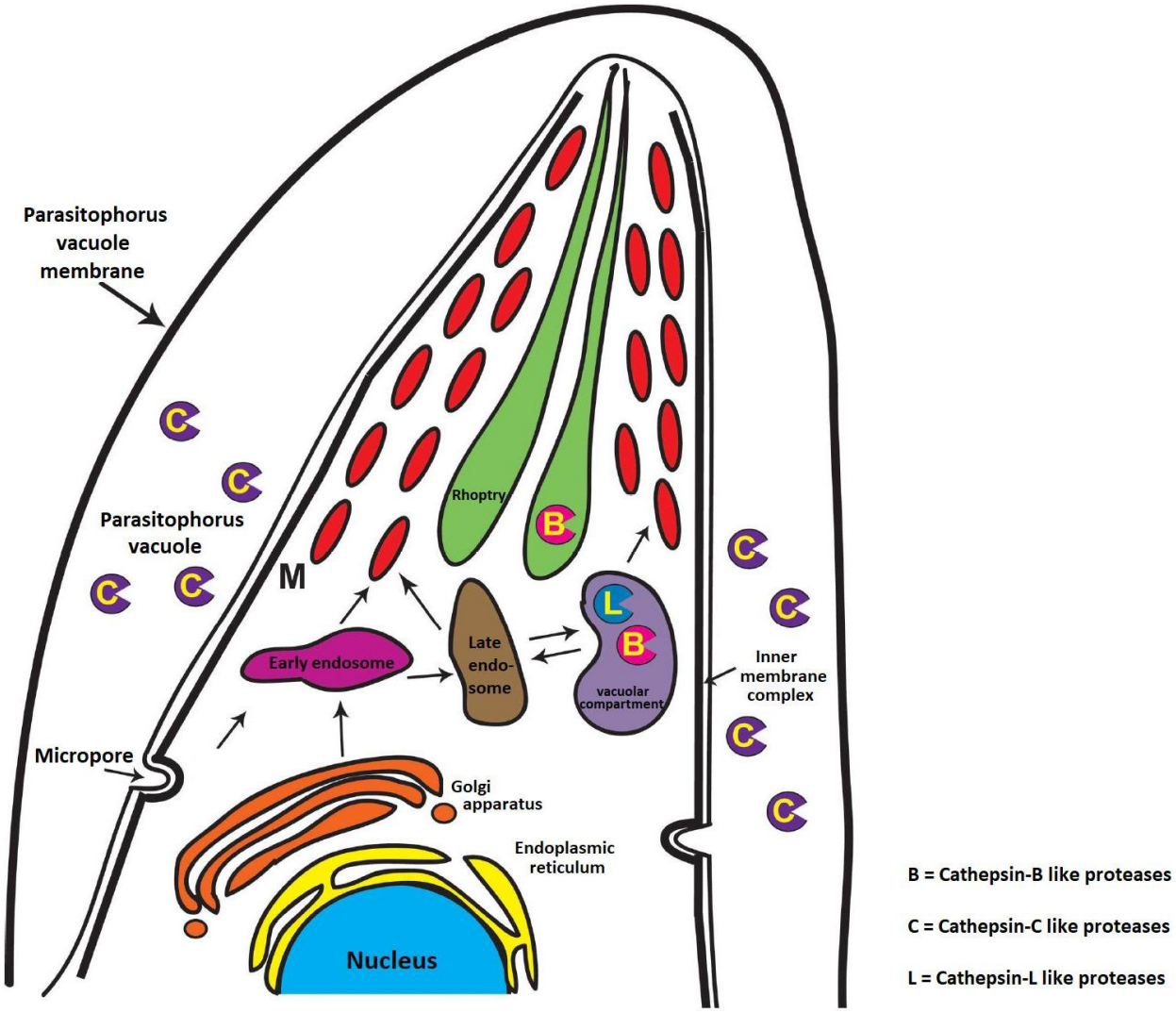

Figure 4.1. The endosomal system of *T. gondii* and the subcellular locations of *T. gondii* cathepsins

Toxoplasma cathepsin *Tg*CPL and *Tg*CPB are predominantly localized in the VAC. The *Tg*CPL facilitates maturation of pro-microneme proteins via the early endosome (EE) and late endosomes (LE). The rhoptry also contains *Tg*CPB which processes pro-rhoptry proteins. The exopeptidase, *Tg*CPC is secreted into the PV following invasion to digest exogenous proteins. Exogenous proteins are endocytosed possibly via the micropore and subsequently trafficked to the VAC for further digestion (Modified from Dou and Carruthers, 2011).

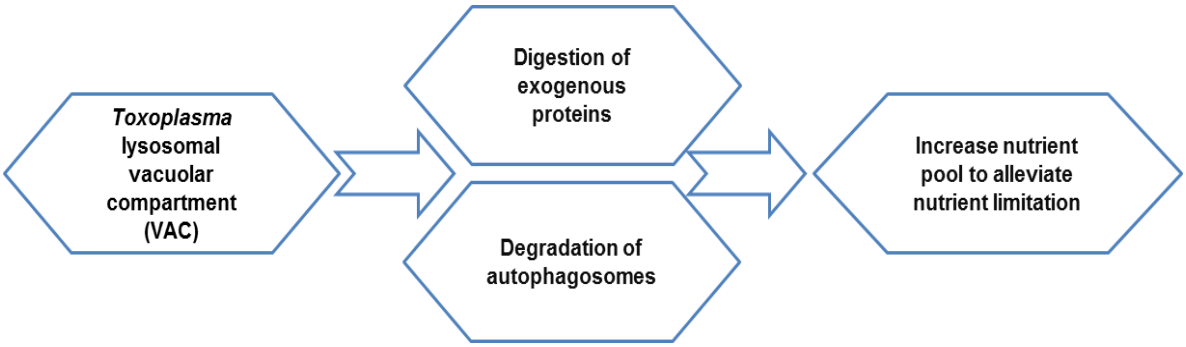

Figure 4.2. The role and function of the *T. gondii* VAC in nutrient acquisition and autophagy to alleviate nutrient limitation

Toxoplasma VAC contains the cysteine proteases *Tg*CPB and *Tg*CPL and function similarly to the mammalian lysosome in degrading proteins. The VAC may also fuse with autophagosomes during autophagy in the parasites. The digested material is then converted to substrates needed for parasite growth and proliferation.

4.2 Results

4.2.1 The cathepsin B inhibitor z-FA-DMK inhibits and induces cyst formation in *T. gondii* (RH and ME49 strain)

Our findings in chapter 3 indicate that the cathepsin B inhibitor, z-FA-FMK inhibits *T. gondii* proliferation and induce cyst formation. Previous study has reported that cysteine proteases such as cathepsin B play a critical role in facilitating parasite invasion and proliferation (Dou and Carruthers, 2011). Since z-FA-FMK possess other side effects besides blocking cathepsin B, it is not clear whether the blocking of *T. gondii* proliferation and cyst formation mediated by z-FA-FMK is due to the inhibition of cathepsin B. To examine this, the effects of z-FA-FMK on *T. gondii* were compared with z-FA-DMK, an analogue of z-FA-FMK, which appears to have no other side effects besides blocking cathepsin B (Green and Shaw, 1981, Liow and Chow, 2013).

To this end, the effects of z-FA-DMK on the formation of plaques in *T. gondii* infected Hs68 cells was first determined. As shown in Figure 4.3A and Figure 4.3B, z-FA-DMK induced a dose-dependent reduction in plaque formation in Hs68 cells infected with both RH and ME49 strains after 96h respectively. Similar to z-FA-FMK, z-FA-DMK also induced a dose- and time-dependent decrease in the formation of PV in Hs68 cells infected with both RH and ME49 *T. gondii* strains (Figure 4.4A and Figure 4.5A, respectively). The total viable parasite following z-FA-DMK treatment was markedly reduced in a dose-dependent manner in Hs68 cells infected with both RH (Figure 4.4B) and ME49 strain (Figure 4.5B) in a dose-dependent manner. Collectively, these results demonstrate that z-FA-DMK induced similar effects on the parasites as seen with z-FA-FMK. Similar to z-FA-FMK, z-FA-DMK was more effective in blocking the proliferation of ME49 strain in Hs68 cells. This is indicated by the greater reduction in PV and parasite number in the ME49 strain at lower concentrations of z-FA-DMK (Figure 4.4 and Figure 4.5). The next step was to examine whether z-FA-DMK could induce formation of cyst wall in Hs68 cells infected with the parasites. Infected Hs68 cells were treated with 100µM z-FA-DMK, which was the most effective concentration in

blocking the proliferation of *T. gondii* (RH and ME49 strain). As illustrated in Figure 4.6, cyst wall formation was readily detected in Hs68 cells infected with both RH and ME49 *T. gondii* strains using DBA-lectin following z-FA-DMK treatment. These results collectively demonstrate that the effects mediated by z-FA-DMK on *T. gondii* infected Hs68 cells are similar to that seen with z-FA-FMK. Both z-FA-FMK and z-FA-DMK are cathepsin B inhibitors which were shown to block *T. gondii* proliferation in a dose-dependent manner followed by induction of cyst formation. This suggest that the inhibition of cysteine proteases such as cathepsin B is likely to be involved in blocking the parasite proliferation and subsequently lead to cyst formation.

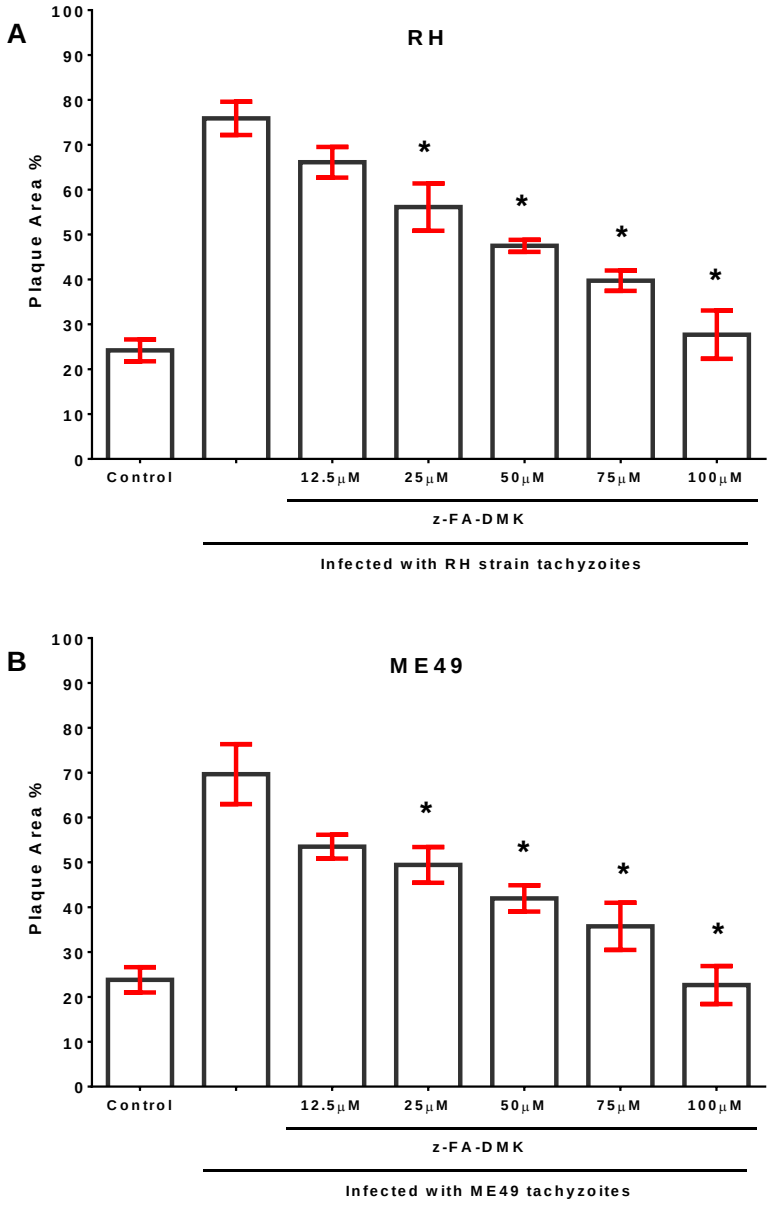

Figure 4.3. Effect of z-FA-DMK on plaque formation in Hs68 cells infected with *T. gondii* (RH and ME49 strain)

Hs68 cells infected with *T. gondii* RH strain (**A**) and ME49 strain (**B**) were treated with various concentrations of z-FA-DMK for 96h. Plaque assay was subsequently performed, and the plaque area was quantified using NIS-Elements Microscope Imaging Software. The results represent the means ± SEM from three independent experiments, where * indicates $p < 0.05$ versus tachyzoite infected treatment.

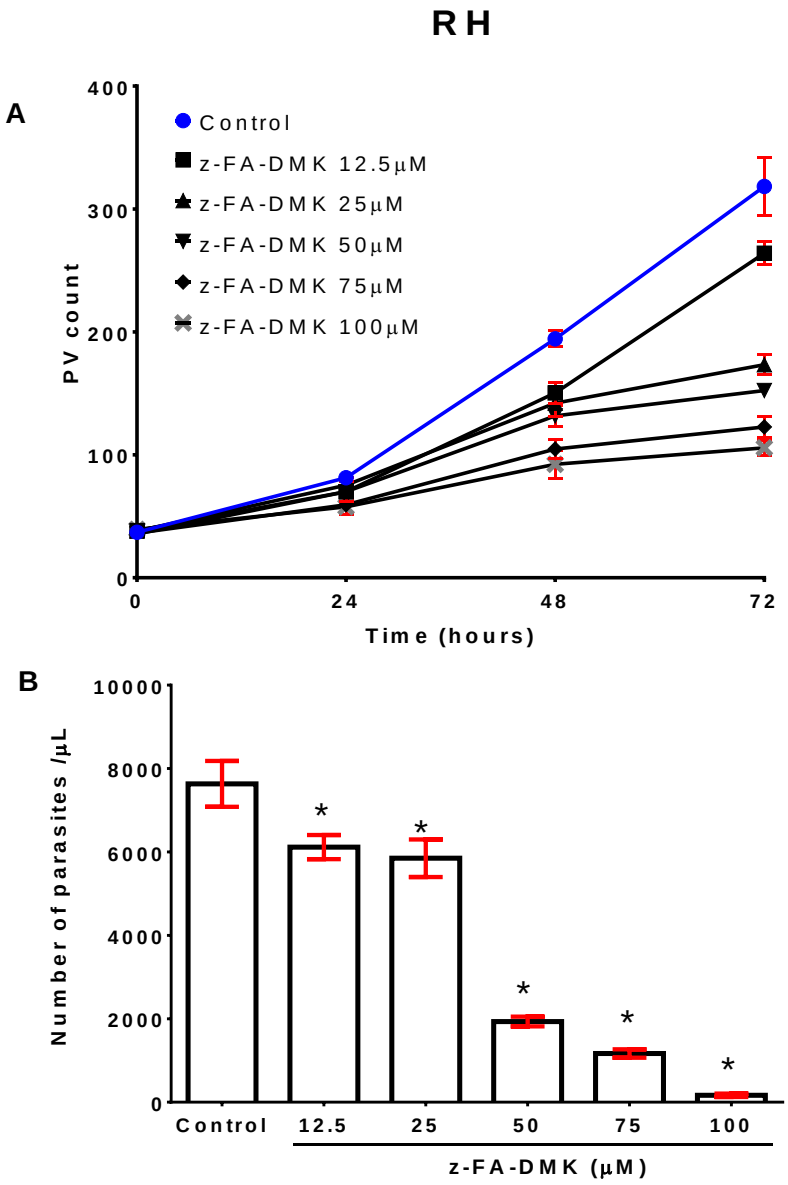

Figure 4.4. Effect of z-FA-DMK on *T. gondii* (RH) tachyzoite proliferation

Hs68 cells infected with *T. gondii* RH strain tachyzoites were treated with various concentrations of z-FA-DMK for different time points where indicated and the number of PV (**A**) and total parasite count in Hs68 cells (after 72h) (**B**) were determined. The number of PV was scored across 10 randomized microscopic field under 40× magnification. The total number of viable tachyzoites was determined using the trypan blue exclusion method as described in Materials and Methods. The results represent the means ± SEM from three independent experiments, where * indicates $p < 0.05$ versus untreated control.

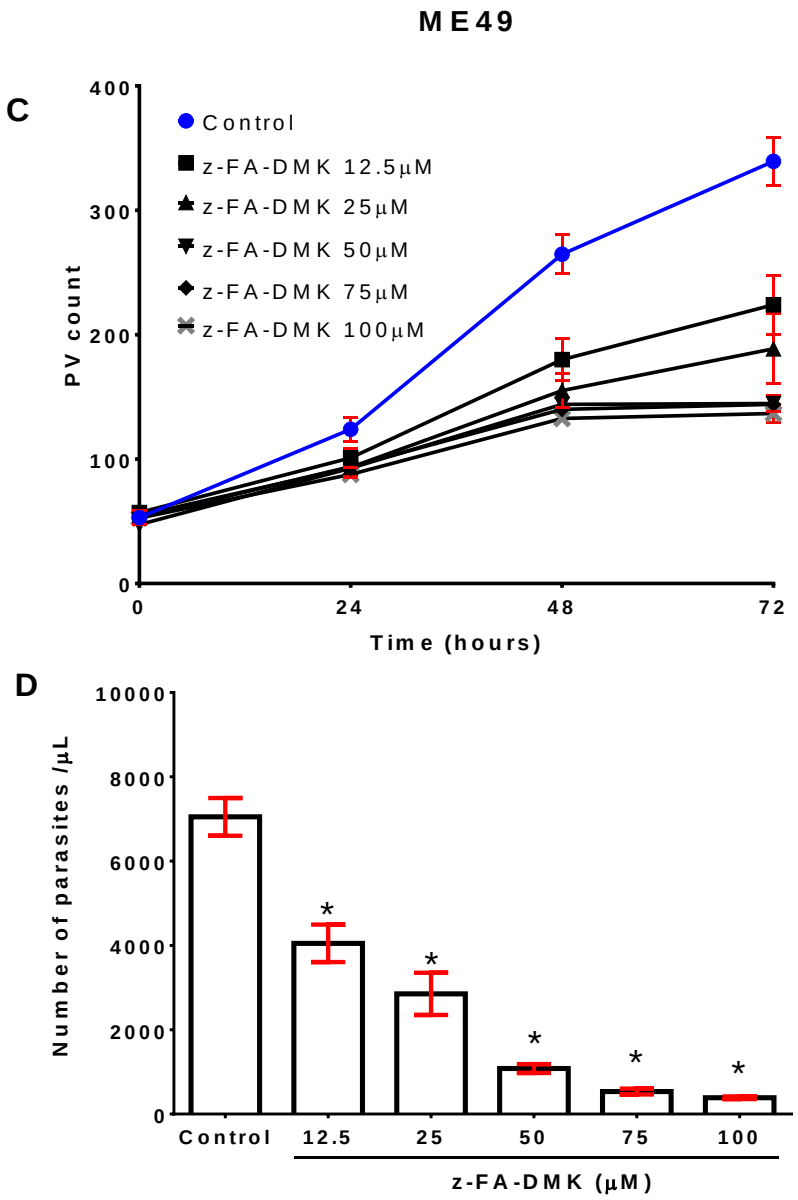

Figure 4.5. Effect of z-FA-DMK on *T. gondii* (ME49) tachyzoite proliferation

Hs68 cells infected with *T. gondii* ME49 tachyzoites were treated with various concentrations of z-FA-DMK for different time points where indicated and the number of PV (**A**) and total parasite count in Hs68 cells (after 72h) (**B**) were determined. The number of PV was scored across 10 randomized microscopic field under 40× magnification. The total number of viable tachyzoites was determined using the trypan blue exclusion method as described in Materials and Methods. The results represent the means ± SEM from three independent experiments, where * indicates $p < 0.05$ versus untreated control.

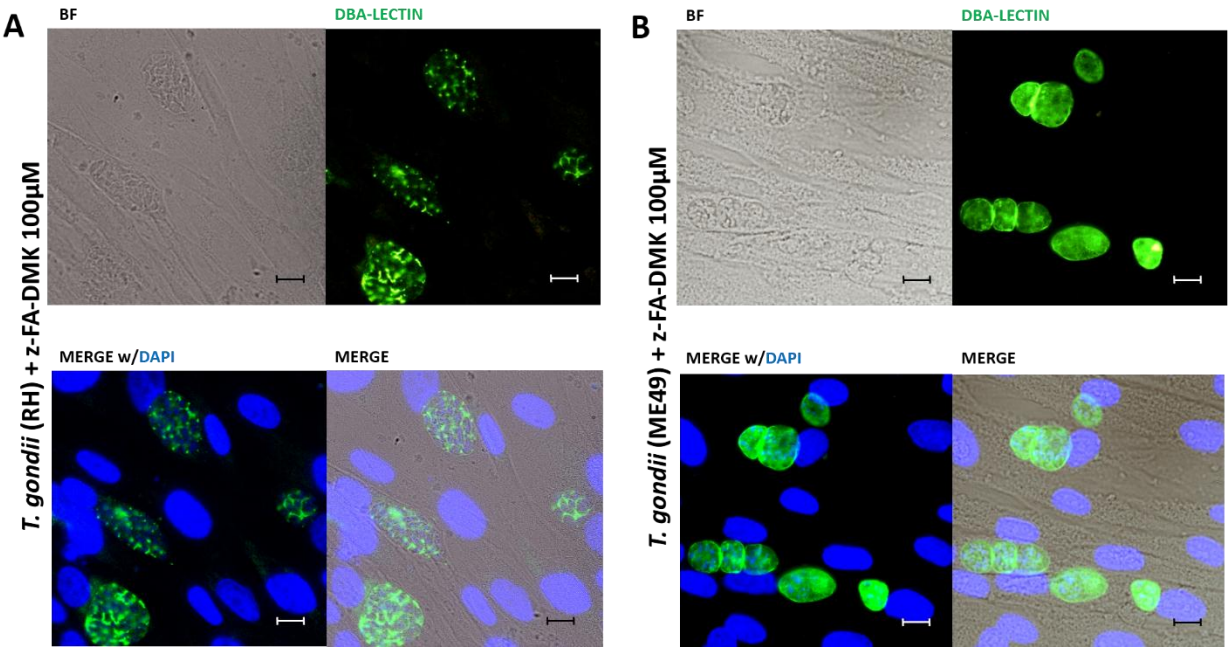

Figure 4.6. Fluorescence microscopy of *T. gondii* stained with DBA-FITC and DAPI

Hs68 cells infected with *T. gondii* (RH or ME49 strains) were treated with 100µM z-FA-DMK for 72h. Following treatments, the infected cells were fixed and stained with DBA-FITC and DAPI as described in Materials and Methods. RH strain (**A**) and ME49 strain (**B**). The parasite morphology and fluorescence staining were examined under 600× magnification using fluorescence microscopy. BF, brightfield. Scale bars, 10µm.

4.2.2 z-FA-FMK and z-FA-DMK dose-dependently inhibits cathepsin B activity in Hs68 cells

Similar to z-FA-FMK, the analogue z-FA-DMK possess similar anti-proliferative effects and was able to induce cyst formation (Figure 4.6) in Hs68 cells infected with *T. gondii* parasites. These results strongly suggest that the inhibition of parasite proliferation mediated by both these cathepsin B inhibitors is most likely be due to the blocking of cathepsin B-like activity in *T. gondii* parasites.

To corroborate the effects of these inhibitors, cathepsin B activity was determined in cell lysates derived from Hs68 cells treated with z-FA-FMK or z-FA-DMK for 6h. As depicted in Figure 4.7A, both z-FA-FMK and z-FA-DMK induced a dose-dependent inhibition (up to 100μM) of cathepsin B activity in the cell lysates with ~70% inhibition in cathepsin B activity after 6h treatment. The cathepsin B activity in live cells was subsequently determined using Magic Red cathepsin B substrate. As shown in Figure 4.7B, both z-FA-FMK and z-FA-DMK dose-dependently (up to 100μM) significantly inhibited cathepsin B activity in live Hs68 cells with ~50% inhibition of cathepsin B activity after 6h treatment.

Collectively, the results shown in Figure 4.7A and 4.7B indicate that cathepsin B activity in Hs68 cells was significantly inhibited by both z-FA-FMK and z-FA-DMK. To further examine the effects of these inhibitors on cathepsin B activity after extended to 72h treatment, live cell imaging of cathepsin B activity in Hs68 cells treated with 100μM z-FA-FMK or z-FA-DMK was carried out. As shown in Figure 4.8, untreated Hs68 cells exhibit a strong red fluorescence within the cytoplasm compartment, demonstrating the normal level of cathepsin B activity in the live cells. In contrast, Hs68 cells treated with z-FA-FMK or z-FA-DMK exhibit a marked reduction in cathepsin B activity as indicated by reduced red fluorescence intensity in the cell. These results demonstrate that the presence of both z-FA-FMK and z-FA-DMK readily inhibited cathepsin B activity in Hs68 cells up to 72h.

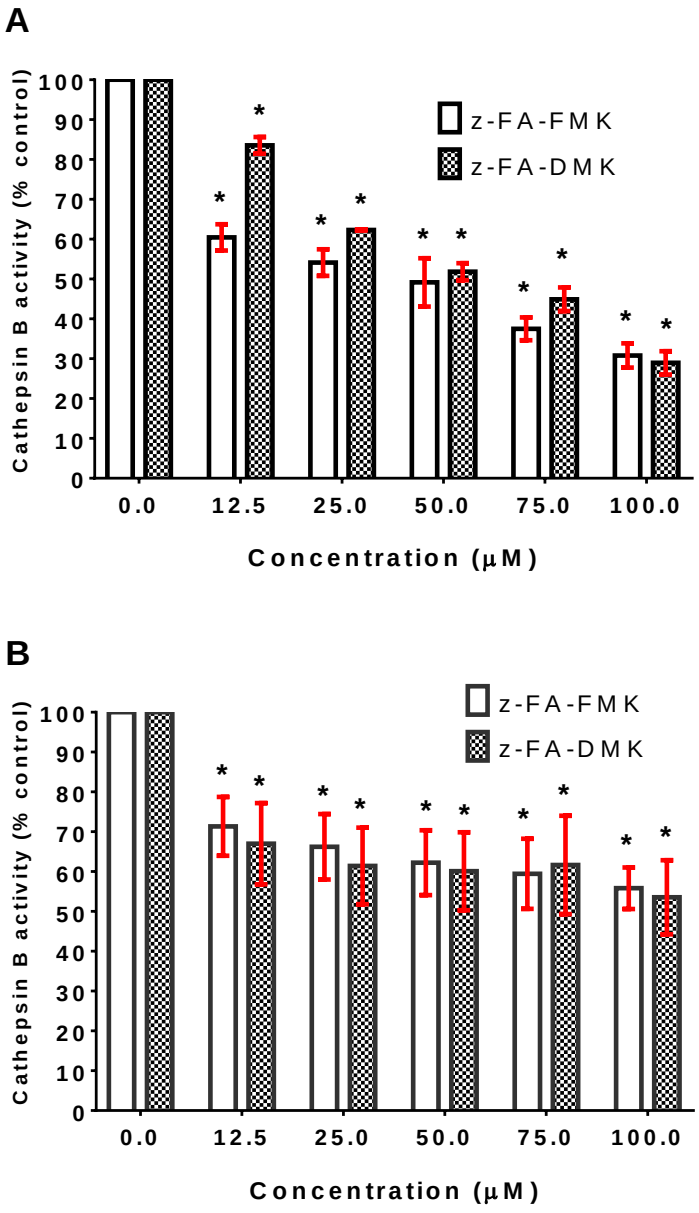

Figure 4.7. Effect of z-FA-FMK and z-FA-DMK on cathepsin B activity in Hs68 cells

Hs68 cells were treated with various concentrations of z-FA-FMK or z-FA-DMK for 6h. Cell lysates were prepared from these cells and cathepsin B activity determined using the fluorogenic substrate z-RR-AMC (**A**) or in live cells using Magic Red cathepsin B assay (**B**) as described in Materials and Methods. The cathepsin B activity from the cell lysates was normalized to protein concentration (30µg). The results are the means ± SEM from three independent experiments, where * indicates $p < 0.05$ versus untreated control.

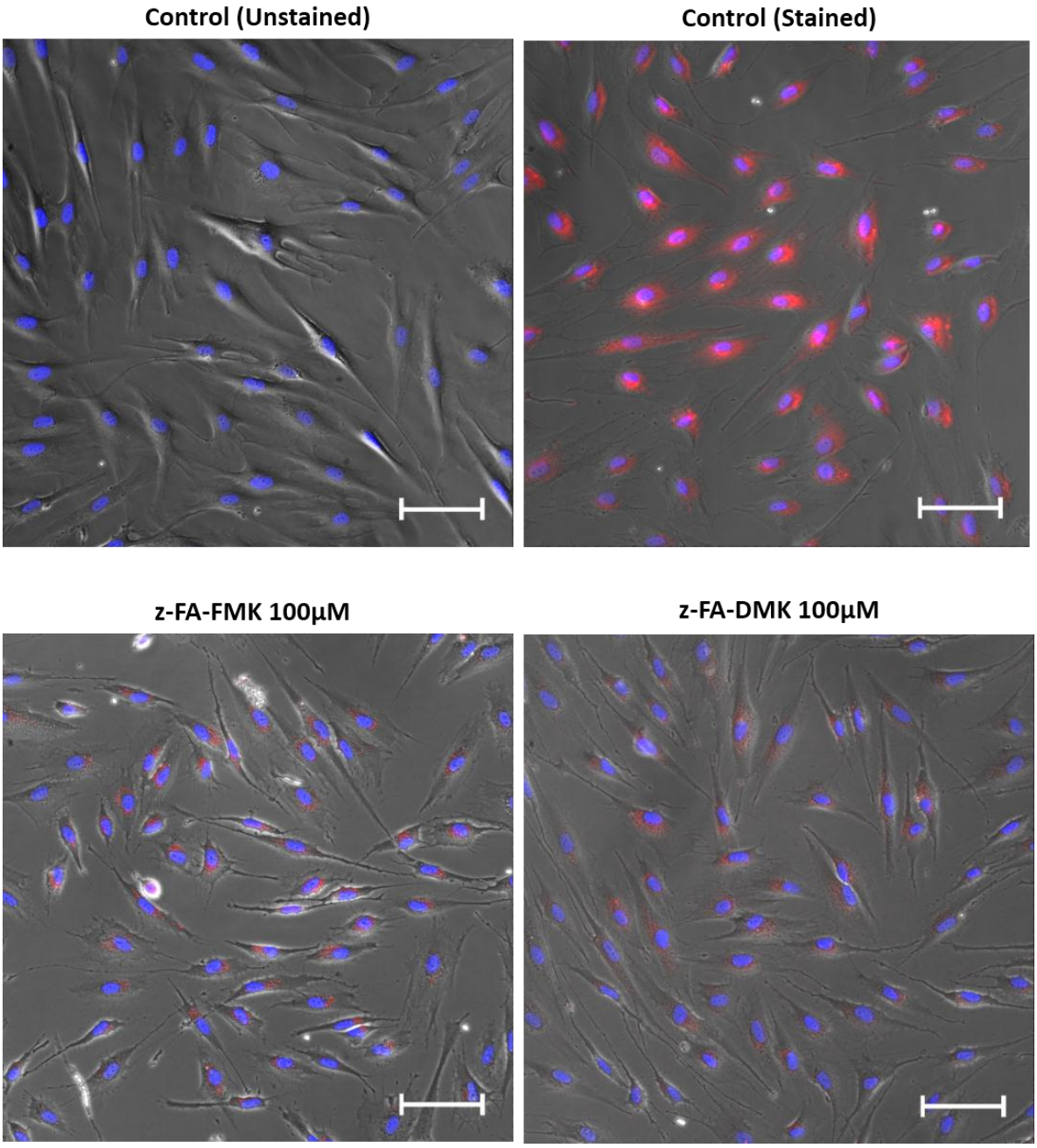

Figure 4.8. Fluorescence live cell imaging of cathepsin B activity in Hs68 cells

Hs68 cells were treated with 100µM z-FA-FMK or z-FA-DMK for 72h. The cells were stained with Magic Red cathepsin B substrate and counterstained with DAPI as described in Materials and Methods. Cells were examined under 20× magnification using fluorescence microscope. Scale bars, 50µm.

4.2.3 z-FA-FMK and z-FA-DMK inhibits cathepsin B activity in extracellular and intracellular *T. gondii* tachyzoites

Since both z-FA-FMK and z-FA-DMK effectively blocked cathepsin B activity in Hs68 cells (Figure 4.7 and 4.8), the effects of these inhibitors on *T. gondii* parasites cathepsin B-like activity was determined. Using live cell imaging, the cathepsin B activity in *T. gondii* infected Hs68 cells following treatment with 100µM z-FA-FMK or z-FA-DMK for 72h were analyzed. As shown in Figure 4.9., Hs68 cells infected with both strains of *T. gondii* (control RH strain and ME49 strain) without z-FA-FMK treatment exhibited a strong red fluorescence within the cytoplasm indicating the presence of cathepsin B activity in the live cells. Specifically, the live *T. gondii* parasites in the PVs (green arrow) were shown to display cathepsin B-like activity. Following z-FA-FMK or z-FA-DMK treatment, there was a marked reduction in cathepsin B activity in the cytosolic compartment as well as within the parasite PV of cells infected with parasites (RH and ME49 strain).

These findings were further corroborated by examining the effect of z-FA-FMK or z-FA-DMK on cathepsin B-like activity in extracellular *T. gondii* parasites. Lysates were prepared from parasites treated with z-FA-FMK or z-FA-DMK and the cathepsin B-like activity was determined using the fluorogenic substrate z-RR-AMC as described in Materials and Methods. As shown in Figure 4.10, the results indicated that both z-FA-FMK (Figure 4.10A) and z-FA-DMK (Figure 4.10B) readily inhibited cathepsin B activity in *T. gondii* (RH strain) in a time-dependent manner as shown by the decreased cathepsin B-like activity in the parasite lysates. The cathepsin B activity in the RH strain parasites was markedly reduced after 4h treatment with z-FA-FMK or z-FA-DMK. Similarly, z-FA-FMK (Figure 4.10C) and z-FA-DMK (Figure 4.10D) also induced a time-dependent inhibition of cathepsin B activity in the ME49 strain parasites.

To confirm these results, the effect of z-FA-FMK or z-FA-DMK on cathepsin B-like activity in *T. gondii* was determined using live imaging of extracellular parasites. As illustrated in Figure 4.11 and 4.12, live untreated extracellular parasites (RH and ME49 strain) exhibit a red fluorescence signal indicating the presence of cathepsin B-like activity in *T. gondii*

parasites. Following treatment with 100µM z-FA-FMK or z-FA-DMK for 6h, the cathepsin B activites in the extracellular parasites of both RH and ME49 strains were markedly diminished (Figure 4.11 and 4.12, respectively). These findings collectively suggest that z-FA-FMK and z-FA-DMK were able to block cathepsin B-like activity in both intracellular and extracellular parasites. Firstly, our results collectively indicate the presence of cathepsin B-like activity was detected in intracellular and extracellular *T. gondii* parasites and was readily blocked by z-FA-FMK and z-FA-DMK. Secondly, since *T. gondii* parasites undergo cyst formation following z-FA-FMK or z-FA-DMK treatment, this shows that cyst formation is not dependent upon cathepsin B-like activity in the parasites.

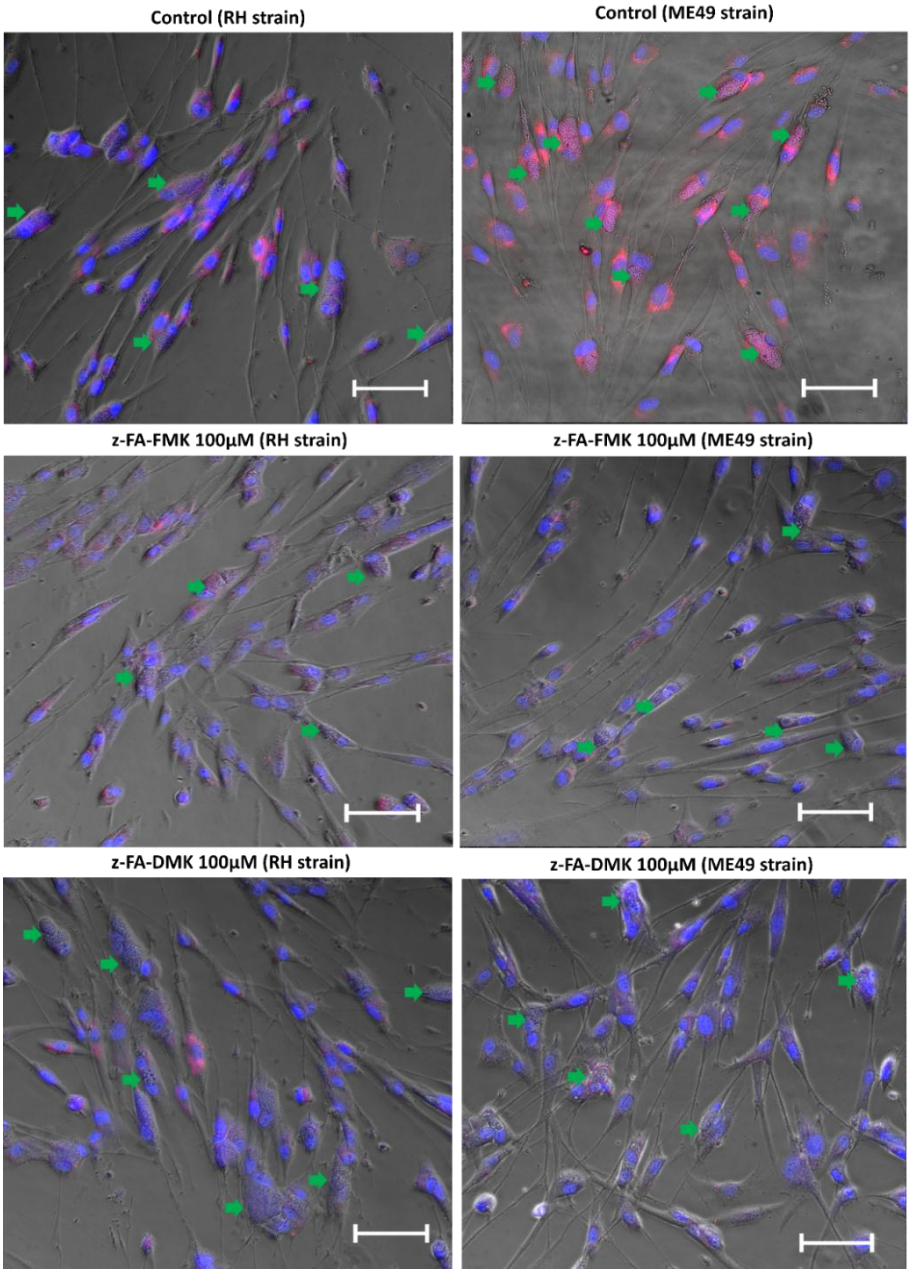

Figure 4.9. Live cell imaging of cathepsin B activity in *T. gondii* infected Hs68 cells

Hs68 cells infected with *T. gondii* were treated with 100µM z-FA-FMK or z-FA-DMK for 72h prior to staining with Magic Red cathepsin B substrate (Red signal), and counterstained with DAPI (Blue signal) as described in the Materials and Methods. Green arrows indicate PV containing *T. gondii* parasites. Cells were examined under 20× magnification using fluorescence microscope. Scale bars, 50µm. (Refer to Appendix: Figure A1-6 for full size images).

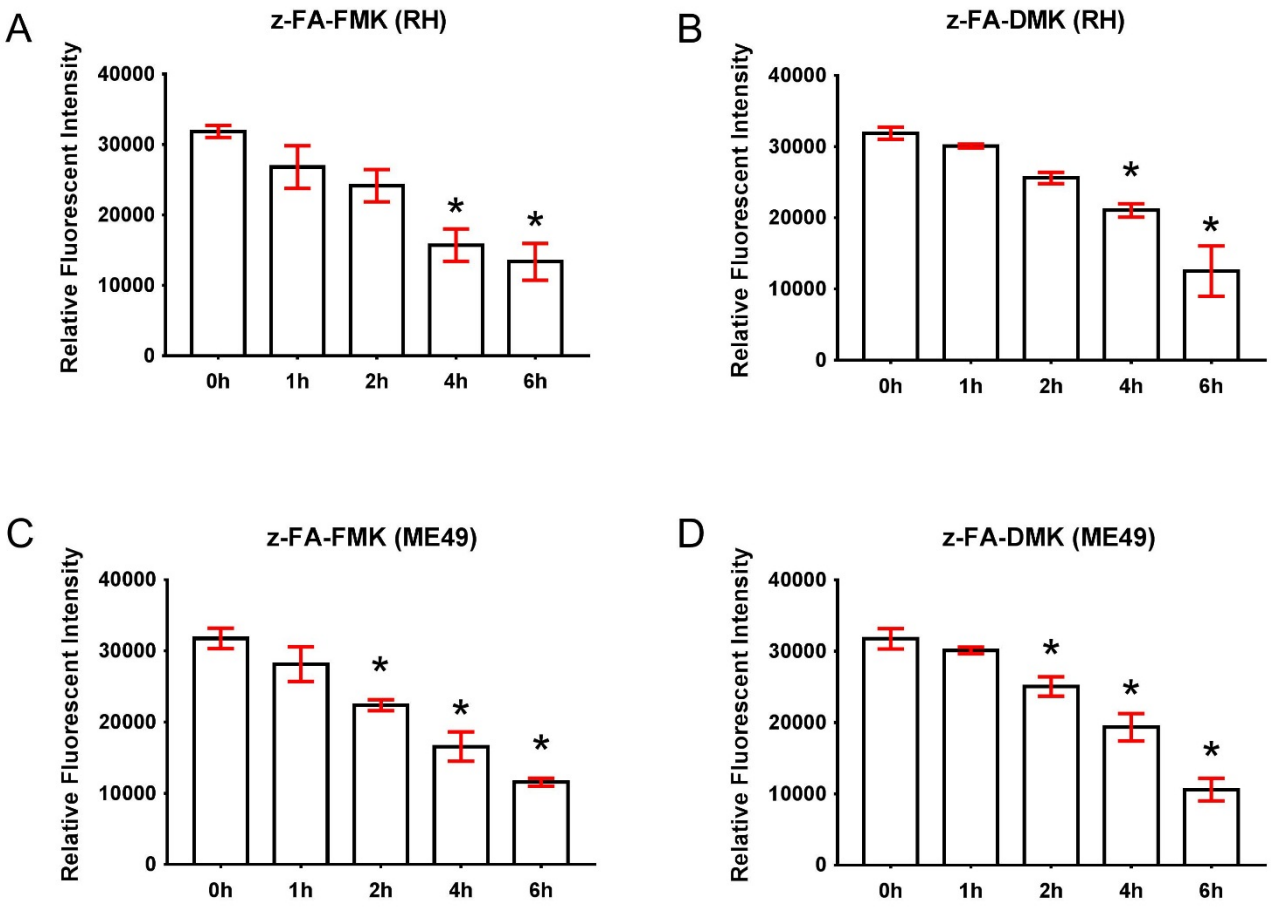

Figure 4.10. Effect of z-FA-FMK and z-FA-DMK on cathepsin B activity in *T. gondii* parasite lysates

Isolated extracellular *T. gondii* parasites from RH strain (**A** and **B**) and ME49 strain (**C** and **D**) were incubated with 100µM z-FA-FMK or z-FA-DMK for the time point where indicated. The cathepsin B activity in the parasites were determined using the fluorogenic substrate z-RR-AMC as described in the Materials and Methods. The cathepsin B activity from the lysates was normalized to protein concentration of 30µg. The results are the means ± SEM from three independent experiments, where * indicates $p < 0.05$ versus 0h treatment.

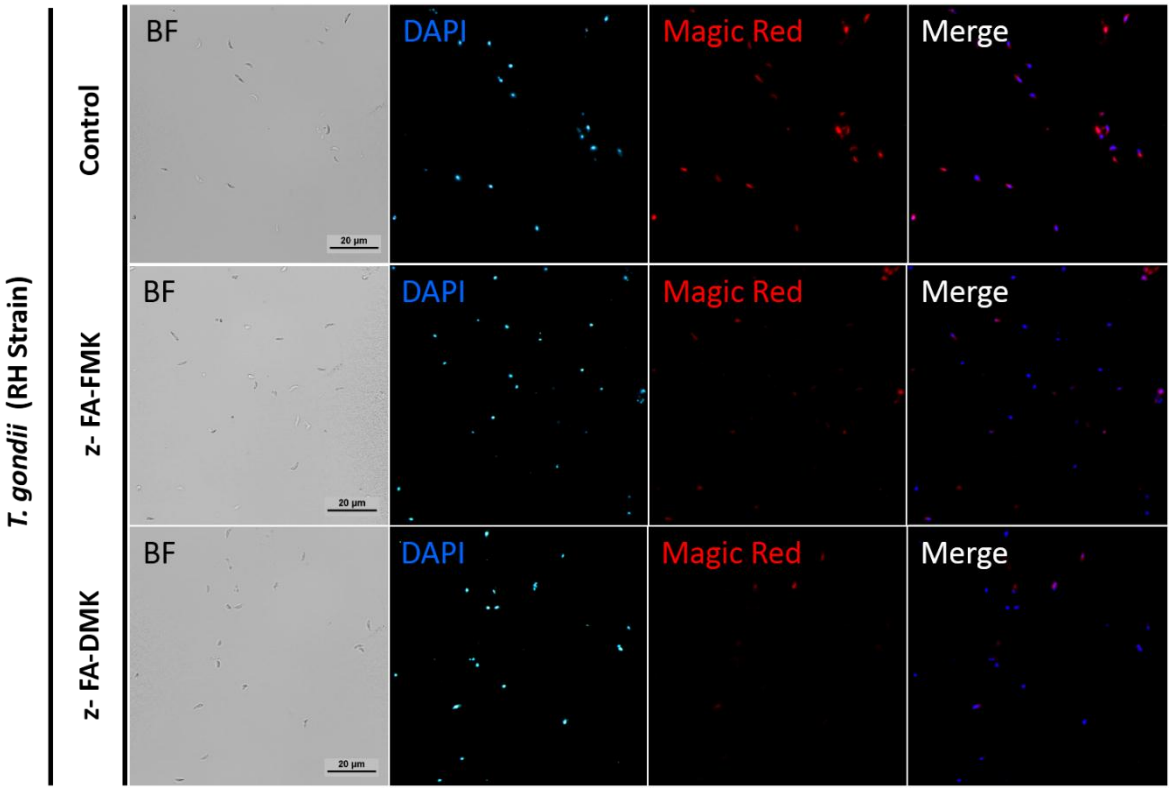

Figure 4.11. Effect of z-FA-FMK and z-FA-DMK on cathepsin B activity in *T. gondii* parasites (RH strain)

Extracellular RH strain *T. gondii* parasites were incubated with 100µM z-FA-FMK or z-FA-DMK for 6h and the cathepsin B activity in the live parasites determined using Magic Red substrate and counterstained with DAPI as described in Materials and Methods. Parasites were examined under 60× magnification using fluorescence microscope. BF, brightfield. Scale bars, 20µm.

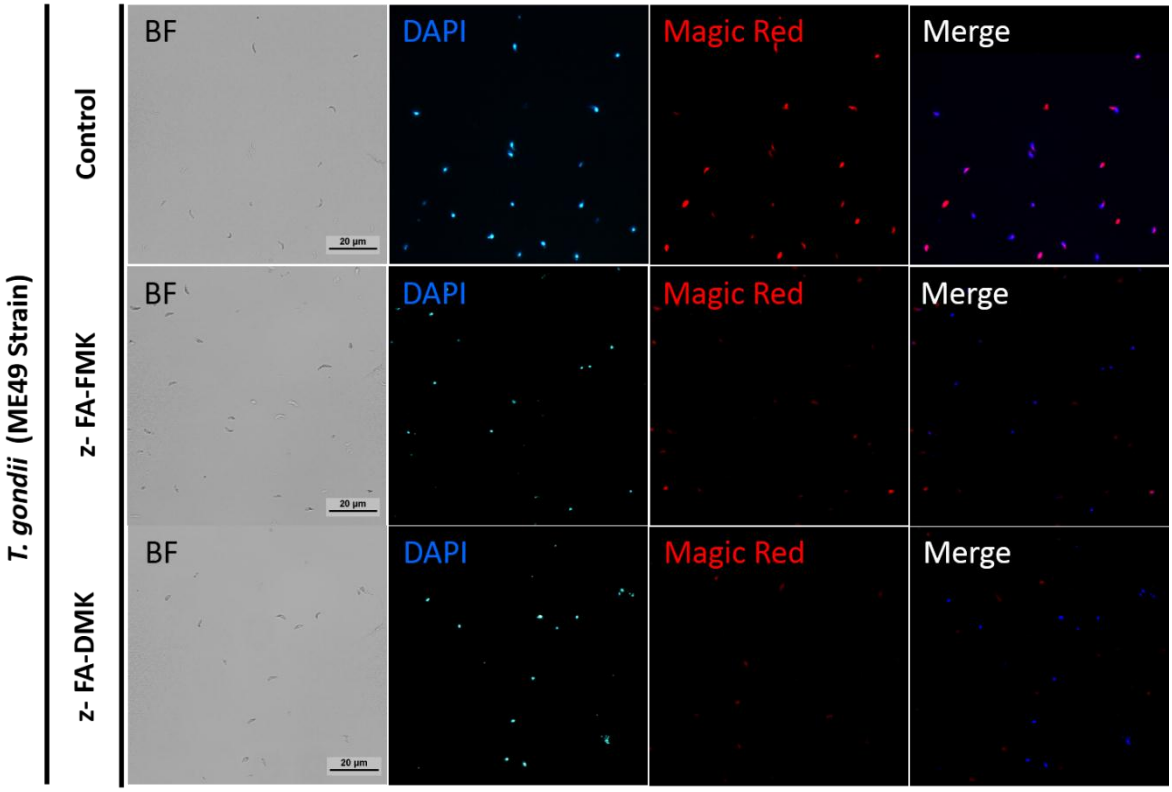

Figure 4.12. Effect of z-FA-FMK and z-FA-DMK on cathepsin B activity in *T. gondii* parasites (ME49 strain)

Extracellular ME49 strain *T. gondii* parasites were incubated with 100µM z-FA-FMK or z-FA-DMK for 6h and the cathepsin B activity in the live parasites determined using Magic Red substrate counterstained with DAPI as described in Materials and Methods. Parasites were examined under 60× magnification using fluorescence microscope. BF, brightfield. Scale bars, 20µm.

4.2.4 Proliferation of *T. gondii* tachyzoites is not dependent on autophagy

Earlier results showed that cathepsin B-like activity in both Hs68 cells (Figure 4.7 and 4.8) and intracellular *T. gondii* parasites (Figure 4.9) were markedly inhibited following z-FA-FMK and z-FA-DMK treatment. These findings suggest that *T. gondii* cyst formation mediated by z-FA-FMK and z-FA-DMK may be associated with the inhibition of cathepsin B-like activity. To this end, studies have been reported that *T. gondii* possess cathepsin B-like protease known as *Tg*CPB, which is associated with the proteolytic function of the VAC (Di Cristina *et al*., 2017, O'Brien *et al*., 2008, Que *et al*., 2002). The VAC is mainly responsible for protein digestion where its disruption could potentially lead to starvation and induction of autophagy in *T. gondii* parasites (Di Cristina *et al*., 2017, Dou *et al*., 2014, Siqueira-Neto *et al*., 2018, Subauste, 2019). The results so far suggest that the cathepsin B inhibitor, z-FA-FMK may be blocking *T. gondii* proliferation by inducing starvation via the disruption of VAC proteolytic function.

To this end, if z-FA-FMK is indeed inducing parasite starvation by disrupting VAC function, then this would lead to the impairment of protein catabolism and induction of autophagy in *T. gondii*. Therefore, the involvement of autophagy in *T. gondii* proliferation was investigated using autophagic inhibitors, Chloroquine (CQ) and 3-Methyladenine (3-MA). Firstly, the role of autophagy is required during normal *T. gondii* parasite proliferation in the absence of z-FA-FMK was examined. Hs68 cells infected with both strains (RH or ME49) *T. gondii* parasites were treated with various doses of CQ or 3-MA across different time points where indicated.

As shown in Figure 4.13, CQ up to 15µM was shown to have minimal effect on formation of new PVs in both RH and ME49 strains of *T. gondii* over 72h (Figure 4.13A and 4.13C respectively). Similarly, CQ up to at 15µM has little effect on total parasite number in both RH and ME49 strains (Figure 4.13B and 4.13D respectively). Similar to CQ, 3-MA which blocks the formation of autophagosomes was found to have little effect on PV formation and total parasite count in Hs68 cells infected with both strains of *T. gondii* (RH and ME49) as shown in Figure 4.14. Collectively, these findings demonstrate that blocking the autophagic

pathway using autophagic inhibitors, CQ and 3-MA, have no significant inhibitory effect on intracellular parasite proliferation under normal conditions and that the parasites were able to progress through the proliferative lytic cycle.

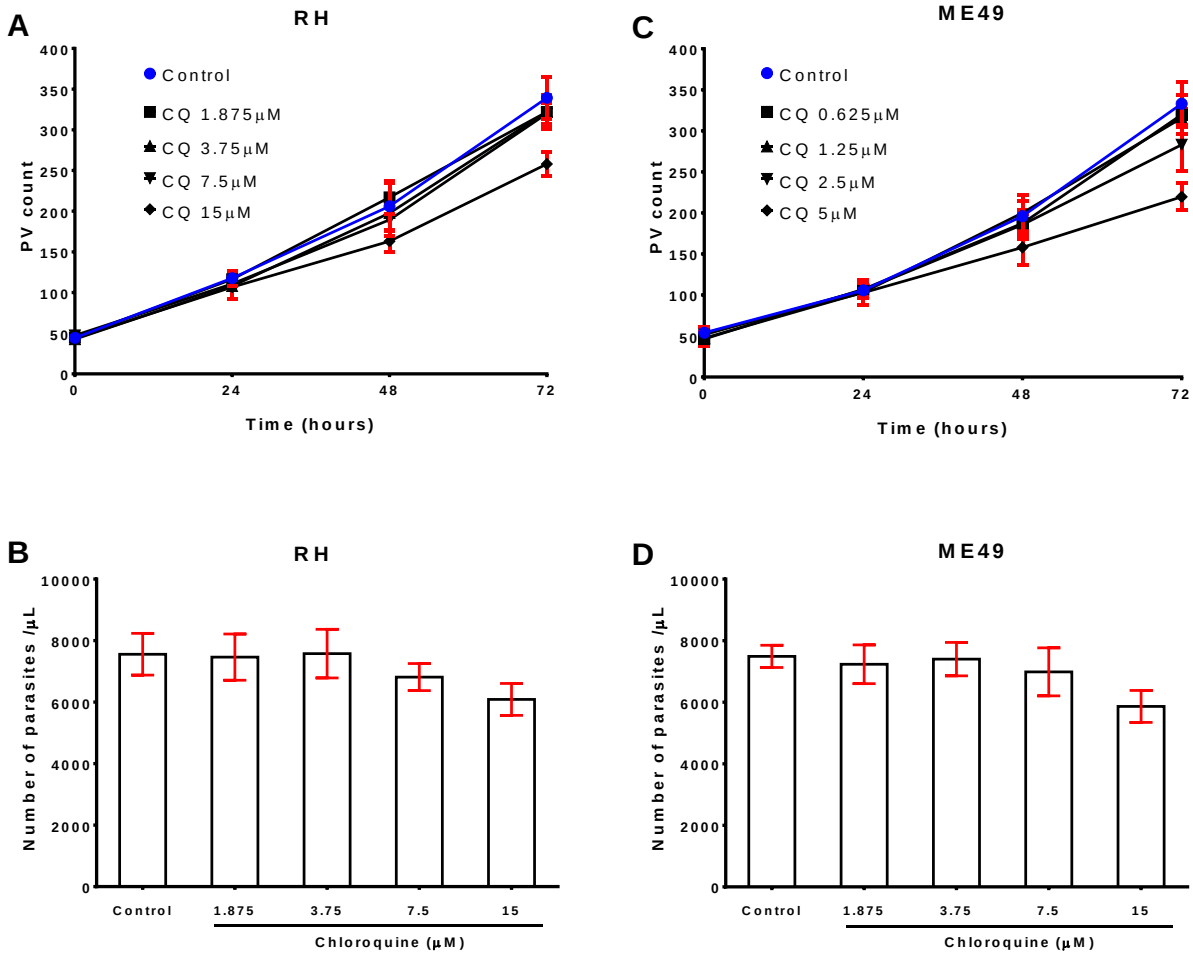

Figure 4.13. Effect of CQ on *T. gondii* tachyzoite proliferation in Hs68 host cells

Hs68 cells infected with *T. gondii*, were treated with various concentrations of CQ. The number of PV were determined at time points where indicated (**A, C**) and parasite count (**B, D**) were determined 72h following CQ treatment. The number of PVs were scored across 10 randomized microscopic field. The number of tachyzoites was determined using the trypan blue exclusion assay as described in Materials and Methods. The results represent the means ± SEM from three independent experiments.

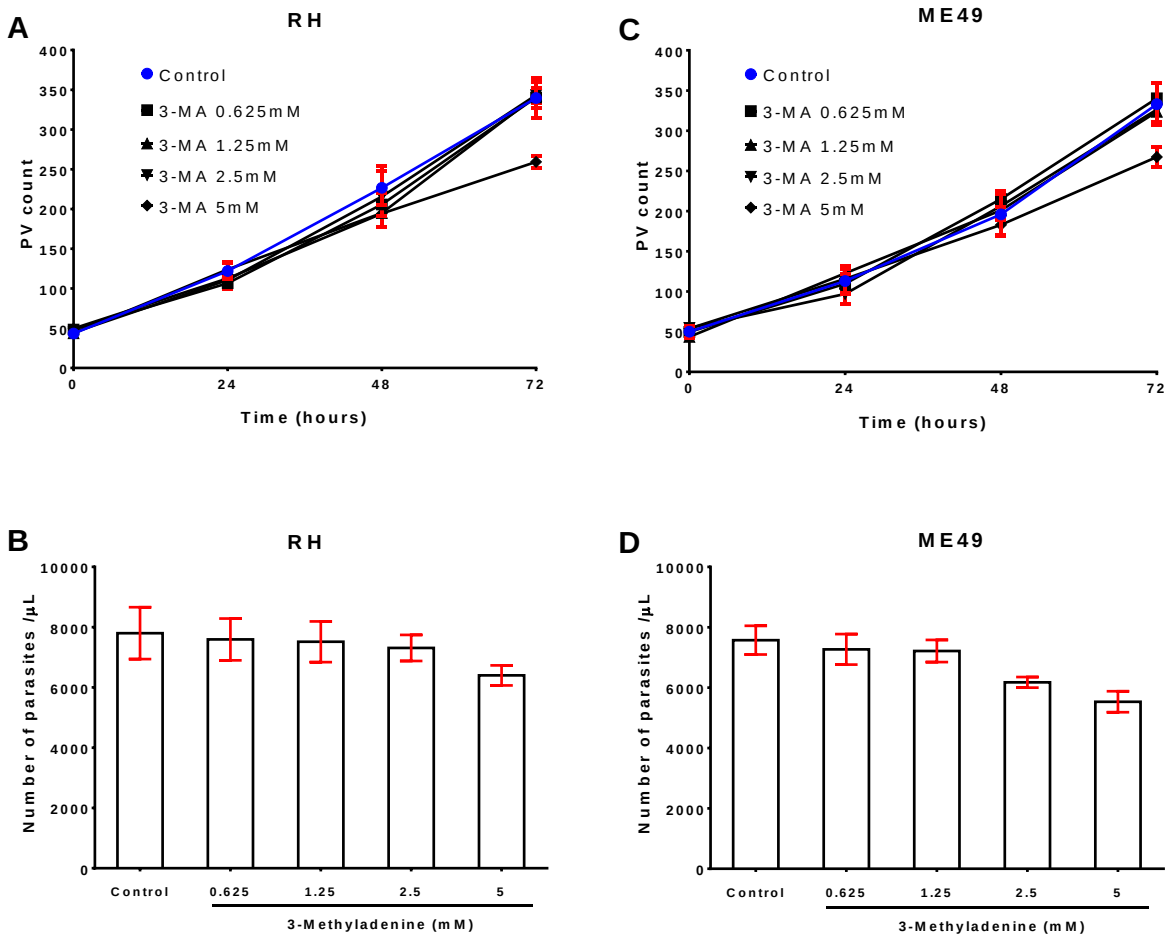

Figure 4.14. Effect of 3-MA on *T. gondii* tachyzoite proliferation in Hs68 host cells

Hs68 cells infected with *T. gondii*, were treated with various concentrations of 3-MA. The number of PV were determined at time points where indicated (**A, C**) and parasite count (**B, D**) were determined 72h following 3-MA treatment. The number of PVs were scored across 10 randomized microscopic field and number of tachyzoites was determined using the trypan blue exclusion assay as described in Materials and Methods. The results represent the means ± SEM from three independent experiments.

4.2.5 Autophagy inhibitor CQ and 3-MA inhibits recovery of *T. gondii* following z-FA-FMK inhibition

The induction of autophagy in *T. gondii* parasites has previously been observed in the parasites following drug treatment or conditions which leads to starvation (Besteiro *et al*., 2011a, Ghosh *et al*., 2012). Therefore, it is not surprising that both CQ and 3-MA have no apparent effect on the proliferation of intracellular *T. gondii* tachyzoites as they were not under any form of stress of starvation. To further corroborate if z-FA-FMK disrupts VAC proteolytic function and leads to nutrient starvation in *T. gondii* parasites, we examined the induction of autophagy in proliferation inhibited parasites following z-FA-FMK treatment. The activation of autophagic pathway following z-FA-FMK treatment would imply that the *T. gondii* parasites are likely to be undergoing starvation due to the disruption of VAC. To this end, Hs68 cells infected with *T. gondii* were treated with z-FA-FMK for 72h before washing off the drug. The infected Hs68 cells were replaced with fresh media supplemented with either CQ or 3-MA and further cultured for 144h. To this end, we examined the effects of blocking autophagy on the ability of z-FA-FMK treated *T. gondii* parasites to regain proliferation over time.

As shown in Figure 4.15A and 4.15C, the number of PVs remain unchanged following 72h post withdrawal of z-FA-FMK in Hs68 cells infected with both strains of *T. gondii* (control). The lack of PV increment during the first 72h post withdrawal of z-FA-FMK could be due to the irreversible effect of the cathepsin B inhibitor. Thereafter, the number of PVs in Hs68 cells start to increase and reaches ~250 PVs in cells infected with both RH and ME49 strains. The presence of CQ dose-dependently inhibited the recovery of proliferation inhibited *T. gondii* (RH and ME49 strain, respectively) indicated by the decrease in PVs following z-FA-FMK withdrawal. Similarly, the increased in total number of parasites in Hs68 cells infected with both RH and ME49 strain after removal of z-FA-FMK was significantly reduced as the concentration of CQ increased (Figure 4.15B and 4.15D respectively). These results showed that CQ at 15μM exhibited the strongest effect on *T. gondii* recovery as indicated by the lowest number of PV and parasite count.

Similarly, the presence of 3-MA also decreased the formation of PVs for RH and ME49 strains following z-FA-FMK withdrawal in a dose-dependent manner (Figure 4.16A and 4.16C, respectively), suggesting that the recovery of encysted *T. gondii* has been impaired. Likewise, the increase in total parasite number in both RH and ME49 strains following z-FA-FMK withdrawal was significantly reduced dose-dependently by the presence of 3-MA (Figure 4.16B and 4.16D, respectively). Similarly, a high concentration of 3-MA (5mM) had the strongest inhibitory effect on encysted *T. gondii* recovery.

Collectively, these results demonstrated that autophagy inhibitors CQ and 3-MA prevented the z-FA-FMK treated parasites from regaining the ability to proliferate upon the withdrawal of z-FA-FMK. This highlights that autophagy appears to be essential for the z-FA-FMK treated *T. gondii* parasites to recover and regain virulence. Hence, the results do suggest that z-FA-FMK may induce stress in *T. gondii* tachyzoites which is associated with nutrient starvation that leads to the induction of autophagy.

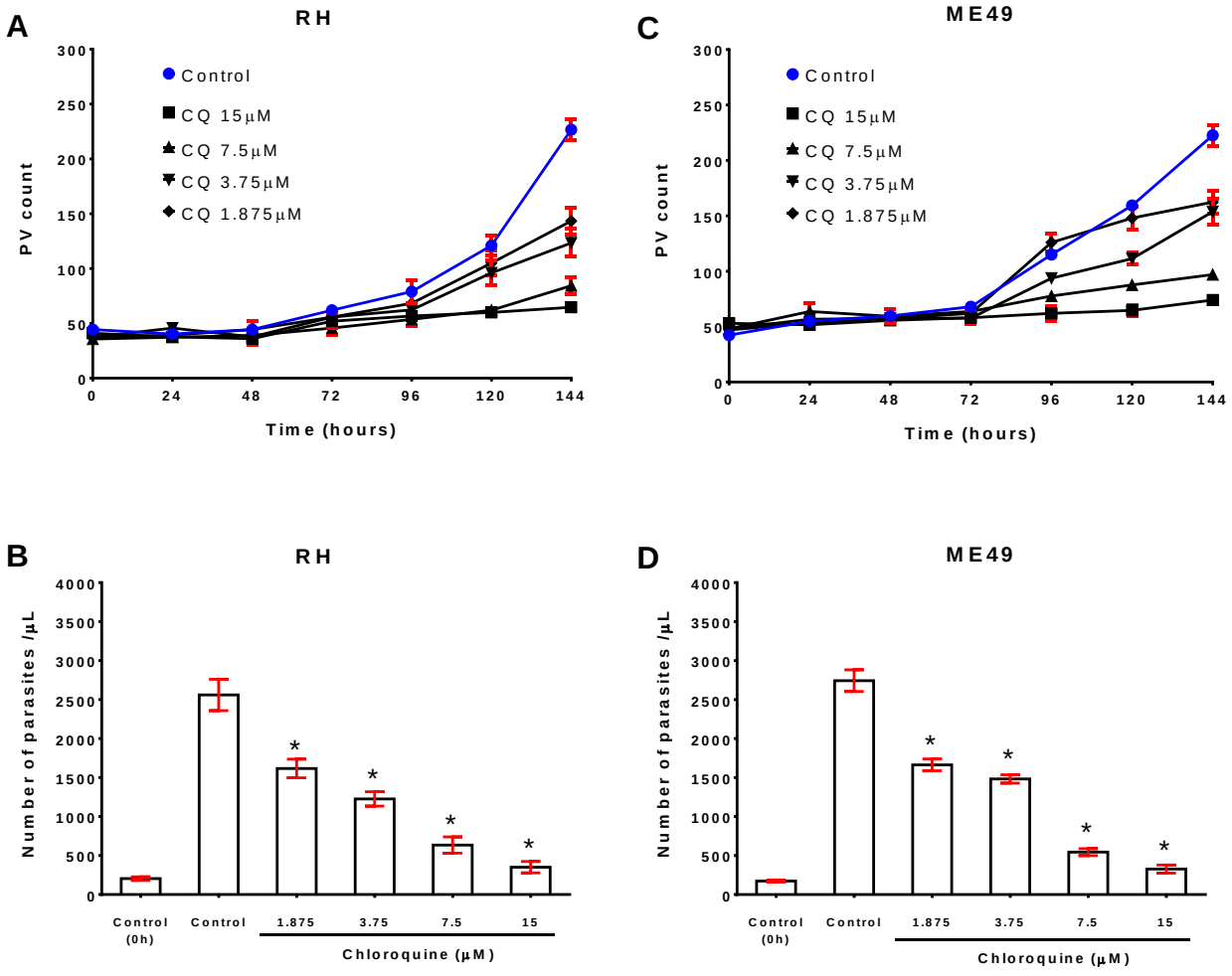

Figure 4.15. Effect of CQ on the recovery of *T. gondii* PV formation following z-FA-FMK withdrawal

Hs68 cells infected with *T. gondii* (RH or ME49 strains) were treated with 100μM z-FA-FMK for 72h. After treatment, the infected Hs68 cells were washed off z-FA-FMK, replaced with fresh media before cultured in the presence or absence of various concentrations of CQ. The number of PVs (**A, C**) in Hs68 cells were determined at the time points where indicated and the total parasite count (**B, D**) was determined after 144h. The PVs were examined under 40× magnification and scored across 10 randomized microscopic field. The number of tachyzoites was determined using the trypan blue exclusion as described in Materials and Methods. The results represent the means ± SEM from three independent experiments, where * indicates $p < 0.05$ versus control.

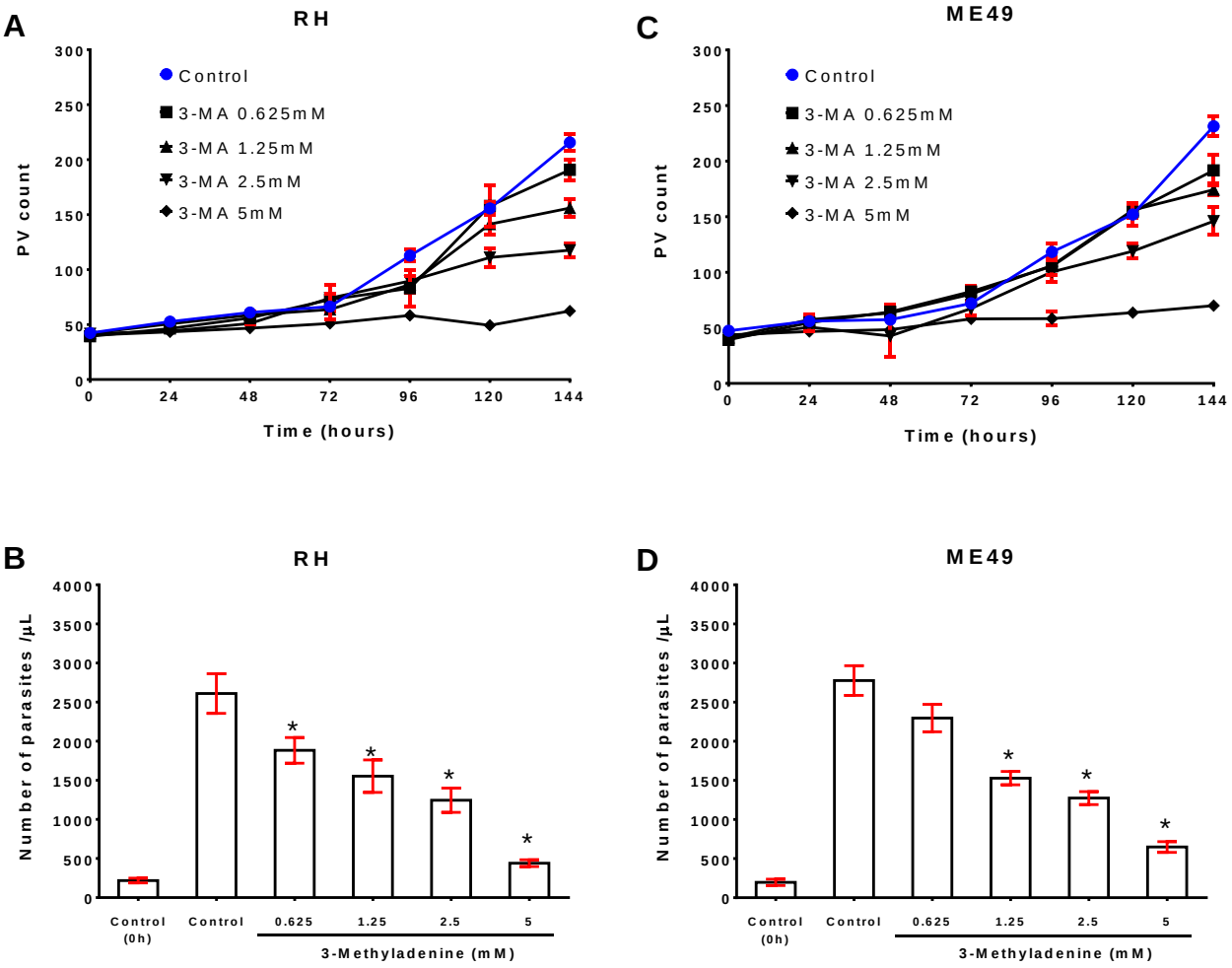

Figure 4.16. Effect of 3-MA on the recovery of *T. gondii* proliferation following z-FA-FMK withdrawal

Hs68 cells infected with *T. gondii* (RH or ME49 strains) were treated with 100µM z-FA-FMK for 72h. After treatment, the infected Hs68 cells were washed off z-FA-FMK, replaced with fresh media before cultured in the presence or absence of various concentrations of 3-MA. The number of PVs (**A, C**) was determined at the time points where indicated whereas the total parasite count (**B, D**) in Hs68 cells was assessed after 144h. The PVs were examined under 40× magnification and scored across 10 randomized microscopic field. The total number of tachyzoites was determined using the trypan blue exclusion as described in Materials and Methods. The results represent the means ± SEM from three independent experiments, where * indicates $p < 0.05$ versus control.

4.3 Discussion

In eukaryotic cells, cathepsin proteases are primarily known to function as lysosomal enzymes that digest endocytosed polypeptides for nutrient acquisition (Dou and Carruthers, 2011). Similarly, protozoan parasites also utilize cathepsin proteases for protein degradation and other specialized functions which are essential for parasite survival (Dou and Carruthers, 2011). For example, the cysteine proteinase cathepsin L in *P. falciparum* has been shown to be vital for the digestion of hemoglobin in the parasite food vacuole (Rosenthal, 2004), while cysteine protease cathepsin B is essential for iron acquisition in *T. brucei* (O'Brien *et al*., 2008). Furthermore, blocking the cysteine proteinase, cruzipain in *T. cruzi* reduced infection and amastigotes replication (Franke de Cazzulo *et al*., 1994, Harth *et al*., 1993). Cathepsins have been shown to be important in *T. gondii* parasites for cell invasion, digestion of host proteins for proliferation (Dou *et al*., 2014, Que *et al*., 2007), and involved in autophagy to maintain the survival of cysts (Di Cristina *et al*., 2017). The redundancy of cathepsin genes is lower in *T. gondii* than in most other studied parasites where it encodes only one cathepsin B (*Tg*CPB), one cathepsin L (*Tg*CPL), and three cathepsin Cs (*Tg*CPC1, 2, and 3), potentially making them more effective drug targets. Therefore, parasite cathepsin proteases have been explored as potential targets for anti-parasitic drug development. Despite the seemingly importance of cathepsin proteases in *T. gondii*, there are currently still no approved drugs targeting this group of enzymes (Siqueira-Neto *et al*., 2018).

Earlier results have shown that z-FA-FMK, which is an irreversible cathepsin B inhibitor, readily blocked *T. gondii* proliferation and induced the formation of cysts in infected Hs68 cells (chapter 3). To ascertain that the effects of z-FA-FMK are due to the inhibition of cathepsin B, the effect of a highly specific cathepsin B inhibitor, z-FA-DMK on *T. gondii* proliferation was compared. Being an analogue of z-FA-FMK, z-FA-DMK has no reported side effects and unreactive towards other classes of proteinases (Green and Shaw, 1981, Liow and Chow, 2013). The results showed that similar to z-FA-FMK, z-FA-DMK was able to inhibit *T. gondii* parasite proliferation dose-dependently and induced cyst formation. These findings suggest that inhibition of cathepsin B is likely to be involved in blocking *T. gondii*

parasite proliferation followed by cyst formation in Hs68 host cells mediated by both z-FA-FMK and z-FA-DMK.

The cathepsin B of *Toxoplasma gondii*, *Tg*CPB have a specific substrate specificity for Arg/Arg substrates, such as the z-Arg-Arg-AMC (z-RR-AMC), where z, acts as the N-terminal blocking group while AMC is a fluorogenic leaving group following substrate hydrolysis (Que *et al*., 2002, Sajid and McKerrow, 2002). Using the cathepsin B specific fluorogenic substrate z-RR-AMC and Magic Red cathepsin B substrate, the results indicate that both cathepsin B inhibitors, z-FA-FMK and z-FA-DMK readily inhibited cathepsin B activity in Hs68 cells and *T. gondii* parasites (RH and ME49 strain) in a dose- and time-dependent manner. Live imaging of cathepsin B activity in Hs68 cells and *T. gondii* parasites using Magic Red cathepsin B substrate further confirm the diminished cathepsin B activity upon z-FA-FMK or z-FA-DMK treatment. Collectively, these findings strongly suggest a correlation between diminished cathepsin B activity and inhibition of *T. gondii* proliferation.

Several studies have proposed that both *T. gondii* cathepsins, *Tg*CPB and *Tg*CPL work in unison in numerous specialized functions to support *T. gondii* infection and persistence. Both *Tg*CPB and *Tg*CPL are predominantly localized in the *Toxoplasma* lysosomal VAC, a lysosome-like organelle where endocytosed host cytosolic proteins are digested for nutrient acquisition (Di Cristina *et al*., 2017, Dou and Carruthers, 2011, McGovern *et al*., 2018). Inhibition of *Tg*CPB with a peptidyl cathepsin B inhibitor or antisense RNA led to impairment of host cell invasion, diminished *in vitro* growth and reduced *in vivo* infection in chick embryo by *T. gondii* (Dou *et al*., 2013, Que *et al*., 2002, Que *et al*., 2004). Treatment of *T. gondii* parasite with the cathepsin inhibitor morpholinurea-leucyl-homophenyl-vinyl sulfonephenyl (LHVS) blocked host cell invasion by inhibiting parasite microneme secretion (Larson *et al*., 2009, Teo *et al*., 2007). Furthermore, *Tg*CPL knockout and inhibition have been shown to impair *T. gondii* cyst survival in chronic infection (Di Cristina *et al*., 2017). The results presented in this chapter which demonstrated the association between cathepsin B inhibition and reduced parasite proliferation are very much in line with these published findings. Since both *Tg*CPB and *Tg*CPL are predominantly situated in the *Toxoplasma* VAC,

their proteolytic function are pivotal for *Toxoplasma* persistence both *in vitro* and *in vivo* (Di Cristina *et al*., 2017). Upregulation of *Tg*CPB and *Tg*CPL have been reported in mice with chronic toxoplasmosis infection, suggesting potential importance of these enzymes in *T. gondii* cysts formation during chronic infection (Pittman *et al*., 2014). In line with this, studies have reported that *Toxoplasma* cyst demise caused by the inhibition of both *Tg*CPB and *Tg*CPL, exhibited excessive accumulation of organellar remnants in the VAC (Di Cristina *et al*., 2017, Siqueira-Neto *et al*., 2018). This suggests that autophagy is likely to be important for bradyzoites during chronic infection, possible involved in organelle turnover during parasite differentiation or as a survival response towards nutritional limitation (Di Cristina *et al*., 2017).

The results in this chapter also demonstrated that both autophagy inhibitor CQ and 3-MA had no significant effect on *T. gondii* tachyzoite proliferation under normal culture conditions. CQ is a well-known anti-malarial drug which also inhibits downstream of the autophagy cascade by impairing autophagosome fusion with the lysosomes (Mauthe *et al*., 2018). On the other hand, 3-MA inhibits type III Phosphatidylinositol 3-kinases (PI-3K) which ultimately blocks the formation of the autophagosome entirely upstream of the autophagy cascade (Stroikin *et al*., 2004). It has been suggested that autophagy in *T. gondii* cysts facilitates the renewal of organelles during the chronic stage or a stress response towards limited nutrient availability (Di Cristina *et al*., 2017). Our results therefore indicate that autophagy is not required in actively proliferating tachyzoites in the absence of stress.

To determine whether z-FA-FMK-treated *T. gondii* parasites are under stress conditions associated with nutrient deprivation, the involvement of autophagy following z-FA-FMK treatment was examined. To this end, we utilize the fact that upon z-FA-FMK withdrawal from *T. gondii* infected Hs68 cells the parasite will slowly recover, and eventually proliferate and resume the lytic cycle. Both autophagy inhibitors, CQ and 3-MA inhibited the recovery of *T. gondii* parasites in Hs68 cells following z-FA-FMK withdrawal in a dose-dependent manner. These results demonstrated that CQ and 3-MA, prevented the *T. gondii* parasites from regaining virulence and the ability to proliferate as shown by the low number of PVs

and decreased total parasite count. This suggested that *T. gondii* parasites in Hs68 host cells treated with z-FA-FMK are dependent on the autophagic process to regain virulence. Therefore, the inhibition of both host and *T. gondii* parasite autophagy using 3-MA could greatly limit amino acid availability, and amino acid deprivation is a potent inducer of autophagy (Ghosh *et al*., 2012, Wang and Klionsky, 2011, Wang *et al*., 2009). The autophagic cascade assumes a cell survival function under nutrient limitation, by selective degradation of dispensable cellular components and organelles in the cell in exchange for increased pools of nutrients to sustain cellular functions and cope with starvation (Klionsky *et al*., 2011, Kristensen *et al*., 2008, Weidberg *et al*., 2011). Therefore, the results demonstrated that autophagy inhibitors CQ and 3-MA, which showed no effect on the proliferation of untreated parasites blocked the recovery of *T. gondii* proliferation following z-FA-FMK withdrawal. Hence, this demonstrates that autophagy is essential for the z-FA-FMK treated parasites in order to regain its proliferation upon withdrawal of z-FA-FMK.

Taken together, our results in this chapter demonstrated that the z-FA-FMK analog, z-FA-DMK was able to block the proliferation of *T. gondii* parasites and induce cyst formation. This suggest that the anti-proliferative effects of these inhibitors are associated with cathepsin B activity inhibition. In line with this, both z-FA-FMK and z-FA-DMK inhibited cathepsin B activity in both Hs68 cells and *T. gondii* parasites. Since cathepsin B is associated with the proteolytic function of VAC in *T. gondii* parasites, z-FA-FMK treatment is likely to induce starvation in *T. gondii* parasites by disrupting protein catabolism mediated via cathepsin B in the VAC. To this end, we have demonstrated that z-FA-FMK treatment is associated with the induction of autophagy in *T. gondii* parasites, possibly as a stress response towards starvation.

CHAPTER FIVE

Role of oxidative stress in the anti-proliferative effects of z-FA-FMK and possible synergistic effects with BSO on *T. gondii* proliferation

5.1 Introduction

Oxygen plays a vital role in the oxidative phosphorylation pathway. It acts as the terminal electron acceptor and drives adenosine triphosphate (ATP) production and major metabolic processes in aerobic organisms (Quijano *et al*., 2015). Reactive oxygen species (ROS) are chemically reactive molecules containing oxygen, which are produced endogenously by living organisms during normal cellular metabolism, predominantly via the incomplete or partial reduction of oxygen (Gorlach *et al*., 2015, Mailloux *et al*., 2013, Mansfield *et al*., 2004). On the other hand, ROS are also generated endogenously in cells upon exposure to xenobiotics or environmental insults (Birben *et al*., 2012, Kurutas, 2016, Martindale and Holbrook, 2002). Additionally, immune effector cells also utilize ROS in a process known as oxidative burst to combat microbial infection (Kwok *et al*., 2004, Liguori *et al*., 2018, Phaniendra *et al*., 2015). Oxidative stress in cells occurs when the balance between antioxidants and pro-oxidants is disrupted, often defined by the depletion of antioxidant levels accompanied by excessive accumulation of ROS (Birben *et al*., 2012, Ozougwu, 2016, Rahal *et al*., 2014). ROS can be classified into free radicals and non-radicals. The former are reactive molecules containing one or more unpaired electrons and the latter consist of 2 free radicals with shared unpaired electrons which give rise to non-radical ROS (Birben *et al*., 2012). The 3 major subclasses of ROS that are of physiological significance are superoxide anions, hydrogen peroxide (H_2O_2) and hydroxyl radicals (Birben *et al*., 2012, Zang *et al*., 2013, Zou *et al*., 2017). Among these classes of ROS, hydroxyl radicals are the most reactive and can readily react with organic and inorganic molecules and cause severe oxidative damage to cells (Birben *et al*., 2012, Phaniendra *et al*., 2015).

Excessive increase in intracellular ROS leads to oxidative stress in a cell and can cause adverse modifications to vital cellular components, mainly lipids, proteins, and DNA, which could lead to cellular dysfunction and cell death (Andreyev *et al*., 2005, Birben *et al*., 2012, Slesak *et al*., 2016, Trachootham *et al*., 2008). Despite the harmful effects associated with ROS, low to moderate concentrations are often found to be involved in physiological

processes or as secondary messengers of signal transduction pathways (Gorlach *et al*., 2015, Reczek and Chandel, 2015).

In order to regulate ROS levels and protect against ROS-mediated damages, aerobic organisms have robust antioxidant systems, including enzymatic and non-enzymatic antioxidants which are extremely efficient in controlling intracellular ROS (Birben *et al*., 2012, Rahal *et al*., 2014, Slesak *et al*., 2016). The non-enzymatic antioxidants have the ability to inactivate ROS rapidly and mainly consist of low molecular weight molecules, including glutathione, ascorbic acid, tocopherols and flavonoids (Mirończuk-Chodakowska *et al*., 2018, Schippers *et al*., 2012, Slesak *et al*., 2016, Waśkiewicz *et al*., 2014). The enzymatic antioxidants, which include superoxide dismutase (SOD), catalase (CAT) and glutathione peroxidase (GPx) work by breaking down ROS and scavenging free radicals (Halliwell, 1999, Simon *et al*., 2000). In living cells, SODs catalyze superoxide radicals into H_2O_2 and oxygen (Fridovich, 1995, Younus, 2018), whereas GPx *and* CATs break down H_2O_2 into water and oxygen (Lubos *et al*., 2011). Enzymatic antioxidants can be classified into primary or secondary enzymatic antioxidants. Primary enzymatic antioxidants such as CAT and SOD react directly with pro-oxidants whereas secondary enzymatic antioxidants such as glutathione reductase (GR) and glutathione-s-transferase (GST) regenerates low molecular weight antioxidant molecules to ensure their continuous antioxidant activity (Halliwell, 1999, Kurutas, 2016).

Most of the pathologically significant parasitic protozoa including *T. gondii* are aerobic organisms and depend on oxidative phosphorylation in the mitochondria to drive cellular function (Turrens, 2004). Obligate apicomplexan intracellular parasites such as *T. gondii* have evolved to cope with the intracellular environment of their host and adapt to the redox state inside the cells (Bosch *et al*., 2015, Peng *et al*., 2003). To overcome these hostile oxidative microenvironments, *T. gondii* have developed a variety of ROS-detoxifying mechanism such as the thioredoxin and glutaredoxin systems (Bosch *et al*., 2015, Kwok *et al*., 2004, Liu *et al*., 2013, Xue *et al*., 2017). These systems act as thiol/disulfide pairs, where glutathione/glutathione disulfide (GSH/GSSG) which plays a critical role in mediating redox

balance while thioredoxins (Trx) is involved in redox signaling and the detoxification of H_2O_2 (Arner and Holmgren, 2000, Jones and Go, 2010). The intracellular antioxidant glutathione exists in both reduced (GSH) and oxidized (GSSG) states. Reduced GSH is able to reduce unstable molecules such as ROS using the cysteine thiol functional group. As a result, the oxidized GSH readily reacts with another reduced GSH to form glutathione disulfide (GSSG) which is subsequently regenerated by glutathione reductase (GSR) (Bahrami *et al*., 2016, Couto *et al*., 2013). Interestingly, *T. gondii* parasites in particular possess cytosolic catalase (CAT) enzyme which is absent in most pathogenic protozoans (Ding *et al*., 2000, Halliwell, 1999, Kwok *et al*., 2004). Cytosolic catalase is primarily involved in the detoxification of host derived peroxides as a result of high substrate turnover of the host cell (Ding *et al*., 2000, Kaasch and Joiner, 2000). Additionally, *T. gondii* also possess 2 superoxide dismutases *Tg*SOD2 and *Tg*SOD3 which are localized to the parasite's single tubular mitochondrion (Melo *et al*., 2000). These different ROS-detoxification and antioxidants work together to protect the parasite against oxidative stress.

Despite having all the different ROS-detoxification mechanisms, *T. gondii* is still vulnerable to oxidative stress. During the early phase of *T. gondii* infection, the host's innate immune system defense mechanism is activated and results in large amount of ROS being generated by the macrophages and neutrophils to eliminate the parasites (Denkers *et al*., 2003). In response to this oxidative stress insult, the parasites will stop proliferating and differentiate from the tachyzoite into the bradyzoite form (Bohne *et al*., 1999, Bosch *et al*., 2015, Pino *et al*., 2007). This is also the reason why healthy individuals following infection with *T. gondii* are usually asymptomatic. However, a dysfunctional immune system would facilitate and allow tissue cysts reactivation and uncontrolled toxoplasmosis with clinical symptoms (Israelski *et al*., 1993, Nath and Sinai, 2003, Sullivan and Jeffers, 2012).

Our previous studies have indicated that z-FA-FMK depletes GSH and induces ROS production in mammalian T-cells besides blocking cathepsin B (Rajah and Chow, 2015, Liow and Chow, 2013). A previous study has suggested that z-FA-FMK inhibits the growth of malaria parasites through the induction of oxidative stress (Vandana *et al*., 2018). The

earlier findings in this study (chapter 3 and 4) also demonstrated that anti-proliferative effects of z-FA-FMK on *T. gondii* parasites which induced cyst formation was mediated via cathepsin B inhibition. As z-FA-FMK is both the irreversible inhibitor of the cysteine protease cathepsin B and a potential pro-oxidant, therefore this prompt us to investigate whether the anti-proliferative effects observed could be contributed by oxidative stress induction as well. Therefore, the main objective in this chapter is to examine if the anti-proliferative activity of z-FA-FMK in *T. gondii* parasites involves oxidative stress and the potential synergistic effect with BSO which blocks GSH biosynthesis.

5.2 Results

5.2.1 Effects of z-FA-FMK and z-FA-DMK on intracellular GSH levels in Hs68 cells and extracellular *T. gondii* tachyzoites

The results in chapter 3 and chapter 4 indicate that the cathepsin B inhibitor, z-FA-FMK was able to inhibit *T. gondii* proliferation and induce cyst formation. Previous studies have indicated that the cathepsin B inhibitor, z-FA-FMK but not z-FA-DMK inhibits T-cell proliferation through the induction of mild oxidative stress (Rajah and Chow, 2015). Therefore, in this present chapter, the involvement of oxidative stress in the anti-proliferative effects induce by z-FA-FMK and its analogue, z-FA-DMK was examined. To this end, the intracellular GSH levels in Hs68 host cells and extracellular *T. gondii* following z-FA-FMK and z-FA-DMK treatment was examined.

As shown in Figure 5.1, both z-FA-FMK and z-FA-DMK at 100µM did not induce significant depletion of intracellular GSH levels in Hs68 cells after 72h. This result suggests that z-FA-FMK behaves similarly to z-FA-DMK in Hs68 cells, which disagrees with previous studies where z-FA-FMK depleted GSH levels in human T-cells (Rajah and Chow, 2015). Subsequently, the effect of z-FA-FMK and z-FA-DMK on isolated extracellular *T. gondii* was examined. As depicted in Figure 5.2A and 5.2B, the results showed that the intracellular GSH levels in both the untreated extracellular *T. gondii* strains (RH and ME49 strain) remained unchanged over 6h. The presence of 100µM z-FA-FMK significantly depleted the intracellular GSH in both the RH and ME49 strains within the first hour and the level remain depleted in a sustained level for 6h. In contrast, 100µM z-FA-DMK has no effect on the intracellular GSH levels in both the *T. gondii* strains. The results collectively indicated that z-FA-FMK at 100µM may be inducing oxidative stress in the redox sensitive parasites directly while having negligible effect on the Hs68 host cells. Conversely, z-FA-DMK did not have any effect on the intracellular GSH in both parasites and Hs68 host cells.

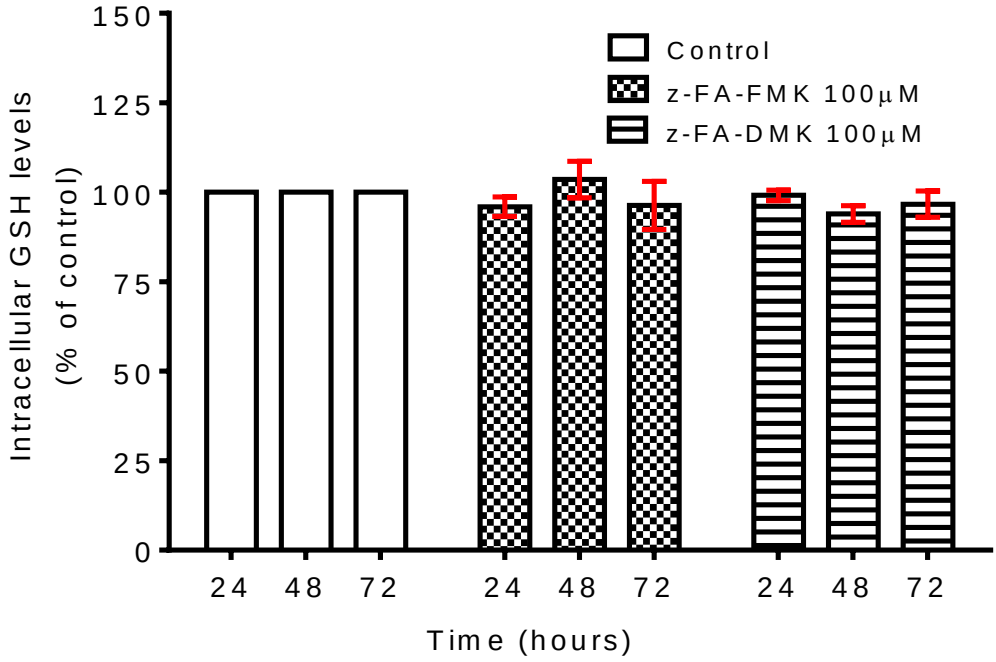

Figure 5.1. Effect of z-FA-FMK or z-FA-DMK on intracellular GSH levels in Hs68 cells

Hs68 cells were treated with 100µM of z-FA-FMK or z-FA-DMK for different time points where indicated. Intracellular GSH levels were measured using the fluorogenic dye MCB as described in Materials and Methods. The results represent the means ± SEM from three independent experiments.

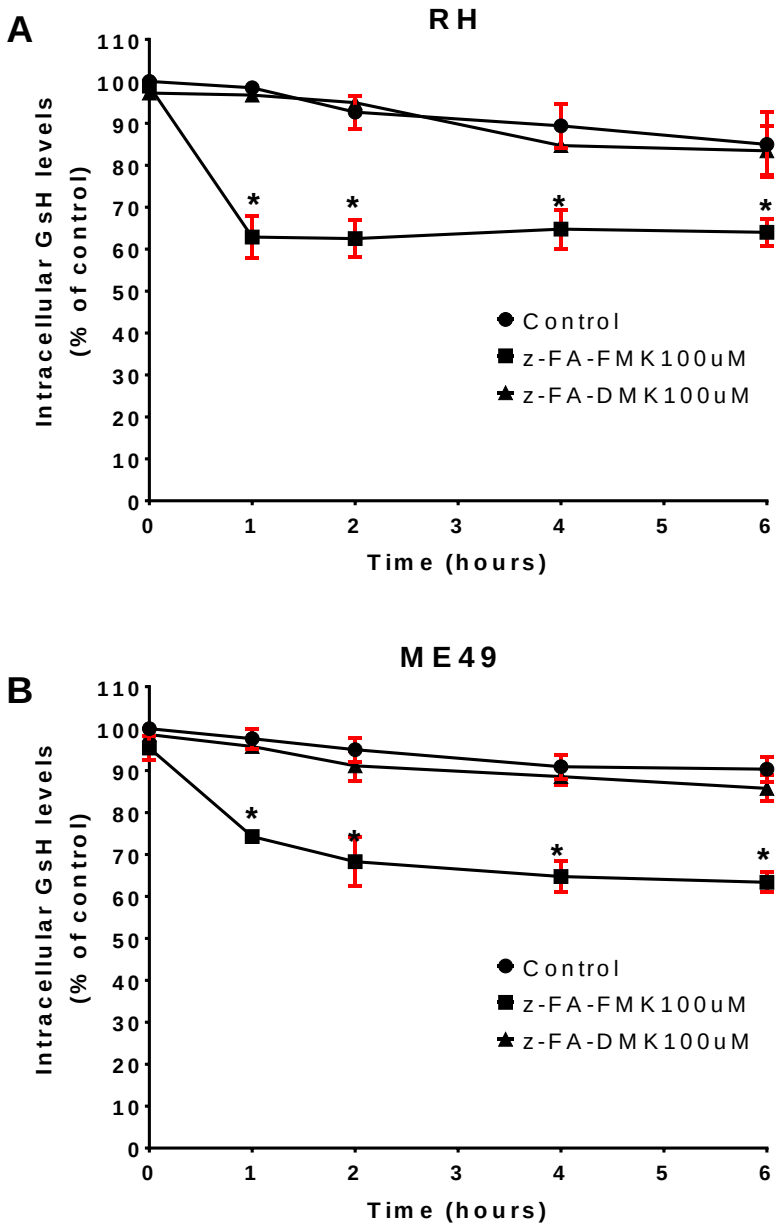

Figure 5.2. Effect of z-FA-FMK on intracellular GSH levels in extracellular *T. gondii* parasites

Isolated tachyzoites RH strain (**A**) or ME49 strain (**B**) were treated with 100µM of z-FA-FMK or z-FA-DMK for different time points where indicated. Intracellular GSH levels were measured using the fluorogenic dye MCB as described in Materials and Methods. The results represent the means ± SEM from three independent experiments, , where * indicates $p < 0.05$ versus 0h untreated control.

5.2.2 z-FA-FMK and z-FA-DMK do not induce ROS production in Hs68 host cells and extracellular *T. gondii* parasites

As shown earlier (Figure 5.1) both z-FA-FMK and z-FA-DMK have no effect on the intracellular GSH levels in Hs68 cells. However, z-FA-FMK significantly depletes intracellular GSH in extracellular *T. gondii* parasites while z-FA-DMK has no effect (Figure 5.2). To reconcile these results and confirm whether z-FA-FMK and z-FA-DMK induce oxidative stress, the production of ROS in Hs68 cells and extracellular *T. gondii* parasites was next determined. The major classes of ROS with physiological significance are superoxide anions, hydroxyl radicals and H_2O_2 (Ozougwu, 2016). To determine the various classes of ROS, Hs68 cells were treated with 100µM z-FA-FMK or z-FA-DMK for various time points where indicated before the amount of ROS generated was determined using redox sensitive dyes DHE (superoxides) and DCFH-DA (peroxyl and hydroxyl radicals). As shown in Figure 5.3, H_2O_2 (500µM) added to Hs68 cells as a positive control, readily induced the increase in ROS (superoxides) by 5-fold (Figure 5.3A and 5.3B), while peroxyl and hydroxyl radicals increased by 15-fold (Figure 5.3A and 5.3B) after 30min when compared to control cells. As shown in Figure 5.3A and 5.3B, both z-FA-FMK and z-FA-DMK, respectively did not induce any increase in superoxide production in Hs68 cells over 72h. Similarly, both z-FA-FMK and z-FA-DMK did not induce significant production of peroxyl and hydroxyl radicals in Hs68 cells over 72h (Figure 5.3C and 5.3D, respectively). These results collectively suggest that z-FA-FMK and z-FA-DMK at 100µM did not induce any notable oxidative stress towards Hs68 cells. Therefore, the reduced proliferation and formation of *T. gondii* cysts in response to z-FA-FMK and z-FA-DMK appears not to be due to intracellular oxidative stress exerted from within the host cells.

Since *T. gondii* parasites would be exposed to the extracellular environment during egress and invasion of a new host cell. Therefore, the effect of z-FA-FMK and z-FA-DMK at 100µM on ROS production in extracellular tachyzoites was examined subsequently. As illustrated in Figure 5.4, all control untreated extracellular parasites showed slight increase in ROS over 6h using DHE (superoxides) and DCFH-DA (peroxyl and hydroxyl radicals)

probes. Both z-FA-FMK and z-FA-DMK at 100µM did not induce any increase in superoxides (Figure 5.4A) or peroxyl and hydroxyl radicals (Figure 5.4C) in extracellular *T. gondii* RH strain parasites over 6h compared to untreated parasites. Similarly, in the avirulent ME49 strain parasites, both z-FA-FMK and z-FA-DMK did not induce accumulation of superoxides (Figure 5.4B) or peroxyl and hydroxyl radicals (Figure 5.4D). Our results collectively indicate that z-FA-FMK and z-FA-DMK did not induce oxidative stress in the parasites or Hs68 host cells following treatments.

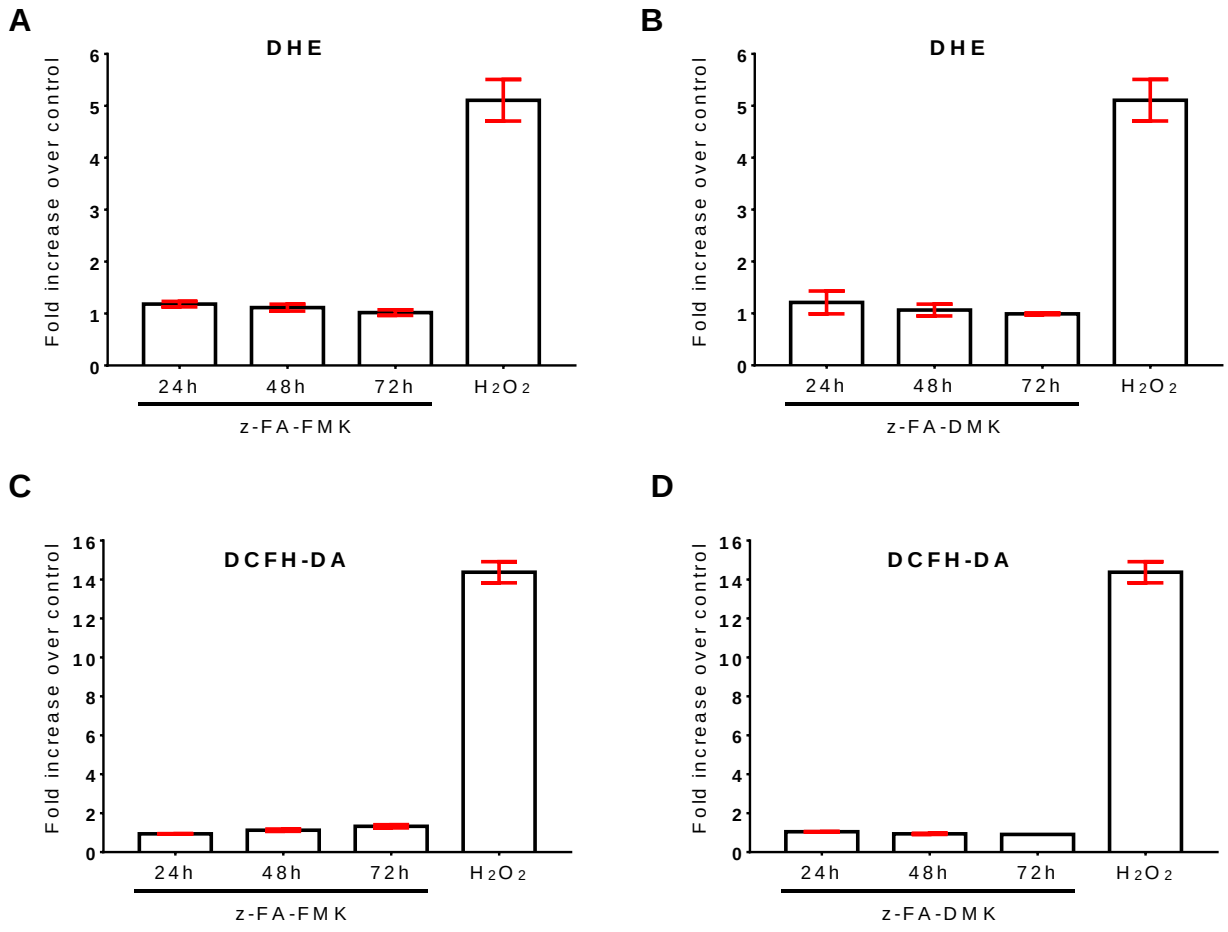

Figure 5.3. Effect of z-FA-FMK and z-FA-DMK on intracellular ROS accumulation in Hs68 cells

Hs68 cells were treated with 100µM z-FA-FMK or z-FA-DMK for different time points where indicated. Accumulation of intracellular superoxides was measured using DHE (**A-B**) or peroxyl and hydroxyl radicals using DCFH-DA (**C-D**) as described in Materials and Methods. The results represent the fold increase of ROS over control ± SEM from three independent experiments.

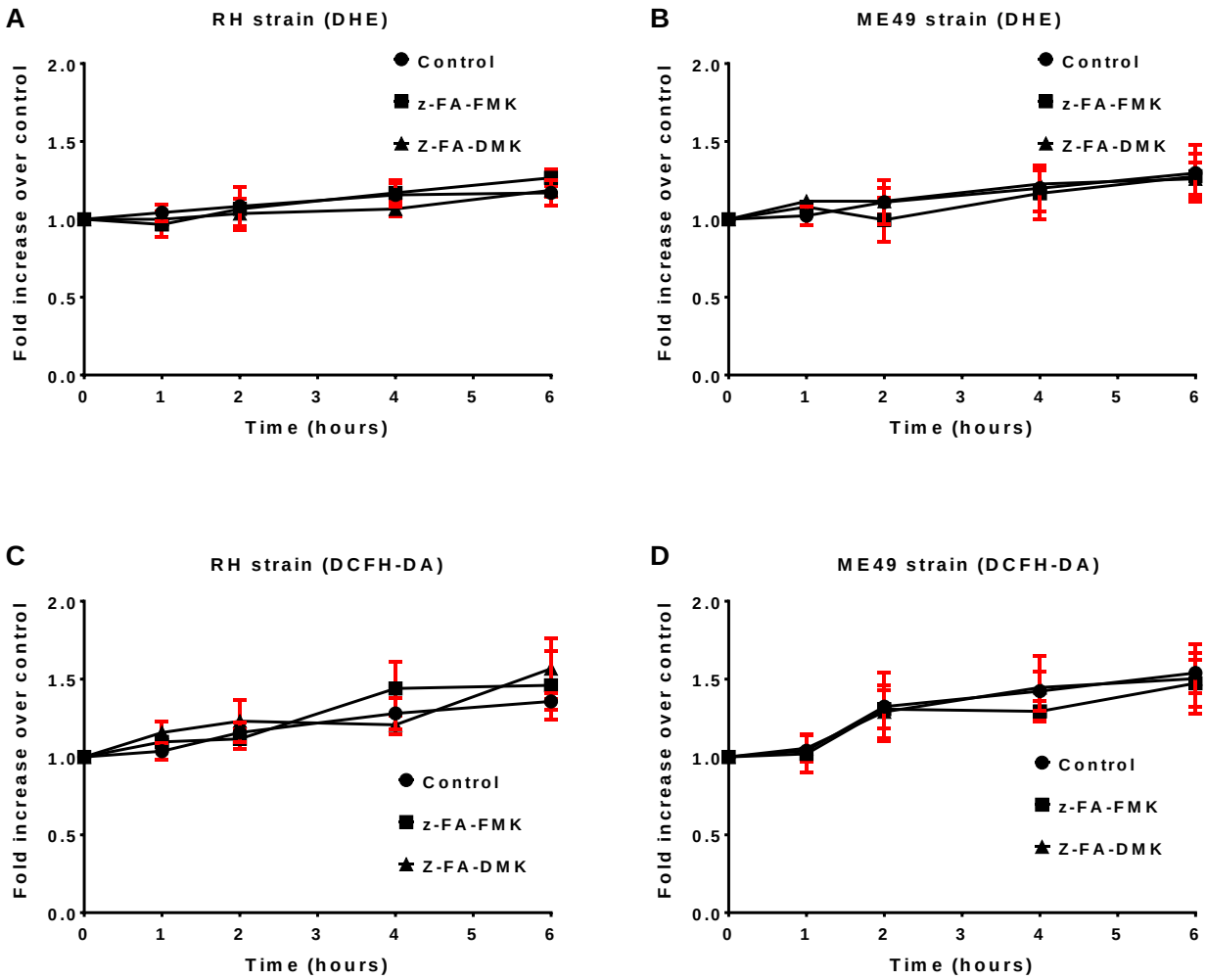

Figure 5.4. Effect of z-FA-FMK and z-FA-DMK on intracellular ROS accumulation in *T. gondii* parasites

Extracellular *T. gondii* parasites were purified and treated with 100µM z-FA-FMK or z-FA-DMK for different time points where indicated. Accumulation of intracellular superoxides was measured using DHE (**A**-**B**) or peroxyl and hydroxyl radicals using DCFH-DA (**C**-**D**) as described in Materials and Methods. The results represent the fold increase of ROS over control ± SEM from three independent experiments.

5.2.3 Intracellular *T. gondii* proliferation is redox sensitive

The results so far have suggested that z-FA-FMK did not induce any increase in ROS production in both Hs68 cells and extracellular *T. gondii* parasites. However, z-FA-FMK but not z-FA-DMK was shown to partially deplete intracellular GSH in extracellular *T. gondii* parasites. These results led us to examine whether reducing the availability of GSH in Hs68 host cells has any effect on *T. gondii* proliferation induced by the z-FA-FMK. To this end, we used BSO to block intracellular GSH production in the Hs68 cells. BSO is a potent inhibitor of the enzyme γ-glutamylcysteine synthetase (γ-GCS), and blocks intracellular GSH synthesis in cells (Drew and Miners, 1984, O'Dwyer *et al*., 1996, Tagde *et al*., 2014). The effect of BSO on the intracellular GSH levels in Hs68 cells was first examined. As shown in Figure 5.5, BSO at 2mM was able to reduce intracellular GSH levels in Hs68 cells by ~35% compared to control cells after 24h and remained unchanged after 72h. As expected, z-FA-FMK did not deplete intracellular GSH levels in Hs68 cells. When Hs68 cells were co-treated with BSO, the depletion of GSH remained similar to BSO alone.

Having established that BSO can reduce intracellular GSH level by ~35%, its effect on *T. gondii* proliferation in Hs68 cells was then examined. As illustrated in Figure 5.6, BSO at 2mM significantly reduced total proliferated parasite number after 72h in both RH strain and ME49 strain. The results suggest that the depletion of GSH antioxidant in the host intracellular environment reduces *T. gondii* parasite proliferation.

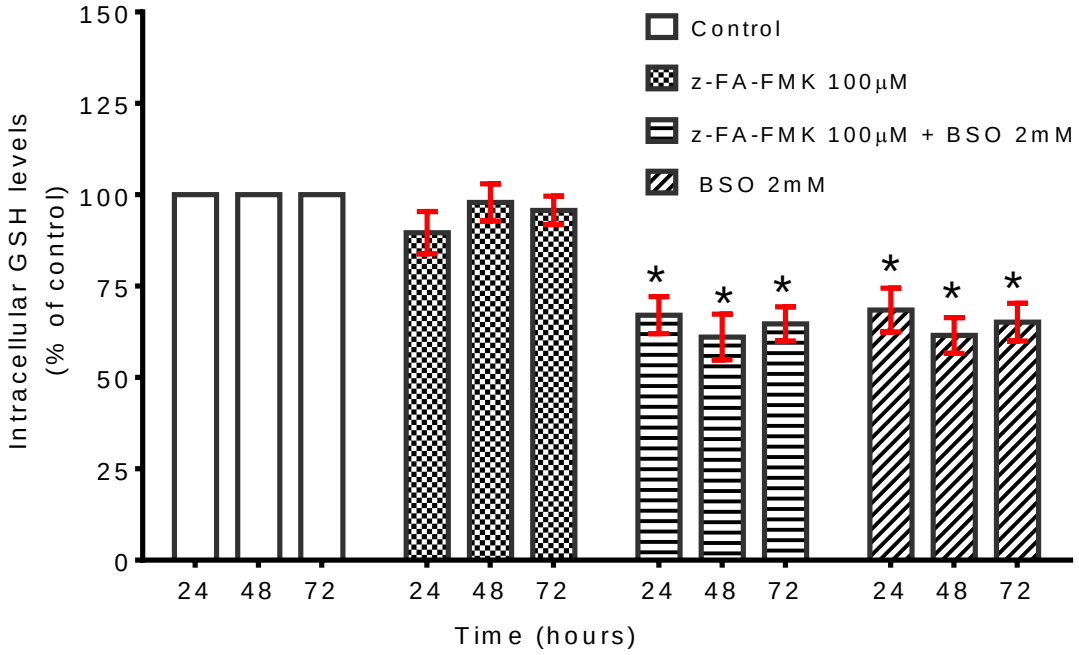

Figure 5.5. Effect of BSO and z-FA-FMK on intracellular GSH levels in Hs68 cells

Hs68 cells were treated with 2mM of BSO or 100µM of z-FA-FMK or both for different time points where indicated. Intracellular GSH levels were measured using the fluorogenic dye MCB as described in Materials and Methods. The results represent the means ± SEM from three independent experiments, where * indicates $p < 0.05$ versus respective untreated control over time.

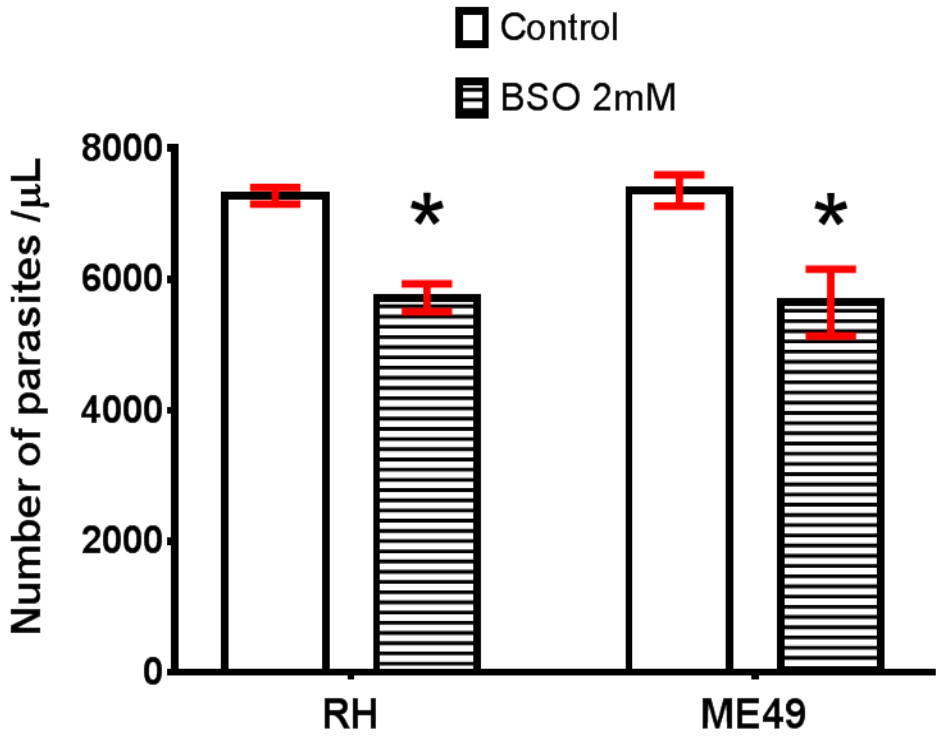

Figure 5.6. Effect of BSO on intracellular *T. gondii* parasite number following 72h treatment

Hs68 cells infected with *T. gondii* tachyzoites RH strain or ME49 strains were treated with 2mM BSO for 72h and the number of tachyzoites was determined using the trypan blue exclusion assay as described in Materials and Methods. The results represent the means ± SEM from three independent experiments, where * indicates $p < 0.05$ versus control.

5.2.4 Depletion of GSH by BSO enhances anti-proliferative effects of z-FA-FMK

Previous study has demonstrated that BSO is able to potentiate the effect of anti-parasitic drugs such as nifurtimox and benznidazole against *T. cruzi* (Faundez *et al*., 2005). BSO was shown to abrogate pyrimethamine and sulfadoxine resistance in malaria parasites (Songsungthong *et al*., 2016). Therefore, whether BSO could potentiate or increase the sensitivity of the intracellular *T. gondii* tachyzoites towards z-FA-FMK treatment was investigated. To this end, Hs68 cells infected with *T. gondii* (RH or ME49 strains) were treated with various concentrations of z-FA-FMK in the presence of 2mM BSO over 72h.

As shown in Figure 5.7 and Figure 5.8, the presence of BSO markedly enhanced the anti-proliferative effects of z-FA-FMK on *T. gondii* RH and ME49 strains, respectively. The number of PV formed over time in RH strain tachyzoites was further reduced in z-FA-FMK-treated host cells infected with parasites in the presence of BSO (Figure 5.7B) compared to z-FA-FMK treatment alone (Figure 5.7A). Likewise, the total parasite count was also reduced, further confirming that BSO potentiated the dose-dependent anti-proliferative effects of z-FA-FMK on the RH strain *T. gondii* as shown in Figure 5.7C. Similarly, BSO also exhibited potential synergistic effect with z-FA-FMK in the ME49 strain parasites (Figure 5.8B) compared to z-FA-FMK treatment alone (Figure 5.8A). As seen with the RH strain, the total number of ME49 strain parasites was also reduced in the presence of BSO plus z-FA-FMK (Figure 5.8C). The results collectively indicated that the presence of BSO resulted in a marked reduction in parasite growth across lower concentrations of z-FA-FMK (<100µM) in both RH and ME49 strain. No enhancement on *T. gondii* proliferation was seen at 100µM z-FA-FMK in the presence of BSO. These results also suggest that the RH strain parasite proliferation is more sensitive to z-FA-FMK plus BSO compared to the ME49 strain. Our findings collectively suggest that the depletion of intracellular GSH mediated by BSO synergistically enhanced the anti-proliferative effects of z-FA-FMK towards RH tachyzoite strain. These results collectively suggest that the anti-proliferative effects induced by z-FA-FMK in *T. gondii* can be enhanced with GSH depletion using BSO.

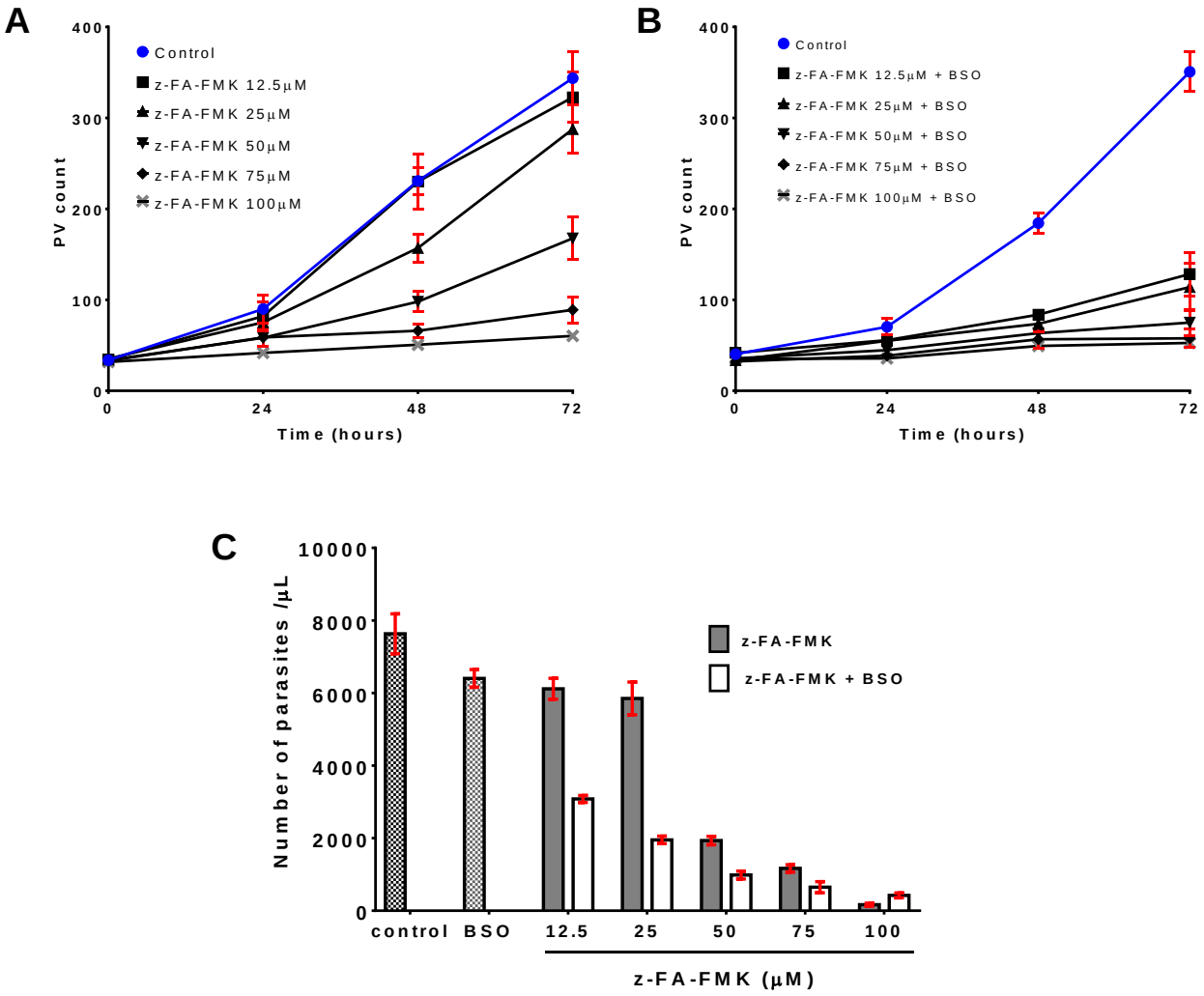

Figure 5.7. Effect of BSO (2mM) on proliferation of z-FA-FMK treated RH strain *T. gondii* tachyzoites

Hs68 host cells were preinfected with the RH strain parasites for 24h before treated with z-FA-FMK or together with BSO. The time course for PV formed in Hs68 cells following z-FA-FMK treatment alone (**A**) or in combination with 2mM BSO (**B**). Total number of viable parasites after 72h following treatment with z-FA-FMK alone or co-treated with 2mM BSO (**C**). The treated Hs68 cells infected with tachyzoites were examined under 40× magnification and the number of PV was scored across 10 randomized microscopic fields. The number of tachyzoites was determined using the trypan blue exclusion assay as described in Materials and Methods. The results represent the means ± SEM from three independent experiments.

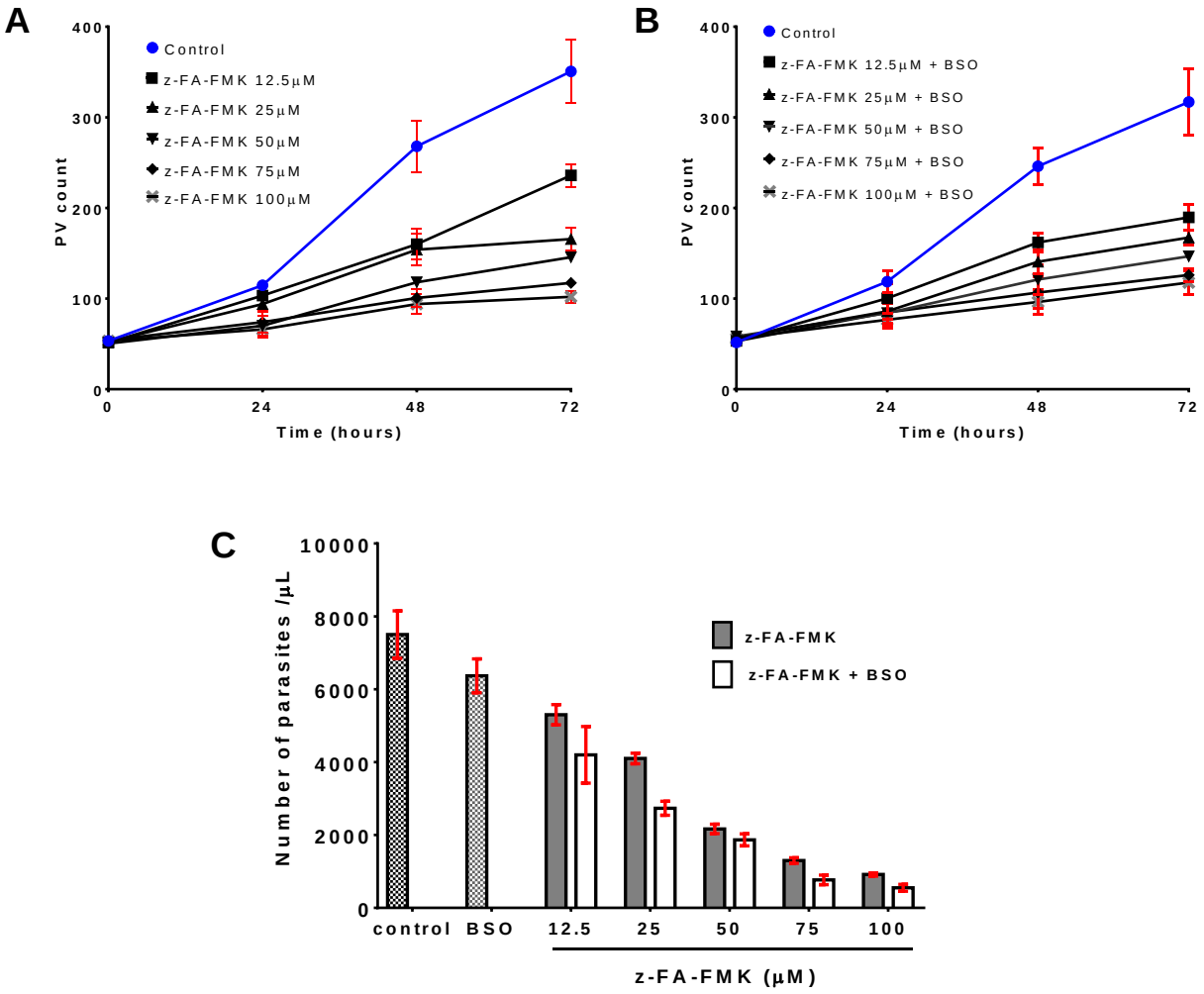

Figure 5.8. Effect of BSO (2mM) on proliferation of z-FA-FMK treated ME49 strain *T. gondii* tachyzoites

Hs68 host cells were preinfected with the ME49 strain parasites for 24h before treated with z-FA-FMK or together with BSO. The time course for PV formed in Hs68 cells following z-FA-FMK treatment alone (**A**) or in combination with 2mM BSO (**B**). Total number of viable parasites after 72h following treatment with z-FA-FMK alone or co-treated with 2mM BSO (**C**). The treated Hs68 cells infected with tachyzoites were examined under 40× magnification and the number of PV was scored across 10 randomized microscopic fields. The number of tachyzoites was determined using the trypan blue exclusion assay as described in Materials and Methods. The results represent the means ± SEM from three independent experiments.

5.3 Discussion

Obligate intracellular parasites including the apicomplexans have complex life cycles and require the transmission from one host to another. The complete lytic cycle of *T. gondii* parasites involves the intracellular proliferation phase and extracellular invasion phase (Blader *et al*., 2015, Jeffers *et al*., 2018, Tu *et al*., 2018). Therefore, obligate intracellular parasites such as *T. gondii* needs to cope with the redox stress which could arise from the intracellular environment of their hosts and/or the extracellular environment (Bosch *et al*., 2015, Peng *et al*., 2003). Oxidative stress is described as the imbalance between anti-oxidant and pro-oxidant levels which is often characterized with the depletion of intracellular GSH pools coupled by accumulation of ROS (Chandra *et al*., 2000, Liguori *et al*., 2018, Orrenius, 2007, Sun, 2010). In physiological conditions, immune effector cells such as macrophage and neutrophils exploit detrimental properties of ROS to combat infections via 'oxidative burst', which rapidly increases the oxidative burden to eradicate the targeted infectious agent (Nguyen *et al*., 2017a, Slauch, 2011).

Earlier findings in chapter 4 indicated that the anti-proliferative effects of z-FA-FMK in *T. gondii* parasites were associated with the inhibition of cathepsin B. However, one of the side effects of z-FA-FMK is acting as a pro-oxidant and inhibits T-cell proliferation via oxidative stress (Rajah and Chow, 2015). In line with this, z-FA-FMK has been reported to inhibit the growth malaria parasites mediated via the induction of oxidative stress via ROS production (Vandana *et al*., 2018). Hence in this chapter, the involvement of oxidative stress on the anti-proliferative effects of z-FA-FMK on *T. gondii* in Hs68 host cells was examined. To this end, we examined the effect of z-FA-FMK and its analog, z-FA-DMK on intracellular GSH levels and ROS production in both Hs68 cells and *T. gondii* parasites. Like z-FA-FMK, z-FA-DMK readily inhibits *T. gondii* proliferation in host cells but has no reported side effects (Green and Shaw, 1981, Liow and Chow, 2013). In the previous study, z-FA-FMK readily depletes intracellular GSH and promotes ROS accumulation in T-cells to block cell proliferation (Rajah and Chow, 2015). In sharp contrast, the results showed that z-FA-FMK and z-FA-DMK have no effect on intracellular GSH levels in Hs68 cells. Surprisingly, the findings

differ from the reported depletion of GSH in human T-cells induced by z-FA-FMK. In the study of *T. gondii* parasites, interestingly z-FA-FMK but not z-FA-DMK induced a moderate decrease in intracellular GSH in extracellular tachyzoites from both ME49 and RH strains. This suggests that z-FA-FMK could be causing a mild oxidative stress in the extracellular parasites but not in the host cells. The results also indicate that it is likely that during the transition between egress and invasion, the extracellular tachyzoites will be affected by z-FA-FMK in the culture media during treatment.

Accumulation of ROS in cells is known to have detrimental effects on cells and parasites (Andreyev *et al*., 2005, Birben *et al*., 2012, Kwok *et al*., 2004, Slesak *et al*., 2016). Aside from the redox balance within the parasite, the host cell also exerts oxidative stress towards the intracellular parasites due to the cell's higher metabolism and substrate turnover in the cytosol or the mitochondria (Andreyev *et al*., 2005, Trachootham *et al*., 2008). Therefore, ROS could directly affect the survivability of the parasite or indirectly via disruption of the oxidative balance of the host cell (Bosch *et al*., 2015). Since *T. gondii* parasites proliferate entirely within the infected host cell, the redox state of the host cell would be an indicator of oxidative stress imposed towards the proliferating parasites. The major classes of ROS with physiological significance are superoxide anions, hydroxyl radicals, and peroxyl radicals (Ozougwu, 2016).

In this study, two different ROS sensitive dyes (DHE and DCFH-DA) were used: DHE for measurement of superoxide anions and DCFH-DA for the specific detection of hydroxyl radicals and peroxyl radicals. The results obtained indicate that both z-FA-FMK and z-FA-DMK does not induce ROS accumulation in Hs68 cells, suggesting that both compounds did not induce oxidative stress in the host cells. Similarly, both z-FA-FMK and z-FA-DMK did not promote increase in ROS in extracellular *T. gondii*. Firstly, the results showed that z-FA-DMK is a specific cathepsin B inhibitor and did not induce any oxidative stress in both Hs68 and *T. gondii* altogether, which is in line with reported studies (Rajah and Chow, 2015). Collectively, these findings suggest that z-FA-FMK does not induce oxidative stress in the

host cells, whereas it may induce mild oxidative stress in the extracellular tachyzoites during the transition period after egressing and finding the next host via the depletion of GSH.

Depleting intracellular GSH in cells will affect the redox balance and several studies have used BSO to block GSH synthesis in cells by inhibiting γ-GCS. The resulting imbalanced redox state was shown to increase the effectiveness of a number of anti-parasitic drugs (Faundez *et al*., 2005, Gibellini *et al*., 2010, Songsungthong *et al*., 2016, Tagde *et al*., 2014). Our results show that BSO at non-toxic concentrations was able to deplete intracellular GSH in Hs68 cells by ~35% and was able to partially reduce intracellular tachyzoite proliferation. As expected, there was no further reduction in intracellular GSH levels in Hs68 host cells treated with both z-FA-FMK and BSO, confirming that z-FA-FMK does not deplete intracellular GSH levels, despite the replenishment of GSH being blocked by the presence of BSO.

However, under this condition, the results suggest that BSO have a potential synergistic effect with z-FA-FMK and further enhanced the anti-proliferative effect of z-FA-FMK on RH strain of *T. gondii*. These results suggest that the inhibition of GSH biosynthesis with BSO, increased the sensitivity of the two strains of parasites to z-FA-FMK. Interestingly, the synergistic effects of BSO were only effective when used with lower concentrations of z-FA-FMK and more pronounced with the RH strain but not apparent in the ME49 strain of *T. gondii*. These findings are very much in line with previous reports where BSO treatment enhances the effects of several anti-parasitic drugs (Faundez *et al*., 2005, Pal and Bandyopadhyay, 2012, Songsungthong *et al*., 2016, Turrens, 2004). Indeed, these results demonstrated that *T. gondii* like other studied parasitic protozoans in general are sensitive and vulnerable to oxidative stress, suggesting that disruption of parasite/host redox homeostasis could be an effective approach to control infections (Bosch *et al*., 2015).

Since *T. gondii* differentiation can be driven by various stress factors (physical and physiological) and preceded by slowed growth (Sullivan and Jeffers, 2012, Sullivan *et al*., 2009). Therefore, the combination of BSO and z-FA-FMK may be introducing imbalanced redox state and starvation via cathepsin B inhibition, which further impedes intracellular

replication which results in the enhancing the potency of z-FA-FMK. These findings suggest that stress inducers against *T. gondii* which acts via different mechanisms could apply a synergistic inhibitory effect towards *T. gondii* proliferation.

In summary, our results have shown that z-FA-FMK and z-FA-DMK both did not induce ROS accumulation in Hs68 cells and extracellular tachyzoites. However, only z-FA-FMK was able to deplete ~35% GSH levels in extracellular tachyzoites. Additionally, the results showed that that the intracellular redox state mediated via the availability of antioxidants affects the proliferation of *T. gondii* parasites. We suggest that oxidative stress is not involved in the anti-proliferative effects of z-FA-FMK on *T. gondii*. Nevertheless, the induction or sensitization towards oxidative stress may be combined with z-FA-FMK to increase the strength of inhibition towards intracellular *T. gondii* parasite proliferation.

CHAPTER SIX

GENERAL DISCUSSION, CONCLUSION AND FUTURE WORK

6.1 General discussion

Toxoplasma gondii is an obligate intracellular opportunistic parasitic protozoan of the apicomplexan phylum that causes toxoplasmosis. Toxoplasmosis is highly prevalent due to the wide host range compatibility, leading to widespread infections in both animals and humans worldwide. The *T. gondii* life cycle involves differentiation between sporozoites, tachyzoites and bradyzoites to facilitate parasite dissemination and persistence (Ferreira da Silva Mda *et al*., 2008, Vonlaufen *et al*., 2008). Toxoplasmosis can be classified into the acute phase and the chronic phase, where the acute infection by tachyzoites which is generally subclinical and asymptomatic (Dubey and Jones, 2008, Montazeri *et al*., 2017). Acute toxoplasmosis may develop into chronic infection, characterized by the differentiation of tachyzoites into bradyzoites which remains dormant as cysts (Weiss and Kim, 2000). Dormant cysts may reactivate and manifest as symptomatic toxoplasmosis in immunocompromised or congenitally infected individuals, leading to severe complications and mortality (Dubey and Jones, 2008, Montazeri *et al*., 2017, Vonlaufen *et al*., 2008).

The current standard treatment for acute toxoplasmosis is pyrimethamine and sulfadiazine. These drugs which possess undesirable side effects are also ineffective against *T. gondii* cysts (chronic toxoplasmosis) (Bosch-Driessen *et al*., 2002b, Schmidt *et al*., 2006, Silveira *et al*., 2002). To date, toxoplasmosis remains incurable due to the resilient cysts which avoid immunodetection and the quiescent metabolic activity of cysts increases the challenges for pharmacological intervention (Samuel *et al*., 2003, Sullivan and Jeffers, 2012, Sullivan *et al*., 2009). The ability of *T. gondii* to differentiate into bradyzoites and form cysts is critical in establishing chronic infection. Therefore, understanding the mechanism that underlie the differentiation of *T. gondii* tachyzoites to bradyzoites and cyst formation may unravel new strategies to combat *T. gondii* infection. (Ferreira da Silva Mda *et al*., 2008). Indeed, an attenuated strain of *T. gondii* that has lost the ability to differentiate into bradyzoites has been used as a vaccine (Toxovax) in sheep to curb zoonotic transmission (Buxton and Innes, 1995, Buxton *et al*., 2007).

The differentiation of *T. gondii* has been widely recognized as a response towards stress or hostile environmental conditions (Ferreira da Silva Mda *et al*., 2008, Vonlaufen *et al*., 2008, Weiss and Kim, 2000). How *T. gondii* responds to stress and differentiates remains elusive and the underlying mechanisms are of major scientific interest. In the present study, the anti-proliferative effect of the irreversible cathepsin B inhibitor z-FA-FMK on two different strains of *T. gondii* (RH and ME49) with different propensity to form cyst *in vitro* using in Hs68 host cells infected was studied.

The main objectives in chapter three were to examine and characterize the anti-proliferative effects of the irreversible cathepsin B inhibitor, z-FA-FMK on Hs68 cells infected with *T. gondii* tachyzoites. Parameters correlating to parasite lytic cycle including PV formation, total viable *T. gondii* parasite number and plaque area formation were looked at. The findings demonstrated that z-FA-FMK dose-dependently impaired the *T. gondii* lytic cycle at multiple stages, which include parasite invasion (PV count), intracellular replication (total parasite count) and egress (plaque formation) in both RH and ME49 strains. The *T. gondii* cathepsin B is involved in the processing of rhoptry proteins which is a secretory organelle required for parasite invasion into cells and its inhibition has been reported to impair cell invasion (Que *et al*., 2002). In line with this, results have also indicated that z-FA-FMK partially blocks *T. gondii* invasion, suggesting the involvement of *T. gondii* cathepsin B inhibition. Interestingly, the findings also clearly demonstrated that z-FA-FMK blocks the overall lytic cycle by inhibiting intracellular *T. gondii* proliferation. Additionally, the avirulent ME49 strain appears to be more sensitive to z-FA-FMK and formed cysts readily as compared to the virulent RH strain.

Most of the reported stress conditions that promote *T. gondii* differentiation into bradyzoites also reduce the proliferation of tachyzoites (Gubbels *et al*., 2008, Sullivan and Jeffers, 2012). There is also evidence to suggest that the trigger for differentiation in *T. gondii* may be a programmed response activated by slow growth and is independent of cellular stress (Bohne *et al*., 1994, Jerome *et al*., 1998, Sullivan *et al*., 2009). Since z-FA-FMK was able to block *T. gondii* proliferation within Hs68 cells, we then examined if *T. gondii* differentiate and

form cysts after z-FA-FMK treatment. The results showed that parasites treated with z-FA-FMK developed cysts wall in both RH and ME49 strains. In line with reported studies, our time-course examination of cyst formation in response to z-FA-FMK indicate that the inhibition of parasite proliferation preceded cyst wall formation. Since cell cycle progression is required for cyst formation, as cell cycle arrest does not trigger bradyzoite differentiation (Gubbels *et al*., 2008). Therefore, is remain unclear if the anti-proliferative effects of z-FA-FMK involves inducing cell cycle arrest in the parasites and more work is needed to confirm this. Next, we further examined if the parasites could regain virulence and proliferation following withdrawal of z-FA-FMK. The results demonstrated that the intracellular parasites gradually regained its proliferation following z-FA-FMK withdrawal. This shows that the anti-proliferative effects of z-FA-FMK in *T. gondii* may be stress related and are reversible over time upon withdrawal. Using this model, the anti-proliferative effects of z-FA-FMK on tachyzoite and bradyzoite interconversion were further characterized.

In chapter four, the objective was to examine if the anti-proliferative effects of z-FA-FMK towards *T. gondii* parasites in Hs68 cells involve cathepsin B inhibition. Cathepsins are cysteine proteases which play important role in the biology of *T. gondii* parasites. Aside from basic catabolic functions and protein processing, cathepsins have been shown to involve in cell and tissue invasion, nutrient acquisition, excystment/encystment and replication (Dou and Carruthers, 2011, Sajid and McKerrow, 2002). As a negative control for z-FA-FMK, one of its analogues, z-FA-DMK which has no reported side effects besides blocking cathepsin B was used (Rajah and Chow, 2015). Similar to z-FA-FMK, z-FA-DMK also effectively inhibited parasite growth and induced cyst formation. These results suggest that the anti-proliferative effect on tachyzoites induced by both z-FA-FMK and z-FA-DMK is through the inhibition of cathepsin B. As expected, both z-FA-FMK and z-FA-DMK inhibited cathepsin B activity in Hs68 cell lysates and in live Hs68 cells. Live cell imaging of cathepsin B activity in *T. gondii* infected Hs68 cells indicate the presence of cathepsin B-like activity in parasite PVs which was reduced following z-FA-FMK and z-FA-DMK treatment. This was corroborated when the cathepsin B activity in *T. gondii* parasite lysates and extracellular parasites were readily inhibited by z-FA-FMK and z-FA-DMK. Collectively, our results

indicated that the anti-proliferative effects of z-FA-FMK and z-FA-DMK are associated with the inhibition of cathepsin B in *T. gondii* parasites.

T. gondii parasites possesses a lysosome-like organelle known as the VAC which is the major site for the cathepsins, *Tg*CPL and *Tg*CPB (Dou and Carruthers, 2011, Parussini *et al*., 2010). *T. gondii* tachyzoites ingests and catabolize host-derived cytosolic proteins in the VAC to drive proliferation (Dou *et al*., 2014, McGovern *et al*., 2018). Studies have shown that *T. gondii* bradyzoites deficient in VAC-localized cathepsins accumulate large quantities of undigested material in the VAC *in vitro*, suggesting that autophagy mediates organelles turnover during parasite differentiation or serves as a survival response to overcome nutrient limitation (Di Cristina *et al*., 2017). The results from this study showed that both autophagy inhibitors, CQ and 3-MA have no effect on *T. gondii* proliferation in Hs68 cells, suggesting that autophagy is not activated under normal culture conditions. However, the proliferation of *T. gondii* which resumes following z-FA-FMK withdrawal were blocked in the presence of CQ and 3-MA. These results demonstrated that autophagy is involved as the parasites began to proliferate to regain infectivity and proliferation following z-FA-FMK withdrawal.

In line with this, rapidly replicating tachyzoites are more metabolically active and require a higher overall nutrient demand than bradyzoites. Proliferating *T. gondii* parasites have also been suggested to parasitize host-derived nutrients sources by recruiting host organelles, autophagic vesicles and even induce autophagy of the infected host cell to increase amino acid pools (Besteiro, 2019, Ghosh *et al*., 2012). These findings are in line with reported studies where autophagy inhibitors such as 3-MA have been reported to block host autophagy which further lowers amino acid availability for the parasite during starvation condition (Wang *et al*., 2009).

Collectively, these findings demonstrated that the anti-proliferative effects of z-FA-FMK on *T. gondii* parasites could involve nutrient starvation through the inhibition of cathepsin B in the VAC to reduce amino acid availability. This could lead to the activation of autophagy as a stress response as amino acid deprivation has been well established to be a potent inducer of autophagy (Wang and Klionsky, 2011). Other than that, the deprivation of the amino acid

arginine has been reported to impede parasite growth and induced differentiation to bradyzoites (Fox *et al*., 2004). Therefore, it is also not surprising that the disruption of VAC cathepsin proteolytic function by z-FA-FMK causes nutrient starvation and activation of autophagy, hence ultimately impeding parasite proliferation and inducing cyst formation.

Most of the current anti-parasitic drugs, such as anti-malarial (chloroquine) and anti-trypanosomal (nifurimox and beta-lapachone) are known to be pro-oxidants and counters parasitic infections by inducing oxidative stress (Turrens, 2004, Pal and Bandyopadhyay, 2012). *T. gondii* parasites are vulnerable to oxidative stress not only intracellularly but also during infection where the host's immune system produces ROS to fight the infection. Therefore, the selective disruption of redox homeostasis in apicomplexa presents an ideal and effective drug target (Bosch *et al*., 2015). In line with this, our previous studies have indicated that the cathepsin B inhibitor, z-FA-FMK but not z-FA-DMK inhibits T-cell proliferation by inducing mild oxidative stress (Liow and Chow, 2013, Rajah and Chow, 2015). Hence the objective in chapter 5 was to examine the involvement of oxidative stress in the anti-proliferative effects induced by z-FA-FMK and z-FA-DMK. In contrast to T-cells, z-FA-FMK has no significant effect on the intracellular GSH level in Hs68 cells. However, z-FA-FMK was shown to partially deplete GSH levels in extracellular *T. gondii* parasites while z-FA-DMK has no effect. To further corroborate if z-FA-FMK and z-FA-DMK causes oxidative stress, the production of ROS in Hs68 cells and extracellular *T. gondii* was examined. To this end, the results demonstrated that both z-FA-FMK and z-FA-DMK did not induce ROS production (superoxides, hydroxyl and peroxyl radicals) in both Hs68 cells and extracellular *T. gondii* parasites. These results indicate that the anti-proliferative effects of both z-FA-FMK and z-FA-DMK is not mediated via the induction of oxidative stress.

However, a number of studies have shown that by altering the redox state of the host cells, particularly by depleting intracellular GSH using BSO increases the efficacy of a number of parasitic drugs (Turrens, 2004, Pal and Bandyopadhyay, 2012, Songsungthong *et al*., 2016, Faundez *et al*., 2005). In support of these reported findings, BSO which blocks GSH synthesis and depletes intracellular GSH in Hs68 cells, markedly enhanced the anti-

proliferative effects of z-FA-FMK. The array of cysteine proteases like cathepsin B in mammalian cells is substantially higher than parasites, which may provide a level of redundancy not found in the parasitic systems (Turk and Guncar, 2003, Sajid and McKerrow, 2002). Hence, the potential of anti-parasitic drugs targeting cathepsins in parasites may be an effective treatment approach towards both acute and chronic phase infections with minimum harm to the host.

Taken together, the results suggest that the depletion of GSH availability could synergistically enhance the anti-proliferative effects of z-FA-FMK towards the RH strain. Our results also imply that stress inducers that work through different mechanism of action such as, cathepsin B inhibition by z-FA-FMK together with GSH depletion mediated by BSO could be combined to amplify the suppression effect towards intracellular *T. gondii* parasite proliferation. The use of BSO in combination with z-FA-FMK could lower the effective dose for required to suppress *T. gondii* proliferation and consequently also helps to minimize any potential side effects of a single drug treatment.

6.2 Conclusion

Taken together, our results indicated that the irreversible cathepsin B inhibitor z-FA-FMK inhibited the proliferation of *T. gondii* tachyzoites in Hs68 cells in a dose-dependent manner. The parasites treated with z-FA-FMK have reduced proliferation and infectivity in Hs68 cells, indicated by less PV formed and impaired proliferative lytic cycle shown by total parasite number and plaque area formation. The inhibition of tachyzoite proliferation by z-FA-FMK subsequently leads to differentiation into bradyzoites and cyst formation. When z-FA-FMK was withdrawn from the Hs68 infected cells, the intracellular parasites gradually recovered and increased proliferation and infectivity. The negative control cathepsin B inhibitor, z-FA-DMK which lacks other non-specific effects also inhibited *T. gondii* parasite replication in Hs68 cells and induced cyst formation similar to z-FA-FMK. Both cathepsin inhibitors, z-FA-FMK and z-FA-DMK blocked cathepsin B activity in Hs68 cells and *T. gondii* parasites. In *T. gondii*, cathepsin B is associated with the proteolytic function of the parasite VAC in protein catabolism. Hence, the anti-proliferative effects of z-FA-FMK and z-FA-DMK may be mediated via starvation by blocking cathepsin B in the VAC. Furthermore, autophagy was shown to be critical during the recovery of the parasites upon withdrawal of z-FA-FMK. In the final chapter, the results showed that z-FA-FMK which was reported as a pro-oxidant in T-cells did not induce ROS production in both Hs68 cells and *T. gondii* parasites. However, the co-treatment of z-FA-FMK with BSO which blocks GSH synthesis potentiated the efficiency of z-FA-FMK in inhibiting *T. gondii* proliferation. Therefore, it appears that z-FA-FMK and BSO may be simultaneously exerting different stress mechanism that can potentiate the inhibition of *T. gondii* proliferation.

6.3 Future work

The results presented in this study could be taken further in several areas to further understand differentiation of *T. gondii* parasites as a response towards z-FA-FMK treatment. Firstly, additional studies could be done to examine the expression of bradyzoite specific antigen markers (BAG-1) and tachyzoite specific markers (SAG-1) following z-FA-FMK treatment. The changes of stage specific markers could be monitored over time to further elucidate the differentiation process in response to z-FA-FMK treatment. Other than that, parasite response to stress and starvation have been shown to activate the translational repression system, indicated by elevation of phosphorylated *Tg*IF2a (Ghosh *et al*., 2012). This represses protein synthesis while enhancing translation of a subset of mRNAs responsible for stress coping response and stage differentiation (Gebauer and Hentze, 2004, Joyce *et al*., 2011). Given that stress is closely associated with the induction of bradyzoite development (Boyce *et al*., 2005, Narasimhan *et al*., 2008, Vonlaufen *et al*., 2008), the phosphorylation status of *Tg*IF2α could be examined in z-FA-FMK treated parasites. In addition, studies have shown that *T. gondii* VAC contains both cathepsin B and L, where the maturation of cathepsin B is dependent on cathepsin L (Di Cristina *et al*., 2017, Dou and Carruthers, 2011, Dou *et al*., 2013, Turk and Guncar, 2003). Hence, the involvement of cathepsin L could be further investigated to examine the potential synergistic effect with cathepsin B inhibitors such as z-FA-FMK. Subsequently, several studies have shown that *T. gondii* parasites induces host cell autophagy to gain access to nutrients for its growth (Pernas *et al*., 2018, Subauste, 2019, Wang *et al*., 2009). Our findings indicate that autophagy is needed for parasites treated with z-FA-FMK to regain proliferation. Therefore, the elevation of autophagy markers in both Hs68 host cells and *T. gondii* parasites following z-FA-FMK could be determined to further confirm the involvement of autophagy and its effect upon extended period of treatment. Some of these studies particularly the synergistic effect of BSO and z-FA-FMK in blocking on *T. gondii* proliferation and infection can be studied further using mice as an *in vivo* model.

APPENDICES

APPENDICES

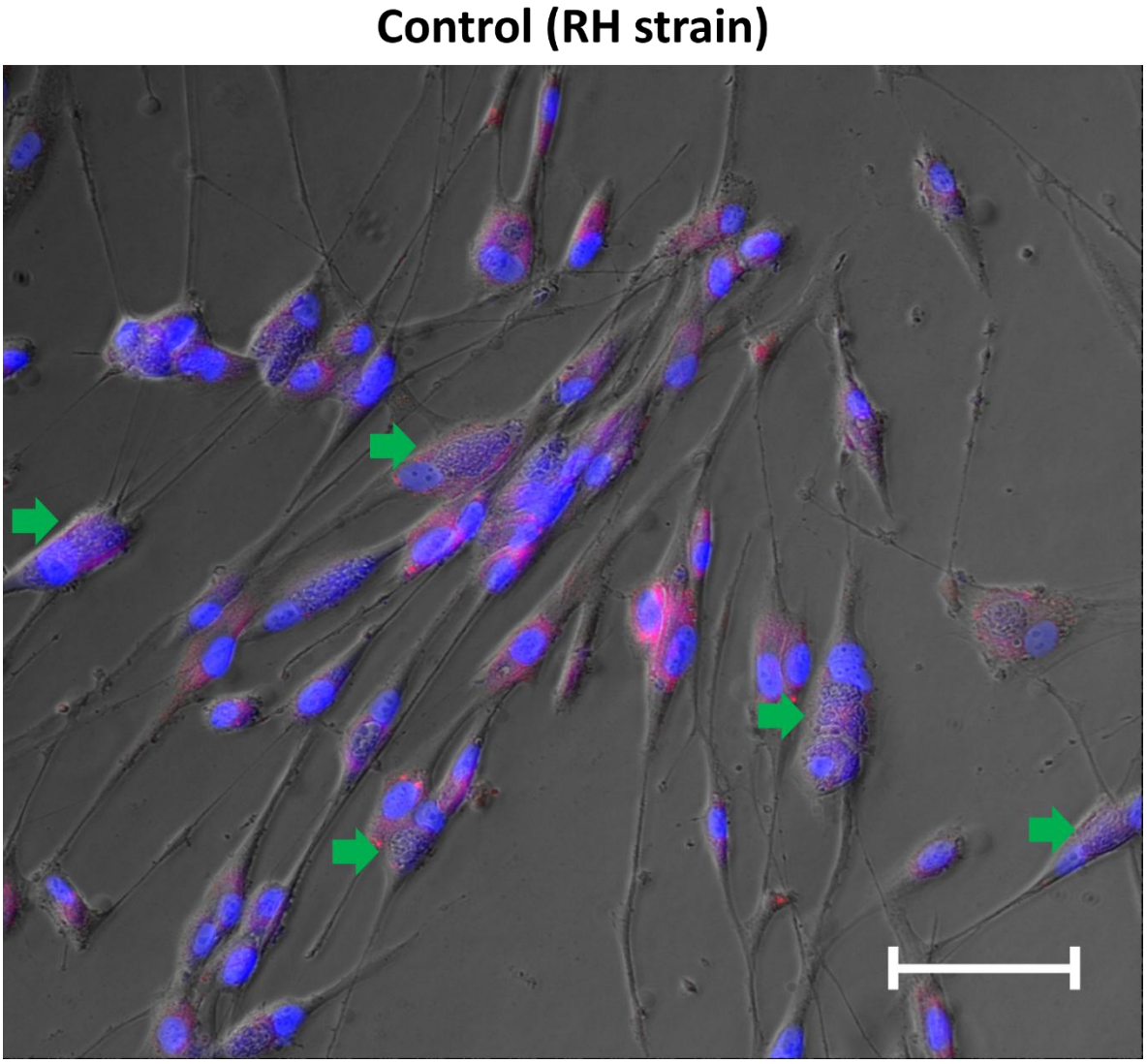

Figure A1: Live cell imaging of cathepsin B activity in *T. gondii* (RH strain) infected Hs68 cells

Hs68 cells infected with *T. gondii* (RH strain) for 72h prior to staining with Magic Red cathepsin B substrate (Red signal), and counterstained with DAPI (Blue signal) as described in the Materials and Methods. Green arrows indicate PV containing *T. gondii* parasites. Cells were examined under 20× magnification using fluorescence microscope. Scale bars, 50μm.

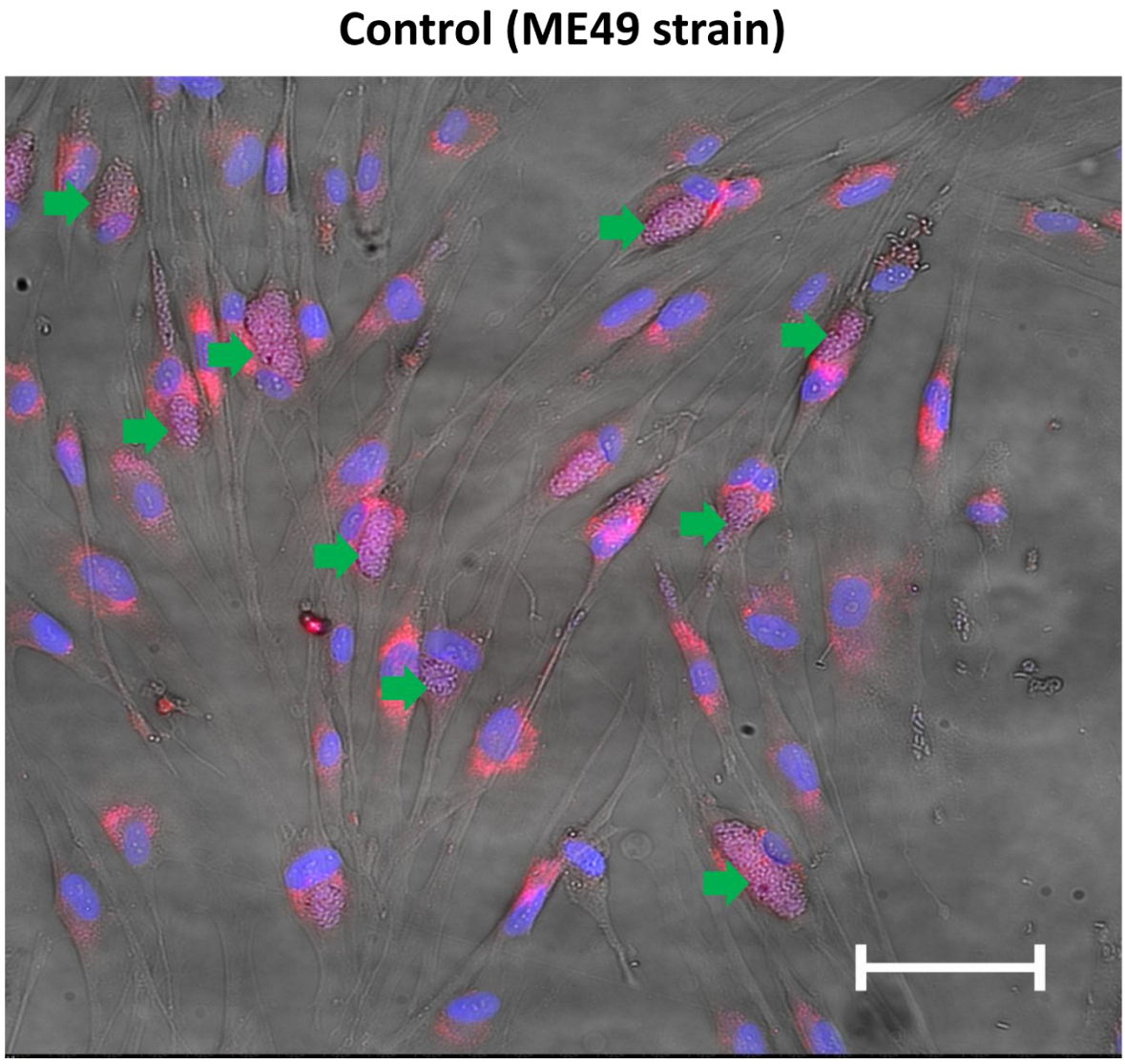

Figure A2: Live cell imaging of cathepsin B activity in *T. gondii* (ME49 strain) infected Hs68 cells

Hs68 cells infected with *T. gondii* (ME49 strain) for 72h prior to staining with Magic Red cathepsin B substrate (Red signal), and counterstained with DAPI (Blue signal) as described in the Materials and Methods. Green arrows indicate PV containing *T. gondii* parasites. Cells were examined under 20× magnification using fluorescence microscope. Scale bars, 50μm.

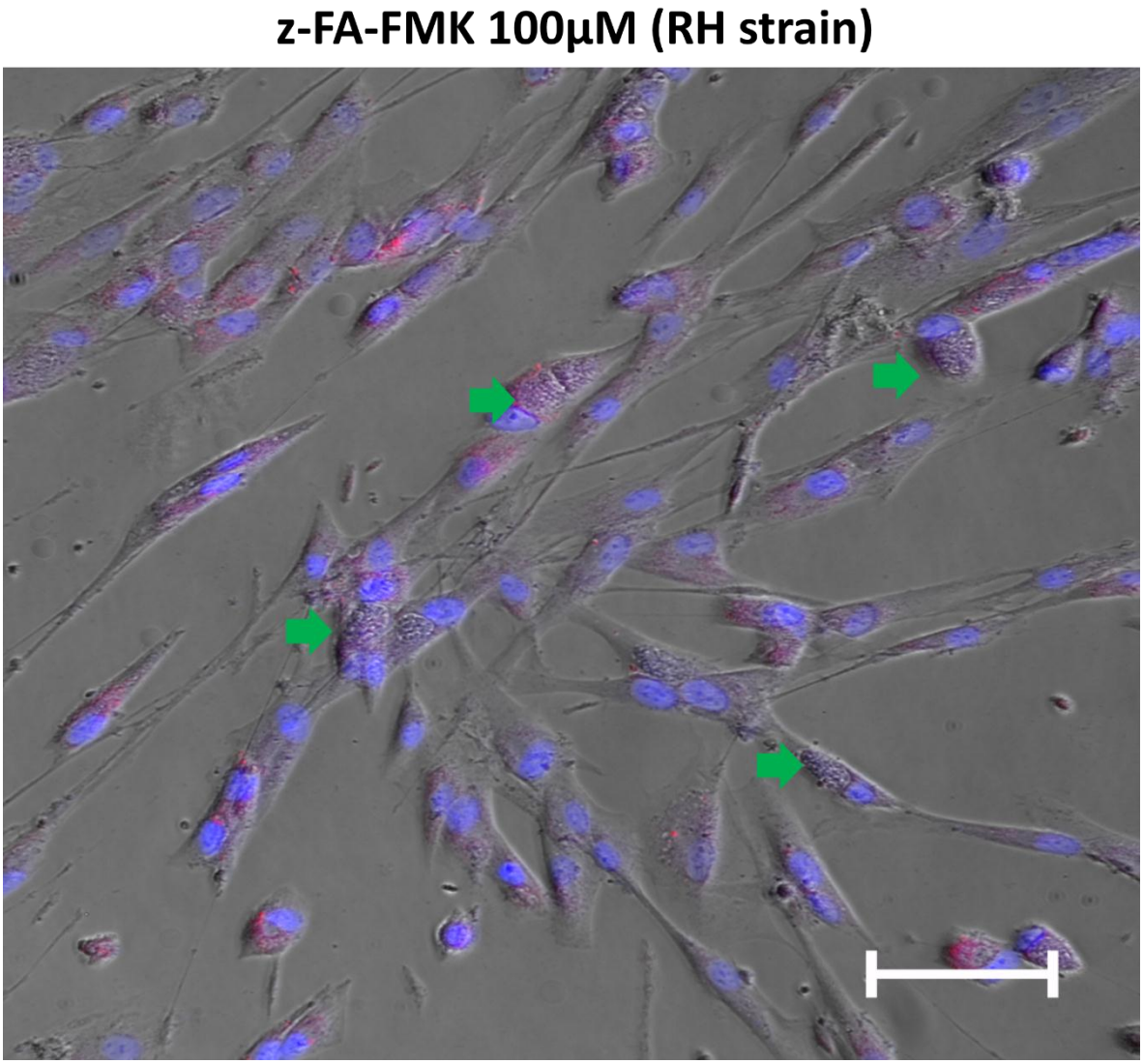

Figure A3: Live cell imaging of cathepsin B activity in *T. gondii* (RH strain) infected Hs68 cells treated with z-FA-FMK

Hs68 cells infected with *T. gondii* (RH strain) were treated with 100µM z-FA-FMK for 72h prior to staining with Magic Red cathepsin B substrate (Red signal), and counterstained with DAPI (Blue signal) as described in the Materials and Methods. Green arrows indicate PV containing *T. gondii* parasites. Cells were examined under 20× magnification using fluorescence microscope. Scale bars, 50µm.

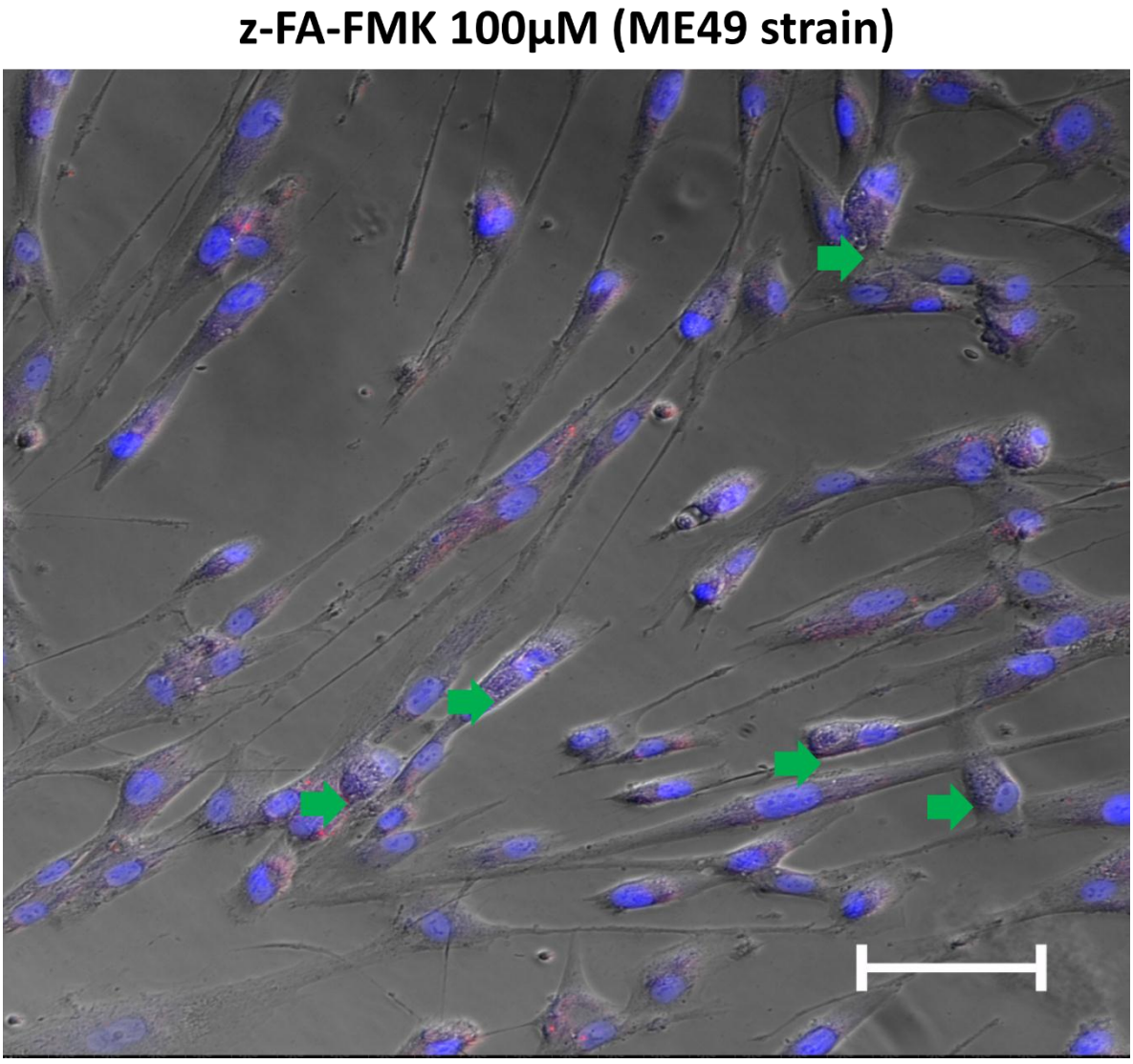

Figure A4: Live cell imaging of cathepsin B activity in *T. gondii* (ME49 strain) infected Hs68 cells treated with z-FA-FMK

Hs68 cells infected with *T. gondii* (ME49 strain) were treated with 100µM z-FA-FMK for 72h prior to staining with Magic Red cathepsin B substrate (Red signal), and counterstained with DAPI (Blue signal) as described in the Materials and Methods. Green arrows indicate PV containing *T. gondii* parasites. Cells were examined under 20× magnification using fluorescence microscope. Scale bars, 50µm.

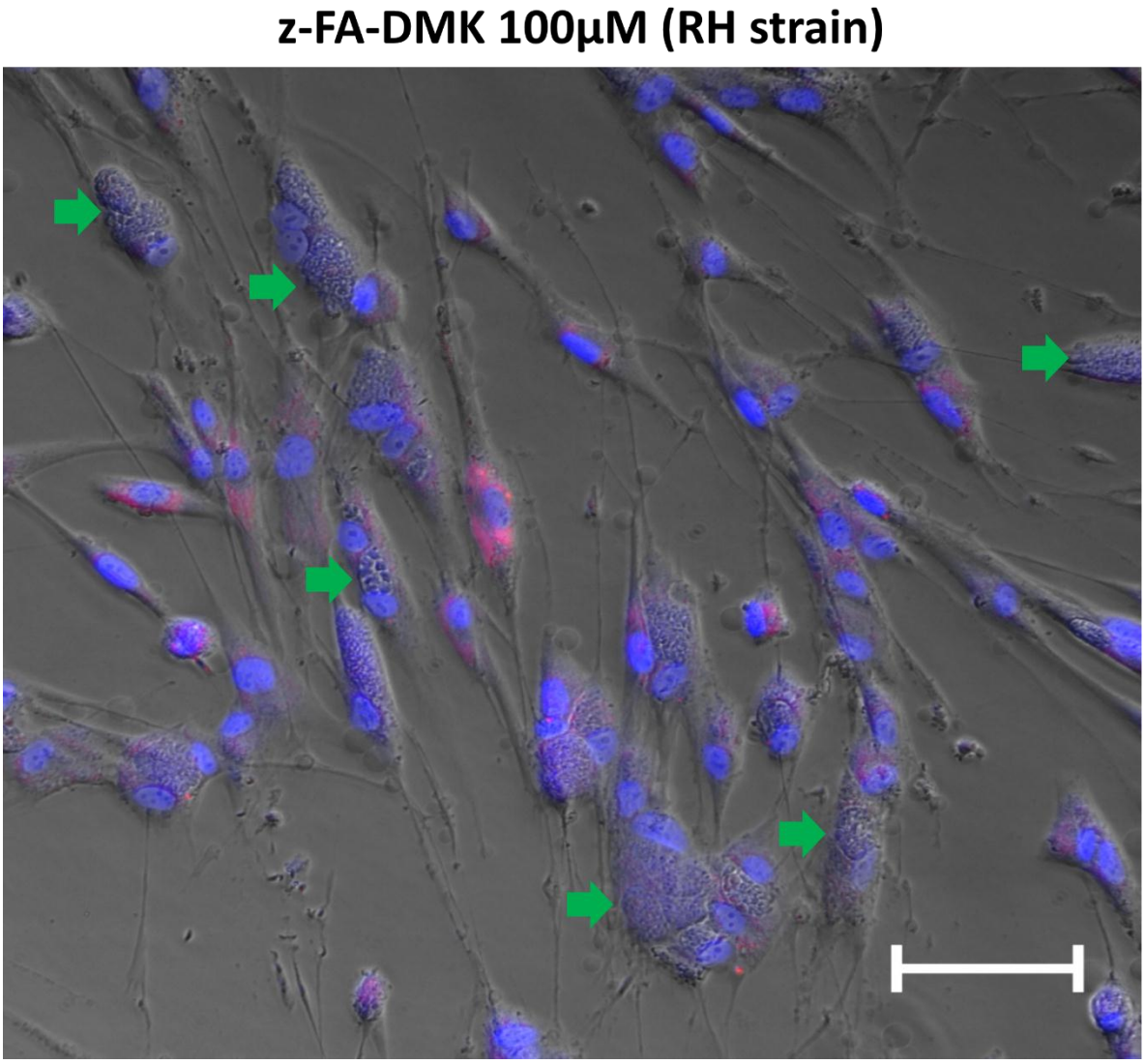

Figure A5: Live cell imaging of cathepsin B activity in *T. gondii* (RH strain) infected Hs68 cells treated with z-FA-DMK

Hs68 cells infected with *T. gondii* (RH strain) were treated with 100µM z-FA-DMK for 72h prior to staining with Magic Red cathepsin B substrate (Red signal), and counterstained with DAPI (Blue signal) as described in the Materials and Methods. Green arrows indicate PV containing *T. gondii* parasites. Cells were examined under 20× magnification using fluorescence microscope. Scale bars, 50µm.

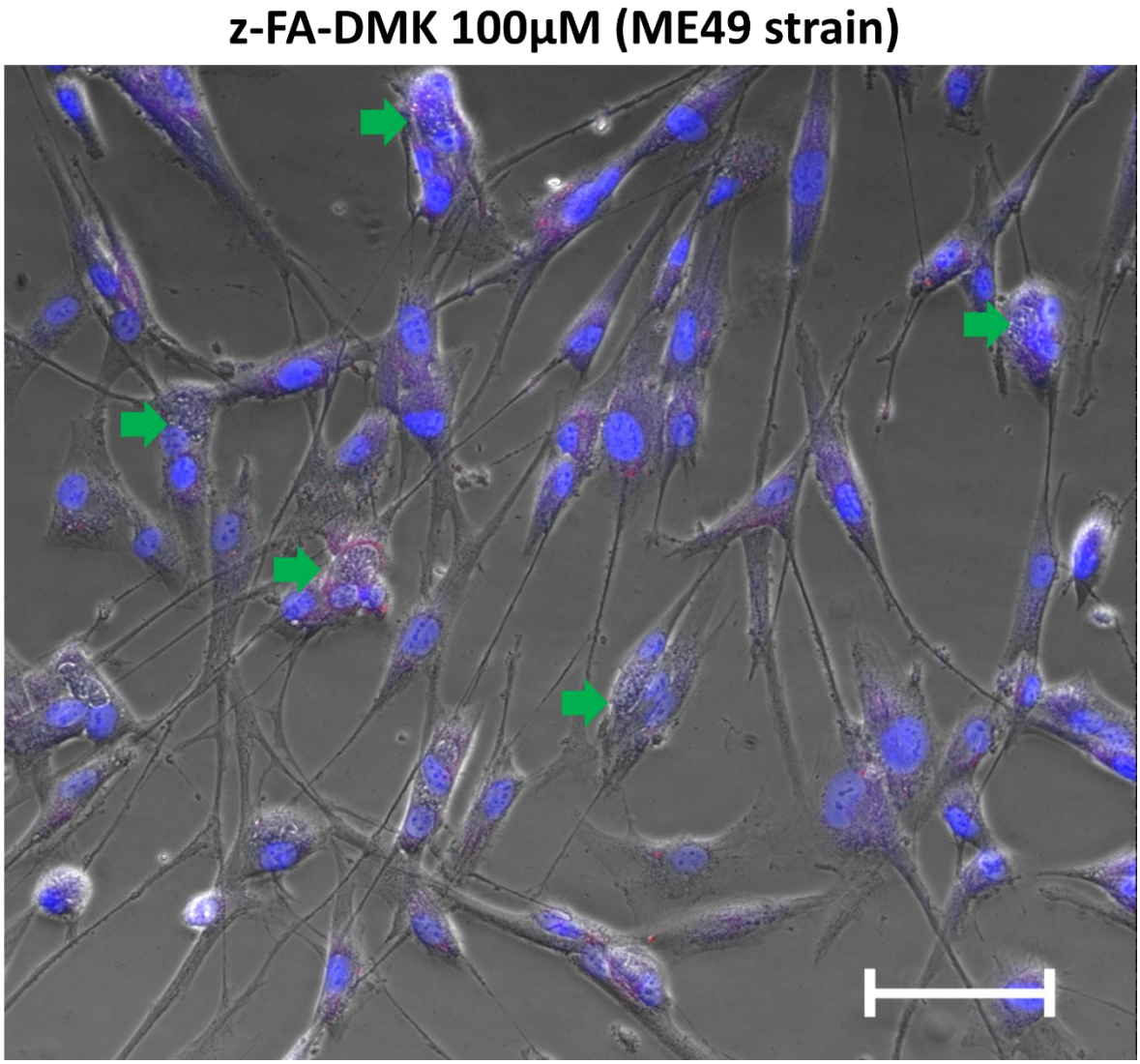

Figure A6: Live cell imaging of cathepsin B activity in *T. gondii* (ME49 strain) infected Hs68 cells treated with z-FA-DMK

Hs68 cells infected with *T. gondii* (ME49 strain) were treated with 100µM z-FA-DMK for 72h prior to staining with Magic Red cathepsin B substrate (Red signal), and counterstained with DAPI (Blue signal) as described in the Materials and Methods. Green arrows indicate PV containing *T. gondii* parasites. Cells were examined under 20× magnification using fluorescence microscope. Scale bars, 50µm.

BIBLIOGRAPHY

AHMED, N. K., MARTIN, L. A., WATTS, L. M., PALMER, J., THORNBURG, L., PRIOR, J. & ESSER, R. E. 1992. Peptidyl fluoromethyl ketones as inhibitors of cathepsin B. Implication for treatment of rheumatoid arthritis. *Biochemical Pharmacology,* 44, 1201-7.

AL-ADHAMI, B. H., NICHOLS, R. A., KUSEL, J. R., O'GRADY, J. & SMITH, H. V. 2006. *Cryptosporidium parvum* sporozoites contain glutathione. *Parasitology,* 133, 555-63.

ALDAY, P. H. & DOGGETT, J. S. 2017. Drugs in development for toxoplasmosis: Advances, challenges, and current status. *Drug design, development and therapy,* 11, 273-293.

ALEXANDER, D. L., MITAL, J., WARD, G. E., BRADLEY, P. & BOOTHROYD, J. C. 2005. Identification of the moving junction complex of *Toxoplasma gondii*: a collaboration between distinct secretory organelles. *PLOS Pathogens,* 1, 17.

ALONSO, A. M., CORVI, M. M. & DIAMBRA, L. 2019. Gene target discovery with network analysis in *Toxoplasma gondii*. *Scientific Reports,* 9, 646.

ANDREYEV, A. Y., KUSHNAREVA, Y. E. & STARKOV, A. A. 2005. Mitochondrial metabolism of reactive oxygen species. *Biochemistry (Moscow),* 70, 200-14.

ARANDA, A., SEQUEDO, L., TOLOSA, L., QUINTAS, G., BURELLO, E., CASTELL, J. V. & GOMBAU, L. 2013. Dichloro-dihydro-fluorescein diacetate (DCFH-DA) assay: a quantitative method for oxidative stress assessment of nanoparticle-treated cells. *Toxicology In Vitro,* 27, 954-63.

ARAUJO, F. G. & SLIFER, T. 2003. Different strains of *Toxoplasma gondii* induce different cytokine responses in CBA/Ca mice. *Infection and immunity,* 71, 4171-4174.

ARNER, E. S. & HOLMGREN, A. 2000. Physiological functions of thioredoxin and thioredoxin reductase. *European Journal of Biochemistry,* 267, 6102-9.

BAHRAMI, S., SHAHRIARI, A., TAVALLA, M., AZADMANESH, S. & HAMIDINEJAT, H. 2016. Blood levels of oxidant/antioxidant parameters in rats infected with *Toxoplasma gondii*. *Oxidative medicine and cellular longevity,* 2016, 8045969-8045969.

BANG, B., BAADSGAARD, O., SKOV, L. & JAATTELA, M. 2004. Inhibitors of cysteine cathepsin and calpain do not prevent ultraviolet-B-induced apoptosis in human keratinocytes and HeLa cells. *Archives of Dermatological Research,* 296, 67-73.

BARANWAL, S., AZAD, G. K., SINGH, V. & TOMAR, R. S. 2014. Signaling of chloroquine-induced stress in the yeast *Saccharomyces cerevisiae* requires the Hog1

and Slt2 mitogen-activated protein kinase pathways. *Antimicrobial Agents and Chemotherapy,* 58, 5552-66.

BARRETT, A. J. & KIRSCHKE, H. 1981. Cathepsin B, Cathepsin H, and cathepsin L. *Methods in Enzymology,* 80 Pt C, 535-61.

BASAVARAJU, A. 2016. Toxoplasmosis in HIV infection: An overview. *Tropical parasitology,* 6, 129-135.

BEN-HARARI, R. R., GOODWIN, E. & CASOY, J. 2017. Adverse event profile of pyrimethamine-based therapy in toxoplasmosis: a systematic review. *Drugs in R&D,* 17, 523-544.

BESTEIRO, S. 2019. The role of host autophagy machinery in controlling *Toxoplasma* infection. *Virulence,* 10, 438-447.

BESTEIRO, S., BROOKS, C. F., STRIEPEN, B. & DUBREMETZ, J. F. 2011a. Autophagy protein Atg3 is essential for maintaining mitochondrial integrity and for normal intracellular development of *Toxoplasma gondii* tachyzoites. *PLOS Pathogens,* 7, p1002416.

BESTEIRO, S., DUBREMETZ, J. F. & LEBRUN, M. 2011b. The moving junction of apicomplexan parasites: a key structure for invasion. *Cellular Microbiology,* 13, 797-805.

BHARTI, A. R., MCCUTCHAN, A., DEUTSCH, R., SMITH, D. M., ELLIS, R. J., CHERNER, M., WOODS, S. P., HEATON, R. K., GRANT, I. & LETENDRE, S. L. 2016. Latent *Toxoplasma* infection and higher *Toxoplasma gondii* immunoglobulin G levels are associated with worse neurocognitive functioning in HIV-infected adults. *Clinical Infectious Diseases,* 63, 1655-1660.

BIRBEN, E., SAHINER, U. M., SACKESEN, C., ERZURUM, S. & KALAYCI, O. 2012. Oxidative stress and antioxidant defense. *The World Allergy Organization journal,* 5, 9-19.

BISIO, H., LUNGHI, M. & BROCHET, M. 2019. Phosphatidic acid governs natural egress in *Toxoplasma gondii* via a guanylate cyclase receptor platform. *Nature Microbiology,* 4, 420-428.

BLACK, M. W. & BOOTHROYD, J. C. 2000. Lytic cycle of *Toxoplasma gondii*. *Microbiology and Molecular Biology Reviews,* 64, 607-623.

BLADER, I. J., COLEMAN, B. I., CHEN, C. T. & GUBBELS, M. J. 2015. Lytic cycle of *Toxoplasma gondii*: 15 years later. *Annual review of microbiology,* 69, 463-85.

BLADER, I. J. & KOSHY, A. A. 2014. *Toxoplasma gondii* development of its replicative niche: in its host cell and beyond. *Eukaryotic cell,* 13, 965-976.

BLADER, I. J. & SAEIJ, J. P. 2009. Communication between *Toxoplasma gondii* and its host: impact on parasite growth, development, immune evasion, and virulence. *APMIS : acta pathologica, microbiologica, et immunologica Scandinavica,* 117, 458-476.

BLUME, M. & SEEBER, F. 2018. Metabolic interactions between *Toxoplasma gondii* and its host. *F1000Research,* 7, F1000 Faculty Rev-1719.

BOHNE, W., HEESEMANN, J. & GROSS, U. 1994. Reduced replication of *Toxoplasma gondii* is necessary for induction of bradyzoite-specific antigens: a possible role for nitric oxide in triggering stage conversion. *Infection and immunity,* 62, 1761-1767.

BOHNE, W., HOLPERT, M. & GROSS, U. 1999. Stage differentiation of the protozoan parasite *Toxoplasma gondii*. *Immunobiology,* 201, 248-54.

BOSCH-DRIESSEN, L. E., BERENDSCHOT, T. T., ONGKOSUWITO, J. V. & ROTHOVA, A. 2002a. Ocular toxoplasmosis: clinical features and prognosis of 154 patients. *Ophthalmology,* 109, 869-78.

BOSCH-DRIESSEN, L. H., VERBRAAK, F. D., SUTTORP-SCHULTEN, M. S., VAN RUYVEN, R. L., KLOK, A. M., HOYNG, C. B. & ROTHOVA, A. 2002b. A prospective, randomized trial of pyrimethamine and azithromycin vs pyrimethamine and sulfadiazine for the treatment of ocular toxoplasmosis. *American Journal of Ophthalmology,* 134, 34-40.

BOSCH, S. S., KRONENBERGER, T., MEISSNER, K. A., ZIMBRES, F. M., STEGEHAKE, D., IZUI, N. M., SCHETTERT, I., LIEBAU, E. & WRENGER, C. 2015. Oxidative stress control by apicomplexan parasites. *Biomed Research International,* 2015, 351289.

BOYCE, M., BRYANT, K. F., JOUSSE, C., LONG, K., HARDING, H. P., SCHEUNER, D., KAUFMAN, R. J., MA, D., COEN, D. M., RON, D. & YUAN, J. 2005. A selective inhibitor of eIF2alpha dephosphorylation protects cells from ER stress. *Science,* 307, 935-9.

BUCHHOLZ, K. R., BOWYER, P. W. & BOOTHROYD, J. C. 2013. Bradyzoite pseudokinase 1 is crucial for efficient oral infectivity of the *Toxoplasma gondii* tissue cyst. *Eukaryotic Cell,* 12, 399-410.

BUXTON, D. & INNES, E. A. 1995. A commercial vaccine for ovine toxoplasmosis. *Parasitology,* 110, 11-6.

BUXTON, D., MALEY, S. W., WRIGHT, S. E., RODGER, S., BARTLEY, P. & INNES, E. A. 2007. Ovine toxoplasmosis: transmission, clinical outcome and control. *Parassitologia,* 49, 219-21.

CABRAL, G. R. A. & DAMATTA, R. 2017. Antimicrobial activities of macrophages and *Toxoplasma gondii* evasion mechanisms. *Toxoplasma gondii: Dangers, life cycle and research*, 39-84

CAPOBIANGO, J. D., BREGANO, R. M., MORI, F. M., NAVARRO, I. T., CAMPOS, J. S., TATAKIHARA, L. T., TALIZIN, T. B., SANTOS, M. D., PEREIRA, T. R., NARCISO, S. G. & REICHE, E. M. 2016. Gestational and congenital toxoplasmosis: a practical approach to disease notification. *Epidemiology and Health Services,* 25, 187-194.

CAPOBIANGO, J. D., BREGANÓ, R. M., NAVARRO, I. T., REZENDE NETO, C. P., CASELLA, A. M. B., MORI, F. M. R. L., PAGLIARI, S., INOUE, I. T. & REICHE, E. M. V. 2014. Congenital toxoplasmosis in a reference center of Paraná, Southern Brazil. *Brazilian Journal of Infectious Diseases,* 18, 364-371.

CARRUTHERS, V. B. 1999. Armed and dangerous: *Toxoplasma gondii* uses an arsenal of secretory proteins to infect host cells. *Parasitology International,* 48, 1-10.

CARRUTHERS, V. B. 2002. Host cell invasion by the opportunistic pathogen *Toxoplasma gondii*. *Acta Tropica,* 81, 111-22.

CARRUTHERS, V. B. 2006. Proteolysis and *Toxoplasma* invasion. *International Journal of Parasitology,* 36, 595-600.

CESBRON-DELAUW, M. F. 1994. Dense-granule organelles of *Toxoplasma gondii*: their role in the host-parasite relationship. *Parasitology Today,* 10, 293-6.

CHANDRA, J., SAMALI, A. & ORRENIUS, S. 2000. Triggering and modulation of apoptosis by oxidative stress. *Free Radical Biology and Medicine,* 29, 323-33.

CHAPARRO, J. D., CHENG, T., TRAN, U. P., ANDRADE, R. M., BRENNER, S. B. T., HWANG, G., COHN, S., HIRATA, K., MCKERROW, J. H. & REED, S. L. 2018. Two key cathepsins, *Tg*CPB and *Tg*CPL, are targeted by the vinyl sulfone inhibitor K11777 in *in vitro* and *in vivo* models of toxoplasmosis. *PLOS ONE,* 13, e0193982.

CHARRON, A. J. & SIBLEY, L. D. 2002. Host cells: mobilizable lipid resources for the intracellular parasite *Toxoplasma gondii*. *Journal of Cell Science,* 115, 3049-59.

CHEN, L. F., HAN, X. L., LI, F. X., YAO, Y. Y., FANG, J. P., LIU, X., LI, X. C., WU, K., LIU, M. & CHEN, X. G. 2018. Comparative studies of *Toxoplasma gondii* transcriptomes: insights into stage conversion based on gene expression profiling and alternative splicing. *Parasites & Vectors,* 11, 402.

CHEW, W. K., WAH, M. J., AMBU, S. & SEGARRA, I. 2012. *Toxoplasma gondii*: Determination of the onset of chronic infection in mice and the *in vitro* reactivation of brain cysts. *Experimental Parasitology,* 130, 22-25.

CLOUGH, B. & FRICKEL, E. M. 2017. The *Toxoplasma* parasitophorous vacuole: an evolving host-parasite frontier. *Trends Parasitol,* 33, 473-488.

COOK, A. J., GILBERT, R. E., BUFFOLANO, W., ZUFFEREY, J., PETERSEN, E., JENUM, P. A., FOULON, W., SEMPRINI, A. E. & DUNN, D. T. 2000. Sources of *Toxoplasma* infection in pregnant women: European multicentre case-control study. *European Research Network on Congenital Toxoplasmosis*. *Bmj,* 321, 142-7.

COPPENS, I., ASAI, T. & TOMAVO, S. 2013. *Biochemistry and metabolism of Toxoplasma gondii. carbohydrates, lipids and nucleotides*.

COPPENS, I., SINAI, A. P. & JOINER, K. A. 2000. *Toxoplasma gondii* exploits host low-density lipoprotein receptor-mediated endocytosis for cholesterol acquisition. *Journal of Cell Biology,* 149, 167-80.

COUTO, N., MALYS, N., GASKELL, S. J. & BARBER, J. 2013. Partition and turnover of glutathione reductase from saccharomyces cerevisiae: a proteomic approach. *Journal of Proteome Research,* 12, 2885-2894.

DA COSTA-SILVA, T. A., DA SILVA MEIRA, C., FRAZZATTI-GALLINA, N. & PEREIRA-CHIOCCOLA, V. L. 2012. *Toxoplasma gondii* antigens: Recovery analysis of tachyzoites cultivated in Vero cell maintained in serum free medium. *Experimental Parasitology,* 130, 463-469.

DE MELO, E. J. & DE SOUZA, W. 1996. Pathway of C6-NBD-Ceramide on the host cell infected with *Toxoplasma gondii*. *Cell Structure and Function,* 21, 47-52.

DENKERS, E. Y., KIM, L. & BUTCHER, B. A. 2003. In the belly of the beast: subversion of macrophage proinflammatory signalling cascades during *Toxoplasma gondii* infection. *Cell Microbiology,* 5, 75-83.

DI CRISTINA, M., DOU, Z., LUNGHI, M., KANNAN, G., HUYNH, M. H., MCGOVERN, O. L., SCHULTZ, T. L., SCHULTZ, A. J., MILLER, A. J., HAYES, B. M., VAN DER LINDEN, W., EMILIANI, C., BOGYO, M., BESTEIRO, S., COPPENS, I. & CARRUTHERS, V. B. 2017. *Toxoplasma* depends on lysosomal consumption of autophagosomes for persistent infection. *Nature microbiology,* 2, 17096.

DING, M., CLAYTON, C. & SOLDATI, D. 2000. *Toxoplasma gondii* catalase: are there peroxisomes in *Toxoplasma*? *Journal od Cellular Science,* 113 (Pt 13), 2409-19.

DOU, Z. & CARRUTHERS, V. B. 2011. Cathepsin proteases in *Toxoplasma gondii*. *Advances in Experimental Medical Biology,* 712, 49-61.

DOU, Z., COPPENS, I. & CARRUTHERS, V. B. 2013. Non-canonical maturation of two papain-family proteases in *Toxoplasma gondii*. *Journal of Biological Chemistry,* 288, 3523-34.

DOU, Z., MCGOVERN, O. L., DI CRISTINA, M. & CARRUTHERS, V. B. 2014. *Toxoplasma gondii* ingests and digests host cytosolic proteins. *mBio,* 5, e01188.

DREW, R. & MINERS, J. O. 1984. The effects of buthionine sulphoximine (BSO) on glutathione depletion and xenobiotic biotransformation. *Biochemical Pharmacology,* 33, 2989-94.

DREWRY, L. L. & SIBLEY, L. D. 2015. *Toxoplasma* actin is required for efficient host cell invasion. *mBio,* 6, e00557-15.

DUBEY, J. P. 1988. *Toxoplasmosis of animals & man*, CRC-Press.

DUBEY, J. P. 1995. Duration of immunity to shedding of *Toxoplasma gondii* oocysts by cats. *Journal of Parasitology,* 81, 410-5.

Dubey, J. P. (1996). *Toxoplasma gondii*. *In S. Baron (Ed.), Medical Microbiology (4th ed.).* Galveston, TX: The University of Texas Medical Branch at Galveston.

DUBEY, J. P. 1998. Advances in the life cycle of *Toxoplasma gondii*. *International Journal for Parasitology*, 28, 1019-1024.

DUBEY, J. P. & JONES, J. L. 2008. *Toxoplasma gondii* infection in humans and animals in the United States. *International Journal for Parasitology,* 38, 1257-1278.

DUBEY, J. P., LINDSAY, D. S. & SPEER, C. A. 1998. Structures of *Toxoplasma gondii* tachyzoites, bradyzoites, and sporozoites and biology and development of tissue cysts. *Clinical Microbiology Reviews,* 11, 267-299.

DUMETRE, A. & DARDE, M. L. 2003. How to detect *Toxoplasma gondii* oocysts in environmental samples? *FEMS Microbiology Reviews,* 27, 651-61.

KASPER, L. H. 2001. Toxoplasmosis. eLS. John Wiley & Sons, Ltd.

DUNAY, I. R., GAJUREL, K., DHAKAL, R., LIESENFELD, O. & MONTOYA, J. G. 2018. Treatment of toxoplasmosis: historical perspective, animal models, and current clinical practice. *Clinical Microbiology Reviews,* 31, e00057-17.

DUSZENKO, M., GINGER, M. L., BRENNAND, A., GUALDRON-LOPEZ, M., COLOMBO, M. I., COOMBS, G. H., COPPENS, I., JAYABALASINGHAM, B., LANGSLEY, G., DE CASTRO, S. L., MENNA-BARRETO, R., MOTTRAM, J. C., NAVARRO, M., RIGDEN, D. J., ROMANO, P. S., STOKA, V., TURK, B. & MICHELS, P. A. 2011. Autophagy in protists. *Autophagy,* 7, 127-58.

DZIERSZINSKI, F., NISHI, M., OUKO, L. & ROOS, D. S. 2004. Dynamics of *Toxoplasma gondii* differentiation. *Eukaryotic Cell,* 3, 992-1003.

ELSHEIKHA, H. M. & KHAN, N. A. 2010. Protozoa traversal of the blood-brain barrier to invade the central nervous system. *FEMS Microbiology Reviews,* 34, 532-53.

ENGEL, J. C., DOYLE, P. S., HSIEH, I. & MCKERROW, J. H. 1998. Cysteine protease inhibitors cure an experimental *Trypanosoma cruzi* infection. *The Journal of experimental medicine,* 188, 725-734.

FAUNDEZ, M., PINO, L., LETELIER, P., ORTIZ, C., LÓPEZ, R., SEGUEL, C., FERREIRA, J., PAVANI, M., MORELLO, A. & MAYA, J. D. 2005. Buthionine sulfoximine increases the toxicity of nifurtimox and benznidazole to *Trypanosoma cruzi*. *Antimicrobial agents and chemotherapy,* 49, 126-130.

FERGUSON, D. J. 2004. Use of molecular and ultrastructural markers to evaluate stage conversion of *Toxoplasma gondii* in both the intermediate and definitive host. *International Journal of Parasitology,* 34, 347-60.

FERGUSON, D. J. P. & DUBREMETZ, J. F. 2014. *Chapter 2 - The Ultrastructure of Toxoplasma gondii.* In: WEISS, L. M. & KIM, K. (eds.) *Toxoplasma gondii* (2nd Edition). Boston: Academic Press.

FERREIRA DA SILVA MDA, F., BARBOSA, H. S., GROSS, U. & LUDER, C. G. 2008. Stress-related and spontaneous stage differentiation of *Toxoplasma gondii*. *Molecular Biosystems,* 4, 824-34.

FLEGR, J., PRANDOTA, J., SOVICKOVA, M. & ISRAILI, Z. H. 2014. Toxoplasmosis-a global threat. Correlation of latent toxoplasmosis with specific disease burden in a set of 88 countries. *PLOS One*, 9, e90203.

FOULON, W., NAESSENS, A., LAUWERS, S., DE MEUTER, F. & AMY, J. J. 1988. Impact of primary prevention on the incidence of toxoplasmosis during pregnancy. *Obstetrics & Gynecology,* 72, 363-6.

FOX, B. A. & BZIK, D. J. 2002. *De novo* pyrimidine biosynthesis is required for virulence of *Toxoplasma gondii*. *Nature,* 415, 926-9.

FOX, B. A., GIGLEY, J. P. & BZIK, D. J. 2004. *Toxoplasma gondii* lacks the enzymes required for *de novo* arginine biosynthesis and arginine starvation triggers cyst formation. *International Journal of Parasitology,* 34, 323-31.

FRANKE DE CAZZULO, B. M., MARTINEZ, J., NORTH, M. J., COOMBS, G. H. & CAZZULO, J. J. 1994. Effects of proteinase inhibitors on the growth and differentiation of *Trypanosoma cruzi*. *FEMS Microbiology Letters,* 124, 81-6.

FRIDOVICH, I. 1995. Superoxide radical and superoxide dismutases. *Annual Review of Biochemistry,* 64, 97-112.

GEBAUER, F. & HENTZE, M. W. 2004. Molecular mechanisms of translational control. *Nature Reviews Molecular Cell Biology,* 5, 827-35.

GHOSH, D., WALTON, J. L., ROEPE, P. D. & SINAI, A. P. 2012. Autophagy is a cell death mechanism in *Toxoplasma gondii*. *Cell Microbiology,* 14, 589-607.

GIBELLINI, L., PINTI, M., NASI, M., DE BIASI, S., ROAT, E., BERTONCELLI, L. & COSSARIZZA, A. 2010. Interfering with ros metabolism in cancer cells: the potential role of quercetin. *Cancers,* 2, 1288-1311.

GILSON, P. R. & CRABB, B. S. 2009. Do apicomplexan parasite-encoded proteins act as both ligands and receptors during host cell invasion? *F1000 Biology Reports,* 1, 64.

GLOR, S. B., EDELHOFER, R., GRIMM, F., DEPLAZES, P. & BASSO, W. 2013. Evaluation of a commercial ELISA kit for detection of antibodies against *Toxoplasma gondii* in serum, plasma and meat juice from experimentally and naturally infected sheep. *Parasites & Vectors,* 6, 85.

GORLACH, A., DIMOVA, E. Y., PETRY, A., MARTINEZ-RUIZ, A., HERNANSANZ-AGUSTIN, P., ROLO, A. P., PALMEIRA, C. M. & KIETZMANN, T. 2015. Reactive oxygen species, nutrition, hypoxia and diseases: Problems solved? *Redox Biology,* 6, 372-385.

GREEN, G. D. & SHAW, E. 1981. Peptidyl diazomethyl ketones are specific inactivators of thiol proteinases. *Journal of Biological Chemistry,* 256, 1923-8.

GRINTZALIS, K., GEORGIOU, C. D. & SCHNEIDER, Y.-J. 2015. An accurate and sensitive Coomassie Brilliant Blue G-250-based assay for protein determination. *Analytical Biochemistry,* 480, 28-30.

GROSS, U., BOHNE, W., SOETE, M. & DUBREMETZ, J. F. 1996. Developmental differentiation between tachyzoites and bradyzoites of *Toxoplasma gondii*. *Parasitology Today,* 12, 30-3.

GRZONKA, Z., JANKOWSKA, E., KASPRZYKOWSKI, F., KASPRZYKOWSKA, R., LANKIEWICZ, L., WICZK, W., WIECZERZAK, E., CIARKOWSKI, J., DRABIK, P., JANOWSKI, R., KOZAK, M., JASKOLSKI, M. & GRUBB, A. 2001. Structural studies of cysteine proteases and their inhibitors. *Acta Biochimica Polonica,* 48, 1-20.

GUBBELS, M. J., WHITE, M. & SZATANEK, T. 2008. The cell cycle and *Toxoplasma gondii* cell division: tightly knit or loosely stitched? *International Journal of Parasitology,* 38, 1343-58.

GUICCIARDI, M. E., DEUSSING, J., MIYOSHI, H., BRONK, S. F., SVINGEN, P. A., PETERS, C., KAUFMANN, S. H. & GORES, G. J. 2000. Cathepsin B contributes to TNF-alpha-mediated hepatocyte apoptosis by promoting mitochondrial release of cytochrome c. *Journal of Clinical Investigations,* 106, 1127-37.

GUIMARAES, E. V., CARVALHO, L. & BARBOSA, H. S. 2009. Interaction and cystogenesis of *Toxoplasma gondii* within skeletal muscle cells *in vitro*. *Memórias do Instituto Oswaldo Cruz,* 104, 170-4.

HALLIWELL, B. 1999. Antioxidant defence mechanisms: from the beginning to the end (of the beginning). *Free Radical Research,* 31, 261-72.

HALONEN, S. K. 2009. Role of autophagy in the host defense against *Toxoplasma gondii* in astrocytes. *Autophagy,* 5, 268-9.

HAMMOUDA, N. A., AMIN, S. M., KHALIFA, A. M., ABOU-EL, N. I., GAAFAR, M. R. & NASR, M. A. 2006. The use of ELISA and immunohistochemistry techniques for detection of *Toxoplasma gondii* antigen in tissues of experimentally infected mice. *Journal of the Egyptian Society of Parasitology,* 36, 925-35.

HARKER, K. S., UENO, N. & LODOEN, M. B. 2015. *Toxoplasma gondii* dissemination: a parasite's journey through the infected host. *Parasite Immunology,* 37, 141-9.

HARTH, G., ANDREWS, N., MILLS, A. A., ENGEL, J. C., SMITH, R. & MCKERROW, J. H. 1993. Peptide-fluoromethyl ketones arrest intracellular replication and intercellular transmission of Trypanosoma cruzi. *Molecular and Biochemistry Parasitology,* 58, 17-24.

HERMAN, M., GILLIES, S., MICHELS, P. A. & RIGDEN, D. J. 2006. Autophagy and related processes in trypanosomatids: insights from genomic and bioinformatic analyses. *Autophagy,* 2, 107-18.

HILL, D. & DUBEY, J. P. 2002. *Toxoplasma gondii*: transmission, diagnosis and prevention. *Clinical Microbiology and Infection,* 8, 634-640.

HILL, D. E., CHIRUKANDOTH, S. & DUBEY, J. P. 2005. Biology and epidemiology of *Toxoplasma gondii* in man and animals. *Animal Health Research Reviews,* 6, 41-61.

HILL, D. E. & DUBEY, J. P. 2018. *Toxoplasma gondii*. *In:* ORTEGA, Y. R. & STERLING, C. R. (eds.) *Foodborne Parasites.* Cham: Springer International Publishing.

HOPPE, H. C., NGO, H. M., YANG, M. & JOINER, K. A. 2000. Targeting to rhoptry organelles of *Toxoplasma gondii* involves evolutionarily conserved mechanisms. *Nature Cell Biology,* 2, 449-56.

HORTUA TRIANA, M. A., MÁRQUEZ-NOGUERAS, K. M., VELLA, S. A. & MORENO, S. N. J. 2018. Calcium signaling and the lytic cycle of the apicomplexan parasite *Toxoplasma gondii*. *Biochimica et Biophysica Acta (BBA) - Molecular Cell Research,* 1865, 1846-1856.

HU, K., JOHNSON, J., FLORENS, L., FRAUNHOLZ, M., SURAVAJJALA, S., DILULLO, C., YATES, J., ROOS, D. S. & MURRAY, J. M. 2006. Cytoskeletal components of an invasion machine--the apical complex of *Toxoplasma gondii*. *PLOS Pathogens,* 2, e13.

HU, K., ROOS, D. S., ANGEL, S. O. & MURRAY, J. M. 2004. Variability and heritability of cell division pathways in *Toxoplasma gondii*. *Journal of Cell Science,* 117, 5697-705.

HUA, A. B., JUSTINIANO, R., PERER, J., PARK, S. L., LI, H., CABELLO, C. M. & WONDRAK, G. T. 2019. Repurposing the electron transfer reactant phenazine methosulfate (PMS) for the apoptotic elimination of malignant melanoma cells

through induction of lethal oxidative and mitochondriotoxic stress. *Cancers,* 11, 590.

HUSSAIN, M. A., STITT, V., SZABO, E. A. & NELAN, B. 2017. *Toxoplasma gondii* in the Food Supply. *Pathogens (Basel, Switzerland),* 6, 21.

INOUE, Y. & KLIONSKY, D. J. 2010. Regulation of macroautophagy in *Saccharomyces cerevisiae*. *Seminars in Cell and Developmental Biology,* 21, 664-70.

ISRAELSKI, D. M., CHMIEL, J. S., POGGENSEE, L., PHAIR, J. P. & REMINGTON, J. S. 1993. Prevalence of *Toxoplasma* infection in a cohort of homosexual men at risk of AIDS and toxoplasmic encephalitis. *Journal of Acquired Immune Deficiency Syndrome,* 6, 414-8.

JACOBS, L., REMINGTON, J. S. & MELTON, M. L. 1960. The resistance of the encysted form of *Toxoplasma gondii*. *Journal of Parasitology,* 46, 11-21.

JACOT, D., DAHER, W. & SOLDATI-FAVRE, D. 2013. *Toxoplasma gondii* myosin F, an essential motor for centrosomes positioning and apicoplast inheritance. *The EMBO Journal,* 32, 1702-1716.

JEFFERS, V., TAMPAKI, Z., KIM, K. & SULLIVAN, W. J., JR. 2018. A latent ability to persist: differentiation in *Toxoplasma gondii*. *Cellular and Molecular Life Sciences,* 75, 2355-2373.

JEROME, M. E., RADKE, J. R., BOHNE, W., ROOS, D. S. & WHITE, M. W. 1998. *Toxoplasma gondii* bradyzoites form spontaneously during sporozoite-initiated development. *Infection and Immunity,* 66, 4838-44.

JOHNSON, V. L., KO, S. C., HOLMSTROM, T. H., ERIKSSON, J. E. & CHOW, S. C. 2000. Effector caspases are dispensable for the early nuclear morphological changes during chemical-induced apoptosis. *Journal of Cell Science,* 113 (Pt 17), 2941-53.

JONES, D. P. & GO, Y. M. 2010. Redox compartmentalization and cellular stress. *Diabetes, obesity & metabolism,* 12, 116-125.

JONES, J., LOPEZ, A. & WILSON, M. 2003. Congenital toxoplasmosis. *American Family Physician,* 67, 2131-8.

JOYCE, B. R., KONRAD, C., WEK, R. C. & SULLIVAN, W. J., JR. 2011. Translation control is critical during acute and chronic stages of toxoplasmosis infection. *Expert Review of Anti-infective Therapy,* 9, 1-3.

KAASCH, A. J. & JOINER, K. A. 2000. Targeting and subcellular localization of *Toxoplasma gondii* catalase. Identification of peroxisomes in an apicomplexan parasite. *Journal of Biological Chemistry,* 275, 1112-8.

KAMENCIC, H., LYON, A., PATERSON, P. G. & JUURLINK, B. H. 2000. Monochlorobimane fluorometric method to measure tissue glutathione. *Analytical Biochemistry,* 286, 35-7.

KANNAN, G., DI CRISTINA, M., SCHULTZ, A. J., HUYNH, M.-H., WANG, F., SCHULTZ, T. L., LUNGHI, M., COPPENS, I. & CARRUTHERS, V. B. 2019. A role for *Toxoplasma gondii* chloroquine resistance transporter in bradyzoite viability and digestive vacuole maintenance. *bioRxiv,* 647669.

KATHURIA, M., BHATTACHARJEE, A., SASHIDHARA, K. V., SINGH, S. P. & MITRA, K. 2014. Induction of mitochondrial dysfunction and oxidative stress in *Leishmania donovani* by orally active clerodane diterpene. *Antimicrobial agents and chemotherapy,* 58, 5916-5928.

KHAN, A. & GRIGG, M. E. 2017. *Toxoplasma gondii*: Laboratory maintenance and growth. *Current Protocols in Microbiology,* 44, 20c.1.1-20c.1.17.

KHAN, I. A., HWANG, S. & MORETTO, M. 2019. *Toxoplasma gondii*: CD8 T cells cry for CD4 help. *Frontiers in Cellular and Infection Microbiology,* 9.

KIM, B., KIM, H. S., JUNG, E.-J., LEE, J. Y., K. TSANG, B., LIM, J. M. & SONG, Y. S. 2016. Curcumin induces ER stress-mediated apoptosis through selective generation of reactive oxygen species in cervical cancer cells. *Molecular Carcinogenesis,* 55, 918-928.

KIM, K. & WEISS, L. M. 2004. *Toxoplasma gondii*: the model apicomplexan. *International journal for parasitology,* 34, 423-432.

KLIONSKY, D. J., BAEHRECKE, E. H., BRUMELL, J. H., CHU, C. T., CODOGNO, P., CUERVO, A. M., DEBNATH, J., DERETIC, V., ELAZAR, Z., ESKELINEN, E. L., FINKBEINER, S., FUEYO-MARGARETO, J., GEWIRTZ, D., JAATTELA, M., KROEMER, G., LEVINE, B., MELIA, T. J., MIZUSHIMA, N., RUBINSZTEIN, D. C., SIMONSEN, A., THORBURN, A., THUMM, M. & TOOZE, S. A. 2011. A comprehensive glossary of autophagy-related molecules and processes (2nd edition). *Autophagy,* 7, 1273-94.

KRATSCHMER, C. & LEVY, M. 2018. Targeted delivery of auristatin-modified toxins to pancreatic cancer using aptamers. *Molecular Therapy - Nucleic Acids,* 10, 227-236.

KRISTENSEN, A. R., SCHANDORFF, S., HOYER-HANSEN, M., NIELSEN, M. O., JAATTELA, M., DENGJEL, J. & ANDERSEN, J. S. 2008. Ordered organelle degradation during starvation-induced autophagy. *Molecular and Cellular Proteomics,* 7, 2419-28.

KURUTAS, E. B. 2016. The importance of antioxidants which play the role in cellular response against oxidative/nitrosative stress: current state. *Nutrition journal,* 15, 71-71.

KWOK, L. Y., SCHLÜTER, D., CLAYTON, C. & SOLDATI, D. 2004. The antioxidant systems in *Toxoplasma gondii* and the role of cytosolic catalase in defence against oxidative injury. *Molecular Microbiology,* 51, 47-61.

LALIBERTE, J. & CARRUTHERS, V. B. 2008. Host cell manipulation by the human pathogen *Toxoplasma gondii*. *Cellular and Molecular Life Sciences,* 65, 1900-15.

LAPINSKAS, P. J. & BEN-HARARI, R. R. 2019. Perspective on current and emerging drugs in the treatment of acute and chronic toxoplasmosis. *Postgraduate Medicine,* 131, 589-596.

LARSON, E. T., PARUSSINI, F., HUYNH, M. H., GIEBEL, J. D., KELLEY, A. M., ZHANG, L., BOGYO, M., MERRITT, E. A. & CARRUTHERS, V. B. 2009. *Toxoplasma gondii* cathepsin L is the primary target of the invasion-inhibitory compound morpholinurea-leucyl-homophenyl-vinyl sulfone phenyl. *Journal of Biological Chemistry,* 284, 26839-50.

LAWRENCE, C. P., KADIOGLU, A., YANG, A. L., COWARD, W. R. & CHOW, S. C. 2006. The cathepsin B inhibitor, z-FA-FMK, inhibits human T cell proliferation *in vitro* and modulates host response to pneumococcal infection *in vivo*. *Journal of Immunology,* 177, 3827-36.

LIGUORI, I., RUSSO, G., CURCIO, F., BULLI, G., ARAN, L., DELLA-MORTE, D., GARGIULO, G., TESTA, G., CACCIATORE, F., BONADUCE, D. & ABETE, P. 2018. Oxidative stress, aging, and diseases. *Clinical interventions in aging,* 13, 757-772.

LIOW, K. Y. & CHOW, S. C. 2013. The cathepsin B inhibitor, z-FA-CMK is toxic and readily induced cell death in human T lymphocytes. *Toxicology and Applied Pharmacology,* 272, 559-67.

LIU, J., WETZEL, L., ZHANG, Y., NAGAYASU, E., EMS-MCCLUNG, S., FLORENS, L. & HU, K. 2013. Novel thioredoxin-like proteins are components of a protein complex coating the cortical microtubules of *Toxoplasma gondii*. *Eukaryotic Cell,* 12, 1588-1599.

LIU, Q., WANG, Z. D., HUANG, S. Y. & ZHU, X. Q. 2015. Diagnosis of toxoplasmosis and typing of *Toxoplasma gondii*. *Parasites & vectors,* 8, 292-292.

LUBOS, E., LOSCALZO, J. & HANDY, D. E. 2011. Glutathione peroxidase-1 in health and disease: from molecular mechanisms to therapeutic opportunities. *Antioxidants & redox signaling,* 15, 1957-1997.

LYONS, R. E., MCLEOD, R. & ROBERTS, C. W. 2002. *Toxoplasma gondii* tachyzoite-bradyzoite interconversion. *Trends in Parasitology,* 18, 198-201.

MAILLOUX, R. J., MCBRIDE, S. L. & HARPER, M. E. 2013. Unearthing the secrets of mitochondrial ROS and glutathione in bioenergetics. *Trends in Biochemical Sciences,* 38, 592-602.

MAMMARI, N., HALABI, M. A., YAACOUB, S., CHLALA, H., DARD, E, M.L. & COURTIOUX, B. 2019. *Toxoplasma gondii* Modulates the Host Cell Responses: An Overview of Apoptosis Pathways. *BioMed Research International,* 2019, 10.

MANSFIELD, K. D., SIMON, M. C. & KEITH, B. 2004. Hypoxic reduction in cellular glutathione levels requires mitochondrial reactive oxygen species. *Journal of Applied Physiology (1985),* 97, 1358-66.

MANY, A. & KOREN, G. 2006. Toxoplasmosis during pregnancy. *Canadian family physician Médecin de famille canadien,* 52, 29-30, 32.

MARTINDALE, J. L. & HOLBROOK, N. J. 2002. Cellular response to oxidative stress: signaling for suicide and survival. *Journal of Cellular Physiology,* 192, 1-15.

MAUTHE, M., ORHON, I., ROCCHI, C., ZHOU, X., LUHR, M., HIJLKEMA, K. J., COPPES, R. P., ENGEDAL, N., MARI, M. & REGGIORI, F. 2018. Chloroquine inhibits autophagic flux by decreasing autophagosome-lysosome fusion. *Autophagy,* 14, 1435-1455.

MCAULEY, J. B. 2014. Congenital toxoplasmosis. *Journal of the Pediatric Infectious Diseases Society,* 3, S30-S35.

MCGOVERN, O. L., RIVERA-CUEVAS, Y., KANNAN, G., NARWOLD JR, A. J. & CARRUTHERS, V. B. 2018. Intersection of endocytic and exocytic systems in *Toxoplasma gondii*. *Traffic,* 19, 336-353.

MELÉNDEZ, A. & LEVINE, B. 2009. *Autophagy in C. elegans,* WormBook, ed. The *C. elegans* Research Community, WormBook, doi/10.1895/wormbook.1.147.1.

MELO, E. J., ATTIAS, M. & DE SOUZA, W. 2000. The single mitochondrion of tachyzoites of *Toxoplasma gondii*. *Journal of Structural Biology,* 130, 27-33.

MIRANDA, K., PACE, D. A., CINTRON, R., RODRIGUES, J. C., FANG, J., SMITH, A., ROHLOFF, P., COELHO, E., DE HAAS, F., DE SOUZA, W., COPPENS, I., SIBLEY, L. D. & MORENO, S. N. 2010. Characterization of a novel organelle in *Toxoplasma gondii* with similar composition and function to the plant vacuole. *Molecular Microbiology,* 76, 1358-75.

MIROŃCZUK-CHODAKOWSKA, I., WITKOWSKA, A. M. & ZUJKO, M. E. 2018. Endogenous non-enzymatic antioxidants in the human body. *Advances in Medical Sciences,* 63, 68-78.

MIZUSHIMA, N. 2007. Autophagy: process and function. *Genes & Development,* 21, 2861-73.

MONTAZERI, M., MEHRZADI, S., SHARIF, M., SARVI, S., TANZIFI, A., AGHAYAN, S. A. & DARYANI, A. 2018. Drug resistance in *Toxoplasma gondii*. *Frontiers in microbiology,* 9, 2587-2587.

MONTAZERI, M., SHARIF, M., SARVI, S., MEHRZADI, S., AHMADPOUR, E. & DARYANI, A. 2017. A systematic review of *in vitro* and *in vivo* activities of anti-*Toxoplasma* drugs and compounds (2006-2016). *Frontiers in Microbiology,* 8, 25.

MONTOYA, J. G. & LIESENFELD, O. 2004. Toxoplasmosis. *Lancet,* 363, 1965-76.

MONTOYA, J. G. & REMINGTON, J. S. 2008. Management of *Toxoplasma gondii* infection during pregnancy. *Clinical Infectious Diseases,* 47, 554-66.

MORLON-GUYOT, J., BERRY, L., CHEN, C. T., GUBBELS, M. J., LEBRUN, M. & DAHER, W. 2014. The *Toxoplasma gondii* calcium-dependent protein kinase 7 is involved in early steps of parasite division and is crucial for parasite survival. *Cellular Microbiology,* 16, 95-114.

NARASIMHAN, J., JOYCE, B. R., NAGULESWARAN, A., SMITH, A. T., LIVINGSTON, M. R., DIXON, S. E., COPPENS, I., WEK, R. C. & SULLIVAN, W. J., JR. 2008. Translation regulation by eukaryotic initiation factor-2 kinases in the development of latent cysts in *Toxoplasma gondii*. *Journal of Biological Chemistry,* 283, 16591-601.

NATH, A. & SINAI, A. P. 2003. Cerebral toxoplasmosis. *Current Treatment Options in Neurology,* 5, 3-12.

NGUYEN, G. T., GREEN, E. R. & MECSAS, J. 2017a. Neutrophils to the ROScue: mechanisms of nadph oxidase activation and bacterial resistance. *Frontiers in Cellular and Infection Microbiology,* 7.

NGUYEN, H. M., BERRY, L., SULLIVAN, W. J., JR & BESTEIRO, S. 2017b. Autophagy participates in the unfolded protein response in *Toxoplasma gondii*. *FEMS Microbiology Letters,* 364.

NGUYEN, H. M., EL HAJJ, H., EL HAJJ, R., TAWIL, N., BERRY, L., LEBRUN, M., BORDAT, Y. & BESTEIRO, S. 2017c. *Toxoplasma gondii* autophagy-related protein ATG9 is crucial for the survival of parasites in their host. *Cellular Microbiology,* 19.

NIEHUS, S., SMITH, T. K., AZZOUZ, N., CAMPOS, M. A., DUBREMETZ, J. F., GAZZINELLI, R. T., SCHWARZ, R. T. & DEBIERRE-GROCKIEGO, F. 2014. Virulent and avirulent strains of *Toxoplasma gondii* which differ in their glycosylphosphatidylinositol content induce similar biological functions in macrophages. *PLOS One,* 9, e85386.

NISHI, M., HU, K., MURRAY, J. M. & ROOS, D. S. 2008. Organellar dynamics during the cell cycle of *Toxoplasma gondii*. *Journal of Cellular Science,* 121, 1559-68.

O'BRIEN, T. C., MACKEY, Z. B., FETTER, R. D., CHOE, Y., O'DONOGHUE, A. J., ZHOU, M., CRAIK, C. S., CAFFREY, C. R. & MCKERROW, J. H. 2008. A parasite cysteine protease is key to host protein degradation and iron acquisition. *Journal of Biological Chemistry,* 283, 28934-43.

O'DWYER, P. J., HAMILTON, T. C., LACRETA, F. P., GALLO, J. M., KILPATRICK, D., HALBHERR, T., BRENNAN, J., BOOKMAN, M. A., HOFFMAN, J., YOUNG, R. C., COMIS, R. L. & OZOLS, R. F. 1996. Phase I trial of buthionine sulfoximine in combination with melphalan in patients with cancer. *Journal of Clinical Oncology,* 14, 249-56.

ODBERG-FERRAGUT, C., RENAULT, J. P., VISCOGLIOSI, E., TOURSEL, C., BRICHE, I., ENGELS, A., LEPAGE, G., MORGENSTERN-BADARAU, I., CAMUS, D., TOMAVO, S. & DIVE, D. 2000. Molecular cloning, expression analysis and iron metal cofactor characterisation of a superoxide dismutase from *Toxoplasma gondii*. *Molecular Biochemical Parasitology,* 106, 121-9.

ORRENIUS, S. 2007. Reactive oxygen species in mitochondria-mediated cell death. *Drug Metabolism Reviews,* 39, 443-55.

OWUSU-ANSAH, E., YAVARI, A. & BANERJEE, U. 2008. *A protocol for in vivo detection of reactive oxygen species*. *Protocol Exchange*

OZGONUL, C. & BESIRLI, C. G. 2017. Recent developments in the diagnosis and treatment of ocular toxoplasmosis. *Ophthalmic Research,* 57, 1-12.

OZOUGWU, J. 2016. *The role of reactive oxygen species and antioxidants in oxidative stress*. Bioscience reports.

PAL, C. & BANDYOPADHYAY, U. 2012. Redox-active antiparasitic drugs. *Antioxidants & Redox Signaling,* 17, 555-82.

PALIT, P., HAZRA, A., MAITY, A., VIJAYAN, R. S. K., MANOHARAN, P., BANERJEE, S., MONDAL, N. B., GHOSHAL, N. & ALI, N. 2012. Discovery of safe and orally effective 4-aminoquinaldine analogues as apoptotic inducers with activity against experimental visceral leishmaniasis. *Antimicrobial Agents and Chemotherapy,* 56, 432.

PARUSSINI, F., COPPENS, I., SHAH, P. P., DIAMOND, S. L. & CARRUTHERS, V. B. 2010. Cathepsin L occupies a vacuolar compartment and is a protein maturase within the endo/exocytic system of *Toxoplasma gondii*. *Molecular Microbiology,* 76, 1340-57.

PENG, B. W., LIN, J., LIN, J. Y., JIANG, M. S. & ZHANG, T. 2003. Exogenous nitric oxide induces apoptosis in *Toxoplasma gondii* tachyzoites via a calcium signal transduction pathway. *Parasitology,* 126, 541-50.

PERNAS, L., BEAN, C., BOOTHROYD, J. C. & SCORRANO, L. 2018. Mitochondria restrict growth of the intracellular parasite *Toxoplasma gondii* by limiting its uptake of fatty acids. *Cell Metabolism,* 27, 886-897.e4.

PHANIENDRA, A., JESTADI, D. B. & PERIYASAMY, L. 2015. Free radicals: properties, sources, targets, and their implication in various diseases. *Indian journal of clinical biochemistry : IJCB,* 30, 11-26.

PINO, P., FOTH, B. J., KWOK, L.-Y., SHEINER, L., SCHEPERS, R., SOLDATI, T. & SOLDATI-FAVRE, D. 2007. Dual targeting of antioxidant and metabolic enzymes to the mitochondrion and the apicoplast of *Toxoplasma gondii*. *PLOS Pathogens,* 3, e115.

PITTMAN, K. J., ALIOTA, M. T. & KNOLL, L. J. 2014. Dual transcriptional profiling of mice and *Toxoplasma gondii* during acute and chronic infection. *BMC Genomics,* 15, 806.

POLJSAK, B., SUPUT, D. & MILISAV, I. 2013. Achieving the balance between ROS and antioxidants: when to use the synthetic antioxidants. *Oxidative Medicine and Cellular Longevity,* 2013, 956792.

POWERS, J. C., ASGIAN, J. L., EKICI, O. D. & JAMES, K. E. 2002. Irreversible inhibitors of serine, cysteine, and threonine proteases. *Chemical Reviews,* 102, 4639-750.

QUE, X., ENGEL, J. C., FERGUSON, D., WUNDERLICH, A., TOMAVO, S. & REED, S. L. 2007. Cathepsin Cs are key for the intracellular survival of the protozoan parasite, *Toxoplasma gondii*. *Journal of Biological Chemistry,* 282, 4994-5003.

QUE, X., NGO, H., LAWTON, J., GRAY, M., LIU, Q., ENGEL, J., BRINEN, L., GHOSH, P., JOINER, K. A. & REED, S. L. 2002. The cathepsin B of *Toxoplasma gondii*, Toxopain-1, is critical for parasite invasion and rhoptry protein processing. *Journal of Biological Chemistry,* 277, 25791-7.

QUE, X., WUNDERLICH, A., JOINER, K. A. & REED, S. L. 2004. Toxopain-1 is critical for infection in a novel chicken embryo model of congenital toxoplasmosis. *Infection and immunity,* 72, 2915-2921.

QUIJANO, C., TRUJILLO, M., CASTRO, L. & TROSTCHANSKY, A. 2015. Interplay between oxidant species and energy metabolism. *Redox biology,* 8, 28-42.

RADKE, J. R., GUERINI, M. N., JEROME, M. & WHITE, M. W. 2003. A change in the premitotic period of the cell cycle is associated with bradyzoite differentiation in *Toxoplasma gondii*. *Molecular and Biochemical Parasitology,* 131, 119-27.

RAHAL, A., KUMAR, A., SINGH, V., YADAV, B., TIWARI, R., CHAKRABORTY, S. & DHAMA, K. 2014. Oxidative stress, prooxidants, and antioxidants: the interplay. *BioMed Research International,* 2014, 19.

RAJAH, T. & CHOW, S. C. 2015. Suppression of human T cell proliferation mediated by the cathepsin B inhibitor, z-FA-FMK is due to oxidative stress. *PLOS One,* 10, e0123711.

RAMIREZ-FLORES, C. J., CRUZ-MIRON, R., ARROYO, R., MONDRAGON-CASTELAN, M. E., NOPAL-GUERRERO, T., GONZALEZ-POZOS, S., RIOS-CASTRO, E. & MONDRAGON-FLORES, R. 2019. Characterization of metalloproteases and serine proteases of *Toxoplasma gondii* tachyzoites and their effect on epithelial cells. *Parasitology Research,* 118, 289-306.

RASNICK, D. 1985. Synthesis of peptide fluoromethyl ketones and the inhibition of human cathepsin B. *Analytical Biochemistry,* 149, 461-5.

RECZEK, C. R. & CHANDEL, N. S. 2015. ROS-dependent signal transduction. *Current Opinion in Cell Biology,* 33, 8-13.

REMINGTON, J. S., ARAUJO, F. G. & DESMONTS, G. 1985. Recognition of different *Toxoplasma* antigens by IgM and IgG antibodies in mothers and their congenitally infected newborns. *Journal of Infectious Diseases,* 152, 1020-4.

REMINGTON, J. S., THULLIEZ, P. & MONTOYA, J. G. 2004. Recent developments for diagnosis of toxoplasmosis. *Journal of clinical microbiology,* 42, 941-945.

REMINGTON, J. S., MCLEOD, R., THULLIEZ, P. & DESMONTS, G., 2006. *Toxoplasmosis. In: Remington, J.S., Klein, J.O. (Eds.), Infectious Diseases of the Fetus and Newborn Infant,* 5th MELÉNDEZ. WB Saunders Company, Philadelphia, USA, 947–1091.

ROBERT-GANGNEUX, F. & DARDÉ, M. L. 2012. Epidemiology of and Diagnostic Strategies for Toxoplasmosis. *Clinical Microbiology Reviews,* 25, 264-296.

ROSENTHAL, P. J. 2004. Cysteine proteases of malaria parasites. *International Journal for Parasitology,* 34, 1489-1499.

ROSENTHAL, P. J., LEE, G. K. & SMITH, R. E. 1993. Inhibition of a *Plasmodium vinckei* cysteine proteinase cures murine malaria. *Journal of Clinical Investigation,* 91, 1052-6.

SABIN, A. B. & FELDMAN, H. A. 1948. Dyes as microchemical indicators of a new immunity phenomenon affecting a protozoon parasite (*Toxoplasma*). *Science,* 108, 660-3.

SAEIJ, J. P., BOYLE, J. P. & BOOTHROYD, J. C. 2005. Differences among the three major strains of *Toxoplasma gondii* and their specific interactions with the infected host. *Trends in parasitology,* 21, 476-81.

SAJID, M. & MCKERROW, J. H. 2002. Cysteine proteases of parasitic organisms. *Molecular and Biochemical Parasitology,* 120, 1-21.

SAMUEL, B. U., HEARN, B., MACK, D., WENDER, P., ROTHBARD, J., KIRISITS, M. J., MUI, E., WERNIMONT, S., ROBERTS, C. W., MUENCH, S. P., RICE, D. W., PRIGGE, S. T., LAW, A. B. & MCLEOD, R. 2003. Delivery of antimicrobials into parasites. *Proceedings of the National Academy of Sciences of the United States of America,* 100, 14281-6.

SCHIPPERS, J. H., NGUYEN, H. M., LU, D., SCHMIDT, R. & MUELLER-ROEBER, B. 2012. ROS homeostasis during development: an evolutionary conserved strategy. *Cellular and Molecular Life Sciences,* 69, 3245-57.

SCHMIDT, D. R., HOGH, B., ANDERSEN, O., HANSEN, S. H., DALHOFF, K. & PETERSEN, E. 2006. Treatment of infants with congenital toxoplasmosis: tolerability and plasma concentrations of sulfadiazine and pyrimethamine. *European Journal of Pediatrics,* 165, 19-25.

SCHOTTE, P., SCHAUVLIEGE, R., JANSSENS, S. & BEYAERT, R. 2001. The cathepsin B inhibitor z-FA.fmk inhibits cytokine production in macrophages stimulated by lipopolysaccharide. *Journal of Biological Chemistry,* 276, 21153-7.

SCORY, S., CAFFREY, C. R., STIERHOF, Y. D., RUPPEL, A. & STEVERDING, D. 1999. *Trypanosoma brucei*: killing of bloodstream forms *in vitro* and *in vivo* by the cysteine proteinase inhibitor Z-phe-ala-CHN2. *Experimental Parasitology,* 91, 327-33.

SEHGAL, A., BETTIOL, S., PYPAERT, M., WENK, M. R., KAASCH, A., BLADER, I. J., JOINER, K. A. & COPPENS, I. 2005. Peculiarities of host cholesterol transport to the unique intracellular vacuole containing *Toxoplasma*. *Traffic,* 6, 1125-41.

SHAW, M. K., ROOS, D. S. & TILNEY, L. G. 2002. Cysteine and serine protease inhibitors block intracellular development and disrupt the secretory pathway of *Toxoplasma gondii*. *Microbes and Infection,* 4, 119-32.

SHEFFIELD, H. G. & MELTON, M. L. 1968. The fine structure and reproduction of *Toxoplasma gondii*. *Journal of Parasitology,* 54, 209-26.

SIBLEY, L. D., CARRUTHERS, V. B., MORDUE, D., MERCIER, C. & HÅKANSSON, S. 1999. Active cell invasion by *Toxoplasma gondii* leads to avoidance of phagocytic processing. *In:* GORDON, S. (ed.) *Advances in Cellular and Molecular Biology of Membranes and Organelles.* JAI.

SILVEIRA, C., BELFORT, R., JR., MUCCIOLI, C., HOLLAND, G. N., VICTORA, C. G., HORTA, B. L., YU, F. & NUSSENBLATT, R. B. 2002. The effect of long-term intermittent trimethoprim/sulfamethoxazole treatment on recurrences of toxoplasmic retinochoroiditis. *American Journal of Ophthalmology,* 134, 41-6.

SIMON, H.-U., HAJ-YEHIA, A. & LEVI-SCHAFFER, F. 2000. Role of reactive oxygen species (ROS) in apoptosis induction. *Apoptosis,* 5, 415-418.

SIMON, S., DE THOISY, B., MERCIER, A., NACHER, M. & DEMAR, M. 2019. Virulence of atypical *Toxoplasma gondii* strains isolated in French Guiana in a murine model. *Parasite (Paris, France),* 26, 60-60.

SINGH, U., BREWER, J. L. & BOOTHROYD, J. C. 2002. Genetic analysis of tachyzoite to bradyzoite differentiation mutants in *Toxoplasma gondii* reveals a hierarchy of gene induction. *Molecular Microbiology,* 44, 721-733.

SIQUEIRA-NETO, J. L., DEBNATH, A., MCCALL, L.-I., BERNATCHEZ, J. A., NDAO, M., REED, S. L. & ROSENTHAL, P. J. 2018. Cysteine proteases in protozoan parasites. *PLOS Neglected Tropical Diseases,* 12, e0006512.

SKARIAH, S., MCINTYRE, M. K. & MORDUE, D. G. 2010. *Toxoplasma gondii*: determinants of tachyzoite to bradyzoite conversion. *Parasitology Research,* 107, 253-260.

SLAUCH, J. M. 2011. How does the oxidative burst of macrophages kill bacteria? Still an open question. *Molecular microbiology,* 80, 580-583.

SLESAK, I., SLESAK, H., ZIMAK-PIEKARCZYK, P. & ROZPADEK, P. 2016. Enzymatic Antioxidant Systems in Early Anaerobes: Theoretical Considerations. *Astrobiology,* 16, 348-58.

SOETE, M., CAMUS, D. & DUBREMETZ, J. F. 1994. Experimental induction of bradyzoite-specific antigen expression and cyst formation by the RH strain of *Toxoplasma gondii in vitro*. *Experimental Parasitology,* 78, 361-70.

SOETE, M., FORTIER, B., CAMUS, D. & DUBREMETZ, J. F. 1993. *Toxoplasma gondii*: kinetics of bradyzoite-tachyzoite interconversion *in vitro*. *Experimental Parasitology,* 76, 259-64.

SONGSUNGTHONG, W., KOONYOSYING, P., UTHAIPIBULL, C. & KAMCHONWONGPAISAN, S. 2016. Inhibition of glutathione biosynthesis sensitizes *Plasmodium berghei* to antifolates. *Antimicrobial agents and chemotherapy,* 60, 3057-3064.

STROBER, W. 2001. Trypan blue exclusion test of cell viability. *Current Protocols in Immunology,* Appendix 3, Appendix 3B.

STROIKIN, Y., DALEN, H., LÖÖF, S. & TERMAN, A. 2004. Inhibition of autophagy with 3-methyladenine results in impaired turnover of lysosomes and accumulation of lipofuscin-like material. *European Journal of Cell Biology,* 83, 583-590.

SU, C., EVANS, D., COLE, R. H., KISSINGER, J. C., AJIOKA, J. W. & SIBLEY, L. D. 2003. Recent expansion of *Toxoplasma* through enhanced oral transmission. *Science,* 299, 414-6.

SUBAUSTE, C. S. 2019. Interplay Between *Toxoplasma gondii*, Autophagy, and Autophagy Proteins. *Frontiers in Cellular and Infection Microbiology,* 9.

SUGI, T., TU, V., MA, Y., TOMITA, T. & WEISS, L. M. 2017. *Toxoplasma gondii* requires glycogen phosphorylase for balancing amylopectin storage and for efficient production of brain cysts. *mBio,* 8, e01289-17.

SULLIVAN, W. J. & JEFFERS, V. 2012a. Mechanisms of *Toxoplasma gondii* persistence and latency. *FEMS Microbiology Reviews,* 36, 717-733.

SULLIVAN, W. J., JR., SMITH, A. T. & JOYCE, B. R. 2009. Understanding mechanisms and the role of differentiation in pathogenesis of *Toxoplasma gondii*: a review. *Memorias do Instituto Oswaldo Cruz,* 104, 155-161.

SUN, S. Y. 2010. N-acetylcysteine, reactive oxygen species and beyond. *Cancer biology & therapy,* 9, 109-110.

SUSS-TOBY, E., ZIMMERBERG, J. & WARD, G. E. 1996. *Toxoplasma* invasion: the parasitophorous vacuole is formed from host cell plasma membrane and pinches off via a fission pore. *Proceedings of the National Academy of Sciences of the United States of America,* 93, 8413-8418.

SUTTERLAND, A. L., FOND, G., KUIN, A., KOETER, M. W., LUTTER, R., VAN GOOL, T., YOLKEN, R., SZOKE, A., LEBOYER, M. & DE HAAN, L. 2015. Beyond the association. *Toxoplasma gondii* in schizophrenia, bipolar disorder, and addiction: systematic review and meta-analysis. *Acta Psychiatrica Scandinavica,* 132, 161-79.

TAGDE, A., SINGH, H., KANG, M. H. & REYNOLDS, C. P. 2014. The glutathione synthesis inhibitor buthionine sulfoximine synergistically enhanced melphalan activity against preclinical models of multiple myeloma. *Blood Cancer Journal,* 4, e229.

TAKASHIMA, Y., SUZUKI, K., XUAN, X., NISHIKAWA, Y., UNNO, A. & KITOH, K. 2008. Detection of the initial site of *Toxoplasma gondii* reactivation in brain tissue. *International Journal for Parasitology,* 38, 601-607.

TENTER, A. M., HECKEROTH, A. R. & WEISS, L. M. 2000. *Toxoplasma gondii*: from animals to humans. *International Journal of Parasitology,* 30, 1217-58.

TEO, C. F., ZHOU, X. W., BOGYO, M. & CARRUTHERS, V. B. 2007. Cysteine protease inhibitors block *Toxoplasma gondii* microneme secretion and cell invasion. *Antimicrobial Agents and Chemotherapy,* 51, 679-88.

THORNTON, L. B., TEEHAN, P., FLOYD, K., COCHRANE, C., BERGMANN, A., RIEGEL, B., STASIC, A. J., DI CRISTINA, M., MORENO, S. N. J., ROEPE, P. D. & DOU, Z. 2019. An ortholog of *Plasmodium falciparum* chloroquine resistance transporter (*Pf*CRT) plays a key role in maintaining the integrity of the endolysosomal system in *Toxoplasma gondii* to facilitate host invasion. *PLOS Pathogens,* 15, e1007775.

TOMAVO, S. & BOOTHROYD, J. C. 1995. Interconnection between organellar functions, development and drug resistance in the protozoan parasite, *Toxoplasma gondii*. *International Journal of Parasitology,* 25, 1293-9.

TOMITA, T., BZIK, D. J., MA, Y. F., FOX, B. A., MARKILLIE, L. M., TAYLOR, R. C., KIM, K. & WEISS, L. M. 2013. The *Toxoplasma gondii* cyst wall protein CST1 is critical for cyst wall integrity and promotes bradyzoite persistence. *PLOS Pathogens,* 9, e1003823.

TRACHOOTHAM, D., LU, W., OGASAWARA, M. A., NILSA, R. D. & HUANG, P. 2008. Redox regulation of cell survival. *Antioxidants & Redox Signaling,* 10, 1343-74.

TRAN, S. L., PUHAR, A., NGO-CAMUS, M. & RAMARAO, N. 2011. Trypan blue dye enters viable cells incubated with the pore-forming toxin HlyII of *Bacillus cereus*. *PLOS One,* 6, e22876-e22876.

TU, V., YAKUBU, R. & WEISS, L. M. 2018. Observations on bradyzoite biology. *Microbes and Infection,* 20, 466-476.

TURK, D. & GUNCAR, G. 2003. Lysosomal cysteine proteases (cathepsins): promising drug targets. *Acta Crystallographica Section D,* 59, 203-213.

TURK, V., STOKA, V., VASILJEVA, O., RENKO, M., SUN, T., TURK, B. & TURK, D. 2012. Cysteine cathepsins: From structure, function and regulation to new frontiers. *Biochimica et Biophysica Acta (BBA) - Proteins and Proteomics,* 1824, 68-88.

TURRENS, J. F. 2004. Oxidative stress and antioxidant defenses: a target for the treatment of diseases caused by parasitic protozoa. *Molecular Aspects of Medicine,* 25, 211-20.

TYMOSHENKO, S., OPPENHEIM, R. D., AGREN, R., NIELSEN, J., SOLDATI-FAVRE, D. & HATZIMANIKATIS, V. 2015. Metabolic needs and capabilities of *Toxoplasma gondii* through combined computational and experimental analysis. *PLOS Computational Biology,* 11, e1004261.

UDONSOM, R., BUDDHIRONGAWATR, R. & SUKTHANA, Y. 2010. Is Sabin-Feldman dye test using T. gondii tachyzoites from animal inoculation still the best method for detecting *Toxoplasma gondii* antibodies? *Southeast Asian Journal of Tropical Medicine and Public Health,* 41, 1059-64.

UFERMANN, C. M., MULLER, F., FROHNECKE, N., LAUE, M. & SEEBER, F. 2017. *Toxoplasma gondii* plaque assays revisited: Improvements for ultrastructural and quantitative evaluation of lytic parasite growth. *Experimental Parasitology,* 180, 19-26.

UTTAH, E., OGBAN, E. & OKONOFUA, C. 2013. Toxoplasmosis: A global infection, so widespread, so neglected. *International Journal of Scientific and Research Publications,* 3.

VAN DOOREN, G. G., REIFF, S. B., TOMOVA, C., MEISSNER, M., HUMBEL, B. M. & STRIEPEN, B. 2009. A novel dynamin-related protein has been recruited for apicoplast fission in *Toxoplasma gondii*. *Current Biology,* 19, 267-76.

VANDANA, SINGH, A. P., SINGH, J., SHARMA, R., AKHTER, M., MISHRA, P. K., SAXENA, A. K., DIXIT, R., RATHI, B., KATYAL, A. & PANDEY, K. C. 2018. Biochemical characterization of unusual cysteine protease of *P. falciparum*, metacaspase-2 (MCA-2). *Molecular and Biochemical Parasitology,* 220, 28-41.

VILLARD, O., CIMON, B., L'OLLIVIER, C., FRICKER-HIDALGO, H., GODINEAU, N., HOUZE, S., PARIS, L., PELLOUX, H., VILLENA, I. & CANDOLFI, E. 2016. Serological diagnosis of *Toxoplasma gondii* infection: Recommendations from the French National Reference Center for Toxoplasmosis. *Diagnostic Microbiology and Infectious Disease,* 84, 22-33.

VINAYAK, S., BROOKS, C. F., NAUMOV, A., SUVOROVA, E. S., WHITE, M. W. & STRIEPEN, B. 2014. Genetic manipulation of the *Toxoplasma gondii* genome by fosmid recombineering. *mBio,* 5, e02021-14.

VONLAUFEN, N., KANZOK, S. M., WEK, R. C. & SULLIVAN, W. J., JR. 2008. Stress response pathways in protozoan parasites. *Cellular Microbiology,* 10, 2387-99.

WANG, K. & KLIONSKY, D. J. 2011. Mitochondria removal by autophagy. *Autophagy,* 7, 297-300.

WANG, Y., WEISS, L. M. & ORLOFSKY, A. 2009. Host cell autophagy is induced by *Toxoplasma gondii* and contributes to parasite growth. *The Journal of Biological Chemistry,* 284, 1694-1701.

WARRING, S. D., DOU, Z., CARRUTHERS, V. B., MCFADDEN, G. I. & VAN DOOREN, G. G. 2014. Characterization of the chloroquine resistance transporter homologue in *Toxoplasma gondii*. *Eukaryotic cell,* 13, 1360-1370.

WAŚKIEWICZ, A., BESZTERDA, M. & GOLIŃSKI, P. 2014. Chapter 7-Nonenzymatic Antioxidants in Plants. *In:* AHMAD, P. (ed.) *Oxidative Damage to Plants.* San Diego: Academic Press.

WATTS, E., ZHAO, Y., DHARA, A., ELLER, B., PATWARDHAN, A. & SINAI, A. P. 2015. Novel approaches reveal that *Toxoplasma gondii* bradyzoites within tissue cysts are dynamic and replicating entities *in vivo*. *MBio,* 6, e01155-15.

WEIDBERG, H., SHVETS, E. & ELAZAR, Z. 2011. Biogenesis and cargo selectivity of autophagosomes. Annual Review of Biochemistry, 80, 125-56.

WEISS, L. M. & KIM, K. 2000. The development and biology of bradyzoites of *Toxoplasma gondii*. *Frontiers in Bioscience,* 5, D391-405.

WEISS, L. M., LAPLACE, D., TAKVORIAN, P. M., TANOWITZ, H. B., CALI, A. & WITTNER, M. 1995. A cell culture system for study of the development of *Toxoplasma gondii* bradyzoites. *Journal of Eukaryotic Microbiology,* 42, 150-7.

WILKING, H., THAMM, M., STARK, K., AEBISCHER, T. & SEEBER, F. 2016. Prevalence, incidence estimations, and risk factors of *Toxoplasma gondii* infection in Germany: a representative, cross-sectional, serological study. *Scientific reports,* 6, 22551-22551.

WILLIAMS, C. F., YARLETT, N., AON, M. A. & LLOYD, D. 2014. Antioxidant defences of *Spironucleus vortens*: Glutathione is the major non-protein thiol. *Molecular and Biochemical Parasitology,* 196, 45-52.

XUE, J., JIANG, W., CHEN, Y., GONG, F., WANG, M., ZENG, P., XIA, C., WANG, Q. & HUANG, K. 2017. Thioredoxin reductase from *Toxoplasma gondii*: an essential virulence effector with antioxidant function. *The FASEB Journal,* 31, 4447-4457.

YAHIAOUI, B., DZIERSZINSKI, F., BERNIGAUD, A., SLOMIANNY, C., CAMUS, D. & TOMAVO, S. 1999. Isolation and characterization of a subtractive library enriched for developmentally regulated transcripts expressed during encystation of *Toxoplasma gondii*. *Molecular and Biochemical Parasitology,* 99, 223-35.

YAN, C., LIANG, L. J., ZHENG, K. Y. & ZHU, X. Q. 2016. Impact of environmental factors on the emergence, transmission and distribution of *Toxoplasma gondii*. *Parasites & Vectors,* 9, 137-137.

YORIMITSU, T. & KLIONSKY, D. J. 2005. Autophagy: molecular machinery for self-eating. *Cell Death & Differentiation,* 12 Suppl 2, 1542-52.

YOUNUS, H. 2018. Therapeutic potentials of superoxide dismutase. *International journal of health sciences,* 12, 88-93.

ZANG, L., HE, H., XU, Q., YU, Y., ZHENG, N., LIU, W., HAYASHI, T., TASHIRO, S., ONODERA, S. & IKEJIMA, T. 2013. Reactive oxygen species H2O2 and *OH, but not O2*(-) promote oridonin-induced phagocytosis of apoptotic cells by human histocytic lymphoma U937 cells. *International Immunopharmacology,* 15, 414-23.

ZHANG, Y. W., HALONEN, S. K., MA, Y. F., WITTNER, M. & WEISS, L. M. 2001. Initial characterization of CST1, a *Toxoplasma gondii* cyst wall glycoprotein. *Infection and Immunity,* 69, 501-7.

ZHAO, G., ZHOU, A., LV, G., MENG, M., SUN, M., BAI, Y., HAN, Y., WANG, L., ZHOU, H., CONG, H., ZHAO, Q., ZHU, X. Q. & HE, S. 2013. *Toxoplasma gondii* cathepsin proteases are undeveloped prominent vaccine antigens against toxoplasmosis. *BMC infectious diseases,* 13, 207-207.

ZHOU, X. W., KAFSACK, B. F., COLE, R. N., BECKETT, P., SHEN, R. F. & CARRUTHERS, V. B. 2005. The opportunistic pathogen *Toxoplasma gondii* deploys a diverse legion of invasion and survival proteins. *Journal of Biological Chemistry,* 280, 34233-44.

ZHU, W., LI, J., PAPPOE, F., SHEN, J. & YU, L. 2019. Strategies Developed by *Toxoplasma gondii* to Survive in the Host. *Frontiers in Microbiology,* 10.

ZOU, Z., CHANG, H., LI, H. & WANG, S. 2017. Induction of reactive oxygen species: an emerging approach for cancer therapy. *Apoptosis,* 22, 1321-1335.

ZWICKER, J. D., DIAZ, N. A., GUERRA, A. J., KIRCHHOFF, P. D., WEN, B., SUN, D., CARRUTHERS, V. B. & LARSEN, S. D. 2018. Optimization of dipeptidic inhibitors of cathepsin L for improved *Toxoplasma gondii* selectivity and CNS permeability. *Bioorganic & Medicinal Chemistry Letters,* 28, 1972-1980.